1. INTRODUCTION

Eales' disease is an idiopathic inflammatory venous occlusion, which primarily affects the peripheral retina veins of the young adults (1, 2). This disease is rarely reported in Western and South East countries, but for unknown reasons it is more common in the Indian subcontinent. The incidence rate is 1 in 200-250 ophthalmic patients evaluated in a tertiary eye care center (3). Predominantly (99 %) affected are males in the age group of 20-45 years and involvement is often bilateral (3). The natural course of the disease varies, there is a complete remission in some cases while in other cases it persistently progress to blindness. The clinical features of the disease are perivascular phlebitis, non-perfusion and neovascularization (NV). Bleeding from NV is most common, usually recurrent and is one of the major causes for visual loss in Eales' disease patients (4). In addition to the above, the formation of epiretinal membrane (ERM) imposes a tractional pull on the retina causing retinal detachment. Timely intervention with vitrectomy, laser photocoagulation or removal of epiretinal membrane helps in partial restoration of vision. Treatment for Eales' disease is mainly based on the symptoms, which the patients present before the clinicians. Often the management of intraocular inflammation is done using oral corticosteroids. Vitreoretinal complications are treated with either laser photocoagulation or other vitreoretinal surgical procedures (5, 6). Classification and assessment the severity of the disease is carried out as per new staging system described by Saxena et al (7).

Earlier, various studies had associated autoimmunity, oxidative stress and exposure to Mycobacterium tuberculin as the cause of disease. Many of these reports strongly associate tuberculosis with Eales' disease, due to the presence of *Mycobacterium tuberculosis* gene in the surgically excised epiretinal membrane, and in the vitreous from the Eales' disease patients (8, 9). The relevance of *M. tuberculosis* in Eales' disease is debatable since the prevalence of the disease in a particular gender, age group and geographical location to the exclusion of other demographics, remains unexplained In addition, tubercular retinal perivasculitis, characterized with the presence of vitreous snowball opacities (10) and is not observed in Eales' disease. Majji *et al* reported the presence of mast cells and eosinophils (11), while Biswas *et al*

demonstrated the infiltration of T lymphocytes in the epiretinal membrane (12). HLA studies were carried to find the association of classical markers for autoimmune condition with Eales' disease. However the study revealed that there was no significant correlation between the HLA predisposition and Eales' disease (13). Inflammatory stage of Eales' disease is associated with raised levels of the inflammatory marker C-reactive protein (14). In addition, elevated levels of pro-inflammatory cytokines such as TNF-α, IL-6, IFN-γ, and IL-1β were also reported in serum (15-17). $CD16^+$ monocytes, a non-classical inflammatory monocytes subset was found to be elevated in the Eales' disease, that secretes TNF-α in the blood (18). They are possible regulators pro-inflammatory cytokines secretion during inflammatory process in the retina (19). The serum protein profile changes like increased in α_2 globulin and α_1 acid glycoprotein were reported (20). A unique protein present in the vitreous, ERM and serum of Eales' disease patients was identified. Previous characterization by our research group revealed that it has iron binding capacity and antioxidant nature and termed as 88 kDa protein. It was considered to be a potential biomarker and probably involved in its etiopathogenesis of Eales' disease. The 88 kDa, protein was purified using HPLC, was characterized to be a glycoprotein, patients The 3 internal and N- terminal peptide residues of 88 kDa protein were identified in the sequencing by Edman automated sequencer. N terminal and internal sequences of the purified sample were searched using BLAST against Human proteins database which could not identify any matches with significance. On characterization, it shared common properties with haptoglobin such as electrophoretic mobility at α2 globulin region, positive acute phase protein and hemoglobin binding. It also agglutinated of red blood cells (RBC). It has anti TBARS activity and 8 % thiols by mass. Since oxidized ferrous ion to ferric ion and it is considered as ferro oxidase (21, 22). Further investigations are required to understand the role of the protein in the etiopathogenesis of Eales' disease. The past and the present studies on Eales' disease are not conclusive about its etiopathogenesis and it remains unknown till date. The diagnosis of Eales' disease is made clinically by omitting various systemic and ocular diseases mimicking in the inflammatory and proliferative phases of the diseases (23). Direct study at proteome levels present a clear depiction of changes occur in pathological changes (24). Various post

translational protein modifications are associated with of ocular diseases such as glaucoma, macular degeneration and cataracts (25). Extensive varieties of proteomics techniques are available to identify proteins and their post translational modifications pertaining ocular environment in diseases (25). Since etiology of Eales disease is unknown till date, a proteomics based study is proposed on to decipher the etiopathogenesis.

Proteomics of Eales' disease is very demanding due to limited availability of ocular tissues and fluids for the analysis. Since clinical management is mainly achieved through the administration of oral corticosteroids and vitrectomy, is performed, only in the cases of recurrent vitreous hemorrhage. This causes a major limitation, in obtaining samples like vitreous and epiretinal membrane, which are from the actual site of the disease. In addition, to the above constraints, no animal model is yet available for studying the disease prognosis. In the attempt of understanding, the mechanism of the disease despite the limitations, this devised study was devised by using blood samples obtained from patients who were diagnosed to have Eales' disease, by an ophthalmologist. The present study describes the serum proteomics approach based on mass spectrometric identification. Eales' disease samples were resolved using native PAGE and 2-dimensional gel electrophoresis to identify the differentially expressed proteins and further to study their effects in endothelial cells by isolating proteins either by purifying or cloning to understand the disease etiopathogenesis.

2. AIM

To evaluate the proteomic biomarkers in Eales' disease, characterize and clone the identified protein biomarker.

Objectives

To evaluate the proteomic biomarkers in Eales' disease:

1. To identify the differentially expressed proteins in serum samples of Eales' disease patients by 2D electrophoresis (2DGE) and Native PAGE.

2. Analyzing the differentially expressed spots by mass spectrometry.

3. To correlate identified protein with the disease stage.

4. To clone the cDNA of identified protein in the mammalian expression vector

5. To transform in the cloned cDNA in the cells and to overexpress and purify the protein.

6. To study the effect of purified protein on angiogenesis in cultured endothelial cells.

7. To study the effect of purified protein in inflammation.

8. To study the role of purified protein in association with iron and copper metabolism

9. To study the role of purified protein in modulation of signaling proteins such as MAPK and NFκB in cultured human retinal pigment cells and endothelial cells.

3. REVIEW OF LITERATURE

British ophthalmologist, Henry Eales in 1880 and 1882, described the series of the clinical picture with recurrent retinal hemorrhages in young adults. Men in ages between 14 to 29 years were affected. All of them had history of epistaxis, dyspepsia, headache, chronic constipation and variation in peripheral circulation. Eales assumed it to be vasomotor necrosis wherein constriction of the alimentary vessels and compensatory dilatation lead to rupture of retinal vessels with subsequent hemorrhage (1, 2). On the other hand, retinal vasculitis (RV) was unexplained by Eales. Involvement of retinal inflammation was explained by Wardsworth (1887) (26). In the next century, Henry Eales has been honored with eponymous for the describing ocular disease of idiopathic pathogenesis and with recurrent vitreous hemorrhage (VH) in young adult males. In 1948 Elliot, recommended that the disease should be called as "periphlebitis retinae" (27). However, equal prevalence of vascular and arteriolar inflammation was later documented by Kimura et al., in the year 1956 and since then Eales' disease was entitled as one of the RV condition (28).

3.1 Clinical Manifestations of the Eales' disease

Most of patients with Eales' disease appear to be asymptomatic in the initial stages of retinal periphlebitis. Some patients present with symptoms such as floaters, blurring of vision or reduction of visual acuity due to substantial VH. Visual acuity of these patients can be limited to perceive hand movements or only light. Bilateral involvement is often seen in patients with Eales' disease. Clinical manifestation of Eales' disease is due to three pathological changes: inflammation, ischemia and NV in the retina or disk, which results in vitreous hemorrhage. During the course of disease, various symptoms of inflammation occur with disparity, although these become less common in later stages. The extent of the vascular sheathing varies. Fundus images of normal eye are shown in Figure 1A and in Figure 1B. In some cases it is simply a thin white line on the both the sides, limiting the vessels and in other cases as the heavy exudates sheathing (Figure 1C). Fundus examination in the early stage of the disease, dilatation and discontinuity of peripheral veins along with perivascular exudates were observed (Figure 1D). In majority of the patients with Eales' disease, retinal non-

perfusion is seen in varying degrees. In the region of hypoxia retinal haemorrhage, there is a subsequent increase in the vascular tortuosity; more persistent collateral formation is seen around the occluded vessels. The vascular abnormalities at these junctions, amid of the peripheral and non-peripheral zones include microaneursyms, Veno-venous shunts, venous beading and occasional hard exudates and cotton - wool spots. NV is usually seen in the retina.

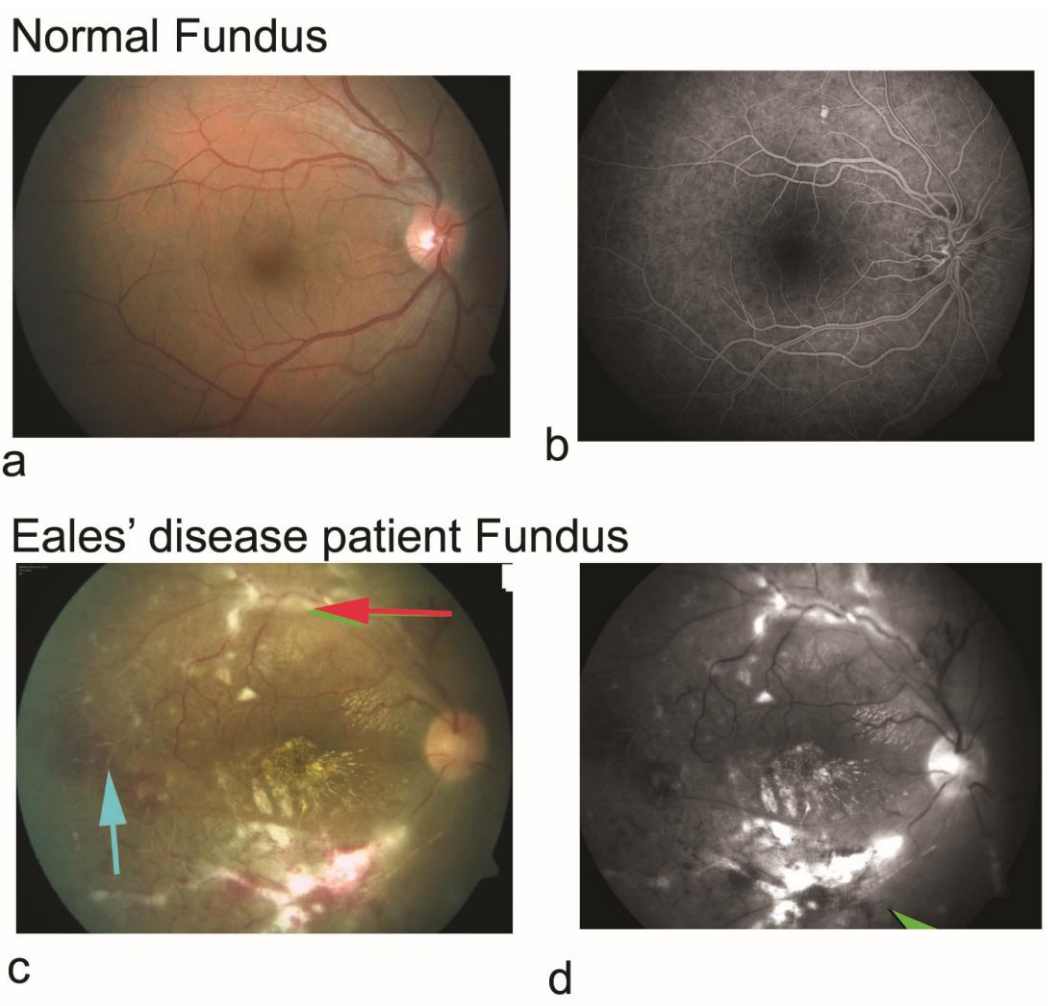

Figure 1: Fundus images
A) Normal fundus image. B) Corresponding fluorescein angiography image of normal fundus. C) Characteristic pattern in Eales' disease and the image illustrates the heavy exudates vascular sheathing by red arrow and thin sheathing by blue arrow. D) Corresponding fluorescein angiography with venous dilatation in the periphery with discontinuity of veins and perivascular exudates is seen along the peripheral veins and marked with green arrow. Images are obtained from Uveitis department, Sankara Nethralaya eye hospital, Chennai

The natural course of Eales' disease is quite variable. Active inflammation is characterized by perivascular clustering and the inflammation of vein with varying degrees of venous insufficiency. Typically an active periphlebitis stage result into ischemic stage followed by NV of the retina and subsequent vitreous hemorrhage. Charmis, (1965) has classified Eales' disease into four stages as given below (Table 1) (28).

Stages	Description
Stage 1	Mild periphlebitis of peripheral retinal capillaries, arteries and veins.
Stage 2	Perivasculitis of the venous capillary widespread and larger veins being affected with vitreous haze.
Stage 3	Neo vessel formation with abundant hemorrhage in the retina and vitreous.
Stage 4	The advanced stage is characterized by massive and recurrent vitreous hemorrhage with retinitis proliferans and tractional retinal detachment (RD)

Table 1. Four stage grading of Eales' disease by Charmis.

Das and Namperumalswamy, (1987) have proposed a different system of grading for Eales' disease, based on the degree and extent of microangiopathy, proliferative retinopathy and VH (29). However, the four-stage classification and the above-described classification are not popular due to the overlapping stages in the clinical manifestation (Table 2).

Stages	Description
Stage 1a	Periphlebitis of small caliber vessels with superficial retinal hemorrhages.
Stage 1a	Periphlebitis of large caliber vessels with superficial retinal hemorrhages.
Stage 2a	Denotes capillary nonperfusion
Stage 2b	Neovascularization elsewhere /of the disc
Stage 3a	Fibrovascular proliferation.
Stage 3b	Vitreous hemorrhage.
Stage 4a	Tractional / combined rhegmatogenous retinal detachment.
Stage 4b	Rubeosis iridis, neovascular glaucoma, complicated cataract and optic atrophy.

Table 2. New grading of Eales' disease stages by Saxena and Kumar (30).

Saxena and Kumar recommended a new grading system derived from visual outcomes in Eales' disease. This system characterized the visual outcomes depending upon the severity of the Eales' disease (30). Till date, no hallmark for grading has been accepted and practiced. In spite of extensive intraocular inflammation and long-standing VH, the lens remains clear. To the clinician, disease can be presented in various stages and hence several modalities of treatment are suggested based on the clinical symptoms. While the etiopathogenesis of Eales' disease remains unclear from the first ever report, various efforts have been taken to identify the etiology, by understanding the:

1. Systemic diseases associated with Eales' disease.
2. Immunological status of patients with Eales' disease.
3. Biochemical abnormalities in Eales' disease.
4. Histopathological characteristics in Eales' disease.

3.2 Systemic diseases associated with Eales' disease

After the first description of Eales' disease (Henry Eales, 1880), several diseases have been associated with disease (5). Although a number of systemic conditions have been reported to be associated with Eales' disease, no study has proved it in large series. The majority of these associations are considered as only occasional. Association of tuberculosis with Eales' disease can be justified and explained below.

3.3 Association with tuberculosis:

Several investigators reported the association of tuberculosis by demonstrating in clinical samples obtained from Eales' disease patients. Gilbert in 1935, reported tubercle bacilli in Eales' disease (31). However, the injection of tubercle bacilli into the homolateral carotid artery of experimental animals had produced periphlebitis in only one of 46 animals (32). It was reported that 1.3 % of patients had ocular manifestations of tuberculosis in a clinical research conducted with 700 patients in a tuberculosis institute (33). However in another study, there were no case of the Eales' disease was reported in the 1,005 patients with tuberculosis (34). Around 41.7 % vitreous samples obtained from the Eales disease patients, the DNA of

mycobacterium tuberculosis (*M.tb*) complex was identified positively by polymerase chain reaction (PCR) (35).

It was reported in two independent studies that around 50 % and 70 % of epiretinal membrane (ERM) samples obtained from Eales disease patients were tested positive with PCR for the presence of Mycobacterium species (8, 35, 36). In a study confirmed that in more than 50 % of vitreous humor samples obtained from the patients with Eales disease, had the presence of *M.tb* genome along with a significant bacillary load. But there were no viable mycobacterium tuberculosis organisms were identified in the bacterial culture of these samples (9).

3.4 Hypersensitivity to tuberculoprotein

The association hypersensitivity to tuberculoprotein is the most favored etiology by many researchers. After exposure to tuberculosis, tuberculin hypersensitivity develops and gives positive Montoux reaction (37, 38). Ashton hypothesized that, the retina of patients with Eales' disease is more particularly primed against the tuberculoprotein (39). It was speculated that Eales' disease patients may carry nonviable organism or DNA of mycobacterium tuberculosis in a significant number of cases. Possible consequence of this antigen re-exposure could be the allergic vasculitis in the retina. Since 70 % of healthy adults in India are Montoux positive which can be attributed to the BCG vaccination, other reliable indicators are needed to be used for the assessment. Other question like the disease occurs in certain geographic areas and predominantly affecting men age groups. The association has been debated since prevalence disease, in the particular gender, age and a geographical location remains unexplained. In addition tubercular retinal perivasculitis, characterized by the presence of vitreous snowball opacities (40) and this is not seen in the Eales' disease patients. The involvement of mycobacterium tuberculosis in the etiopathogenesis of Eales' disease is not clearly understood till date.

3.5 Immune-mediated mechanism - Histopathological studies

Some of the studies had considered involvement of possible immunological mechanism in Eales' disease. Evaluation of ERM from patients with Eales' disease revealed massive infiltration of chronic inflammatory cells. Immuno typing of these cells revealed that they were T cells and monocytes (activated macrophages). The absence of polymorphonuclear cells indicates that the inflammatory tissue damage is chronic in nature. In addition to the above formation of neovascular channels were also observed (41, 42). These findings suggest that leukocytes play an important role in the development of RV in Eales' disease.

3.6 Biochemical studies in Eales' disease

In serum samples of Eales' disease patients, increased α-globulins and decreased albumin levels, and 23 kDa protein were reported (43). Other studies identified raised levels of vascular endothelial growth factor (VEGF), epidermal growth factor (EGF), transforming growth factors (TGF-α and TGF-β), platelet-derived growth factor (PDGF), insulin-like growth factor I (IGF-I) (44).

3.7 Immunological Studies

Elevated levels of serum IgG and IgA in patients with Eales' disease was reported (45). Muthukarupan et al. (1989) found normal T lymphocyte subsets and the optimal antibody response to retinal S antigen (46). Biswas et al., (1998) have found higher phenotypic frequencies of human leukocyte antigen (HLA) B51, DR 1 and DR 4 to be associated with Eales' disease (47).

3.8 Inflammation in Eales' disease

Eales' disease is an ocular inflammatory disease, and various markers of inflammation were reported in the ocular and systemic environment. In the inflammatory stage of the Eales' disease is associated with raised levels of the inflammatory marker C-reactive protein and circulating interleukin (IL-6) (14, 48). In addition, non-classical inflammatory subsets of monocytes expressing $CD16^{+}$ were found to be increased in Eales' disease. These subsets of cells are one of the key regulators in proinflammatory cytokines secretion (49). It was also positively correlated with the serum levels of

proinflammatory cytokines such as IL-6, TNF-α, IFN-γ, and IL-1β (19). Murugeswari et al reported raised levels of IL-6, IL-8, MCP-1 and TNF-α cytokines were found to be elevated in both in ocular (vitreous) and systemic circulation (serum) of patients with Eales' disease (44).

3.9 Role of Iron and copper in Eales' disease:

Iron and copper are vital micronutrients. For the synthesis of a variety of enzymes and other proteins that are involved in respiration, redox reactions and other metabolic pathways. Yet these two metals are potentially dangerous by their ability to participate in one-electron transfer reactions. This enables them to be powerful catalysts of autoxidation reactions. For instance, conversion of H_2O_2 to $OH^{\bullet-}$ and decomposition of lipid peroxides to reactive peroxyl and alkoxyl radical. It is not only free metal ions that are catalytic. Heme and certain heme proteins can decompose lipid peroxides and interact with H_2O_2 to cause extensive structural and functional damage to the biomolecules. Therefore, it is necessary to regulate the metabolism of these metal ions carefully, which are vital for physiological functions, but becomes toxic when critical limit are exceeded. Moreover, iron is a potent producer of most reactive hydroxyl radicals and can be the reason, for the considerable oxidative stress (50).

3.10 Oxidative stress and antioxidant defense in Eales' disease:

Oxidative stress and inflammation have been shown to be co-dependent. Since, inflammation is an important clinical picture of Eales' disease, various studies about role oxidative stress is presented here.

A variety of oxidative stress bio-markers were assayed in serum, plasma, monocytes, epiretinal membrane and vitreous of patients with Eales' disease. Oxidative stress, hydroxyl radicals and decreased antioxidants levels were reported in vitreous, serum and monocytes obtained from Eales' disease patients (51-53). Bhooma et al., (1997) investigated the levels of antioxidant vitamins and levels of thiobarbituric acid reactive substances (TBARS) in erythrocytes of patients with Eales' disease (54). They found the reduced levels of vitamin A, E and C and elevated TBARS in

erythrocytes of patients with Eales' disease, when compared with control subjects. Subsequently Sulochana et al., (1999) had reported diminished activity of glutathione peroxidase (GPx), superoxide dismutase (SOD), and increased accumulation of TBRAS in vitreous of patients with Eales' disease (55).

In addition, nitrostative stress was also demonstrated in Eales' disease. In similar to reactive oxygen species, reactive nitrogen species damages DNA, lipids and proteins and act as an oxidizing agent as well as nitrating agent. Peroxynitrite ($ONOO^-$) is generated from the rapid reaction involving NO and $O_2^{\bullet-}$, can result in oxidation, nitration (addition of NO_2) or nitrosation (addition of NO). NO can be formed from by three nitric oxide synthase (NOS) isoforms present in tissues: neuronal NOS (nNOS), endothelial NOS (eNOS), and inducible NOS (iNOS). For production of NO, iron, O_2, and reducing equivalents, are required. NO has a high - affinity binding to heme and non-heme iron (56). TBARS levels were also reported to be higher along with increased iNOS protein expression and the 3 nitrotyrosine (NTYR) in the Eales' disease monocytes (57). NTYR is a stable product of tyrosine nitration, biomarker of protein damage induced by peroxynitrite and other reactive nitrogen species (56). NO is produced constitutively in nano molar levels by eNOS and nNOS isoforms in the cells. INOS expression in monocytes and macrophages is stimulated by inflammation and produces NO in micro molar amounts. After activation NO can overwhelm Cu, Zn-SOD reaction and produce ONOO. Peroxynitrite inactivates MnSOD by nitration of the critical tyrosine-34 residue (56).

3.11 Involvement of Iron in pathogenesis of the Eales disease.

Iron is, involved in various ocular diseases, like age related macular degeneration (ARMD), cataract, glaucoma and conditions which results in intraocular haemorrhage (59). Notable changes in iron homeostasis were observed in patients with Eales' disease viz., increased ferric (Fe^{3+}) to ferrous (Fe^{2+}) ion ratio in the serum and elevated iron levels in vitreous and monocytes, of patients with Eales' disease (53, 57 60). Fe^{3+} and $OH^{\bullet-}$ are formed when Fe^{2+} reacts with H_2O_2.The increased levels OH free radicals were reported in the monocytes from Eales' disease patients by using electron spin resonance spectrometry (52). $OH^{\bullet-}$ is a rapidly reacting molecule and a very strong oxidizing agent. Its' movement is diffusion limited and it is able to react

with all components of DNA bases as well as the deoxyribose backbone. DNA damage marker, 8-OHdG was found to be elevated using Gas chromatography-Mass spectrometry technique in the leucocytes patients with Eales' disease (57). Treatment with iron chelator desferrioxamine, caused abrogation of $OH^{\bullet -}$ radical production, reduction in TBARS level, and increased SOD activity in monocytes from Eales' disease patients (53, 56). The increased level of advanced glycation end product - carboxy methyl lysine despite normoglycemic status of the Eales' disease patients, confirms the involvement of iron induced glycoxidation in Eales' disease (53).

Desferrioxamine acts as a powerful iron chelator, inhibits the Fenton reaction and prevent the formation $OH^{\bullet -}$. In oxidative stress or in induced inflammation, desferrioxamine treatment had ameliorated the complications of oxidative stress and mitigated the severity of inflammation. From the above results it can be inferred the $OH^{\bullet -}$ radical formed during an iron catalyzed reaction caused 8-OHdG and TBARS. Restoration of SOD activity after, vitamin supplement, desferrioxamine treatment suggests the exhaustion of antioxidants due to overproduction of free radicals.

The novel 88 kDa protein have iron binding capacity and antioxidant role (22)**.** The proteins which are involved in the regulation of iron metabolism are transferrin, haptoglobin (Hp) and Haemopexion (Hpx). Dietary iron imported by the Divalent metal transporter-1, present in the apical side of absorptive cells, reduces Fe^{3+} to form Fe^{2+} with duodenal cytochrome B. The iron thus, imported is either stored as ferritin (a cytosolic iron-storage molecule) or secreted into plasma by ferroportin (basolateral iron exporter) (61). The plasma enzymes ceruloplasmin and hephaestin reconvert Fe^{2+} to Fe^{3+} that bind to transferrin, and transferred to the heme group. In case of iron overload; hepcidin, a regulatory protein of iron absorption, triggers the degradation of ferroportin, thereby, preventing release of excess iron into the circulation. The hepcidin, a key regulator of iron homeostasis is also induced by inflammation. In addition to the oxidative stress, nitrostative stress was also demonstrated in Eales' disease. The presence of excess iron and copper in monocytes along with $OH^{\bullet -}$ radical, it is expected to damage biomolecules.

3.12 Role of Copper in Eales' disease:

Copper ions are potent catalysts of free radical damage. They are involved in converting H_2O_2 to $OH^{\bullet-}$, breaking lipid peroxides, catalyze autoxidation reactions (especially of ascorbate) and are extremely effectual in causing oxidative damage to DNA and thereby stimulating peroxidation of low density lipoproteins (62). Elevated levels of copper and ceruloplasmin in Eales' disease were reported (53 ,60). Like iron, copper must be handled carefully. The molecular weight of ceruloplasmin is 132 kDa. Ceruloplasmin is secreted into circulation to be excreted into bile. Ceruloplasmin is mostly synthesized in liver, lungs and brain. Ceruloplasmin has been shown to possess the ferroxidase activity and it oxidizes Fe^{2+} to Fe^{3+} and thus facilitates iron loading on to transferrin. Thus ceruloplasmin acts an antioxidant by mitigating the generation of radical production by sequestering copper ions and through its ferroxidase activity, it also aids in regulation of iron levels.

3.13 Copper transporting proteins:

Copper transporter 1 (CTR1) is involved in transporting Cu (I) across the plasma membrane, and taken up by intracellular copper chaperones for like Copper chaperone for superoxide dismutase (CCS), Antioxidant Protein 1 (ATOX1) and Cytochrome c oxidase copper chaperone (COX 17). These chaperones delivers copper to superoxide dismutase (SOD), glutathione (GSH) and Metallothionein (MT) (63). Export of copper occurs through ATP7A and ATP7B to regulate homeostasis (64, 65).

CTR1 is a member of a family of proteins that provide Cu to the copper chaperone to specific intracellular proteins like Cu, Zn superoxide dismutase or compartments such as the secretory machinery or mitochondria. Two CTR1 dependent Cu transports are possible: the first – direct Cu transport mediated by CTR1 across the plasma membrane, and the second via endocytosis of the Cu-CTR1 complex. The second mechanism is thought to be meant for Cu storage or supply of Cu to specific metabolic processes in intracellular organelles. During Cu deficiency, excess of CTR1 present in physiological conditions for Cu uptake and during excess degradation of CTR1 protein occurs leading to feedback inhibition, thus maintaining Cu homeostasis (Petris et al. 2003) (66). Mouse embryonic fibroblasts lacking CTR1 showed Cu

accumulation indicating its important role in physiological processes and embryo development (Liang et al. 2009) (67). Another low affinity Cu transporter CTR2 is present in the cell. Blair et al showed mouse embryonic cells with CTR2 knockdown showed increased uptake of Cu due to presence of CTR1 but also induced uptake of cisplatin an anticancer drug which is transported through CTR1. Thus CTR2 knockdown helps in increased sensitivity to platinum drugs (Blair et al. 2009) (68). Cu modulates angiogenesis by causing changes in the growth factors and extracellular matrix. In various types of tumors, raised levels Cu was observed. Their levels were positively correlated with progression of the disease. Goodman et al recommended that Cu deficiency could be a possible therapeutic strategy for cancer treatment. Increased Cu levels were reported in ocular diseases with neovascularization such as Eales' disease, PDR in CTR1 silencing suppressed angiogenesis not only *in vitro* but also *in vivo* experiments (53, 69). All these findings suggest that hypersensitivity to tuberculosis, inflammation, iron and copper and oxidative stress plays pivotal role in the pathogenesis of disease.

To understand the relevance of iron and copper homeostasis in pathophysiology of Eales' disease, proteins involved in their metabolism have to be studied.

3.14 Proteomic approach for potential biomarker discovery

Mass spectrometry based proteomics is a powerful tool identification of proteins and instrument to decipher biological processes. MS based proteomics, is a powerful approach for discovery of proteins, which is widely applied in the understanding the diseases of unknown etiology such as juvenile idiopathic arthritis, type-1 diabetes and Behcet’s disease. Only a few studies have reported the about systemic proteome of changes in Eales' disease. Since the disease is diagnosed by excluding other mimicking diseases sickle cell retinopathy, syphilis rheumatoid arthritis, tuberculosis and sarcoidosis with several investigations, the identification of the differentially expressed proteins in Eales' disease will be useful to identify the biomarkers which will be preventive or protective and to decipher disease pathogenesis. For profiling proteins and two strategies are available, namely viz, top-down proteomics approach for the analysis of whole proteins, whereas bottom-up approach is to study peptides in proteolytic digests.

3.15 Top-down proteomics approach:

The two-dimensional gel electrophoresis (2DGE) is the well-recognized top-down approach for the profiling of protein. It presents variations in the protein expression and covalent modification depending upon the variations in staining intensity and electrophoretic mobility respectively. For the identification of proteins mass spectrometry is used. Proteins of interest were extracted by in-gel digestion by identification differentially expressed spots in the gel, which are excised and made into smaller pieces, and then peptides are extracted, and then analyzed by mass spectrometry. Based on peptide mass and fragmentation information, computer algorithms can identify proteins by comparing with protein databases. On the other hand, there are a few limitations for 2DGE. Mainly detection sensitivity; technique favored to detect highly abundant proteins commonly below 120 kDa and protein solubility; difficulty in resolving basic proteins and integral membrane proteins. Till date, laboratories have screened only below 10 % of the plausible size of a proteome in mammalian cells by 2DGE which is not more than some hundred proteins (70).

3.16 Bottom up / shotgun proteomics approach:

A protein profiling strategy, multidimensional LC/MS/MS, engages proteolytic digestion of solution containing mixture of proteins, and then separation of peptides by chromatography prior to the sequencing by MS/MS. Frequently, before digestion, separation of proteins and enrichment of particular proteins are carried out, such as protein chromatography or organelle purification. A modified approach in which proteins are resolved by polyacrylamide gel electrophoresis (SDS/ non-denaturing PAGE), and bands of interest are excised and subjected to in-gel proteolytic digestion of proteins prior to analysis by LC/MS/MS.

Due to superior software used in the current mass spectrometers, sequencing of peptides can be made by the data-dependent acquisition. In these acquisitions, all the ions are automatically chosen and fragmented by MS/MS, and hence very large number of spectra can be obtained in a single reversed phase analysis (70).

3.17 Introduction to Mass Spectrometry

Mass Spectrometry is a powerful analytical technique. It is used for the identification and quantification of compounds in a sample, and thus the structural and chemical properties of those molecules could be deciphered. Mass spectrometer (MS) has popular choice of all the proteomic approaches available so far. Mass spectrometry identifies the molecular mass of a charged particle based on its mass-to-charge (*m/z*) ratio and plot of ion abundance versus *m/z is* called mass spectrum. The primary step is the production of gas phase ions. It is achieved with electron ionization, in analysis of various compounds by mass spectrometry. This molecular ion splits into fragments and each primary product ion derivative also undergoes fragmentation, and so on. All these ions are sorted in the mass spectrometer depending upon their mass-to-charge ratio, and are identified in ratio to their abundance.

3.17.1 Electrospray Ionization

The Electrospray Ionization **(**ESI**)** is a soft ionization technique. It is widely employed in the making of gas phase ions without causing any fragmentation to thermo-labile larger bio-molecules. Advantage of this method is that it is non-destructive so it is well suited for small proteins and peptides. At atmospheric pressure, ESI generates ions by spraying a fine mist of ions (electrically created) into the inlet of a mass spectrometer. Small droplets of liquid are formed due to the potential difference set between the capillary (in which liquid flows) and the inlet of the mass spectrometer. These droplets enters into a heating device which evaporates solvent or a device which can induce fragmentation of the droplets into more and more smaller sizes until they reached the Rayleigh limit (Point at which the charge repulsion exceeds the surface tension), ions are desorbed and forms bare ions, then send out into the ion optics of the mass spectrometer. ESI converts solution-phase molecules into gas-phase ions and, multiply charged ions are produced (71).

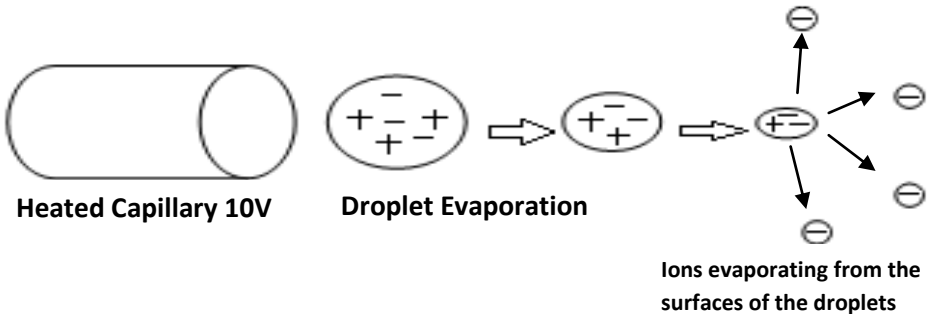

Figure 2: Schematic representation of Electron spray Ionization (ESI)

3.17.2 Matrix-assisted laser desorption ionization

MALDI-Tof-MS is a versatile method. It employed to analyze various ranges of macromolecules present in cells to tissues. It is a method used for the identification of biomolecules such as peptides, proteins, oligosaccharides and oligonucleotides. Factors such as high accuracy, sensitivity, ability to desorb high-molecular-weight thermo labile molecules, wide mass range (1–300 kDa), makes MALDI-Tof-MS as a potential method for identification. MALDI is a more practical and consistent method to in which pulsed-laser is used to produce ions in. This forms ions in packets and mass spectrometer can either measure a complete mass spectrum without scanning a mass range. Lasers induce rapid thermal heating of matrix, in turn, causes molecules to desorb molecules and ions into the gas phase. Both methods, however, show promise for the discovery of biomarkers (72).

3.17.3 Time-of-Flight (TOF)

TOF analyzer measures time taken by an ion to travel a specific distance after being accelerated with a high potential. Due to the mass difference of ions, velocity differs among them. To produce higher resolution than the linear systems Reflectron systems are employed. GC-TOF, ESI-TOF, MALDI-TOF and hybrid instruments are also available.

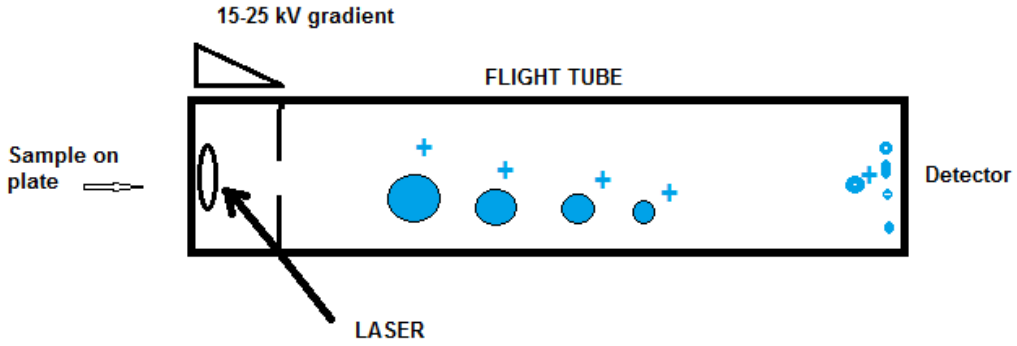

Figure 3: Schematic representation of time of flight analyzer (TOF)

3.17.4 Quadrupoles

This uses dc (direct current) voltage and rf (radio frequency). They are low resolution instruments and functions at lower voltages (<500V). Ions are produced and accumulated in the trap and gradually ejected by escalating the rf voltage. The trapped ions can be further dissociated to create a product ion spectrum within the analyzer. The most of ion traps are bench-top instruments and they are used for regular analysis.

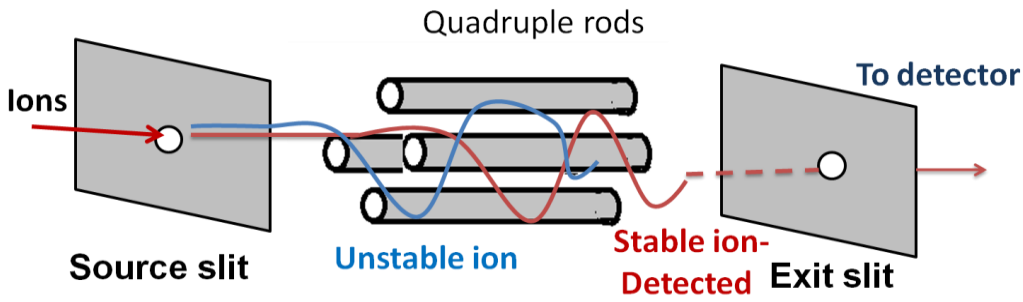

Figure 4: Schematic representation of quadrupole analyzer.

3.17.5 Types of tools to analyze MS data

Developments in mass spectrometry driven proteomics is dependent on robust bioinformatics software packages (Pheny, PEAKS, Mascot, Tandem, Sequest and Ommsa) for large-scale data analysis. Computational task is to select proteins from

the database. Two major steps are involved, in which MS/MS spectrum is used for the identification a peptide sequence from the database and identified peptides are aligned together for the identification of proteins from the database (71, 73).

3.17.6 Applications MS in proteomics

After discovery of MS, proteomics are rising rapidly in the fields of clinical and biological research. It has hugely contributed to biology, may also have greater influence in clinical diagnosis. MS-based proteomics can be used in identifying patterns of differentially expressed proteins in clinical samples such as serum. These analyses have greater potential in the diagnosis as well as classifying stage of diseases like cancers. Mass spectrometers with higher resolution, mass accuracy, dynamic range, and accurate quantification can be used in clinical diagnosis. Proteins are converted to their mature form through a sequence of post-translational protein processing. These changes are regulatory in nature and reversible conditions. Mainly protein phosphorylation and glycosylation are good examples. They control the biological function through a number of mechanisms. Mass spectrometric methods had ascertained the types and sites of modifications based on past studies in single, purified proteins. Protein post translational modifications can be determined by comparing possible mass and fragments of a protein sequence with measured details (73).

3.18 Cloning

A clone is a precise copy of an organism, organ, single cell or macromolecule (DNA). Genetically identical molecules, cell or organisms all derived from a single ancestor is called as cloning. Once a clone is produced it can be used in many areas of biomedical and industrial research.

DNA cloning / molecular cloning is the process of creating multiple copies of a specific DNA sequence after isolation and expressing it in the *in vitro* condition. Cloning is often employed to augment DNA fragments containing genes, or any DNA sequence such as non-coding sequences, promoters, randomly fragmented DNA

chemically synthesized oligonucleotides. Cloning is used in various biological experiments and in applications such as producing recombinant proteins.

Therapeutic cloning has a key role in medical treatment. It is performed by somatic cell nuclear transfer. It is largely used to cultivate organs, which can be used substitute the non-functional organ. The dividing egg is often the source of the totipotent stem cells and grown in a suitable media, depending upon organ to be harvested. Reproductive cloning is to create the exact copy of an existing organism by a technique called as somatic cell nuclear transfer. Reproductive cloning is only restricted for research purpose. It may used to repopulate endangered species, and for the production of organism / animals with specific characteristics (drug- producing / genetically unique).

3.19 *In vitro* angiogenesis assays

Pathological angiogenesis is comparatively less regulated and complex when compared with physiological angiogenesis. Many *in vitro* and *in vivo* assays are available in all these years, and selection of the most appropriate assay key to the success. Most of the *in vitro* assays are based on endothelial cell characters such cell adhesion, migration, proliferation and differentiation which are considered to be essential in the angiogenesis process. For *in vitro* angiogenesis assays HUVECs are preferred. In physiological condition most of the endothelial cells remains quiescent. In contrary in culture conditions, it exhibits pro-angiogenic properties when stimulated. In the cell proliferation assay, protein of interest can be tested whether it is proliferative or anti-proliferative in nature. Induction of cell migration by protein of interest can be studied by various methods. The scratch assay of cells is one such, in which of migration of cells towards the scratched area was studied. In the transwell migration assay or in Boyden chamber assay extent of cell migration across matrix is studied. In the tube formation assay angiogenesis assay in endothelial cells are plated in sub-confluent densities and this measures the ability of the cells to form capillary (tube) like structure in the presence of extracellular matrix support. Pro and anti angiogenic nature of proteins can be screened by this assay (74).

3.20 Research gap

Eales' disease was first described in the year of 1880 by Henry Eales and till date, no diagnostic markers are available since its etiopathogenesis remains as an enigma. Vitrectomy is only performed in cases of recurrent vitreous hemorrhage and this causes a major limitation in obtaining vitreous samples from the Eales' disease patients. In addition, to the above, no animal model is available for studying the disease prognosis. Although a number of the studies associate the disease with presence of Mycobacterium and none has further substantiated, it is suspected as the latent infection of tuberculosis. Eales disease is associated with the both ocular inflammation and tuberculin protein sensitivity. This suggests the involvement of immunologic reactions whose mechanism remains unknown. In the attempt of understanding mechanism, despite of the limitations, serum proteomics study was devised using blood samples obtained from Eales' disease patients. Identification, of differentially expressed proteins and validating their role in disease pathogenesis and identifying interacting proteins, may help in understanding the disease pathogenesis. This will help in clinical intervention, development of specific diagnostic tests, which remains as the prime importance in the management of Eales' disease.

4. SCOPE AND PLAN OF WORK

Scope

Etiopathogenesis of Eales' disease not clearly known and no biomarkers are available. This work uses proteomic approach for identifying differentially expressed proteins and validating their interactions and role. This will have great importance in understanding etiopathogenesis of the Eales' disease.

Plan of work includes the following

1. Identification the differentially expressed serum proteins- 88 kDa protein in Eales' disease by mass spectrometry.
2. ELISA validation of identified proteins
3. Protein interactions of identified proteins by Mass spectrometric analysis and western in co-immunoprecipitated samples.
4. Molecular cloning to identify protein interactions
5. Evaluation of iron and copper metabolism in Eales disease
6. Preliminary screening of purified protein in HUVECs *by vitro* angiogenic assays and screening of purified protein in ARPE-19 cells for in inflammation
7. MAPK (p38) and NFκb of signaling in purified protein treated cells.

5.0 MATERIALS AND METHODS

5.1 Fine chemicals and kits

All fine chemicals were purchased from Sigma-Aldrich (St. Louis, MO), Bio-Rad (Hercules, CA) and Merck Millipore (Mumbai, India). The Serotransferrin immunoturbidimetry kit was procured from Biosystems. Human ELISA kit for Haptoglobin (E-80HPT), Galectin-1 (DGAL10) and C3 Human ELISA kit (ab108823) were procured from Immunology Consultants Laboratory (Portland, OR) and R & D systems (Minneapolis, MN), respectively. CTR1 ELISA kit (E94493Hu , USCN, USA)

Lipopolysaccharides from *Salmonella enterica* serotype typhimurium (L6143) and purified Haptoglobin (Phenotype 2-2) human plasma ≥95% purity (SRP6508), were purchased from Sigma -Aldrich, Missouri, USA. ARPE-19, CRL-2302™, Adult retinal pigment epithelial cell line and COS-7 (ATCC® CRL-1651™) African green monkey kidney fibroblast-like cell line SV40 transformed were purchased from procured from the American Type Culture Collection (ATCC, Virginia, USA). Biotinylated Lectins SAMBUCUS NIGRA (Elderberry) bark -B-1305, PHASEOLUS VULGARIS leucoagglutinin (PHA-L) - B-1115. (Vector Labs, California, USA).

5.2 Other Chemical and reagents

Chemical / Reagent	Catalog number, Suppliers
2-mercaptoethanol	194705, MP
8-Anilino-1-naphthalenesulfonic acid	A1028, Sigma
Acetic acid	ACBA630139, Merck
Acetonitrile	34967, Fluka
Acrylamide	A3553, Sigma
Agar	014011, SRL
Agarose	50004, Lonza
Ammonium bicarbonate	A6141, Sigma
Ammonium persulphate	0148134, SRL

Chemical / Reagent	Catalog number, Suppliers
Ammonium sulfate	QD1Q610103, Merck
Ampicillin	A0166, Sigma
Bis Acrylamide	161-0201, Bio-rad
Borax	27965, Fisher scientific
Boric acid	Q12Q622480, Merck
Bovine serum albumin (BSA)	MB083, Himedia
Brilliant Blue G	B0770, Sigma
Bromopheno blue	AA1A601068, Merck
Calcium chloride	ME7M570903, Merck
Citric acid	ME8M581042,Merck
Cobaltous chloride	27790, BDH
Collagen	C3511, Sigma
Copper (II)chloride	C3279, Sigma
Copper chloride	C3279, Sigma
Diethylaminoethoanol (DEAE)	D0909, Sigma
Disodium hydrogen phosphate	QJIQ611768, Merck
Dipotassium hydrogen phosphate	MG9M591711, Merck
Dithiothreitol (DTT)	161-0611, BIORAD
Formic acid	56302, Fluka (Sigma)
Glycerol	DC4P640148, Merck
Glycine	G8790, Sigma
Guanidine hydrochloride	074843, SRL
HEPES	Sigma
Hydrochloric acid	CE4C6404448, Merck
Hydrogen peroxide	18755, Fisher scientific
Imidazole	RM 559, Himedia
Iodo acetamide (IAA)	163-2109, BIORAD
Isopropylβ-D-1-thiogalactopyranoside (IPTG)	I6758, Sigma
Kanamycin disulfate salt	K1876, Sigma

Chemical / Reagent	Catalog number, Suppliers
L-Homocysteine	H4628, Sigma
L-Homocysteine thio lactone	H6503, Sigma
Methanol	65524, SRL
Paraformaldehyde	MA0M60057,Merck
Potassium chloride	MC4M540102, Merck
Potassium dihydrogen phosphate	MH0M602423, Merck
Potassium iodide	MLM8M583734, Merck
Silver nitrate	Sigma
Sodium Dodecyl sulphate	L3771, Sigma
Sodium Azide	1687, Loba chemie
Sodium carbonate	QB4Q649519, Merck
Sodium chloride	QB4Q640044, Merck
Sodium dihydrogen phosphate	17845, Merck
Sodium hydroxide	QE2Q620871, Merck
Sodium iodide	RM706, Himedia
Sodium thiosulfate	17536, Merck
TEMED	194019, MP
Trifluro acetic acid	AJ0A600708, MERCK
Triton-X-100	10655, fisher scientific
Trizma Base	T6066, Sigma
Trypsin	TC245, cell culture grade , Himedia
Trypsin , proteomics grade	T6567, Sigma
Tween 20	SJ3S630526, MERCK
Urea	194857, MP

5.2.1 Bacterial Strains

Name	Source
M15 (pREP4)	Qiagen, USA

5.2.2 Plasmid vectors

Plasmid name	Feature	Supplier
pQE 30-Xa	T5 Promoter, double Lac operon, 6X His tag, Factor Xa recognition site & Multiple cloning site	Qiagen
P3XFLAG-Myc-CMV	CMV promter, Lac operon, c-Myc, FLAG tag, Multiple cloning site	Sigma

5.2.3 Media

Media	Catalog number, Supplier
Dulbecco's modified eagle medium (DMEM)-F12 media	D8900-1, Himedia
Endothelial Basal media (EBM)	CC-3156, Lonza
Endothelial Growth media (EGM) -2 single Quote	CC-4176, Lonza
Luria-Bertani (LB) broth	M1245, Himedia

5.2.4 Molecular weight standards

Name	Catalog number, Supplier
Broad range protein marker	0231104700A, Genei
DNA 100 – 1000 base pair	GM343, Gene technologies
DNA 500 – 10 kilo base pair	M103O-1, Gene technologies
Unstained protein MW marker	26610,Thermo scientific

5.2.5 Antibodies

Name	Catalog number, Supplier
Anti-complement C3, (rabbit,	ab117244 Abcam
Anti-haptoglobin (goat)	SC-68667, Santa Cruz biotechnology
Anti- galectin-1 (goat)	AF1152, R&D systems
Anti-IgG (mouse)	SC -2025, Santa Cruz biotechnology
Anti-IgG (rabbit)	SC -2027, Santa Cruz biotechnology
Goat anti rabbit IgG – HRP	SC-2004, Santa Cruz biotechnology
Goat anti mouse	SC-2005, Santa Cruz biotechnology
Rabbit anti goat IgG – HRP	SC-2768, Santa Cruz biotechnology

5.2.6 Kits

Name	Catalog number, Supplier
Coomassie Plus (Bradford) Assay Kit	23236, Pierce, Thermo scientific
ECL prime Western Blotting detection reagent	RPN2232, Amersham
Infusion cloning kit	638909, Takara Clontech
iScript cDNA synthesis kit	170-8891, Bio-Rad
MinElute Gel extraction kit	28604, Qiagen
Pierce Co-immuno precipitation kit	26149, Thermo Scientifics
Qiagen plasmid min kit	12123, Qiagen
Qiaprep Spin Miniprep	27104, Qiagen
Albumin depletion kit	Prot BA, Sigma
Clean up Kit	GE
Tandem affinity purification kit	1100, Sigma

5.2.7 Miscellaneous materials

Materials	Catalog number, Supplier
0.22 μm Cellulose acetate	8160, Corning
Cell culture T25 Non vented & Vented flask	430168 & 430720, Corning
Cell culture T75 Non vented & Vented flask	430639 & 430641, Corning
Microtiter plate, 96 well, clear bottom	655101, Geriner bio one
Micro titre plate, 96 well, opaque bottom	655076, Geriner bio one
PVDF	10600023, Amersham

5.2.8 Instruments

Name	Company
Agilent Series 1100 HPLC	Hewlett Packard, USA
Biologic Duo flow (Low pressure Liquid)	Bio-Rad, USA
DU 800 Spectrophotometer	Beckman Coulter,
Fluorchem FC3	Protein simple, USA
GeneAmp PCR system 9700	Applied Biosystem, USA
Spectramax M2^{e}	Molecular Devices, USA
Xevo G2-S Qtof ESI MS	Waters, USA

5.3 Selection of patients and control subjects

5.3.1 Sample information

The study had been approved by the Institute's Human Research Ethics Committee. Experiments involving human subjects were performed in strict adherence to the tenets of the Declaration of Helsinki. Written consents were obtained from all the participants. Patients diagnosed with Eales' disease by an ophthalmologist after detailed fundus examination. Active vasculitis in the Eales' disease is characterized by the presence of serous exudates in the region of the retinal veins with retinal edema. Additionally, occlusion of veins, neovascularization, and fibrovascular scar formation with or without vitreous haemorrhage were seen in all patients. Participants were

included in the study after recording personal details such as their names, identification numbers, ages, and their gender, in addition to their medical history.

Inclusion criteria: Males in ages between 15 to 45 years, with retinal periphlebitis, neovascularization and vitreous haemorrhage not associated with choroiditis, anterior uveitis, parsplanitis or any other retinal vascular diseases which mimic Eales' disease.

Exclusion criteria: Other retinal vasculitis conditions, which mimic Eales' disease, were eliminated by ordering laboratory tests. Subjects/ patients with the habit of smoking, alcohol addiction, with other systemic inflammatory diseases were also excluded. The consecutive sampling method was employed and every subject meeting the inclusion criteria selected until the study period. And the inclusion of participants is based selective which is a non-probability sampling techniques. The total numbers of 22 Eales' disease, patients were enrolled cases in the study. For controls, male healthy volunteers were included. A total number of 21 males, who were age and sex-matched healthy adults, non-smokers and non-drinkers without any history suggestive of Eales' disease or any other systemic inflammatory diseases, were recruited into the control group. They were non diabetic, non-alcoholics and free from the systemic diseases. They were not taking any kind of antioxidant supplements. All these information were obtained by performing laboratory investigations and detailed physicians checkup.

5.3.2 Blood tests

From the participants, 14 mL of blood was drawn after overnight fasting into EDTA containing tubes. Plasma were separated from blood cells by centrifugation at 3000 g at 25 ˚C for 10 min, carefully aspirated and stored at -80 ˚C up to 2 weeks for other investigations. 4 mL venous blood samples collected from subjects were allowed to clot and then centrifuged at 3000 rpm for 5 min. The serum was carefully aspirated and stored at -80 °C.

5.3.3 Separation of peripheral blood mononuclear cells

Ten mL of heparinized venous blood sample was used for separation of mononuclear cells. 5 mL of blood was carefully overlaid with 5 mL of histopaque density gradient solution (Sigma, USA) and centrifuged at 2,700 rpm for 30 min at RT. After centrifugation, the middle layer containing cells (monocytes and lymphocytes) were cautiously aspirated and rinsed thrice with 1X Phosphate buffered saline (PBS) pH 7.4. After the final wash, the pellet was carefully aspirated and re-suspended. 10 µL of the cell was used to assess the viability of the cell by trypan blue dye exclusion test. Then the cells were processed for further investigations.

5.4 Protein estimation

5.4.1 Bicinchoninic acid assay

Principle

This assay is based on the principle reduction of Cu^{2+} ion to Cu^{+} by the peptide bonds in proteins which are dependent on temperature. The amount of Cu^{2+} reduced is proportional to the quantity of protein in the sample solution. To each of Cu^{+} ion, two molecules of BCA chelates and forms a purple-colored product which absorbs light at a wavelength of 562 nm (75).

Materials

- BCA kit- Thermo Fisher Scientific, USA
- Sample

Procedure

1. 5mL of Solution A was mixed with 100 µl of solution B. 200 µl from the mixture was added to 96 well plates.
2. Standards (125 – 1000 µg / mL) and samples of 5 µl volume were added to the well. Normal saline 5 µl was added to blank well.

3. The plate was kept for incubation for 30 min at 37 °C and read in the Spectramax max m2e plate reader at 562 nm.

4. The standard curve was plotted and the protein concentrations of the test samples were calculated by extrapolating the values in the standard graph.

5.4.2 Bradford method

Brilliant Blue G-250 dye can be present in three forms such as neutral -green color, cationic red color, and anionic blue in color. This dye protonated and exists as the red cationic form with Amax of 470 nm in the acidic condition. On binding with protein, it becomes a stable unprotonated blue form with Amax of 595 nm and measured using a spectrophotometer or microplate reader.

Materials

- Bradford- Thermo Fisher Scientific, USA
- Sample
- Normal saline – 0.9 % NaCl in distilled H_2O

Procedure

1. To a 96 well plate, 10 µl of the sample, lysis buffer and standards were added and 90 µl of normal saline was added.
2. Bradford reagent 100 µl was added and kept for incubation for 10 min at RT and read at 595 nm.
3. A standard curve was plotted against known standard concentration.
4. Samples were extrapolated onto the standard curve to calculate the protein concentration.

5.4.3 Lowry Method

Principle

In this method, proteins reacts with the alkaline copper sulphate solutions to form copper-peptide bond protein complexes. When Folin-Ciocalteau reagent is added- the copper protein complexes this reduces the phosphomolybidic acid in the reagent to give blue colored complex, which is read at 660 nm (76).

Reagents

1. Sodium carbonate: 2 % solution in 0.2N NaOH
2. Copper sulphate: 0.5 % solution in 1 % sodium potassium tartrate.
3. Alkaline copper solution: 50mL of reagent 1 was mixed with 1.0mL of reagent 2.
4. Standard bovine serum albumin (BSA): 1mg/mL in dH_2O.
5. Folin- Ciocalteau reagent: One volume of Folin-Ciocalteau reagent (E-Merck, India) was diluted with one volume of water prior to use.

Procedure

To the protein sample 5.0 mL of alkaline copper sulphate solution was added and allowed to stand at room temperature (RT). Then 1.0 mL of Folin-Ciocalteau reagent was added and allowed to react for 20 min at RT. Then the absorbance was measured at 640 nm. The amount of protein in the test sample was calculated from the standard graph generated using BSA standard (50 – 250 μg). The protein content in the serum was expressed as g/dL, in case of purified protein and in cell lysates it was expressed as mg / mL.

5.5 Polyacrylamide Gel Electrophoresis (PAGE) (77)

Reagents

a) Acrylamide (30 %) was prepared by weighing 29.2 g of acrylamide and 0.8 g of N, N'bismethylene acrylamide and dissolving in 50 mL of Milli Q (MQ) water and made upto 100 mL with MQ water.

b) 1.5 M Tris-HCl -pH 8.8

c) 0.5 M Tris-HCl pH 6.8

d) 10 % ammonium persulfate in MQ water

e) N, N, N', N; - tetraethylenediamine (TEMED) – (Bio Rad, CA, USA).

f) 10 % sodium dodecyl sulfate (SDS)

g) Sample buffer: SDS-1.6 mL, Glycerol 0.8 mL, 0.5 M Tris-HCl pH 6.8 -1.0 mL, MQ water- 4.0 mL 10 % β Mercaptoethanol-0.4 mL, 0.05 % bromophenol blue -0.2 mL. For SDS PAGE, one volume of sample was mixed with 3 volumes of sample buffer, boiled in water bath for 5 min and then loaded onto the gel. Native PAGE (NPAGE) the sample buffer was prepared by omission of 10 % SDS and β mercaptoethanol.

h) Running Buffer: 25 mM (3.03 g) Tris base, 192 mM (14.40 g) glycine and 0.1% (1.0 g) SDS in l L of MQ water (pH 8.3). For NPAGE the buffer was prepared by omission of SDS.

Protocol for preparation of gel

S.No.	Reagents	Stacking gel (4 %)	Separating gel (10 %)
1.	Acrylamide 30 % (mL)	1.33	2.5
2.	TRIS HCl (mL)	2.5 (pH 6.8)	3.33 (pH 8.8)
3.	MQ H_20 (mL)	6.1	4.17
4.	10 % APS (µl)	50	50
5.	10 % SDS (µl)	100	100
6.	TEMED (µl)	5	10

Table 3. Reagents used for SDS PAGE.

i) For NPAGE, the gels were prepared by omission of SDS. Electrophoresis was performed by Bio-Rad mini Protean II system (CA, U.S.A). After electrophoresis, the gels were stained for 2 h in Coomassie brilliant blue R-250, and then destained using 40 % methanol, 10 % acetic acid and 50 % water and then stored under water.

5.5.1 Coomassie Stain:

a) Coomassie brilliant blue R 250:

Staining solution **(**0.25 %) was prepared by dissolving 250 mg Coomassie brilliant blue R 250 in methanol (40 mL) and glacial acetic acid (10 mL) final volume is made upto 100 mL with MQ water. The contents were stirred at RT for 1 h and filtered through Whatman No.1 filter paper and used for staining (78).

b) Modified Colloidal Coomassie G-250:

Staining solution was prepared by dissolving 5 % aluminum sulfate (14-18-hydrate) in MQ water, followed by the addition of reagents in the mentioned sequential order 10 % ethanol (96 %), 0.02 % Coomassie brilliant blue G-250, 2 % orthophosphoric acid (85 %). The solution finally made up to 1L with MQ water (79).

5.5. 2 Silver staining

Principle: Silver staining was done to detect proteins on NPAGE by the method described by Morrissey (80). Silver staining is based on binding of silver ions to proteins. After electrophoresis, proteins are fixed, exposed to silver nitrate and developed to form a black precipitate of silver.

Procedure

Step 2 - Silver staining:

Materials Required:

- Sodium thiosulphate -120 mg/ 100 mL of MQ H_2O.
- Stain - Silver nitrate - 250 mg/ 125 mL of MQ H_2O with 50 µl of formalin
- Developer -Sodium carbonate - 2 % of sodium carbonate with 50 µl of formalin
- Stopping solution- 5 % acetic acid

After electrophoresis, the gels were fixed using 30 % methanol and 10 % acetic acid for 30 min. The gels were then washed in Milli Q water for 30 min with an intermittent change of water. After this step the gels were treated with 10 % glutaraldehyde for 30 min and then washed thoroughly in Milli Q water for 30 min with a change of water every 10-min. This step was followed by incubation with 0.1 % silver nitrate for 30 min. Then the gels were briefly washed with water for 2-3 min and then developed using 3.0 % sodium carbonate containing 100 µl of 40 % formaldehyde. After the visualization of protein bands, the reaction was arrested by the addition of saturated citric acid solution until complete neutralization of sodium carbonate was achieved. The gels were then stored under water.

5.6 Native Preparative Gel Electrophoresis-Protein purification

Purification of 88 kDa protein from the Eales disease patient's serum:

1. Serum samples obtained from fourteen Eales' disease patients were pooled and protein was estimated. Total protein of 1.075 g protein per 14 mL of serum was subjected to 70 % ammonium sulphate precipitation. The precipitate was dialyzed with 10 mM PBS pH 7.4, for 48 h and buffer was changed regularly at every 4-6 h interval.

2. After the dialysis, the sample was centrifuged at 10,000 rpm for a period of 30 min at 4-8 ºC; the supernatant was subjected to purification by native preparative gel electrophoresis.

3. Protein estimation was by carried out using Coomassie (Bradford) Protein Assay method. Samples were run (non denaturing condition) in 7.5 % gel with 1 X running buffer preparative electrophoresis apparatus (Bio-Rad, CA, USA) and the proteins were eluted using 0.05 mM Tris glycine buffer, pH 8.3.

4. Eluted samples were collected in fresh tubes (5 mL/tubes) at a flow rate of 0.5 mL per min with continuous buffer elution system (Bio-Rad LPLC).

5. Eluted fractions were screened at 280 nm in a spectrophotometer for protein quantity (Beckman DU 800, CA, and U.S.A.).

6. These fractions resolved in native gel electrophoresis (slab) and stained by silver stain. The fractions enriched with α, β regions, 88 kDa protein bands were pooled. The pooled fractions lyophilised (VirTis 2KBTXL-75 Benchtop SLC Lyophilizer-Freeze Dryer) and stored at -80°C until further purification.

7. At each stages of the protein purification, the presence of the 88 kDa protein was confirmed with 7.5 % native PAGE. The serum obtained from patients with Eales' disease is used as positive control.

5.7 HPLC Purification

The method was adopted from Sulochana et al (2001) (81).

1. The partially purified fractions (from preparative electrophoresis) enriched with 88kDa band were from were pooled and protein content was measured by Bradford method. The samples were concentrated by lyophilisation using the VirTis freeze dryer (NY, USA).

2. The 50 mg of protein concentrate was further purified in HPLC with octadecylsilyl (ODS) reversed phase column.

3. In brief the equilibration of column was carried out 10 mM phosphate buffer with 0.1 M sodium chloride pH 7.4. Isocratically elution was carried out at the flow rate of 0.2 mL/min by the aforesaid buffer with 50 % methanol.

4. The absorbances at 280 nm of eluted fractions were monitored. They were also tested for their anti-TBARS activity and electrophoretic mobility (88 kDa).

5. Fractions positive for above mentioned tests were pooled and rechromatographed in the conditions mentioned until the protein resolved as a homogenous peak.

6. The purity of HPLC resolved protein was re-checked with native PAGE electrophoresis followed by silver staining. The purified protein was dialyzed against 10 mM PBS buffer pH 7.4, and used for further characterization studies.

5.8 Co immunoprecipitation- IP

This method was adopted from protocol published by Jain et al (82).

Principle:

Co-immunoprecipitation (Co-IP) approach is used for studying protein: protein interactions, using a specific antibody to immunoprecipitate the antigen (bait protein) and co-immunoprecipitate other proteins with the antigen (prey proteins). This method allows pull down of interacting proteins. Further, after pull down assay these proteins are subjected to dithiothreitol (DTT) treatment to reduce the disulphide bridges and alkylated with Iodoacetamide (IAA). The next step involves tryptic digestion of proteins into smaller peptides which are submitted to a mass spectrometer. The mass spectrometer identifies the peptides based on their Mass/charge (m/z) ratio.

Materials required.

- Peripheral blood mononuclear cell (PBMC) – 5 mL of heparinized blood was collected. Histopaque (Sigma) a density gradient was used to separate mononuclear cells. 5 mL of histopaque was added to 15 mL falcon tube which was carefully overlaid with 5 mL of blood. Tubes were centrifuged at 5000 rpm for 30 min and the mononuclear cells were immediately separated to a different tube and washed with PBS thrice (5min each).

- Cell lysates – Prepared in membrane protein extraction reagent (MPER, Thermo Scientific) in the presence 10 µl of protease inhibitor cocktail (1 mg/ mL)

Procedure:

Co-immunoprecipitation

1. Protein content of serum samples was estimated and 500 µg of protein from control subjects and Eales' disease patients were used.

2. Samples were precleared to remove any non-specific binding proteins, by incubating for 3 h, with A/G beads (Santa Cruz Biotechnology, USA) at 4 °C under rotary agitation.

3. After incubation, the contents were centrifuged at 2000 rpm for 2 min, 4 °C.

4. The supernatants were incubated with 1 µg of specific antibodies for 12 h at 4 °C under rotary agitation to allow the formation of antibody-antigen complex.

5. For haptoglobin immunoprecipitation, anti haptoglobin antibody, anti-IgG antibody (mouse, sc-2025) was used as negative control.

6. For complement C3 immunopreciptation, anti-complement C3 antibody (rabbit, ab181147) was used and IgG antibody (rabbit, sc-2027) was used as negative control.

7. The antigen antibody complex, were incubated for 2 h, at 4 °C with A/G beads under rotary agitation

8. After incubation, the tubes were centrifuged, and the supernatant was decanted. Beads were boiled at 95 °C for 2 min with 0.2 % RapiGest (Waters Corporation) in Tris pH 8.5, for 5 min to elute of protein bound to the A/G beads.

9. The supernatant of the solution obtained from centrifugation was made into two aliquots. One of them was subjected to in-solution digestion by trypsin as described and with an extra step of adding 200 mM HCl before sample extraction and analyzed by mass spectrometry.

10. Simultaneously the other aliquot of supernatant was boiled with 2X Lamelli buffer at 95 °C and resolved in 10 % SDS- PAGE and subjected to western blot.

11. Silver stained gel protein bands were excised into smaller pieces and subjected to tryptic digestion for mass spectroscopy to identify the interacting partners.

5.9 DNA extraction from PBMC and Serum samples.

From PBMC samples ED patients and control subjects, DNA was extracted by using a NucleoSpin Tissue extraction kit 740952.50 (Germany) by following manufacturers guidelines.

- Lysis Buffer T1
- Lysis Buffer B3
- Wash Buffer BW
- Wash Buffer B5
- Elution Buffer BE
- Proteinase K
- Proteinase Buffer PB
- NucleoSpin® Tissue Columns
- Collection Tubes (2 mL)

Procedure

1. For the pre-lysis, buffer T1 (180 µL) and proteinase K solution (25 µL) was added to the sample and vortex mixed.
2. The mixture was incubated at 56 °C at least 1–3 h with occasional vortexing.
3. Buffer B3 (200 µL) was incubated at 70 °C for 10 min after vigorously mixed. The mixture was centrifuged for 5 min at high speed 11,000 x g and to remove particulates. The supernatant was transferred to a microcentrifuge tube
4. DNA binding condition of the column was adjusted by adding 210 µL of 96–100 % pure ethanol to the sample and vigorously vortexed. Sample was then applied to the column and centrifuged for 1 min at 11,000 x g. Flow-through was discarded and the centrifugation step may be repeated if the sample was not completely drawn through the matrix.

5. Washing the silica membrane: In the first wash, the membrane was washed with Buffer BW (500 µL) by centrifuging columns for 1 min at 11,000 x g and flow-through was discarded. In the second wash buffer B5 (600 µL) was added to the column and centrifuged for 1 min at 11,000 x g. Flow-through was discarded and residual ethanol was removed by centrifuging at 11,000 x g, 1 min.

6. Highly pure DNA was eluted in a fresh 1.5 mL tube after addition 100 µL of prewarmed buffed BE (70 °C) and followed by 1 min incubation at RT and centrifuged 1 min at 11,000 x g.

5.10 Tryptic Digestion

This method was adopted from protocols published by Shevchenko (83) and Kinter (84).

Materials required:

- Destain for silver stained gels: 100 mM Sodium thiosulfate and 30 mM Potassium ferricyanide prepared in deionized water.
- Ammonium bicarbonate buffer (NH_4HCO_3) (100 mM) - 7.90 mg / mL in MQ water.
- DTT 100 mM - 1.5 mg /100 µl of 0.1 M NH_4HCO_3
- Iodoacetamide IAA 200 mM - 37 mg /100 µl in 0.1 M NH_4HCO_3

5.10.1 In-gel tryptic digestion

1. Gel bands were cut into smaller cubes, and then placed into a 1.5 mL tube. Gels were washed with MQ water for 5 times.

2. The gel pieces were incubated with a destaining solution (100 mM Sodium thiosulfate and 30 mM Potassium ferricyanide)

3. The gel pieces were washed with MQ water until they become clear.

4. Depending on the volume of gel pieces, 100-500 µL cetonitrile was added to and then incubated for 15 min at RT.

5. The supernatant was decanted and 100mM of NH_4HCO_3 was added and incubated at RT for 5 min.

6. Step 3-4 is repeated for 3 times.

7. The supernatant was decanted and gel pieces were completely dried in the vacuum concentrator (Speed Vac, Thermo Scientific) for 15 min. Then 150 µL of 10 mM DTT was added and incubated for 45 min at 56°C.

8. The supernatant was decanted and 150 µL of IAA was added, incubated in the dark for 30 min at RT, and then steps 4-5 were repeated for once.

9. Trypsin (12.5 ng/ µL) was added to the gel incubated on ice for 30 min. The excess solution was removed; 100 mM NH_4HCO_3 was added to cover up gel pieces and incubated at 37 °C for 16 h.

10. The supernatant was collected after centrifugation at 14000 rpm for 1 min. For extracting peptides, 50 µL of 0.1 % formic acid in 50 % acetonitrile was added to the gel pieces and was incubated for 15 min at RT. This step was repeated thrice to extract the peptides from the gel. The extracts were pooled, and dried in a vacuum concentrator (Speed Vac, Thermo Scientific).

11. The dried peptides were reconstituted in 2 % acetonitrile and 0.1 % formic acid (40µL) in MQ water and centrifuged at 14,000 rpm for 10 min, and filtered through a 0.2 µ spin column filter, and the filtrate were transferred to mass spec vials.

5.10.2 In solution tryptic digestion

1. The protein concentration of 1 µg in 50 µl of 100 mM NH_4HCO_3 was used for digestion.

2. Proteins were then reduced with 100 mM DTT at 56 ºC for 20 min

3. This was followed by alkylation with 200 mM iodoacetamide and 100 mM of NH_4HCO_3 in the dark at 37 ºC for 30 min.

4. The samples were digested with 1:50 (w/w) gold grade trypsin for 16 h at 37 ºC.

5. To arrest trypsin action, 2 µL of formic acid was added and incubated at 37 °C for 20 min.

6. Vortexed and centrifuged the samples at 10000 rpm for 5 min and the samples were filtered through a 0.2 µ spin column filter which had been made pre-wet by 50 mM NH_4HCO_3, and the filtrate was dried in a vacuum concentrator (Speed Vac, Thermo Scientific).

7. The dried peptides were reconstituted in 2 % acetonitrile and 0.1 % formic acid (40 µL) in MQ water and centrifuged at 14,000 rpm for 10 min, and the resultant supernatant was transferred to mass spec vials.

8. Supernatant was transferred to clean, the fresh vials and steps 12 - 15 were performed as mentioned above for in-gel procedure above and submitted to mass spectrometer.

5.11 Analysis by MALDI Mass Spectrometry (85)

1. Bovine serum albumin (BSA) was tryptic digested and used as a control sample.

2. Both the tryptic digested test samples and control samples were analyzed in triplicates.

3. The Protein identification by peptide mass fingerprint was carried out using a MALDI -TOF MS (Brukers Biosystems). Database searches were carried out on an online Mascot server (www.matrixscience.com) against Homo sapiens protein database of SWISS PROT released on 2016.

4. Carbamidomethyl (C) and Oxidation (M) were selected as fixed modification and variable modification respectively.

5. The parameters chosen were Mass value selected was monoisotopic, protein mass was set as unrestricted, peptide Mass tolerance allowed was ± 0.5 Da, peptide charge state selected as 1+ and maximum missed cleavages allowed was 1.

5.12 UPLC-Mass Spectrometry configurations for analysis

Tryptic digested peptides from the samples were subjected to nano-scale LC separations with a nano ACQUITY system (Waters Corporation, USA) for LC-MS analysis. The Symmetry C18 (180 μm × 20 mm, 5 μm) was used as trapping column whereas as analytical column, BEH C18 (75 μm × 250 mm, 1.7 μm) was used.

Solvent A (0.1 % formic acid in MQ water) and solvent B (0.1 % formic acid in acetonitrile) were the two solvents used for LC separations.

MassPREP protein digestion standard (MPDS) containing a mixture of the tryptic digests of, yeast enolase, rabbit glycogen phosphorylase b, yeast alcohol dehydrogenase and bovine serum albumin was used as standard and analyzed sub-pmol/μL level in water: acetonitrile + 0.1 % formic acid. Each sample with 0.5 μg of completely digested protein was subjected to the trapping column and then flushed with 0.1 % of solvent B for 2 minutes at a flow rate of 15 μL/min.

Elution of the sample was achieved at a flow rate of 250 nL/min by gradually increasing the organic solvent concentration from 3 % to 40 % of solvent B over 90 min.

The precursor ion masses and associated fragment ion spectra of the tryptic peptides was measured using Xevo G2-S QTof mass spectrometer (Waters Corporation) coupled to the chromatographic system. The MS/MS spectrum from [Glu1]-Fibrinopeptide B (human - Sigma Aldrich, UK) m/z 785.8426, was used to calibrate the TOF analyzer of mass spectrometer externally. The monoisotopic mass of the doubly charged species in MS mode was used for post-acquisition data correction. The Glu1]-Fibrinopeptide B was delivered at 500 fmol/μL to the mass spectrometer via a Nano Lock Spray interface using the direct infusion line of a nano ACQUITY system at a flow rate of 500 nL/min, which is sampled every 60 s. Accurate mass data

were collected through a data independent mode of acquisition, the trap collision energy was ramped from 10 eV to 30 eV with the transfer collision energy at 10 eV the collision cells. The spectral acquisition scan rate was typically 1.0 s with a 0.1 s interscan delay.

Data processing

ProteinLynx Global Server v2.4.5 (Waters Corporation, Milford, USA) was used for processing the LC-MS^E data. In brief, lockmass-corrected spectra were centroided, deisotoped, and charge-state-reduced to produce a single and accurately measured monoisotopic mass for each of the peptide its associated fragment ions. The initial correlation of a precursor and a potential fragment ion is achieved by means of time alignment.

Database searches

All data were searched for using PLGS v2.4.5 against the *Homo sapiens* database. A fixed modification of carbamidomethyl-C was specified, and variable modifications included were deamidation N, acetyl N-terminus, oxidation M and deamidation Q. Allowed missed trypsin cleavages were one. The precursor and fragment ion tolerances were determined automatically. The initial protein identification criteria used by the IdentityE algorithm within PLGS required the detection of at least three fragment ions per peptide, seven fragment ions and a minimum of one peptide per protein.

5.13 Mass Spectrometry Data Analysis in the Web-Based Tools

1. DAVID version 6.7 (Database for Annotation, Visualization and Integrated Discovery) (86) and PANTHER version 10.0 (Protein ANalysis THrough Evolutionary Relationships) (87) used for functional annotation of all proteins by their GO number were used.

2. The MS identified proteins were screened for their involvement in biological process, against the background population of proteins / genes in database of Homo sapiens.
3. In the DAVID Bioinformatics resource, the UniProtKB accession number was chosen and the ID lists were pasted to establish a gene list. The function "Functional annotation table" using GO were chosen.
4. The mean was compared using modified fisher exact test and with Bonferroni adjustment.
5. The Cut off *p* value was set <0.0001 and more than one 1.5 fold overrepresented proteins are considered to be significant.
6. The results were reconfirmed in the PANTHER by using the batch ID upload. Statistical enrichment test was used creating an annotated table with the GO terms and only the categories with p-value more than 0.05 are accepted and overrepresentation more than 1.5 fold.

5.14. 2 Dimensional gel electrophoresis (88, 89)

Materials required

For Isoelectric Focusing

- Rehydration buffer
- Sample rehydration tray
- Isoelectric focusing equipment
- IPG strips

For second dimension

- Polyacrylamide resolving gel mixture: 12 % (w/v) (29:1) acrylamide:*bis*-acrylamide, 375 mM Tris–Cl (pH 8.8), 0.1 % SDS, 0.1 % APS and 0.06 % TEMED
- Running buffer - pH 8.3: 190 mM Gly, 25 mM Tris–Cl and 1 % (w/v) SDS.

- Glass plates, spacers
- Multiple gel caster
- Power pack - PowerPac™ Universal Power Supply, Bio-Rad
- Densitometer with PDquest software (Bio-Rad GS 800)
- Rocker
- Vacuum dryer for concentrating samples (SpeedVac,Thermo Fisher)
- Coolant box, 1.5-mL capped microcentrifuge tubes,
- Microcentrifuge
- Vortex mixer.
- Coomassie brilliant blue R-250

5.15 Sample preparation: Albumin and immunoglobin depletion from the serum samples using PROTBA kit (Sigma Aldrich, Missouri, USA) (90). Column Equilibration

1. For removing storage solution from the resin, the spin columns were placed in collection tubes and centrifuged at 8,000 rpm for 5–10 s and the solution collected in tubes was discarded.

2. The spin columns were centrifuged at 8,000 rpm for 5–10 seconds after addition of 0.4 mL equilibration buffer to the resin. The solution collected in the tubes was discarded.

3. The equilibration step is repeated twice and after the final step, spin column was centrifuged for 30 s and saved.

Depletion of Albumin and IgG from serum

1. Serum sample 50 μL was added along with the 100 μL equilibration Buffer on the top of the packed medium of spin column and incubated at the RT for 5–10 min.

2. The spin columns were centrifuged at 10,000 rpm for 60 s.

3. Elute is reapplied on the top of resin and incubated for 10 min at RT for optimal depletion.

4. The spin columns were centrifuged in the same collection tube for 60 s.

5. The twice depleted serum left in collection tube and was combined with the wash for the optimal protein recovery.

6. Unbound proteins from the spin column were removed by centrifuging for 60 s after incubating with equilibration buffer (125 µL) on the top of the resin.

7. The albumin/IgG depleted serum/plasma at were cleaned up with 2-D Clean-Up Kit.

5.16 2-D Clean-Up Kit

Reagents

- Precipitant,
- Co-precipitant,
- Wash buffer chilled to -20 °C,
- Wash additive.

All steps were carried out on the ice. And samples were centrifuged at 12000 x g with cap-hinges of 1.5 mL microcentifuge tubes facing outward.

1. Protein solution (1–100 µl of volume) with 1–100 µg protein was transferred to a 1.5-mL tube.
2. And the tubes were kept for 15 min on ice (4–5 °C) after the addition of 300 µl of precipitant which was mixed well by vortexing.
3. To the mixture of protein and precipitant, 300 µl of co-precipitant was added and vortex mixed.

4. Tubes were centrifuged at 12 000 × g for 5 min.
5. Immediately after the supernatant was removed by carefully with pipette without disturbing the pellet.
6. After brief centrifugation, remaining supernatant in tubes were carefully removed without leaving any visible liquid.
7. 40 µl of co-precipitant was added carefully over the pellet (without disturbing) and on kept in ice for 5 min. Supernatant was removed from the tubes, after 5 min of centrifugation.
8. To disperse the pellets, on top of each, 25 µl of deionized water was added and mixed by vortexing for 5–10 s.
9. 1 mL of prechilled wash buffer (1 h at -20 ºC) and 5 µl of wash additive were added to each tube and vortexed until pellets fully dispersed.
10. The tubes were incubated at -20 °C for at least 30 min and vortexed intermittently for 20–30 s.
11. The tubes were centrifuged at 12 000 × g for 5 min and the supernatant was carefully removed. The resultant pellet was air dried no more than 5 min.
12. Each pellet was resuspened in an appropriate volume of rehydration buffer for first-dimension isoelectric focusing.

5.17 Procedure for whole serum

1. Serum of volume 6.25 µl was added to 10 µl of a solution containing 10 % SDS (w/v) and 2.3 % Dithiothreitol (DTT) (w/v).
2. The sample was boiled at 95 ºC for 5 min and then made upto volume of 500 µl with a solution containing 8 M urea, 4 % CHAPS (w/v), 40 mM Tris , 65 mM DTT and a trace amount of bromophenol blue.
3. Final diluted serum samples; of 45 µg protein concentration was loaded onto the first dimensional isoelectric focusing.

5.18 Rehydration of Immobilized pH gradient (IPG) strip and isoelectric focusing (IEF)

1. IPG strips were rehydrated (pH 4-7 and 3-10 (17 cm)) with 300 µL rehydration solution containing [7 M urea, 2 M thiourea, 4 % CHAPS, DTT (65 mM) and 2% IPG Buffer pH 3-10] using Rehydration Tray for overnight 16h corresponding to 60-100 µg protein per 100 µL.
2. Isoelectric focusing was performed for 40,000 volt h in gradient mode in Protean Iso-electro focusing Cell (Bio-Rad, Pennsylvania, USA) following instructions given by the supplier.
3. After IEF, the IPG strips were subjected to reduction and alkylation for a period of 15 min on a rocker, using 2 % dithiothreitol and 2.5 % iodoacetamide respectively in equilibration solution containing 6 M urea, 0.375 M Tris–HCl, 2 % SDS, 20% glycerol.
4. The equilibrated strips with were initially rinsed with water and excess equilibration buffer was removed by blotting onto Whatman paper and afterwards the strips in were rinsed in SDS-running buffer.
5. The second-dimension separation was with SDS-PAGE. 12.5 % polyacrylamide gels were used and resolved in large electrophoretic system (protean II Xi, Bio-Rad, USA).
6. On the top of separating gels, equilibrated IPG strips were placed and layered with hot 0.5 % agarose solution (Running buffer with trace of bromophenol blue).
7. Initially, current of 16 mA per gel was applied for the initial 20 min of run and then current of 20mA per gel was applied and proteins were separated until dye front reaches the bottom of cassette.
8. Gels were stained with silver stain.

5.19 ELISA Protocol

Materials required:

- ELISA kit
- Serum

Principle:

Target was detected with a biotin – conjugated antibody. Avidin conjugated to HRP was added to which TMB substrate exhibited changes in color. The reaction was terminated with sulphuric acid and color was read at 450 nm.

Minimum detectable dose (MDD) of Galectin-1 ranged from 0.008-0.129 ng/mL. The Linearity of the assay was within the dynamic range of the assay (0.313-20 ng/mL).For the Complement C3 ELISA sensitivity is 0.6 ng /mL and dynamic range of the assay is 0.625 ng/mL - 40 ng /mL.

5.19.1 ELISA- CTR1

1. Standards and samples were prepared in accordance with instruction provided by manufacturer. 100 µl of sample / standard were added to each well and incubated for 2 h at 37 °C.

2. The liquids were decanted and without washing 100 µl of diluted detection A reagent was added and incubated for 1 h at 37 °C.

3. Each well is washed thrice with 350 µl of wash buffer provided.

4. To each well, working solution of detection reagent B (100 µl) was added and incubated for 30 min at 37 °C.

5. The aspiration/wash processes were repeated for total 5 times as conducted in step 4.

6. Substrate Solution of 90 µl was added to each well. With a sealer, plate was covered and incubated for 10 - 15 min at 37 °C in the dark. Substrate solution color changed to blue, and then stop solution of 50 µl was added to each well. Yellow color developed at the end of the reaction.

7. Mixed well and read at 450nm using an ELISA plate reader (Spectramax $M2^e$).

5.19.2 For galectin-1 and complement C3 estimation:

1. Serum samples were diluted 1:100,000 with diluent and 25 μL volume of diluted samples were used for the estimation of complement C3
2. Undiluted serum 10 μL was used for galectin-1 estimation.
3. Samples were incubated for 2 h in pre-coated wells (Anti-complement C3 /galectin-1 antibodies).
4. This was followed by 5 times of washing with wash buffer provided by manufacturer.
5. 100 μL volumes of HRP conjugates of specific antibodies were added to each well.
6. Plates were incubated for a period of 60 min, followed by 5 times of washing.
7. After incubation, TMB substrate chromogen of 100 μL was added to the wells and then incubated for 15 min.
8. After 100 μL of stop solution was added to each wells and followed by reading plates at 450nm in Spectramax M2e immediately.

5.19.3 ELISA estimation for haptoglobin:

1. Serum samples 1:50,000 appropriately diluted with diluents.
2. 100 μL volumes diluted serum samples were used for the haptoglobin estimation.
3. Samples were incubated for a period of 15 min in haptoglobin antibodies pre-coated wells and then 5 times of washing with wash buffer provided by manufacturer.
4. Plate was incubated for 15 min after addition of 100 μL of HRP conjugated haptoglobin antibody to each of the well.
5. This was followed by 5 times of washing of plates with wash buffer.

6. 100 µL of TMB substrate chromogen was added to each wells and incubated for 5 min.
7. Immediately after the addition of 100 µL stop solution, plates were read at 450 nm in Spectramax M2e.
8. The linearity of the assay was within range 0.3125-200 ng/mL.

5.20 Serum iron, Ferritin, Serotransferrin and serum transferrin receptors in serum:

Serum iron and serum total iron binding capacity were determined by a fully automated analyzer (Dade Behring, Siemens, USA as by the methods described (91). Ferritin in serum and was determined by the method of (92). Transferrin and serum transferrin receptor in serum were determined by Kreutzer and Samuelson et.al (93,94). All these assays were performed after equilibrating all materials to RT (21-25 °C) in duplicates including standards and samples as per manufacturer instructions.

5.20.1 Ferritin

Principle:

Anti-human ferritin antibodies in the kit are latex coated particles, which can be agglutinated by ferritin present in samples. This latex particles' agglutination is measured spectrophotometrically and proportional to the concentration of ferritin in sample.

Procedure:

1. Pipette 6 µL of saline (blank) and 6 µL of ferritin standard at varying concentration diluted with normal saline in to the corresponding 96 flat bottom well plates.
2. 6 µL of serum and peripheral blood mononuclear cells was added directly to the well apart from blank and the standards well.

3. Then 200 µL of chromogen was added to all the wells and was incubated for 5 min at 37 ºC.

4. After incubation, the plate was read at 540 nm using a plate reader (Molecular devices Spectramax M2e). The detection limit is up to 4 µg.

5.20.2 Transferrin

Principle :

Transferrin in the sample agglutinates of latex coated anti-human transferrin antibodies in the kit. This turbidity is measured by spectrophotometer and proportional to the concentration of transferrin

Procedure :

1. Pipette 2 µL of water (blank) and 2 µL of transferrin standards into the corresponding 96 well plates.

2. 2 µL of serum and peripheral blood mononuclear cells was added directly to the well apart from blank and the standards well.

3. Then 200 µL of chromogen was added to all the wells and incubated for 5 min at 37ºC. After incubation is over, the plate was read at 540 nm. The detection limit of transferrin is up to 4.8 mg.

5.20.3 Serum transferrin receptors

Procedure:

1. 100 µl of diluted standards, dilution buffer (blank) and samples were loaded into the wells.

2. The plate was incubated at RT for 1 h, in rocker at 300 rpm and with 300 µl of wash solution the wells were washed thrice.

3. After the final wash, 100 µl of conjugate solution was added into each well and incubated at RT for 1 h, in rocker.

4. With 300 µl of wash solution, the wells were washed thrice, followed by addition of 100 µl substrate solution to each well and then incubated for 10 min at RT.

5. The colour development was arrested with Stop Solution (100 µl). The absorbance was read at 450 nm. The detection limit of s TFR is up to 2 ng.

5.21 Haptoglobin phenotyping

Materials required

- **Polyacrylamide resolving gel mixture**: 5 % (w/v) (29:1) acrylamide:*bis*-acrylamide, 375 mM Tris–Cl (pH 8.8), 0.1 % (w/v) APS and 0.06 % (v/v) TEMED)
- **Running buffer** 25 mM Tris–Cl (pH 8.3), 190 mM Glycine,
- **Staining solution :** 5 mL of 0.2% (w/v) 3, 3, 5, 5-tetramethylbenzidine in methanol, 1 mL of 1 % (w/v) potassium ferricyanide, 10 mL of 5 % (v/v) glacial acetic acid, 0.5 mL dimethylsulfoxide (DMSO), and 150 µL of 30 % (w/w) H_2O_2 as described (95).
- 10 % Hemoglobin solution and Serum samples

Procedure

1. Polyacrylamide Gel electrophoresis (NPAGE): 5% separating gel mixture was poured up to 70 % of the plate, overlaid with water saturated butanol and allowed to polymerize.

2. Then 3.5 % stacking gel was poured and comb was placed and allowed to polymerize.

3. After polymerization comb was removed and washed twice with H_2O

4. Haptoglobin–hemoglobin complexes were formed on incubating fresh serum with 2 µL of hemoglobin solution (10 %) for 5 min at RT.

5. Proteins were loaded was resolved in constant volt mode (100 V) till the run was over.

6. The complex formed was resolved in constant voltage by applying 100 V until tracking dye reaches the bottom of the plate.

7. Resolved native PAGE gel was stained with 3, 3, 5, 5-tetramethylbenzidine and documented using densitometer Bio-Rad GS 800.

5.22 Lectin Blot

SDS-PAGE

1. Separating gel was poured up to 70 % of glass plates (1.5 mm spacer) were overlaid with water saturated butanol and allowed to polymerize.
2. Then stacking gel was poured and comb was placed and allowed to polymerize.
3. After polymerization comb was removed and washed twice with water.
4. Serum samples were estimated and 50 μg of proteins were resolved.
5. Electrophoresis was performed at 100V current till the run was over.

Transfer

1. The gel was removed, allowed to be equilibrated with transfer buffer for 20 min.
2. PVDF membrane of required size was cut and incubated in the transfer buffer for 20 min.
3. The gel and PVDF membrane were sandwiched in the mini transfer unit of western blot apparatus without any air bubble.
4. The transfer was performed under 100 V of electric field for 1 h in the ice cold buffer.
5. Then the membrane was taken and washed thrice in TBST each for 5 min
6. The membrane was kept on blocking buffer for 1 h (1 % BSA in TBST for 1h) at RT under mild rocking

7. Washed thrice in TBST.
8. 2-µg/mL biotinylated lectin was incubated for 30 min
9. Washed in TBST for 5 times.
10. Then incubated with streptavidin conjugated with horseradish peroxidase for 30 min at RT.
11. The membrane was washed in TBST thrice and twice with TBS, developed using chemiluminol and documented using fluorchem FC3 chemidoc instrument

5.23 Western Blot

In this method protein sample is resolved in SDS-PAGE and electro transferred onto PVDF / nitrocellulose membrane. The protein in membrane is detected with specific primary antibody and enzyme labeled secondary antibody (raised against species of primary antibody). HRP and chemiluminescent substrate were commonly used.

Materials required:

- Same materials required for casting SDS PAGE
- TBS (Tris buffered saline)
- Transfer buffer – Same composition as running buffer, except addition of 200 mL of methanol made up to 1000 mL using dH_2O. Stored at -20°C.
- Blocking buffer - 5 % skimmed milk (nonfat dry milk) prepared with 1X TBST.
- Washing buffer-TBST: 0.1 % tween-20 in 1X TBS
- Secondary antibody
- Luminescent Mixture – Equal volume of HRP substrate peroxide solution and HRP substrate luminol reagent were mixed and added just before use.
- Nitrocellulose membrane
- Whatmann filter paper no.1
- Mini transfer western blot- Bio Rad

Protocol

SDS-PAGE

1. Glass plates with 1.5 mm spacer were, cleaned and clamped together
2. Separating gel mixture was poured up to 70 % of the plate, overlaid with water saturated butanol and allowed to polymerize.
3. Then stacking gel was poured and comb was placed and allowed to polymerize.
4. After polymerization comb was removed and washed twice with water.
5. The sample containing 50 µg of protein equal part of 2X SDS sample buffer was added and boiled at 95 ˚C for 5 min and resolved at 100V, until the tracking dye reaches the bottom of the plates.

Transfer

1. The gel was cut and incubated in the transfer buffer for 20 min.
2. Nitrocellulose / PVDF membrane of required size was cut and incubated in the transfer buffer for 20 min.
3. The gel and nitrocellulose membrane / PVDF were sandwiched in the mini transfer western blot without any air bubble.
4. The transfer was performed under 100V of electric field for 1 h in the ice cold buffer.
5. Then the membrane was taken and washed thrice in TBST each for 5 min
6. The membrane was kept on blocking buffer for 1 h at RT under mild rocking
7. Washed thrice in TBST (5 times each).
8. The Blot was incubated with primary antibody at 4°C for overnight.
9. Washed in TBST (5 times).
10. Incubated in secondary antibody for 2 h at RT.

11. The membrane was washed in TBST thrice and twice with TBS, developed using chemiluminol and documented using fluorchem FC3 chemidoc instrument.

5.24 Cell culture procedure (96)

5.24.1 Cryopreservation and retrieval cells:

A Cryo protective agent, dimethyl sulfoxide (DMSO), was used in combination with complete medium for cryopreserving cells. Purpose of DMSO is to reduce the freezing point and lowering the rate of cooling. Steady freezing rate greatly prevents the ice crystal formation and cell damage. The cells were trypsinised grown, after reaching the 90 % of confluence. The pellet was reconstituted in growth medium containing 20 % FBS and 10 % DMSO. Cells were kept in one degree step down coolant and later stored in liquid nitrogen. The number of cells were counted using hemocytometer and diluted with accordingly to get a final concentration of 10^6 - 10^7 cells/mL. When needed for study, each vial of the cryopreserved cells was removed from storage and rapidly thawn to prevent ice crystals formation. To optimize the recovery, cells were plated at a high density. Cells taken from liquid nitrogen were thawed at 37 °C and resuspended in fresh 5 mL of growth medium. Subsequently cells were centrifuged at 1500 rpm for 10 min and supernatant was decanted. The cell pellet was suspended in fresh growth medium and seeded onto gelatin coated culture dishes.

5.24.2 Gelatin preparation

Gelatin of 100 mg (Sigma Aldrich) was dissolved in 100 mL of PBS and sterilized at 110 °C in 110 lbs pressure for 15 min. This was used for coating tissue culture dishes / flask for cells from passage 2- 5.

5.24.3 Cell counting:

Materials Required:

- Trypan Blue (0.4 % in PBS)
- Haemocytometer

Principle:

It is a dye exclusion method where only the membrane of the live cells excludes the trypan blue and the cell remains unstained. The dead cell membrane is permeable to the dye and stains blue.

Procedure:

1. Cell suspension of 20 µl was equally mixed with dye and 10 µl of it was loaded.
2. The total count of cells in the four corners (WBC counting squares) was counted.
3. The numbers of dead and live cells were counted separately to calculate the % viability.

Calculation

No of cells counted = *X*

Therefore, cells /mL Y= *X**2 (dilution factor) *10^4

Total no. of cells = *Y* * volume of the total medium trypsin inactivation.

10^4- 1000*10 (i.e. 1 µl - 1000 µl conversion, depth factor)

5.24.4 Serum starvation of cells:

Cells were grown to required confluence in 6 well plates; the medium was removed and added 2 mL of 1 % EBM medium was added. Serum starvation was performed for 4 h at 37°C in 5 % CO_2 incubator.

5.25 Wound healing assay (97)

Materials required:

- 0.1 % gelatin
- 6-well plates
- HUVECs
- EGM medium

- 1 % EBM medium
- 4 % Para formaldehyde – 0.4 g of paraformaldehyde (Merck) dissolved in 10 mL of 1 X PBS at 60 °C for 30 min was freshly prepared.
- PBS

Principle:

Cell migration is a process induced by various growth factors and chemokines that are associated with complex signaling. Cell migration occurs in normal condition of wound healing, cell differentiation and embryonic development and pathological condition like tumor and metastasis.

Procedure:

1. A wound was created in monolayer of cells with a sterile 200 µl tip in a 6-well plate.
2. Cells were exposed to the appropriate conditions and kept at 37 °C incubator for overnight.
3. The medium was removed and 500 µl of 4 % paraformaldehyde was added to all wells and kept at RT for 30 min for fixation.
4. Cells were washed with PBS twice gently. Photographs were taken from 3 different fields and analyzed (Liang, Park, & Guan, 2007).

5.26 Angiogenesis assay-In vitro tube formation assay:

Materials required:

- 96-well culture plates- kept at 4 °C
- ECM matrix- Millipore - kept at 4 °C
- Microtip - kept at 4 °C

- EGM medium
- HUVECs

Principle:

The assay measures the capacity of endothelial cells to form capillary (tube) like structure in the presence of extracellular matrix support when plated at sub confluent densities. This assay helps in screening pro and anti-angiogenic molecules. When a plated, endothelial cell gets attached to the surface and creates mechanical forces on the neighboring extracellular support matrix. This generates guidance pathways or a track that in turn aids cellular migration. The resultant cords of cells will ultimately leads to formation of hollow lumens. The comparisons between cells with and without treatment are measured in parameters such as tube length, size and number of junctions (98).

Procedure:

1. Human umbilical vein endothelial cells (HUVEC) were isolated from the fresh umbilical cords by methods described earlier [99] and grown to confluence at 37 ˚C in 5 % CO_2. The growth medium is 10 % FBS supplemented EGM.

2. All the plates and consumables were pre cooled at 4 °C. The ECM matrix 1 mL was mixed with 100 µl of 10X ECM buffer.

3. Matrigel (BD Biosciences) ECM gel solution of 50 µl was allowed to get polymerized in each well of a 96-well plate by incubating at 37 ˚C for 30 min.

4. VEGF of 10 ng/mL concentration was used as positive control.

5. HUVEC were serum starved for 16 h and 20,000 cells were seeded into each wells of the Matrigel-pre-coated 96 well microtiter plate.

6. The cells were treated with haptoglobin in concentrations of 1, 2.5, 5.0 and 10 µg/mL and incubated for 6 h.

7. The medium was carefully removed without disturbing the tubes and fixed it with 4 % paraformaldehyde.

8. The development of these tubular network was observed with microscope and then photographed. The degree of tube formation was estimated by determining the length of the tubes in the 3 random fields and distances were calculated with ImageJ software (National Institutes of Health).

5.27 Proliferation assay by using crystal violet (100)

Materials required

- 6-well plates
- Crystal violet staining solution (0.5 %)
- 0.5 g crystal violet powder (Sigma-Aldrich), 80 mL distilled water and 20 mL methanol. Stain was made by dissolving crystal violet powder in water and then adding methanol.
- EBM medium
- HUVECs

Principle

A method to detect the cell proliferation with crystal violet dye staining and measured by the amount of crystal violet uptake by the cell which indicates the newly synthesized DNA. Cell death results loss of adherence and subsequent lost from the population of cells, and thus reducing the amount of crystal violet staining in a culture.

Procedure

1. Cells were grown at 37°C in 5 % CO_2 incubator and seeded in a 24 well plate (3,000 / well). Cells were grown to 60 % of confluence. Three wells were medium without cells served as controls for nonspecific binding of the crystal violet dye.

2. Then the cells were serum starved with 1 % EBM medium for overnight.

3. The medium was aspirated from the wells, and fresh medium supplemented with haptoglobin was added (concentration 1-15 µg /mL). Without allowing cells to dry out the cells were treated in triplicate wells for each concentration. Untreated cells reminded as controls.

4. The medium was aspirated, and washed twice in a gentle stream of water without hitting the cell monolayer directly. After water from the wells were immediately aspirated. The plates were inverted on the filter paper and remaining liquid was removed by tapping the plate gently.

5. Cells were kept for 24 h, and then cells were washed in PBS twice and 0.2 mL of stain was added to each well.

6. 200 µL of 0.5 % crystal violet staining solution was added to each well, and incubated for 20 min at RT on a rocker.

7. Plates were washed four times in a stream of tap water as described in Step 4. After washing, plates were air-dried without lid for at least 2 h at RT.

8. 500 µL of methanol was added to each well, and the plates were incubated with its lid on for 20 min at on a rocker at RT.

9. The optical density of each well were measured at 570 nm (OD570) with a plate reader and average OD of the wells without cells from the OD of each well on the plate was subtracted. The OD570 of the wells without cells, were processed identically to wells with cells.

10. OD values average of untreated cells were set at 100 % and compared with the average OD values of stimulated cells with the OD570 values of the controls.

11. The mean and the standard error of the mean were calculated for at least three independent experiments.

5.28 Molecular Cloning and Over Expression of galectin-1 (101)

p3XFLAG-Myc-CMV™-26 Expression Vector, Catalog Number E7283

p3XFLAG-Myc-CMV™-26 is a shuttle vector that can be used in both in E. coli and mammalian cells. It is a 6.3 kb derivative of pCMV51 and used to create protein with N-terminal 3 flanking FLAG epitopes (Asp-Tyr-Lys-Xaa-Xaa-Asp) and C-terminal c-myc (EQKLISEEDL) tags in mammalian cells. Optimal replication of vector is seen in host with SV40 T antigen (COS-7 cells).The vector encodes for FLAG and c-myc epitopes the multiple cloning sites.

5.28.1 Control plasmid -p3XFLAG-CMV-7-BAP

p3XFLAG-CMV-7-BAP is 6.2 kb in size and a derivative of PCMV51 vector. It is used for transient expression of alkaline phosphatase bacterial protein with N-terminal 3X-FLAG (3 adjacent FLAG) tag and these epitopes are encoded by vector in the upstream of the multiple cloning region 2.

5.28.2 FLAG M2 antibody

The enterokinase recognition sequence in the 3rd FLAG epitope region, allows cleavage of the 3XFLAG peptide from the purified fusion protein. The transcription of FLAG-fusion constructs is steered by the promoter-regulatory region of the human cytomegalovirus 4.

5.28.3 Sequence retrieval of galectin-1

The galectin-1 gene was mapped to 22q13.1 chromosome and the complete gene sequence of human is available in the NCBI database with the Reference Sequence of NM_002305.3. The coding sequence of galectin-1 gene lies from 37675606 to 37679802 bp of the total. In order to clone, a primer was designed to amplify the nucleotide sequence from (408 bp) of the CDS region.

5.28.4 Galectin 1 (LGALS1), mRNA CDS sequence Homo sapiens

ATGGCTTGTGGTCTGGTCGCCAGCAACCTGAATCTCAAACCTGGAGAGTG
CCTTCGAGTGCGAGGCGAGGTGGCTCCTGACGCTAAGAGCTTCGTGCTGA
ACCTGGGCAAAGACAGCAACAACCTGTGCCTGCACTTCAACCCTCGCTTC
AACGCCCACGGCGACGCCAACACCATCGTGTGCAACAGCAAGGACGGCG
GGGCCTGGGGGACCGAGCAGCGGGAGGCTGTCTTTCCCTTCCAGCCTGGA
AGTGTTGCAGAGGTGTGCATCACCTTCGACCAGGCCAACCTGACCGTCAA
GCTGCCAGATGGATACGAATTCAAGTTCCCCAACCGCCTCAACCTGGAGG
CCATCAACTACATGGCAGCTGACGGTGACTTCAAGATCAAATGTGTGGCC
TTTGACTGA

5.28.5 FASTA sequence of galectin-1, protein Length: 135; Mass (Da):14,716

>sp|P09382|LEG1_HUMAN Galectin-1 OS=Homo sapiens GN=LGALS1 PE=1
SV=2

MACGLVASNLNLKPGECLRVRGEVAPDAKSFVLNLGKDSNNLCLHFNPRFN
AHGDANTIVCNSKDGGAWGTEQREAVFPFQPGSVAEVCITFDQANLTVKLPD
GYEFKFPNRLNLEAINYMAADGDFKIKCVAFD

5.28.6 PCR amplification of galectin1 cDNA for infusion cloning:

Coding sequences of galectin-1

ATGGCTTGTGGTCTGGTCGCCAGCAACCTGAATCTCAAACCTGGAGAGTG
CCTTCGAGTGCGAGGCGAGGTGGCTCCTGACGCTAAGAGCTTCGTGCTGA
ACCTGGGCAAAGACAGCAACAACCTGTGCCTGCACTTCAACCCTCGCTTC
AACGCCCACGGCGACGCCAACACCATCGTGTGCAACAGCAAGGACGGCG
GGGCCTGGGGGACCGAGCAGCGGGAGGCTGTCTTTCCCTTCCAGCCTGGA
AGTGTTGCAGAGGTGTGCATCACCTTCGACCAGGCCAACCTGACCGTCAA
GCTGCCAGATGGATACGAATTCAAGTTCCCCAACCGCCTCAACCTGGAGG
CCATCAACTACATGGCAGCTGACGGTGACTTCAAGATCAAATGTGTGGCC
TTTGACTGA

5.28.7 Designing of infusion specific primers

Infusion cloning primers were designed with the manufacturer's online tool with selected vector (p3XFLAG-Myc-CMV™-26), galectin-1 sequence and restriction enzymes (HindIII and XbaI I). The CDNA was used for preparation of the galectin1 cDNA insert for cloning. Template was with the designed infusion primer as below.

- **Forward primer** (the restriction site of HindIII)**:**
  TGACGATGACAAGCTTATGGCTTGTGGTCTGGTC (Tm = 53.2ºC).
- **Reverse primer** (the restriction site of XbaI):
  GTTTTTGTTCTCTAGATCAGTCAAAGGCCACACATT (Tm = 52.2ºC)

  PCR product length:408 bp

Contents	Volume, µl
DNTPs	4 µL
Buffer (10 X)	2.5 µl
FP (10 pmols)	1.5 µL
RP (10 pmols)	1.5 µL
Taq Polymerase	0.3 µl
Milli-Q water	13.2 µl
cDNA	2.0 µl
Total volume	25µl

Table 4. PCR reaction mixture

PCR was carried out in a thermocycler (Eppendorf Mastercycler EPS Gradient) according to the manufacturer's instructions.

Initial denaturation	**95 ºC, 2 min**	
Denaturation	95 ºC, 30 s	**29 times**
Annealing	55.7 ºC, 30 s	
Extension	72 ºC, 50.0 s	
Final extension	72 ºC, 5 min	

Table 5. PCR reaction protocol

The *Pfu* polymerase was used for amplification and reactions were set for 20 µl volume. Amount of primers for used for each reaction were 5 µmol. A negative control was also set. (The above reaction mix was prepared, instead of DNA, MQ water was added) PCMV vector plasmid of 1000ng was digested with HindIII and XbaI for overnight at 37 ºC. These products were separately run in 1 % agarose gel and eluted with Qiagen Gel extraction Kit PCR and quantitated with a Nanodrop

5.28.8 Linearization of p3XFLAG-Myc-CMVvector

Vector was linearized using the selected HindIII and XbaI restriction enzymes. The reaction mixture was prepared as mentioned in the below table. The reaction mixture was incubated at 37 ºC for 16 h. The digested product was run in 1 % agarose gel along with molecular weight markers. After electrophoresis, gel elution was carried out to purify the digested product by gel extraction method.

Reagents	Volume	Final Concentration
10XBuffer	2 µL	1 X
DNA	5 µL	2 µg
XbaI I	0.5 µL	2 U
Hind III	0.5 µL	2 U
Milli-Q water	2 µL	
Total volume	10 µL	

Table 6. Reaction protocol for vector digestion

5.28.9 Infusion reaction and transfection

The infusion reaction was performed as per the manufacture's instruction. Infusion reaction mixture contained linearized vector and DNA insert in the molar ratio 2:1 with infusion enzyme.

Reagents	Volume µL
5X In-Fusion HD Enzyme Premix	2.0 µL
Linearized Vector (100 ng)	4.0 µL
PCR DNA insert (45 ng)	2.6 µL
Milli-Q water	1.4 µL
Total volume	10.0 µL

Table 7. Reaction protocol for infusion reaction

The total reaction volume was made up to 10 µL using sterile Milli Q H_2O. The Reaction mixture was incubated at 50 °C for 15 mins, and then was placed on ice. Then the infused vector DNA product was transfected into the competent cells and inoculated onto the selective LB plate.

5.28.10 Transformation of p3XFLAG-Myc-CMVvector into competent M15 *E.coli* strain

Transformation is an important step in the cloning process. In transformation, foreign DNA will be taken up by bacteria under laboratory conditions. There are two types of transformation methods: chemical method and electroporation method. The method here followed is a chemical transformation method using calcium chloride.

Chemical method includes two steps: 1) Bacterial cells were converted to competent cells to take up the plasmid DNA after treating with polyvalent cations ($CaCl_2$ / $MgCl_2$). At a low temperature, bacterial cells were exposed to cations, resulting in transiently opening of membrane channels. 2) Second phase involved heat shock. Competent bacterial cells were mixed with plasmid DNA and were exposed to 42 °C for 60 – 120 s and then the cells were recovered in complete LB media and inoculated onto the selective LB agar plate. The competent cells, which were successfully transformed and expressing the plasmid was grown on the selective LB agar plate.

Recovery phase is where the heat shock competent cells were suspended in the sterile LB media and was incubated at 37 °C for 1 h. Then the cells were inoculated onto the selective LB plate. The competent cells, which are successfully transformed and expressing the plasmid was grown on the selective LB agar plate.

Transfecting clone into COS-7 cells.

1. On the prior day, cells were seeded in 60mm dish with full growth media to reach 70–90 % confluency.
2. 1 µg of plasmid DNA (clone) was made up in solution 500 µL with basal DMEM high glucose media without antibiotic and serum.
3. 1.5 µL of ICAfectin 441 reagent was made up in 500 µL basal media.
4. Both solutions were pipette mixed together and incubate for 5 min at RT.
5. The mixture was slowly dispensed in the dish and supplemented with 50 µL of FBS / fresh growing medium after 4 h of incubation. Transfected cells were visualized.

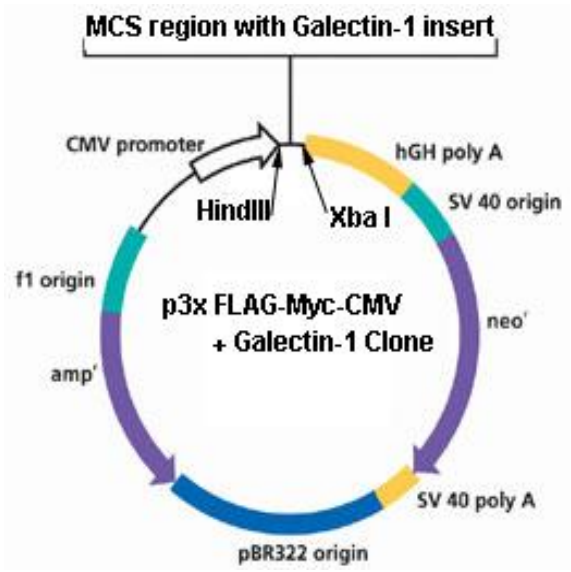

Figure 5: Vector map of p3X FLAG -Myc-CMV with galectin-1. Image is adapted from Sigma manual.

5.28.11 FLAG HA Tandem Affinity Purification Kit TP0010

Manufactures guidelines were followed -TP0010.

Tandem Affinity Purification is applied for isolating of protein complexes. To a known "bait" protein, a tandem affinity tag was added and used to pull down endogenous proteins that interact with the tagged protein. Proteins purified are

suitable for mass spectrometry (MS) analysis. Antibodies against FLAG tags and affinity resins derived were highly specific compared to other existing epitope-tagging systems.

Binding to ANTI-FLAG M2 resin

Lysates preparation

1. RIPA + protease inhibitor (PI) cocktail was prepared with approximately 4 mL .
2. Appropriate amount of ANTI-FLAG M2 resin was aliquoted into a clean tube or vial. Washed thrice with RIPA buffer, then centrifuged at 3,000 X g for 30 s. All remaining final wash was removed carefully without losing any resin.
3. FLAG HA fusion protein confirmed with the western blotting. ANTI-FLAG® M2 resin from step 2 was added to the sample extract.
4. This mixture was incubated for 2h to overnight at 4 °C with gentle rocking or agitation.

Removing the unbound protein.

5. Tube from step 4 was centrifuged at 3,000 X g at 4 °C for 2 min. The Most of supernatant (unbound protein) was removed as much of the supernatant with a pipette without disturbing the resin and discarded. The remaining supernatant and resin was transferred into a spin column that has been placed into a collection tube. 500 mL RIPA + PI cocktail was added to each spin column and centrifuged at 3,000 X g at 4 °C for 30 s.
6. The tip was reinserted into column and 500 µl of the RIPA + PI cocktail was added. The samples were agitated for several min at 4 °C.
7. Tip was removed from the column and the spin column centrifuged at 3,000 X g at 4 °C for 30 s after placing the column in a same 2 mL collection tube. Column washings with unbound protein were discarded.
8. Wash steps 6-7 were repeated two more times.

The first elution of the protein complex using 3XFLAG peptide.

9. Tip was reinserted into column and placed in a new collection tube.

10. Preparing the 3XFLAG peptide: 5mg/mL 3XFLAG peptide stock solution was prepared by adding TBS, 3 mL of 5 mg/mL 3XFLAG peptide stock of (150 ng/mL final concentration) was used for elution.

11. Tandem FLAG tagged protein was eluted with 2.5 times elution 3XFLAG peptide. Elution volume was incubated 10 min.

12. Tip was removed and the column was placed in a clean tube and centrifuged at 3,000 X g for 1 min. The eluted protein was preserved.

13. The second elution was performed (Steps from 11-12) and samples were pooled.

5.29. Expression and purification of the recombinant proteins: PE35 of *Mycobacterium tuberculosis* H37RV. [101]

Vector sequence:

Human PE35 was cloned in the bacterial expression pQE30-Xa vector by infusion cloning method. Infusion cloning is based on the principle of sequence and ligation independent cloning (SILC) (102). Here, target DNA will contain single stranded nucleotide (15 – 22 no's) over hangs on both ends. These over hangs will be complementary to the selected vector restriction site and allow annealing of insert DNA to vector during the infusion reaction.

5.29.1 Features of pQE 30-Xa vector

It is a bacterial expression vector that works based on the T5 promoter transcription-translation system. This T5 promoter is controlled by two lac operon operator sequence. The high translation rate of gene of interest is ensured by the presence of Ribosomal Binding Site (RBS II). The gene of interest will be inserted into plasmid with the help of restriction enzyme sites in the multiple cloning sites. The expressed protein will contain 6X His tag at N-terminal, which help in single step affinity

purification of over expressed protein. Factor Xa recognition site is encoded between His tag and protein sequence, enabling removal of his tag from the target protein after purification using the enzyme Factor Xa. The vector contains β-lactamase gene (bla), hence the bacterial strain transformed exhibit resistance to ampicillin antibiotic.

5.29.2 Sequence retrieval of PE35

MTB, PE35 gene was mapped to 5q23 chromosome. Complete gene sequence of human PE35 with the NCBI Accession ID NC_000962.3 and with the version ID of NM_002317.5 is available in the NCBI database. The coding sequence of PE35 gene lies from 435074 to 4351044. In order to clone the PE35, a primer was designed to amplify the nucleotide sequence from (300 bp) of the PE35 CDS region.

5.29.3 Designing of infusion specific primers

The nucleotide sequence of PE35 was retrieved from the NCBI database as described below. Infusion cloning primers were designed with the manufacturer's online tool with selected vector (pQE30-Xa vector), PE35 sequence and restriction enzymes (StuI and HindIII).

Forward primer**:** (has the restriction site of StuI)

GGTATCGAGGGAAGGCCTATGGAAAAAATGTCACATGATC

Reverse primer: (has the restriction site of HindIII)

TCAGCTAATTAAGCTTCTATTCGGCGAAGACGCC

5.29.4 PCR amplification of PE35 gene for infusion cloning

Mycobacterium Tuberculosis H37RV expresses the PE35 protein. The genomic DNA was used for preparation of PE35 gene insert for cloning. Template was with the designed infusion primer as below. A negative control was also set. (The above reaction mix was prepared where instead DNA, Milli-Q water was added)

Contents	Volume, µl
DNTPs	4 µL
Buffer (10 X)	2.5 µl
FP (10 pmols)	1.5 µL
RP (10 pmols)	1.5 µL
Taq Polymerase	0.3 µl
Milli-Q water	13.2 µl
DNA	2.0 µl
Total volume	25µl

Table 8. PCR reaction mixture

Coding sequences of PE35

ATGGAAAAAATGTCACATGATCCGATCGCTGCCGACATTGGCACGCAAGT
GAGCGACAACGCTCTGCACGGCGTGACGGCCGGCTCGACGGCGCTGACGT
CGGTGACCGGGCTGGTTCCCGCGGGGGCCGATGAGGTCTCCGCCCAAGCG
GCGACGGCGTTCACATCGGAGGGCATCCAATTGCTGGCTTCCAATGCATC
GGCCCAAGACCAGCTCCACCGTGCGGGCGAAGCGGTCCAGGACGTCGCCC
GCACCTATTCGCAAATCGACGACGGCGCCGCCGGCGTCTTCGCCGAATAG

PCR profile

Steps	Temperature and duration	
Initial denaturation	95 ºC, 2 min	
Denaturation	95 ºC, 30 s	36 times
Annealing	58 ºC, 30 s	
Extension	72 ºC, 50.0 s	
Final extension	72 ºC, 5 min	
Hold	4 ºC at ∞	

Table 9. PCR reaction protocol

The PCR product was run in 2 % agarose gel and was visualized using ethidium bromide under UV light. The PCR-amplified PE35 DNA was eluted by gel extraction method.

5.29.5 Linearization of pQE-30Xa vector

Vector was linearized using the selected StuI and HindIII restriction enzymes. The reaction mixture was prepared as mentioned in the below table. The reaction mixture was incubated at 37 ℃ for 16 h. The digested product was run in 1 % agarose gel along with molecular weight markers. After electrophoresis, gel elution was carried out to purify the digested product by gel extraction method.

Reagents	Volume	Final Concentration
10X Buffer	2 µL	1 X
DNA	5 µL	2 µg
Stu I	0.5 µL	2 U
Hind III	0.5 µL	2 U
Milli-Q water	2 µL	
Total volume	10 µL	

Table 10. Reaction protocol for vector digestion

5.29.6 Infusion reaction and transfection

The infusion reaction was performed as per the manufacture's instruction. Infusion reaction mixture contained linearized vector and DNA insert in the molar ratio 2:1 with infusion enzyme. The total reaction volume was finally made up to 10 µL with sterile MQ water. The reaction mixture was immediately placed on ice after 15 mins of incubation at 50 °C. Then the infused vector DNA product was transfected into the competent cells and inoculated onto the selective LB plate.

Reagents	Volume, µL
5X In-Fusion HD Enzyme Premix	2.0 µL
Linearized Vector (100 ng)	4.0 µL
PCR DNA insert (45 ng)	2.6 µL
Milli-Q water	1.4 µL
Total volume	10.0 µL

Table 11. Reaction protocol for infusion reaction

5.29.7 Transformation of pQE-30-Xa + PE35 vector into competent M15 *E.coli* strain Transformation is an important step in the cloning process. In transformation, foreign DNA will be taken up by bacteria under laboratory conditions. The method here followed is a chemical transformation method using calcium chloride as described above.

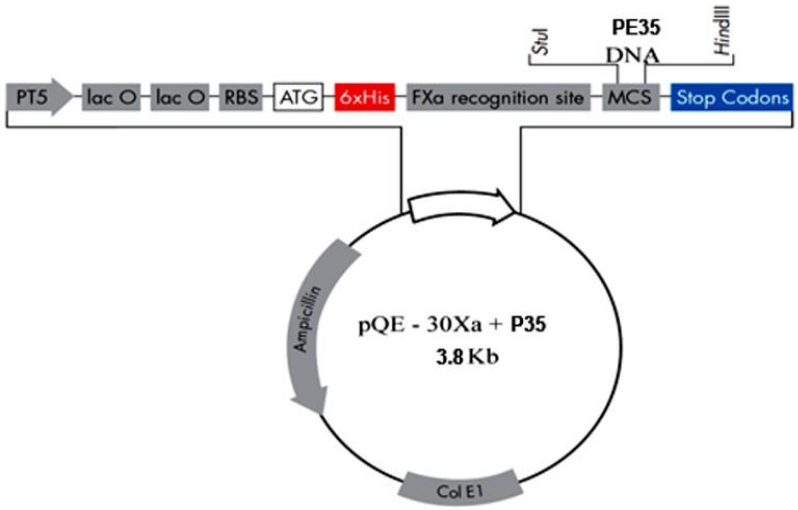

Figure 6: pQE-30-Xa + PE35 vector map, adapted from Qiagen

Recovery phase is where the heat shock competent cells were suspended in the sterile LB media and was incubated at 37 ^{o}C for 1 h. Then the cells were inoculated onto the selective LB plate. The competent cells, which are successfully transformed andexpressing the plasmid will grow on the selective LB agar plate.

Reagents required:

1. Luria-Bertani (LB) media (autoclaved)
2. 1 M $CaCl_2$ (filter sterilized)
3. 0.1 M $CaCl_2$ (filter sterilized)
4. 50 % Glycerol (sterilized by steaming)
5. 1 M $CaCl_2$ + 15 % glycerol (sterilized by steaming)
6. Sterile LB media, non-selective (Sterilized by autoclaving)
7. Sterile LB agar plate (ampicillin 100 µg / mL and kanamycin 25 µg / mL)

Competent cell preparation

1. Overnight culture of *E.coli* strain was diluted with sterile LB media to 1 % final concentration and incubated at 37 ^{o}C.
2. Cells were pelleted down when culture is in growth phase i.e. optical density (OD) of the culture was between 0.4 and 0.6 at 600 nm wavelength.
3. Then cells were re-suspended in 0.1 M $CaCl_2$ and were incubated at 4 ^{o}C for 30 mins.
4. The cells were centrifuged at 15,000 rpm for 10 mins at 4 ^{o}C.
5. Then the pellet was re-suspended in 1 M $CaCl_2$ with 15 % glycerol. Thus the bacterial cells were converted to the competent bacterial cells, which can take up the exogenous plasmid DNA. The cells will be competent for 6 months at -80 ^{o}C.

Transformation procedure

1. Plasmid DNA was added to competent cells and incubated at 4 ^{o}C for 30 min. Generally, 25 ng of plasmid DNA was recommended for 50 µL of the competent cells.

2. The cells were exposed to 42 ^{o}C for 90 s and immediately transferred to 4 ^{o}C, providing heat shock to the cells.

3. After heat shock, the cells were incubated with 750 µL of LB media at 37 °C for 1 h with gentle shaking.

4. The cells were centrifuged at 10,000 rpm for 3 min; the pellet was re-suspended with 300 µL of LB media. The 300 µL inoculums was inoculated onto selective LB agar plate (kanamycin 30 µg / mL and ampicillin 100 µg / mL) by spread plate method and was incubated at 37 °C for 24 h.

5. Transformed competent cells, which expressed plasmid containing antibiotic resistant gene were grown on the selective plate.

6. To confirm the transformation, plasmid was isolated from the clones on a selective LB agar plate. The isolated plasmid was subjected to restriction digestion with StuI and HindIII and the restriction product was subjected to 2 % agarose gel electrophoresis.

5.29.7 DNA sequencing

To confirm that there was no mutation in the insert DNA, the isolated vector constructs were subjected to DNA sequencing. The sequencing was performed based on the Sanger's dideoxy method in ABI 3100 - Avant Genetic Analyzer. With the infusion primers the PE35 insert DNA was amplified from the isolated plasmid DNA and was sequenced. The resulting sequence was analyzed by Bio-edit software.

5.29.8 Expression of recombinant PE35 in M15 (pREP4) *E.coli*

5.29.8.1 Optimization of recombinant PE35 expression

Expression of insert DNA in the pQE-30Xa vector is controlled by double lac promoter and T5 operator system. The allolactose, a metabolite of lactose, starts transcription of the lac operon. It's analog Isopropyl β-D-1-thiogalactopyranoside (IPTG) used in expression systems, due its advantage over the allolactose in being not

metabolized by *E.coli*, thus maintaining the concentration constant throughout the induction. IPTG binding to the lac operon and results in the release of tetrameric repressor from the lac operator and thus allows the binding of DNA polymerase to the T5 operator system and leads to the transcription of the gene. IPTG is. Expression of PE35 from M15 (pREP4) was standardized for concentration and time of IPTG induction (0.2 – 1 mM) and time for induction (2, 4, 6 and 16 h) at 30 ^{o}C. The conditions were examined and the optimal concentration and time were standardized and used further. After inducing with the respective conditions, 20 µL of broth was boiled with 5 µL of 5X Laemmli buffer and subjected to 10 % SDS –PAGE and visualized by Coomassie staining.

5.29.8.2 Purification of recombinant PE35

Purification was based on one step affinity purification using Ni-NTA (Nickel – Nitrilotriacetic acid) agarose beads.

Materials required

1. Ni-NTA (Nickel – Nitrilotriacetic acid) agarose beads
2. Protease inhibitor cocktail (PIC)
3. Lysis buffer: 50 mM sodium dihydrogen phosphate, 300 mM sodium chloride and 8 M urea with PIC, pH 8.0.
4. Wash buffer: 30 mM of imidazole in lysis buffer.
5. Elution buffer: 250 mM of imidazole in lysis buffer.

Consecutive 6 histidine residues (6X His tag) exhibits higher affinity towards the Ni-NTA. Due to the presence 6X His tag at N-terminal of the recombinant PE35 protein, it was bound to the Ni-NTA with higher affinity than other *E.coli* proteins. The bound PE35 was eluted by affinity displacement. After treating with *E.coli* lysate Ni-NTA agarose beads were washed with 25 mM imidazole buffer to remove any non-specifically bound proteins. Then PE35 was eluted with 250 mM imidazole buffer.

Preparation of M15 (pREP4) cell lysate:

After IPTG induction the cells were pelleted down by centrifugation at 7,500 rpm for 20 mins. Then the pellet was suspended in lysis buffer. The cell suspension was sonicated for 30 s for 3 cycles. To separate protein from cell debris, the whole content is centrifuged at 10,000 rpm for 30 mins. The supernatant was further purified.

Ni-NTA agarose beads were packed into a column. The column was then equilibrated with lysis buffer. The supernatant was passed through the equilibrated Ni-NTA column. To remove any non-specific proteins, the column was washed with 10 mL of wash buffer. Then bound the 6X His tag PE35 was eluted from the column by treating the column with 10 mL elution buffer. Throughout the process 0.2 mL / min flow rate was maintained. Then the fractions were examined by performing electrophoresis on a 10% SDS-PAGE gel to determine the fraction containing PE35.

5.29.9. In-Fusion reaction and transformation

In-Fusion reactions were carried out as per manufacture's instruction. In brief, reaction mixture of 10 µl volume in 0.2 mL, consisting of 5X In-Fusion HD Enzyme Premix, insert and vector (2:1 ratio), infusion enzyme and molecular grade water was incubated for 15 min at 50 °C (Thermocycler). The in-fusion product was added to the chemically competent cells (X1-Blue) thawed on ice. For 30 min cells were incubated on ice, followed by 45 s heat shocks transformation at 42 °C, and 750 µl LB broths was added to the cells. After 1 h incubation time cells were centrifuged and a volume of 200 µl LB broth was added. The culture was smeared on the LB plate supplemented with 100 µg/mL of ampicillin and incubated overnight at 37 °C.

5.29.10 Plasmid extraction:

The prominent colonies were picked up from the culture plates and allowed to grow for overnight, in tubes containing 5 mL of LB supplemented with ampicillin (100 µg/mL) with constant shaking speed of 250 rpm. The plasmids were eluted with Qiagen Miniprep Kit from 3 mL of culture was RE digested with HindIII and Xba1. PCR was for insert is carried over.

5.3 *Insilico* approach for identification interacting partners of haptoglobin:

Using haptoglobin (HP) protein sequence were submitted in different protein- protein interaction server like Biogrid, STRINGv9.1, intact and FpClass.

5.4 Galectin-1 gene knockdown by small interference RNA

Knockdown of galectin-1, in HUVEC and ARPE-19 cells was performed with DsiRNA. The efficacy of galectin-1 knock down was assessed by western blot. The sequences of the siRNA for galectin-1, 5′GCUGCCAGAUGGAUACGCUUCAAG3', 5'CUUGAAUUCGUAUCCAUCUGGCAGCUU-3 were purchased from IDT.

Cells were transfected with ICAFectin442 as per manufacturer's guidelines.

In previous day to transfection, cells were plated in 1 mL full growth medium and allowed to reach 70-80% confluence at the time of transfection (4 x 10^5 cells per well).

Transfection with DsiRNA complex

1. The growth medium was removed 30 min before transfection and 500 µL fresh medium with without serum was added.

2. 5, 10, 20 and 30 nM siRNA was made up in 100 µL of basal medium without antibiotics and serum.

3. Transfecting reagent (ICAFectin442) was vortexed and working solution were made up by mixing 4µL of ICAFectin 442 in 100 µL of basal medium containing neither serum nor antibiotics.

5. Both solutions were mixed together by pipette and incubated for 15 min at RT.

6. The entire volume is dispensed drop by drop into the wells and plates were swirled for homogenous suspension.

5.4 PCR for screening gene of Mycobacterial PE35.

Primers were designed using Primer3 (103). Each PCR reaction mixture was prepared for the 10 μL reaction volume.

It consists of 200 nM of each of the forward (5'CACGCAAGTGAGCGACAAC3') and reverse primers (5'GGATGCCCTCCGATGTGAAC3'), 2× EmeraldAmp GT PCR Master Mix, 50ng of DNA and RNase-free water. The PCR reaction was carried out with a initial denaturation step at 95 ºC for 10 min, 15 s for next 39 cycles, annealing step at 58 ºC for 30 s and 72 ºC for 1 min, the final extension step is carried out for 5 min at 72 °C in a thermal cycler (Eppendrof, U.S.A.). Both the positive control (reaction mixtures with *M. tuberculosis* DNA) and negative control (without template DNA) were run along with samples. The products were resolved in 2 % agarose gel with ethidium bromide in TAE buffer and imaged.

5.5.1 RNA extraction

Principle

TRI reagent is a monophasic solution of guanidine thiocyanate and phenol. This solution aids the in the instant RNase activity. Biological samples are homogenized or lysed in TRI Reagent. The chloroform is subsequently added for separating the homogenate into aqueous and organic phase. RNA is retained in the aqueous phase, DNA is partitioned to the interphase, and protein to the organic phase. The propanol addition to aqueous phase, precipitates RNA from the solution. The RNA isolated is appropriate for any downstream applications such as RT-PCR.

Materials required

- TRIzol (Sigma)
- DNA RNase free H_2O, tips and vials
- Cooling centrifuge

- Chloroform (Merck)
- Iso propanol (Merck)
- Ethanol (Merck) – 70 % made in DEPC treated H_2O

Procedure:

1. Cells were trypsinised, transferred to tubes and centrifuged at 1500 rpm. The pellet was incubated for 5 min at RT with 1 mL of TRIzol reagent.
2. 200 µl of chloroform was added to these tubes, invert mixed for 15 s and incubated at RT for 3 min.
3. These tubes were centrifuged at 12000 rpm for 15 min.
4. The aqueous layer was carefully aspirated into a new tube without disturbing the protein layer.
5. Iso-propanol (2- propanol -500 µl) was added and mixed well by inverting and incubated at RT for 10 min and then centrifuged at 12000 rpm for 10 min..
6. The supernatant was decanted and 1 mL of 70 % alcohol was added to the pellet and incubated at RT for 2-3 min.
7. These tubes were centrifuged at 14000 rpm for 5 min and the supernatant was discarded air dried for 3 min.
8. Finally, 20 µl of RNase free H_2O was added and stored at -80°C (2 µl was taken for quantification and gel electrophoresis)

5.5.2 Conversion of RNA to cDNA:

RNA was converted to cDNA using iScript RT-PCR Kit (Bio-Rad) following the manufacturer's protocol using the reagents provided in the kit.

Procedure

Step 1: The following reaction mix was prepared

RNA Template	**- X µl (1 µg)**
5x I script Reaction Mix	-4 µl
Reverse Transcriptase	- 1 µL
Nuclease free water	- make up to 20 µl

Table 12. cDNA conversion reaction mixture

Step 2: The following protocol was followed for cDNA conversion

Temperature	Duration
25 ˚C	5 min
42 ˚C	30 min
85 ˚C	5 min
4 ˚C	∞

Table 13. cDNA conversion protocol

Steps	**Temperature and duration**	
Initial denaturation	95 ºC, 10 min	
Denaturation	95 ºC, 1 min	36 times
Annealing	60 ºC, 1 min	
Extension	72 ºC, 1 min 30 s	
Final extension	72ºC, 5 min	
Hold	4 ºC at ∞	

Table 14. PCR reaction protocol for amplification of IL-6, IL-8, MCP-1, TNF-α, haptoglobin, complement C3, galectin-1, 18S rRNA and VEGF

Steps	Temperature and duration	
Initial denaturation	95 ºC, 2 min	
Denaturation	95 ºC, 30 s	30 times
Annealing	58.3 ºC, 30 s	
Extension	72 ºC, 30.0 s	
Final extension	72ºC, 5 min	
Hold	4 ºC at ∞	

Table 15. PCR reaction protocol for amplification of CTR1

5.5.3 Quantitative PCR

S.No	Target	Forward Primer (5'-3')	Reverse primer (5'-3')
1.	*IL-6*	TGCAATAACCACCCCTGA	ATTTGCCGAAGAGCCCTCAG
2.	*IL-8*	CCAAACCTTTCCACCCCA	AACTTCTCCACAACCCTCTG
3.	*MCP-1*	CCCCAGTGACCTGCTGTT	AGCTTCTTTGGGACA CTTGC
4.	*TNF – α*	GGGAGAGAAGCAACTAC	TCAGTATGTGAGAGGAAGAGAA
5.	*18 S rRNA*	GTGGAGCGATTTGTCTGG	GGACATCTAAGGGCATCCACAG
6.	*Galectin-1*	CTCAAACCTGGAGAGTGC	CGTTGAAGCGAGGGTTGAAG
7.	*Haptoglobin*	CCCCGAAAAGAAGACAC	GATCCCAGTCGCATACCAGG
8.	*Complement C3*	CTGTCCATCACCACCGAC	TTTTACCACCAGCGAGCCC
9.	*VEGF*	CGGTATAAGTCCTGGAGC	GCCTCGGCTTGTCACATCTG
10.	*CTR1*	CTTAGACTGGCTGCCAAA	AGAGTAAGGGGGGGCCAAAG

Table 16. List of primers used in the study

S.No	Target	Forward Primer (5'-3')	Reverse primer (5'-3')
1	*PE35*	CACGCAAGTGAGCGACAAC	GGATGCCCTCCGATGTGAAC
2	*FAD*	GGAGAAAACCGAACCCAAGC	GATCTTAACCGTCACCCCCT

Table 17. List of *Mycobacterial* primers used in the study

RNA isolation was carried out with the TRIzol reagent (Sigma) and converted to cDNA by using IScript Bio-Rad Kit, as instructed in standard protocols. Quantitative

PCR was carried out with SYBR Green on the Roche light cycler real-time PCR system. Primers were designed as per Basu-Thronton et al (104).

Each PCR reaction mixture was prepared for 10 μL containing 200 nM of each of the forward and reverse primers, 2× SYBR Green PCR Master Mix, and 50 ng of cDNA and RNase-free water. The PCR reactions steps were as follows: Initial denaturation at 95 ºC for 10 min, and 15 s for the next 39 cycles, annealing was at 60 ºC for 30 s and extension was at 62 ºC for 1 min. All reactions were performed in triplicate and normalized to internal control β tubulin mRNA (105). The triplicate average of Ct values for the internal control gene 18S rRNA (Internal control Gene Experimental (IE), and Internal control Gene Control (HC)) and the gene of interest (Tested Experimental (TE), Tested Control (TC)) at control and various treatment conditions were calculated. And then difference between the gene of interest and internal control gene at control condition was calculated (TE-IE= ΔCTE). Similarly difference between the gene of interest and internal control gene at various treatment conditions was calculated (TC-IC = ΔCTC). The difference change in mRNA expression of the gene of interest and of internal control gene (ΔCTE-ΔCTC) was calculated as Double Delta Ct Value (ΔΔCt) and 2^-ΔΔCt was the expression fold change.

Relative expression was presented using the $2^{-\Delta\Delta CT}$ method as follows

C_T	:	Cycle threshold value
ΔC_T	:	Gene C_T – β-tubulin C_T
Calibrator	:	Control sample ΔC_T
$\Delta\Delta C_T$	:	ΔC_T – Calibrator
Fold Change	:	$2^{-\Delta\Delta CT}$

5.6 Statistical analysis

Results are reported as the mean ± standard error of mean. Box whisker plots were generated through graph pad prism (Version 5.0) from the ELISA data. These plots show a statistical summary with the median, quartiles and range. Student *t*-test was

used to compare the mean of protein levesl between the Eales' disease patients and control serum samples. The Chi-square test was used to compare the number of individuals with different haptoglobin phenotypes among the two groups. Two-way ANOVA along with Bonferroni posttests was used to compare the mean of fold changes among LPS treated ARPE-19 and haptoglobin co-treated cells. One-way ANOVA along with Tukey posttest was used to compare the mean of fold changes after comparison.

6. RESULTS

Objective.1. To identify the differentially expressed proteins in serum samples of Eales' disease patients by 2D electrophoresis (2 DGE) and native PAGE analyzing the differentially expressed spots by mass spectrometry.

6.1.1 Identification of the differentially expressed spots in serum of Eales' disease patients by Two-dimensional gel electrophoresis (2DGE) of serum sample - cup loading.

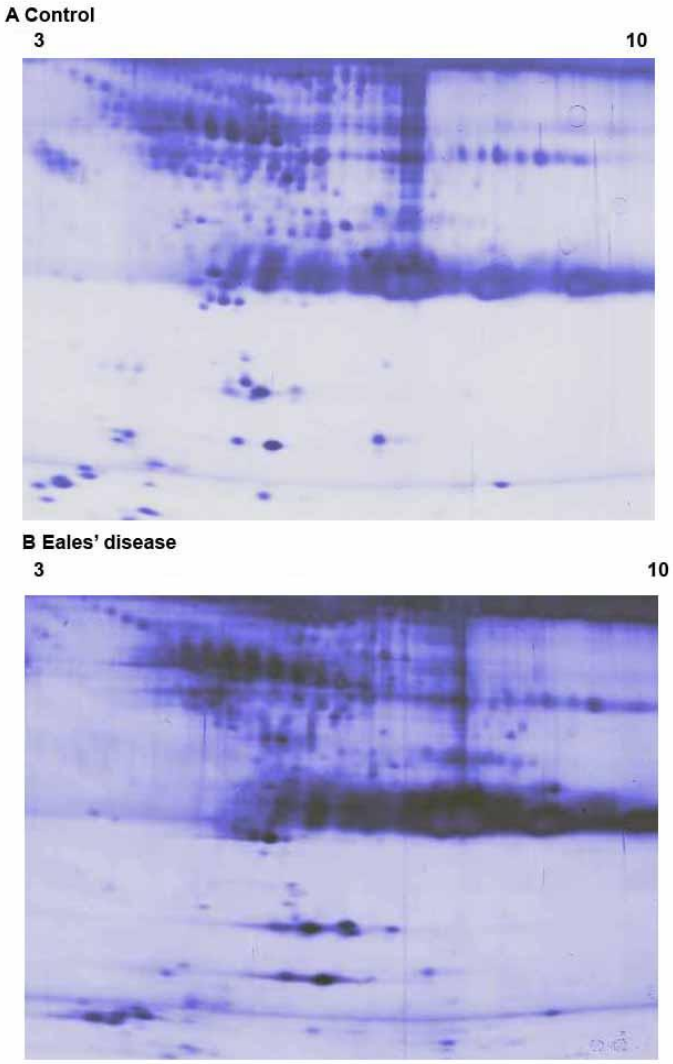

Figure 7: Representative 2DGE image of undepleted serum samples.
Pooled serum obtained from the control subject (n=3) and Eales' disease patients (n=3) stained by colloidal coomassie stain were resolved in 2DGE.

Serum samples obtained from the control subjects and Eales' disease patients were initially screened with 2DGE 3-10 Immobilized pH gradient Nonlinear (IPG - NL) strips. Protein samples of 150 µg were loaded in strips and isoelectric focusing was carried out with 40000 Voltage hours. The strips were equilibrated and resolved in 10 % SDS page gel and later stained with colloidal coomassie stain (Figure 7).

6.1.2Analysis by PDquest

Three spots corresponding to haptoglobin such as 3201, 2402 and 3194 were found to be increased in comparison to the control samples. Spot 5601, corresponding to serum amyloid protein was found to be 3.6 fold increased in comparison to control (Figure 8)

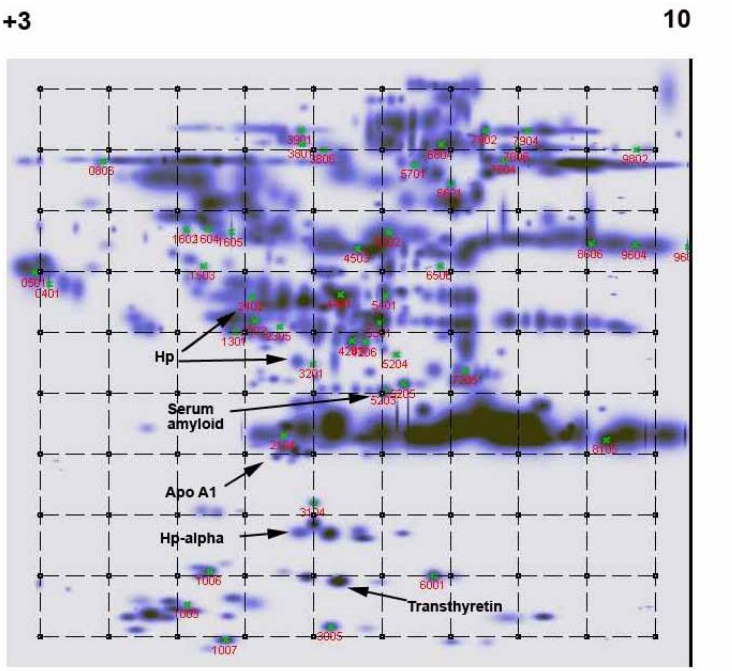

Figure 8: Master gel image for undepleted serum samples resolved by 2DGE. Gel images of control serum and Eales' disease serum were compared with standard 2DGE pictures in the Swiss 2Dpage. Proteins like haptoglobin and serum amyloid protein were increased in Eales' disease serum.

6.1.3 2D gel electrophoresis (2DGE) of albumin and immunoglobulin depleted serum samples

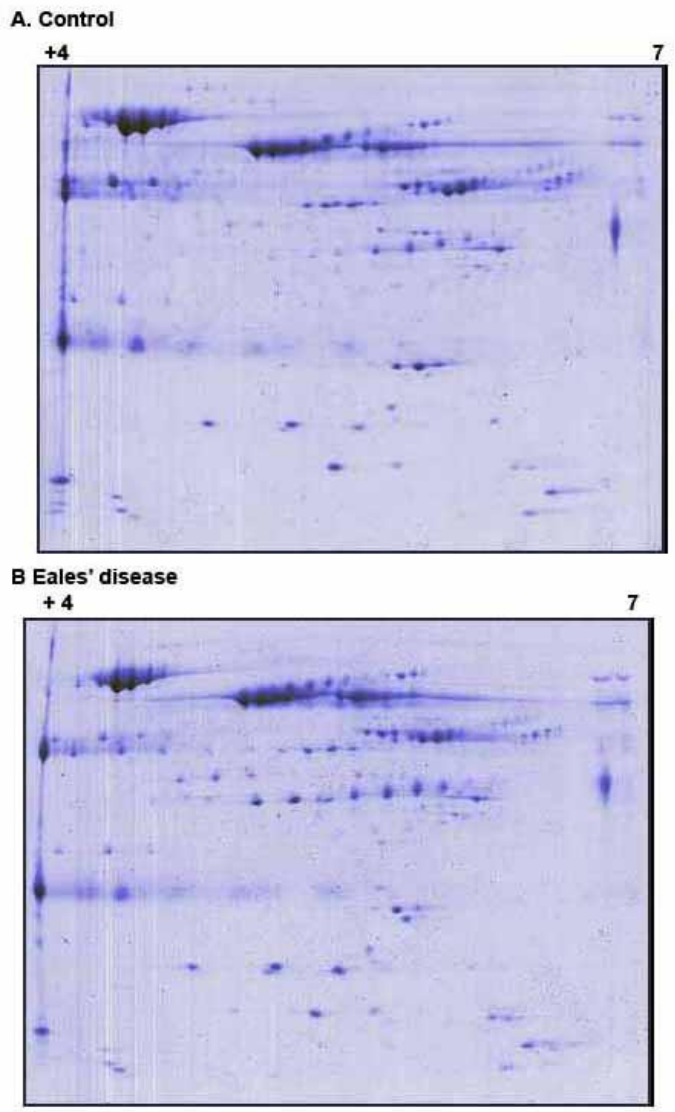

Figure 9: Representative 2DGE image of albumin depleted serum samples. 2DGE of pooled serum obtained from the control subject (n=3) and Eales' disease patient (n=3) stained with colloidal coomassie stain.

Serum samples of control subjects and Eales' disease patients were albumin and immunoglobulin depleted with the depletion kit (PROT-BA Sigma, CA, USA). Protein samples of 150 μg concentrarion were rehydrated in the IPG strips 4-7 NL and

isoelectric focused. The IPG strip were equilibrated and resolved in 10 % SDS page. After electrophoresis, gels were stained with colloidal coomassie stain (Figure 9).

6.1.4 Comparison by PDquest

Three spots corresponding to haptoglobin such as 3202, 3303 and 4201 were found to be increased in comparison to the control samples (Figure 10).

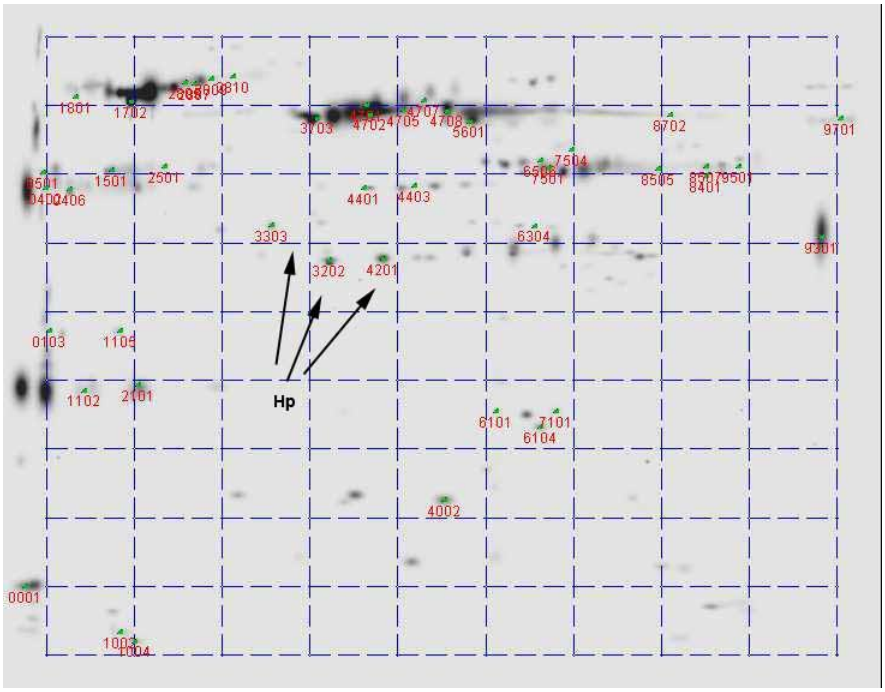

Figure 10: Master gel image of albumin depleted serum samples, resolved by 2DGE. The pictures were compared with standard 2DGE pictures in Swiss 2Dpage. Haptoglobin was found to be increased in Eales' disease serum.

6.2 Screening for 88 kDa bands in serum of Eales' disease patients and mass spectrometric identification of 88 kDa band

Serum samples from control subjects and Eales' disease patients were screened. The presence of 88 kDa bands in serum samples of Eales' disease patients is shown in Figure 11. It was identified in the alpha 2 globulin region of the gel and the regions containing this band were excised and ingel tryptic digested.

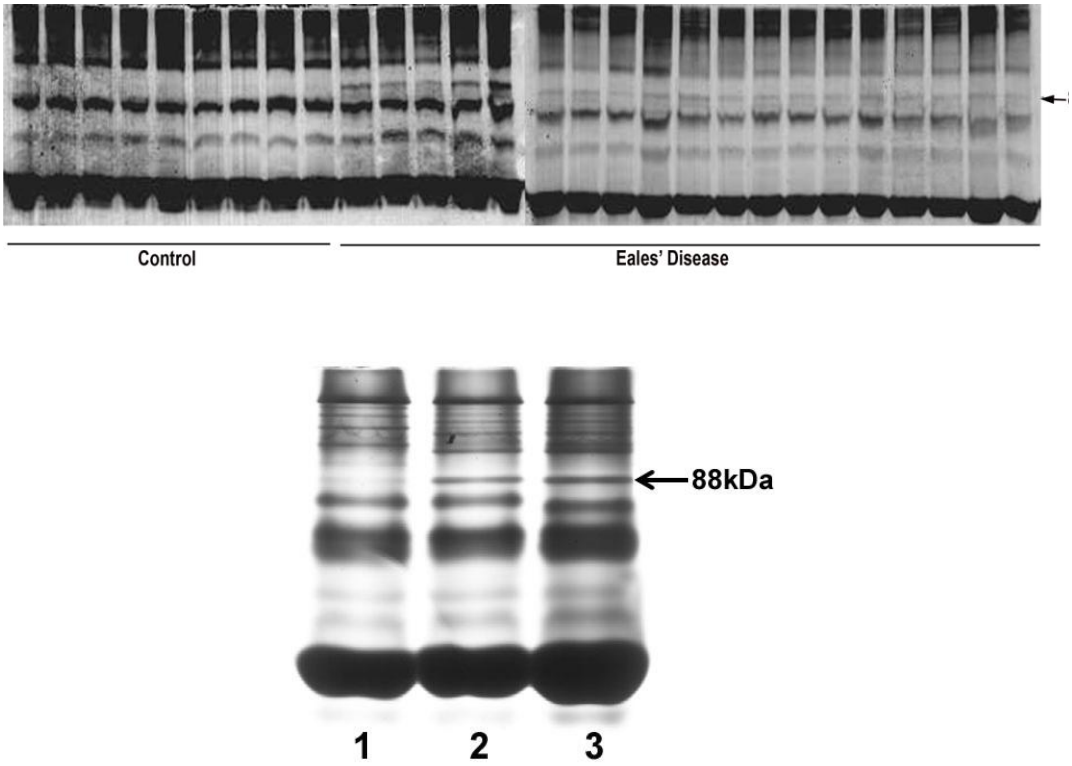

Figure 11: The representative image of serum proteins resolved in native PAGE. Samples were obtained from control subjects and patients with Eales' disease. Protein of 50 μg was resolved on a 7.5 % polyacrylamide gel under non denaturing conditions and subsequently stained with colloidal coomassie stain. Lane 1 depicts sample from healthy volunteers - control and whereas the lane 2 and 3 represents the samples obtained from patient with Eales' disease. The presence of the 88 kDa band is identified in the lane 2 and 3, indicated by an arrow in the image.

6.2.1 Identification of complement C3 by MALDI MS

Samples were resolved in native page and 88 kDa band was tryptic digested. Supernatant (10μL) was analyzed by peptide mass fingerprinting using MALDI. The peptide masses obtained by MALDI analysis were searched against protein databases. Complement C3b fragments were identified with scores greater than 56 and were considered statistically significant ($p<0.05$) by the MASCOT analysis (Figure 12) .

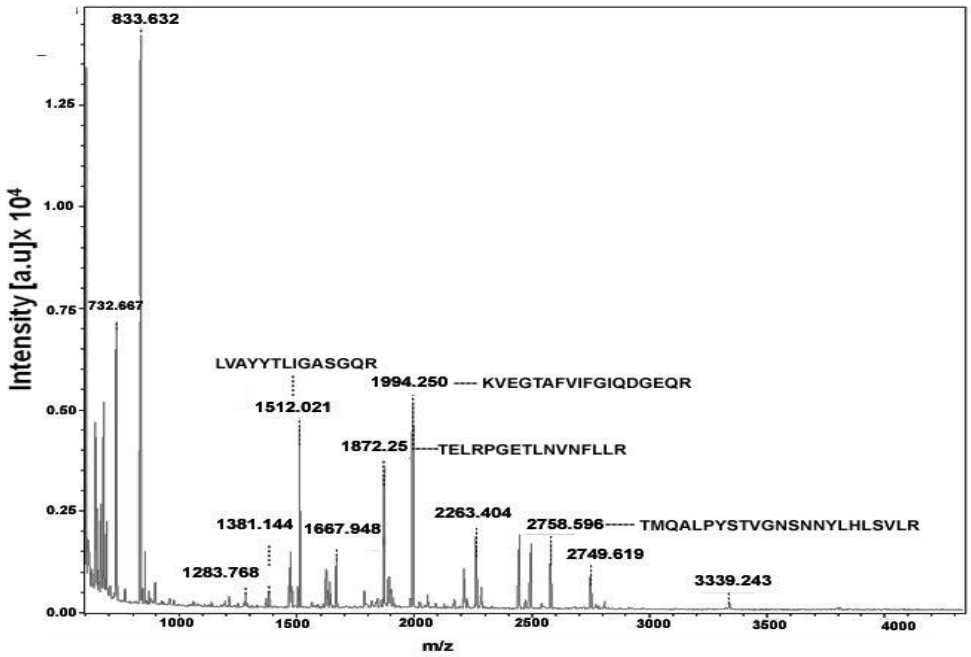

Figure 12: MALDI - MS spectrum of the 88 kDa protein. Peptides identified in the analysis were indicated in the spectrum. Peptides with corresponding m/z values of complement C3 are given in the spectrum.

6.3 Nano liquid chromatography–electrospray ionization–tandem MS (LC-ESI-MS/MS) and data analysis

6.3.1 Identification of 88 kDa band protein as complex of proteins.

The reproducibility of LC-ESI-MS/MS analysis was confirmed with triplicates of the 88 kDa band excised from 3 different ED patient serum samples. The analysis revealed a total number of 42 proteins, including complement and coagulation components, immunoglobins and transport proteins. Most of these proteins belong to serine proteases of chymotrypsin family and serpins family. The hits were identical in all the three independent samples analyzed. Among these hits highest scoring proteins hits were haptoglobin, an iron-binding protein that helps in hemoglobin clearance and complement C3. In addition, the proteins in complement pathway, regulatory proteins and blood coagulation pathway were also obtained (Table 18).

Protein Accession Protein Description	Protein Score	Protein. avgMass	Protein Seq Cover (%)	Protein Matched Peptide IntenSum
P00738 Haptoglobin	66603.21	45889.68	66.26	1.39E+07
P02768 Serum albumin	52063.33	71362.71	77.01	8189692
P00739 Haptoglobin related protein	37747.57	39542.86	48.56	7721190
P02647 Apolipoprotein A I	26517.27	30777.87	53.18	546066
P02787 Serotransferrin	20788.27	79345.08	57.74	1396145
P01024 Complement C3	19443.52	188688.1	53.94	4639550
P01834 Ig kappa chain C region	15834.84	11779.94	80.19	147108
P01861 Ig gamma 4 chain C region	14001.72	36453.84	32.11	279043
P00751 Complement factor B	8444.882	86901.64	31.41	934103
P01876 Ig alpha 1 chain C region	7561.822	38510.08	36.83	331059
P01009 Alpha 1 antitrypsin	7245.382	46907.71	51.44	308399
P0CG06 Ig lambda 3 chain C regions	6870.708	11408.59	69.81	124458
P02743 Serum amyloid P component	6674.922	25501.21	26.46	53914
P01857 Ig gamma 1 chain C region	6630.649	36619.19	42.12	58721
P02790 Hemopexin 2	5692.093	52417.79	39.18	56497
P02749 Beta 2 glycoprotein 1	5124.225	39609.83	36.23	67124
P00450 Ceruloplasmin 1	3944.894	123060.8	19.62	69285
P04004 Vitronectin	3442.725	55104.04	16.74	48615
P02652 Apolipoprotein A II	3410.937	11289.09	46	70066
P01877 Ig alpha 2 chain C region	3287.537	37324.73	35.29	20379.76
P10909 Clusterin	2461.443	53064.97	28.73	43448
P05155 Plasma protease C1 inhibitor	1949.719	55382.4	19.8	56143

P19823 Inter alpha trypsin inhibitor	1673.244	106919.8	18.82	77512
P0C0L5 Complement C4 B	1384.759	194291.5	19.09	0
P0C0L4 Complement C4 A	1384.759	194382.5	19.15	40370
P19827 Inter alpha trypsin inhibitor	1229.482	101845.5	12.51	49434
P01011 Alpha 1 antichymotrypsin	1197.121	47822.05	17.26	14536
P04196 Histidine rich glycoprotein	1064.669	60547.83	7.81	15086
P35858 Insulin like growth factor binding protein complex	991.679	66776.41	17.52	9720
P27169 Serum paraoxonase arylesterase	941.1029	39902.45	15.49	22358
P22792 Carboxypeptidase N 2	909.9385	61412.12	14.86	21053
P51884 Lumican	839.5626	38771.22	19.23	15911
P31276 Homeobox protein Hox C13	810.32	35778.02	7.27	295572
P01019 Angiotensinogen	684.5562	53439.43	13.81	10974
P00747 Plasminogen	681.78	93306.41	22.59	29104
P05160 Coagulation factor XIII B	603.5076	77791.87	10.44	15752
P00734 Prothrombin	442.2777	71519.66	10.45	16260
P29622 Kallistatin	422.3022	48713.13	18.27	8055
P06396 Gelsolin	342.4955	86096.82	10.23	18680
P36955 Pigment epithelium derived factor	173.386	46483.34	11. 96	10216.5
P01031 Complement C5 OS	89.9455	190016.3	2.8	10648
P03952 Plasma kallikrein	63.7332	73479.81	3.29	11247

Table 18. List of proteins identified in 88 kDa band by ESI LC MS with their characteristics.

Functional Annotation Chart was used to study the proteins which are significantly enriched with a modified Fisher's exact test (EASE score). In this analysis acute phase proteins and complement activation pathways were significantly enriched (Table 19).

Term	Count	%	P Value	List Total	Fold Enrichment	Bonferroni	FDR
GO:0002526 acute inflammatory response	13	35.13	4.96E-18	35	51.27	4.33E-15	7.70E-15
hsa04610: Complement and coagulation cascades	11	29.72	1.93E-15	18	45.033	2.26E-14	1.21E-12
GO:0004866 endopeptidase inhibitor activity	10	27.02	2.47E-11	31	28.88	2.89E-09	2.82E-08
GO:0030414 peptidase inhibitor activity	10	27.02	4.01E-11	31	27.37	4.69E-09	4.58E-08
GO:0032101 regulation of response to external stimulus	10	27.02	1.39E-10	35	24.30	1.22E-07	2.16E-07
GO:0004857 enzyme inhibitor activity	11	29.72	2.67E-10	31	17.06	3.12E-08	3.05E-07
GO:0006954 inflammatory response	14	37.83	4.12E-13	35	16.64	3.60E-10	6.40E-10
GO:0009611 response to wounding	18	48.64	1.14E-15	35	13.12	9.70E-13	1.72E-12
GO:0005615 extracellular space	24	64.86	6.57E-22	35	12.79	4.66E-20	6.82E-19
GO:0006952 defence response	17	45.94	2.82E-13	35	10.68	2.47E-10	4.39E-10
GO:0044421 extracellular region part	25	67.56	4.86E-20	35	9.51	3.45E-18	5.04E-17
GO:0048878 chemical homeostasis	10	27.02	3.34E-06	35	7.5	0.002917	0.00519
GO:0005576 extracellular region	34	91.89	7.07E-26	35	6.17	5.02E-24	7.34E-23
GO:0042592 homeostatic process	11	29.72	1.02E-05	35	5.66	0.008838	0.015771
GO:0006508 proteolysis	12	32.43	3.27E-05	35	4.40	0.028184	0.050782

Table 19. Functional Annotation table for list of proteins identified in 88 kDa band by in PANTHER software. In statistical overrepresentation test of PANTHER software complement activation pathway ($p<0.05$) was found to be highlighted (Figure 13).

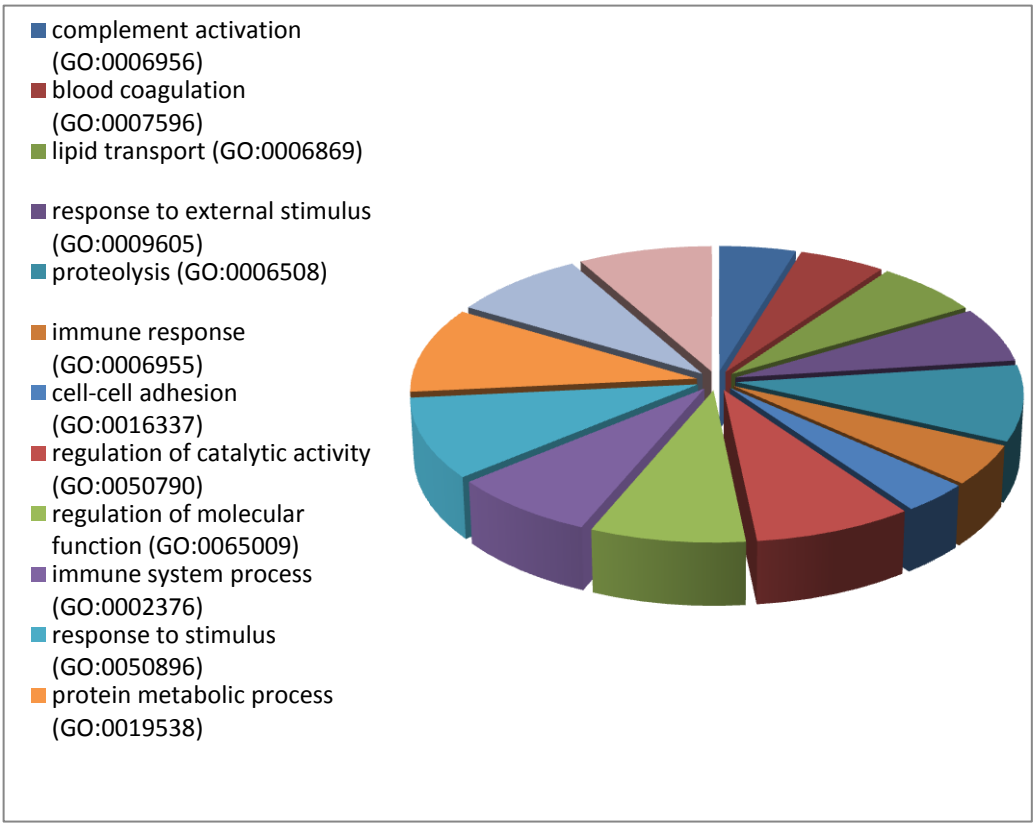

Figure 13: PANTHER analysis of biological pathway with the proteins identified in 88 kDa band in serum of Eales' disease patients.

6.3.2 Purification of 88 kDa protein from Eales disease patient's serum by preparative electrophoresis:

Serum samples of Eales' disease patients were resolved in the preparative scale electrophoresis under native condtions for identifying the presence of the 88 kDa protein and for purification. The fractions, positive for 88 kDa were tryptic digested and analyzed by LC-ESI-MS/MS (liquid chromatography–electrospray ionization–tandem MS). The analysis revealed hits of haptoglobin, complement C3 and galectin-1 along with other proteins in all the three samples (Figure 14 & Table 20).

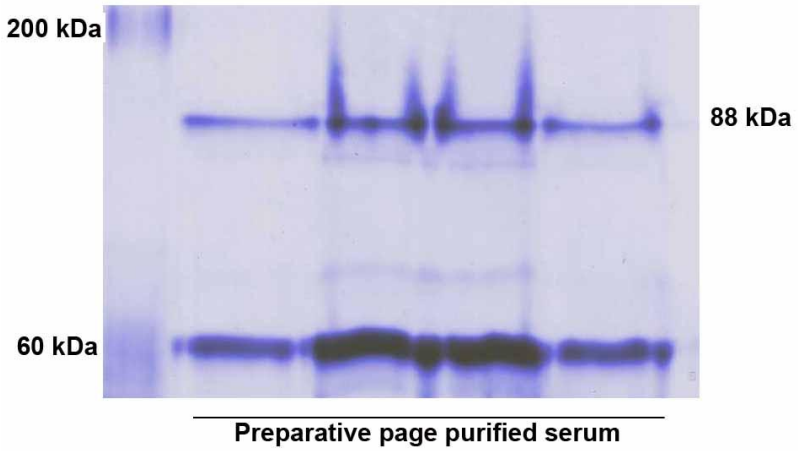

Figure 14: Serum samples of Eales' disease patients were fractioned in preparative native page for the identification of the 88 kDa band.

Protein Entry protein Description	Protein score	Protein avg Mass	Protein seq Cover (%)	Protein Matched Peptide Inten Sum
P00738 **Haptoglobin**	2059.269	45889.68	25.12	99888
P01024 **Complement C3**	2494.473	188688.1	36.68	372557
P02768 **Serum albumin**	4208.022	71362.7109	36.78	2612830
P02787 **Serotransferrin**	3639.538	79345.0824	41.69	690242
P02790 **Hemopexin**	1126.671	52417.7931	27.06	142448
P02763 **Alpha 1 acid glycoprotein 1**	289.1357	23739.6925	8.46	20653
P16402 **Histone H1**	141.6171	22349.921	9.5	36682
Q9UKV3 **Apoptotic chromatin condensation inducer in the nucleus**	76.6768	152260.852	7.38	28780
Q5T200 **Zinc finger CCCH domain containing protein 13**	11.8571	197319.921	0.48	988

Table 20. The list of proteins identified with ESI MS of 88 kDa positive fractions in preparative native page electrophoresis of the Eales' disease serum. Uni-Prot accession numbers are listed along with the PLGS scores, sequence coverage and intensity.

6.3.3 Identification of purified 88 kDa protein as haptoglobin, complement C3 and galectin-1 by ESI-MS

The purified 88 kDa protein fraction was subjected to in-sol tryptic digestion followed by LC-ESI-MS/MS analysis. This analysis yielded only three hits, namely haptoglobin, complement C3 and galectin-1 as shown in (Table 21) and in (Figures 15, 16 and 17). The reproducibility of the analysis was ascertained by analyzing samples in three sets. The presence of only three hits highlights the purity of the sample.

It is notable that the analysis of in-gel tryptic digested 88 kDa band from Eales' disease patient serum and the in-sol tryptic digested purified 88 kDa fraction gave the similar hits of haptoglobin and complement C3, along with galectin-1.

Protein Accession & Protein Description	Protein score	Protein. Avg Mass	Protein Seq Cover (%)	Protein Matched Peptide Inten Sum
P00738 Haptoglobin	1995.474	45889.68	57.14	580473
P01024 Complement C3	783.7782	188688.1	28.26	650537
P09382 Galectin 1	9758.473	15057.8861	76.3	766672

Table 21. The list of proteins identified with ESI MS of the 88 kDa protein in the ED serum. Uni-Prot accession numbers are listed along with the PLGS scores, sequence coverage and intensity.

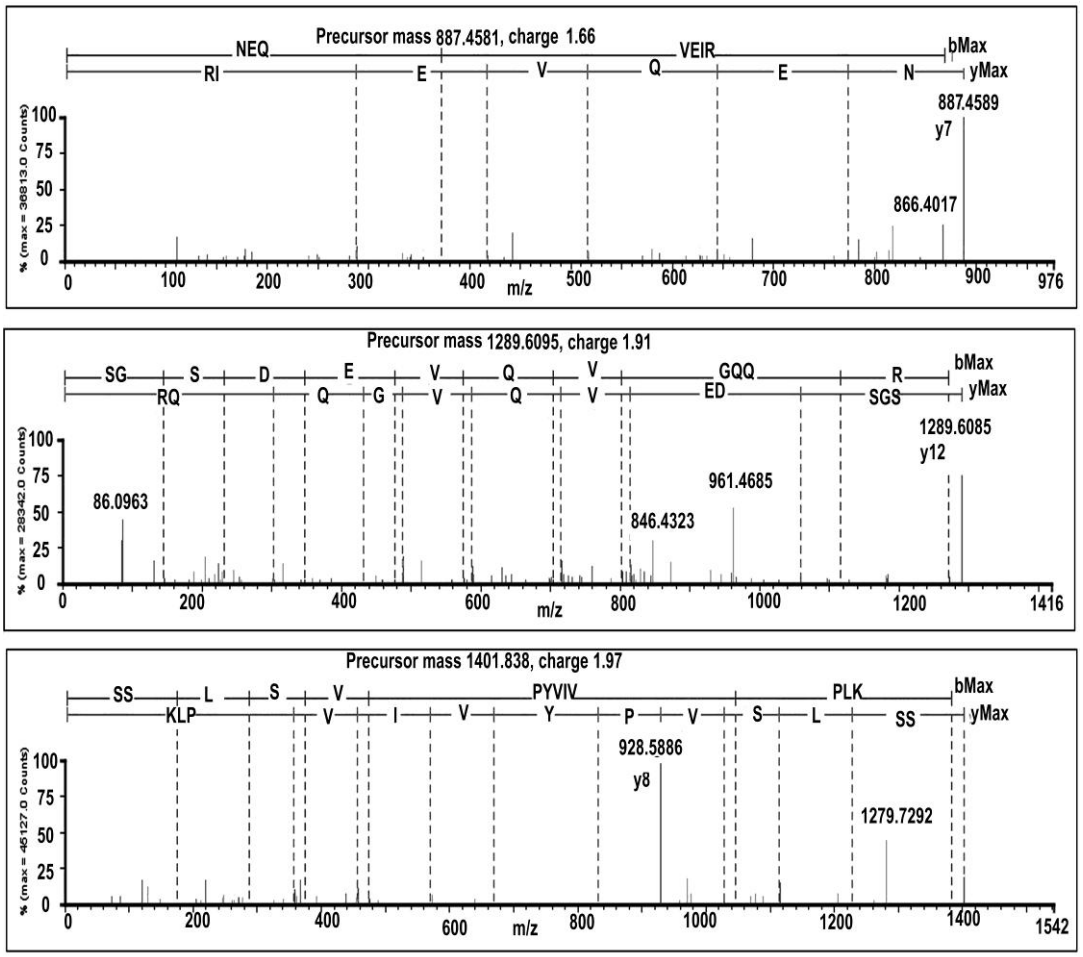

Figure 16: The MS MS spectrum from ESI MS for the second top scoring hit (complement C3) of the 88 kDa protein. Three unique peptides of complement C3 are identified from the precursor mass of 887.4581- NEQVEIR, 1289.6085 - SGSDEVQVGQQR and 1401.838- SSLSVPYVIVPLK.

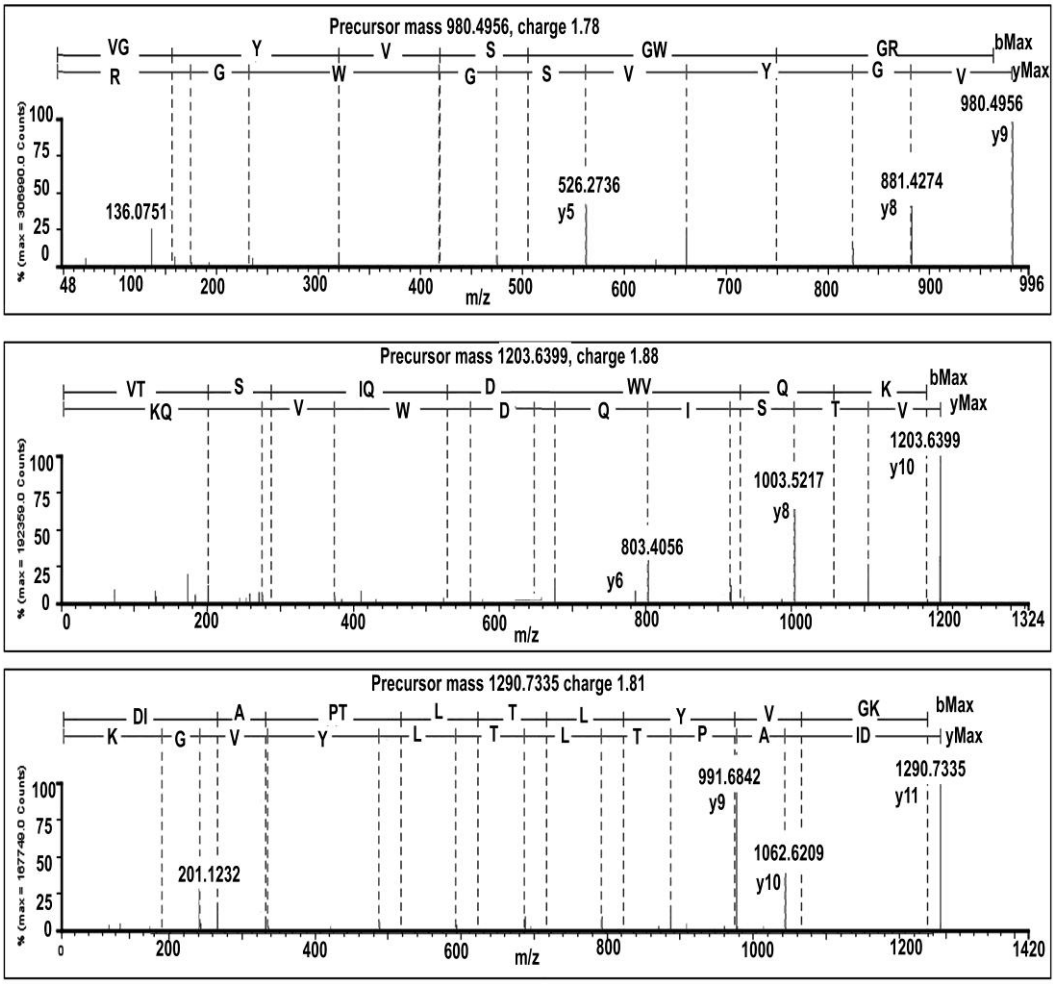

Figure 15: The MS/ MS spectrum from ESI MS for the top scoring hit - haptoglobin in purified 88 kDa protein. Three unique peptides of haptoglobin are identified from the precursor mass of 980.4956- VGYVSGWGR, 1203.6399 - VTSIQDWVQK and 1290.7335-DIAPTLTLYVGK. All these peptides occur with high intensity

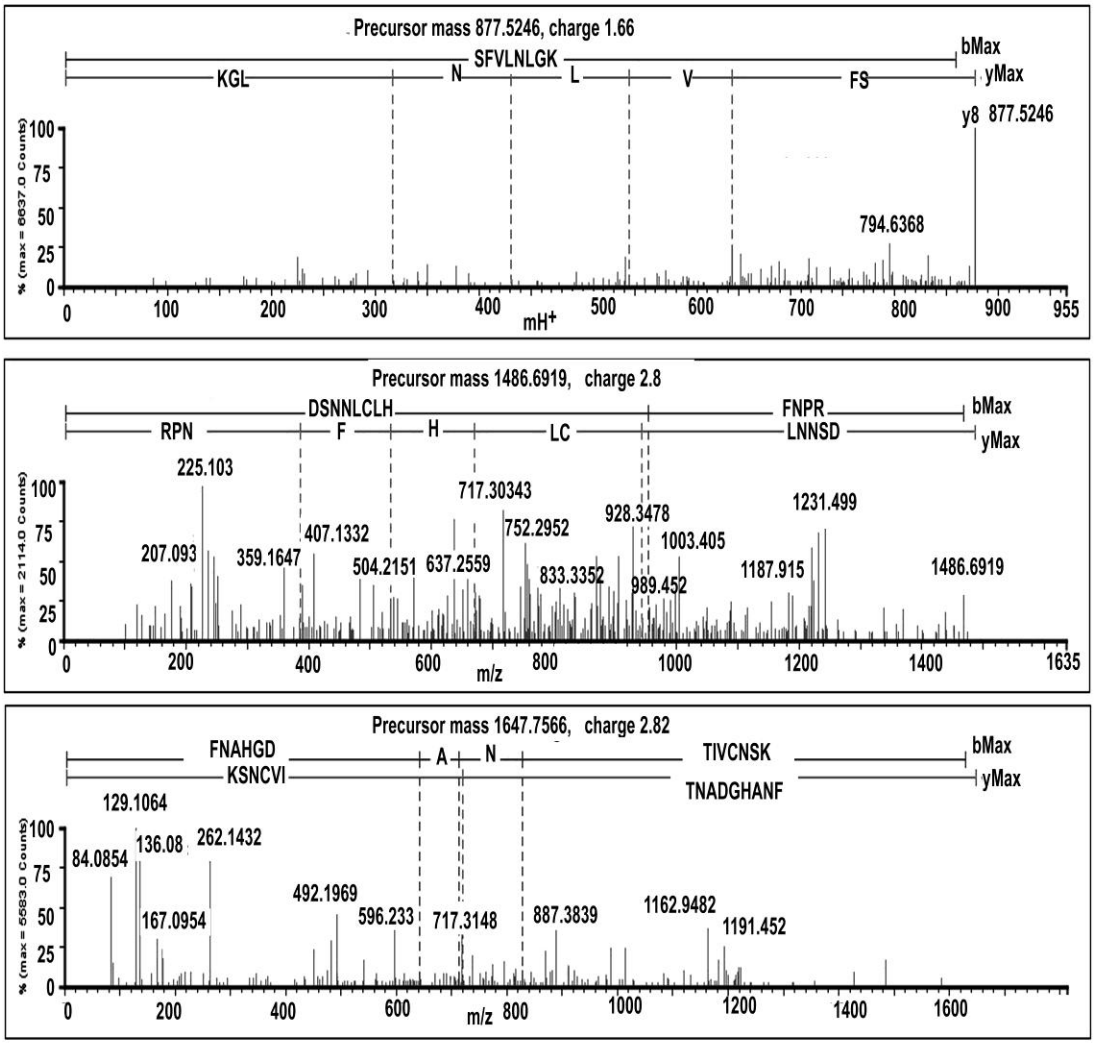

Figure 17: The MS MS spectrum from ESI MS for the third top scoring hit - galectin-1 in 88 kDa protein. Three unique peptides of galectin-1 are identified from the precursor mass of 877.5246-SFVNLGK, 1486.6919 -DSNNLCHFNPR and 1647.7566- FNAHGDTIVCNSK.

Objective 2: To correlate the identified protein with the disease.

6.4 Validation of the major protein identified:

Expression levels of the top scoring proteins identified in purified 88 kDa protein were estimated by ELISA in serum samples from Eales' disease patients (n=20) and healthy control subjects (n=20) and also compared. Serum levels of haptoglobin complement C3, and galectin-1 proteins were estimated by ELISA**.** Elevated levels of haptoglobin, decreased galectin-1 level and unaltered C3 levels were found in the serum of Eales' disease patients in comparison to control subjects' serum. Levels of complements C3 were unaltered and statistically non-significant. Serum galectin-1 levels were found to be significantly lower in Eales' disease samples when compared to controls. Further, the levels of haptoglobin in serum were found to be significantly increased in comparison to control subjects (Figure 18).

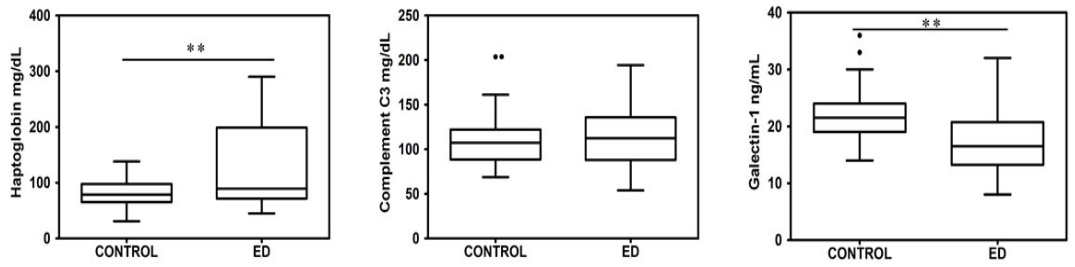

Figure 18: Serum levels of haptoglobin, complement C3, and galectin-1 proteins were estimated by ELISA. The levels of haptoglobin in serum were found to be significantly increased in Eales' disease (ED) patients in comparison to control subjects. (n -20, the levels of haptoglobin in Control-80.72 ± 25.33, ED-131.12 ± 72.88, p=0.008). Unaltered levels complement C3 in control serum 330.21 ± 49.4 mg/dL; Eales' disease patients serum 340.1294 ± 42.48541 mg/dL and difference among these groups (n-20) was non-significant. Significantly lowered serum galectin-1 levels of Eales' disease patients in comparison to controls (n-20, Control-22.50 ± 5.15 ng/dL, ED- 17.25 ± 5.46 ng/dL, p=0.003).

6.5 Comparative levels of top scoring 88 kDa proteins estimated by ELISA, with MS quantified levels in partially purified 88kDa protein and purified 88 kDa proteins.

Levels of haptoglobin complement C3 and galectin-1 were measured in serum by ELISA and compared with the levels measured by MS by HI3 analysis of 88 kDa protein band and of purified 88 kDa protein fraction (Table 22). Note: Mass spectrometry based protein estimation in whole serum (immunodepleted for albumin and immunoglobin) yielded 227 mg/dL of haptoglobin and 100 mg/dL of complement C3 meanwhile galectin-1 was undetected.

Protein Accession protein Description	Serum levels ELISA (n=20)	Protein in 88 kDa protein resolved in Preparative PAGE (n=3)	88 kDa Purified protein (n=3)
P00738 Haptoglobin	131.12 ± 72.88 mg/dL	48.76 ± 11.25 ng/µL	6.6 ± 0.02ng/µL
P01024 Complement C3	113.9 ± 37.49 mg/dL	12.2 ± 2.415ng/µL	2.95 ± 1.09ng/µL
P09382 Galectin 1	17.25 ± 5.46 ng/mL	0.27 ± 0.06 ng/µL	1.8 ± 0.8ng/µL

Table 22. The three proteins identified in purified 88 kDa protein were measured in serum and in 88 kDa band. Amount of haptoglobin was found to be increased serum of Eales' disease patients and in 88 kDa protein.

6.6. Co-immunoprecipitation experiments

Mass spectrometric identification of complement C3 interacting partners in co-immunoprecipitated C3 serum sample:

For further confirmation, co-immunoprecipitation experiments were carried out. To address whether complement C3 associates with the haptoglobin, complement C3 from human serum was immunoprecipitated and analyzed by mass spectrometry. The result identified haptoglobin and other complement cascade proteins (Table.23).

Protein Accession Protein Description	Protein Score	Protein Avg Mass	Protein Seq Cover (%)	Protein Matched Peptide Inten Sum
P01009 Alpha 1 antitrypsin precursor	417.1919	46907.7136	18.9	97386
P01023 Alpha 2 macroglobulin precursor	24292.5	164703.861	52.44	7748787
P02760 AMBP protein precursor	1169.088	39911.9931	25	77459
P00450 Ceruloplasmin precursor	755.918	123060.7982	39.44	494497
P01024 Complement C3 precursor	15001.28	188704.1377	54.12	4759200
P01028 Complement C4 precursor	2067.683	194368.4845	37.67	733193
P01031 Complement C5 precursor	400.3875	190042.4292	17.6	167061
P08603 Complement factor H precursor H factor 1	3948.684	143801.7924	47.52	876580
P02679 Fibrinogen gamma chain precursor	59371.25	52124.0191	62.25	7053887
P00738 Haptoglobin 2 precursor	70515.26	45889.6837	59.11	8435820
P01876 Ig alpha 1 chain C region	53302.52	38510.0827	58.07	5411943
P01877 Ig alpha 2 chain C region	24848.03	37306.6938	65	3138973
P01766 Ig heavy chain V III region BRO	22477.41	13340.8229	25	392701
P01871 Ig MU chain C region	10950.55	50241.2317	55.73	1008537
P19827 Inter alpha trypsin inhibitor heavy chain	783.733	101845.5159	22.72	244855
P20742 Pregnancy zone protein precursor	2277.249	165318.8601	13.23	931058
P02787 Serotransferrin precursor	545.1461	79331.0555	23.35	297914
P14639 Serum albumin precursor	834.3349	71184.296	11.04	126794
P02743 Serum amyloid P component precursor	474.6092	25501.2065	13.45	58262
P00761 Trypsin precursor EC 3 4 21 4	5179.762	25093.8291	36.36	905720
P04004 Vitronectin precursor Serum spreading factor s	2894.299	55104.0374	20.92	182319

Table 23. List of proteins identified in immunoprecipitates of complement C3 by ESI LC MS with their characteristics.

Protein accession Protein Description	Protein score	Protein avg Mass	Protein seq Cover (%)	Protein Matched Peptide Inten Sum
P02768 Serum albumin	26460.01	71362.71	69.95	1.94E+07
P01857 Ig gamma 1 chain C region	10717.36	36619.19	73.94	1674231
P02787 Serotransferrin	8692.873	79345.08	60.46	1942442
P68871 Hemoglobin subunit beta 2	8006.901	16112.48	68.03	286542
P01834 Ig kappa chain C region	7614.438	11779.94	83.96	642319
P69905 Hemoglobin subunit alpha	3428.981	15314.6	33.1	134732
P01860 Ig gamma 3 chain C region	2385.701	42313.49	37.4	596777
P0CG06 Ig lambda 3 chain C regions	1863.642	11408.59	65.09	138844
P01859 Ig gamma 2 chain C region	1767.989	36527.98	39.26	423293
A0M8Q6 Ig lambda 7 chain C region	1654.87	11473.76	46.23	130671
P02766 Transthyretin	1652.427	16001.1	40.14	41924
P02790 Hemopexin	828.3835	52417.79	40.04	185274
P01009 Alpha 1 antitrypsin	779.28	46907.71	24.88	224875
Q6P587 Acylpyruvase FAHD1 mitochondrial	654.6217	25128.15	21.43	289497
P02763 Alpha 1 acid glycoprotein 1	473.7783	23739.69	30.85	38464
P10909 Clusterin	455.2224	53064.97	14.92	59827
P01011 Alpha 1 antichymotrypsin	453.6974	47822.05	19.39	88144
P36955 Pigment epithelium derived factor	449.2569	46483.34	22.49	109099
P02647Apolipoprotein A I	408.8636	30777.87	32.21	40695
P01777 Ig heavy chain V III region	228.8666	12673.26	15.97	10744
Q8WXA9Splicing regulatory glutamine lysine rich protein 1	188.669	59437.39	12.2	27041
Q6UW01 Cerebellin 3	143.0499	21634.67	12.68	1898
Q8TF64PDZ domain containing protein	135.1703	34323.83	13.46	45193
P00450 Ceruloplasmin	129.9434	123060.8	8.54	36260
Q5T0J7 Uncharacterized protein	125.3106	26916.98	18.88	14392
Q8NGT5 Olfactory receptor	115.1356	35957.47	2.9	12328
Q496M5 Inactive serine threonine protein kinase	109.1867	36728.56	15.18	19232

Table 24. Negative control for complement C3 immunoprecipitation.

In order to determine whether haptoglobin interacts with complement C3, haptoglobin from human serum was immunoprecipitated and analyzed by mass spectrometry. And we identified complement C3 as interacting protein along with haptoglobin binding proteins (Table 25).

Protein Accession Protein Description	Protein Score	Protein Avg Mass	Protein Seq Cover (%)	Protein Matched Peptide IntenSum
P01834 Ig kappa chain C region	97581.79	11779.94	88.68	2566082
P0CG05 Ig lambda 2 chain C regions	75366.1	11464.66	82.08	2056561
P01857 Ig gamma 1 chain C region	70320.09	36619.19	57.88	3578893
P01861 Ig gamma 4 chain C region	63427.84	36453.84	54.43	3795989
B9A064 Immunoglobulin lambda like polypeptide	61150.36	23405.44	30.84	1614594
P01859 Ig gamma 2 chain C region	58688.41	36527.98	64.11	4075787
P00738 Haptoglobin	57333.56	45889.68	65.52	5083795
P68871 Hemoglobin subunit beta	53413.3	16112.48	93.2	774912
P01876 Ig alpha 1 chain C region	51174.47	38510.08	65.44	2602259
P01023 Alpha 2 macroglobulin	31886.53	164716.9	55.43	4509670
P01621 Ig kappa chain V III region	28988.68	10842.94	56	141975
P01622 Ig kappa chain V III region	26745.18	11902.21	22.94	97499
P01877 Ig alpha 2 chain C region	26387.48	37324.73	62.35	1568492
P00739 Haptoglobin related protein	20653.39	39542.86	43.97	1918384
P02768 Serum albumin	18080.76	71362.71	65.85	1471460
P01764 Ig heavy chain V III region	16330.95	12753.42	35.04	46078
P01765 Ig heavy chain V III region	15545.48	11726.22	26.09	38108

Protein Accession Protein Description	Protein Score	Protein Avg Mass	Protein Seq Cover (%)	Protein Matched Peptide IntenSum
P01593 Ig kappa chain V I region	13508.42	12106.42	31.48	45116
P01617 Ig kappa chain V II region	12546.83	12172.72	32.74	58257
P0C0L5 Complement C4 B	8783.288	194291.5	34.12	1058353
P0C0L4 Complement C4 A	8783.288	194382.5	34.17	1087454
P69905 Hemoglobin subunit alpha OS	8046.841	15314.6	54.93	156624
P02647 Apolipoprotein A I	7559.909	30777.87	41.57	165152
P20742 Pregnancy zone protein	4646.01	165345.9	6.68	762243
P01009 Alpha 1 antitrypsin	4046.111	46907.71	44.02	386329
P08603 Complement factor H	3664.805	143772.7	36.64	313973
P04264 Keratin type II cytoskeletal 1	2840.325	66209.9	27.02	213902
P06312 Ig kappa chain V IV region	2491.878	13494.12	29.75	48122
P01598 Ig kappa chain V I region	2215.684	11902.32	32.41	137886
P00747 Plasminogen	1391.025	93306.41	23.58	143102
P04004 Vitronectin	1296.971	55104.04	14.44	29388
P01781 Ig heavy chain V III region	1276.06	11885.37	26.72	9653
P01717 Ig lambda chain V IV region	1179.903	11630.83	17.76	8635
P01024 Complement C3	880.9597	188688.1	19.96	142136
P10909 Clusterin	824.9657	53064.97	25.39	32764
P02787 Serotransferrin	713.8206	79345.08	20.77	93155
P27169 Serum paraoxonase arylesterase1	599.9766	39902.45	13.24	43740
P06396 Gelsolin OS	387.588	86096.82	7.93	31438
P01019 Angiotensinogen	149.6979	53439.43	5.15	11260
P00751 Complement factor B	137.8617	86901.64	7.46	14933

Table 25. List of proteins identified in immunoprecipitates of haptoglobin by ESI LC MS with their characteristics.

Protein Entry Protein Description	Protein score	Protein avg Mass	Protein seq Cover (%)	Protein Matched Peptide Inten Sum
P02768 Serum albumin	39554.7	71362.71	76.52	3.15E+07
P02787 Serotransferrin	18675.23	79345.08	67.77	7065844
P02790 Hemopexin	5399.003	52417.79	42.21	717419
P02647 Apolipoprotein A I	2527.709	30777.87	48.69	178572
P01857 Ig gamma 1 chain C region	1625.793	36619.19	49.7	174534
P69905 Hemoglobin subunit alpha	1495.004	15314.6	26.76	32975
P68871 Hemoglobin subunit beta	1021.143	16112.48	38.1	47473
P01834 Ig kappa chain C	654.6534	11779.94	29.25	44947
P02774 Vitamin D binding protein	181.3151	54560.49	21.94	71049
P01011 Alpha 1 antichymotrypsin	161.5645	47822.05	11.58	58663
P00450 Ceruloplasmin	149.8954	123060.8	13.24	77645
P05204 Non histone chromosomal protein	126.8086	9392.68	18.89	33461

Table 26. Negative control for haptoglobin immunoprecipitation.

To further confirm the interaction, complement C3 and haptoglobin co-IP samples were probed by western blot. The Eales' disease patients' serum was immunoprecipitated with complement C3 antibody and western blot for both C3 and haptoglobin was done. Presence of Haptoglobin and C3 in serum of ED patients was identified in the western blot analysis by probing the co-IP samples with respective antibodies (Figure 19).

Complement C3 is known as an acute-phase protein and has been reported to be elevated in the serum during inflammation. The presence of complement C3 and complement C3-interacting protein complex was identified in the serum samples which includes haptoglobin by co- Immunoprecipitation. The property of haptoglobin binding to complement C3 was also confirmed in the serum by co-immunoprecipitation.

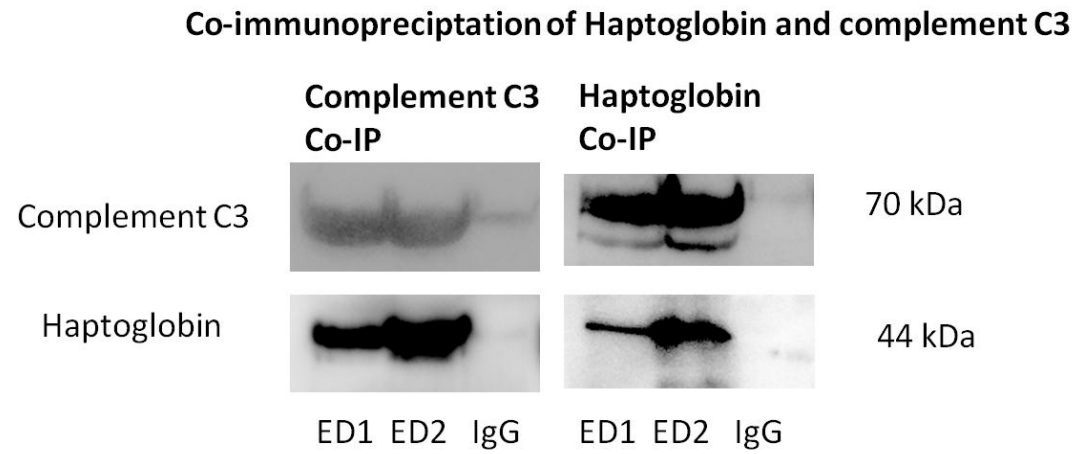

Figure 19: Western blots of co-immunoprecipitated samples.

6.7 Glycosylation status of haptoglobin by lectin blot:

Increased haptoglobin protein expression was identified Eales' Disease serum of patients' serum. Increased, tri-antennary and tetra-antennary glycopeptides (containing β (1-4) linked mannose residues with-1, 6-N-acetylglucosamine branches) and decreased α 2-6-linked sialic acid residues were seen in haptoglobin from Eales' disease patients by lectin blots when compared to control subjects (Figure. 20).

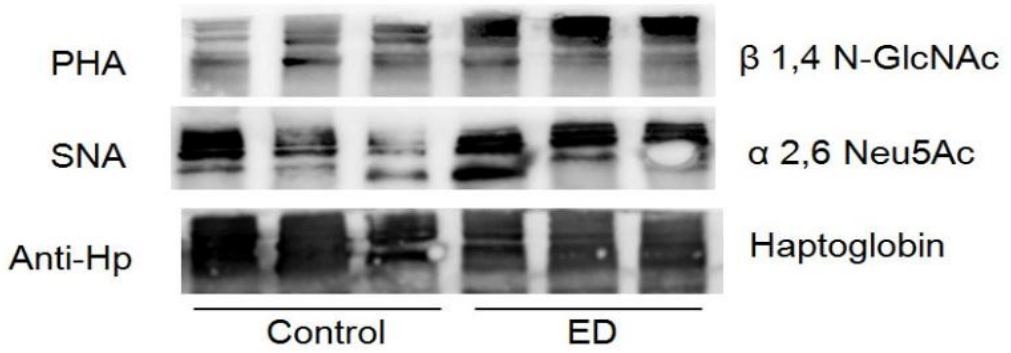

Figure 20: Lectin blots of Eales' disease patients and control subjects. Increased levels of biantennary glycans in haptoglobin were seen by PHA. Decreased levels α-2, 6-sialic acid was identified in haptoglobin by SNA lectin blot. The presence of haptoglobin is confirmed by western blot.

6.8 Glycosylation status of haptoglobin by Mass spectrometry

Four N-glycosylation sites N184, N207, N211 and N241 are reported in haptoglobin N glycosylation status of haptoglobin was identified in control and Eales' disease patients. The peptide MVSHHN184LTTGATLINEQWLLTTAK from haptoglobin is glycosylated and difference between control and Eales' disease samples were seen and the MS analysis (Table 27) and identified one of these glycosylated peptide. In the glycosylation profiling of control serum haptoglobin, N184 residue was identified to be mono sialylated biantennary species (Figure 21) and Eales disease patients 184 residue was found to be nonsialylated biantennary N-glycan (Figure 22)

MVSHHNLTTGATLINEQWLLTTAK		
Sample	**Eales' disease**	**Control**
Peptide mhp	**3936.859**	**4593.0691**
Precursor charge	**3+**	**4+**
Retention time	**54.4982**	**56.2942**
Peptide Glycan	**Man2HexNAc2+Man3HexNAc2**	**Man2HexNAc2NeuAc1+Man3HexNAc2**

Table 27. Comparison of peptide sequences MVSHHNLTTG ATLINEQWLL TTAK of haptoglobin among the Eales' disease patients and control subjects.

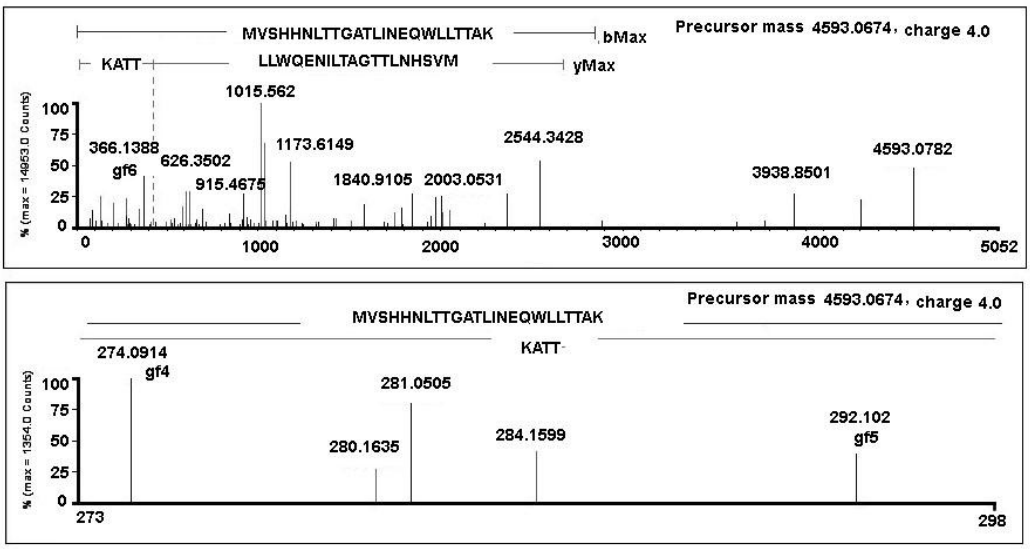

Figure 21: N-Glycosylation of haptoglobin peptide MVSHHNLTTGATLINEQWLLTTAK from control subjects sample.

The mass of the peptide was 4593.0674 with identified glycan of Man2HexNAc2NeuAc1+Man3HexNAc2. The mhp identified were 366.1395 (ManHexNAc), 292.1027 (NeuAc1) and 657.2354 (Man HexNAc NeuAc) and indicative of sialation.

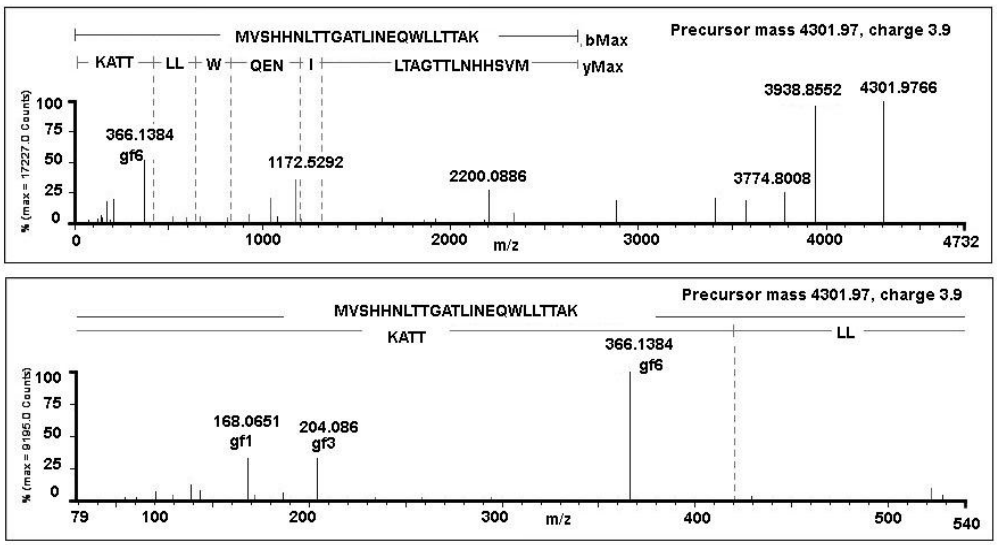

Figure 22: N-Glycosylation of haptoglobin peptide MVSHHNLTTGATLINEQWLLTTAK from Eales' disease patients' samples. The mass of the peptide was 4301.97 and identified to contain Man2HexNAc2+Man3HexNAc2 glycosylation. In Eales' disease patients samples mhp values are 292 Da lesser than controls which accounts loss of one sialic acid residue. Glyan residues were identified by the mhp values 204.0867 (HexNAc) and (ManHexNAc) 366.1395.

6.9 Identification of haptoglobin interacting partners by *in silico* approach

Interacting partners of haptoglobin, were identified by bio-informatics' analysis using protein-protein interaction prediction servers (FpClass, BIOGRID, MINT and STRING). They have database of predicted interaction partners based on Affinity Capture-MS, Affinity Capture-Western, Affinity Capture-RNA, Two hybrids, and pull down methods (Table 28).

S.NO	FpClass	BIOGRID	MINT	STRING
1	A2M	ALB	APOE	APOA1
2	ABCA1	ATP7B	APOA1	APOE
3	AGT	DDX19B	MIS12	MIS12
4	AHSG	ELAVL1	WASL	IL6
5	ALB	GADD45G	TBL1X	MB
6	AMBP	GDPD1	GADD45G	HBB
7	APOA1	GRB2	TGM2	CD163
8	APOBEC3A	HBB	RPL11	HBA2
9	APOC1	LAMC3	GRB2	HBA1
10	APOC2	MIS12	SMAD3	TF
11	APOC3	MVP	MVP	
12	APOE	NARG2	RBBP6	
13	APOH	RBBP6		
14	APP	SMAD3		
15	AZU1	TBL1X		
16	BP1	TGM2		
17	C1R	TP63		
18	C1S	VKORC1		
19	**C3**			
20	C5AR1			
21	ABL2			
22	ADC			
23	ASL			
24	ASS1			
25	AZIN1			
26	BMP2			
27	CAD			
28	CCNA2			
29	CCNB1			
30	CCNB2			
31	CCT2			
32	CCT3			
33	CCT5			
34	CDC20			
35	CDC6			
36	CDK1			
38	CKS1B			
39	CKS2			
40	EIF5			
41	ENOPH1			

Table 28. The predicted interacting partners of haptoglobin using different protein-protein interaction server. It is shows that many proteins interact with haptoglobin

6.10 Haptoglobin phenotyping

Haptoglobin phenotype screening was carried out in serum of Eales' disease patients and compared with control samples. Identified phenotype is tested for its anti-inflammatory potential in ARPE-19 cells to understand its relevance to the disease. Serum samples obtained from control subjects and Eales' disease patients were screened by using native PAGE with peroxidase staining. The three different phenotypes are easily distinguishable by a characteristic pattern of bands representing haptoglobin-hemoglobin complexes. Out of 21 controls, 17 samples were haptoglobin 2-2 type, while 4 samples were 2-1 type. In 22 cases of Eales' disease patients samples 15 were haptoglobin 2-2, 6 were 2-1 and 1 was 1-1 type as shown (Figure 23).

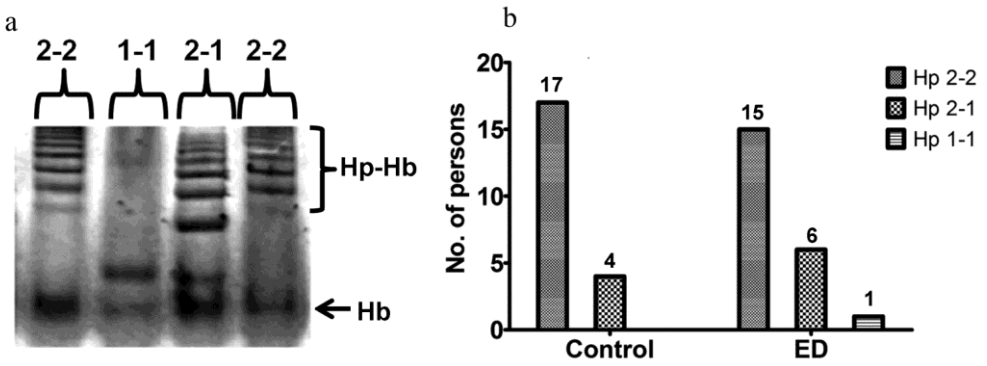

Figure 23: Representative image of haptoglobin phenotyping carried out in 5 % native PAGE with tetramethylbenzidine staining. Lane 1& 4 is haptoglobin 2-2: a series of more slowly migrating bands similar to that of haptoglobin 1-1, Lane 2 is haptoglobin 1-1: a single rapidly migrating band and Lane 3 is haptoglobin 2-1: slowly migrating bands. Hemoglobin is marked by an arrow.

6.11 Iron and copper in Eales disease

Levels of Iron Ferritin, Transferrin and Serum transferrin receptor

Haptoglobin 2-2 phenotype is the major phenotype identified in Eales' disease patients. It was reported that HIV patients with this phenotype are more prone to hemoglobin / iron-driven oxidative stress since its complex with hemoglobin is cleared from the circulation with a lesser competence (106, 107). Since Eales' disease is associated with oxidative stress and altered iron levels in PBMC and serum, it is essential to assess the status of iron in the disease. The serum levels of iron, ferritin, transferrin, and serum transferrin receptor were estimated. Levels of serum iron were 82 ± 8 µg / dL in control subjects and 93 ± 7 µg / dL in Eales' disease patients and the difference among them were insignificant $P < 0.298$. Serum ferritin levels were 31.9 ± 3.9 µg / L in control subjects and 81.1 ± 7.8 µg / L in Eales' disease, $p<0.002$. There was a significant increase in the level of serum ferritin in Eales' disease patients compared to the controls. Levels of serum transferrin were 397.9 ± 26.8 mg / dL in control subjects and 330.2 ± 11.0 mg / dL in Eales' disease. There was a decrease in the serum transferrin levels in Eales' disease patients compared to the controls and the difference among them were insignificant. Difference in the levels of serum transferrin receptor were not significant when compared to controls (control subjects - 4.37 ± 0.57 mg / L, and in Eales' disease patients - 4.92 ± 0.52 mg / L, $p< 0.47$). Thus, the above results indicate that, both iron and ferritin are associated and have role in vascular eye diseases (Figure 24).

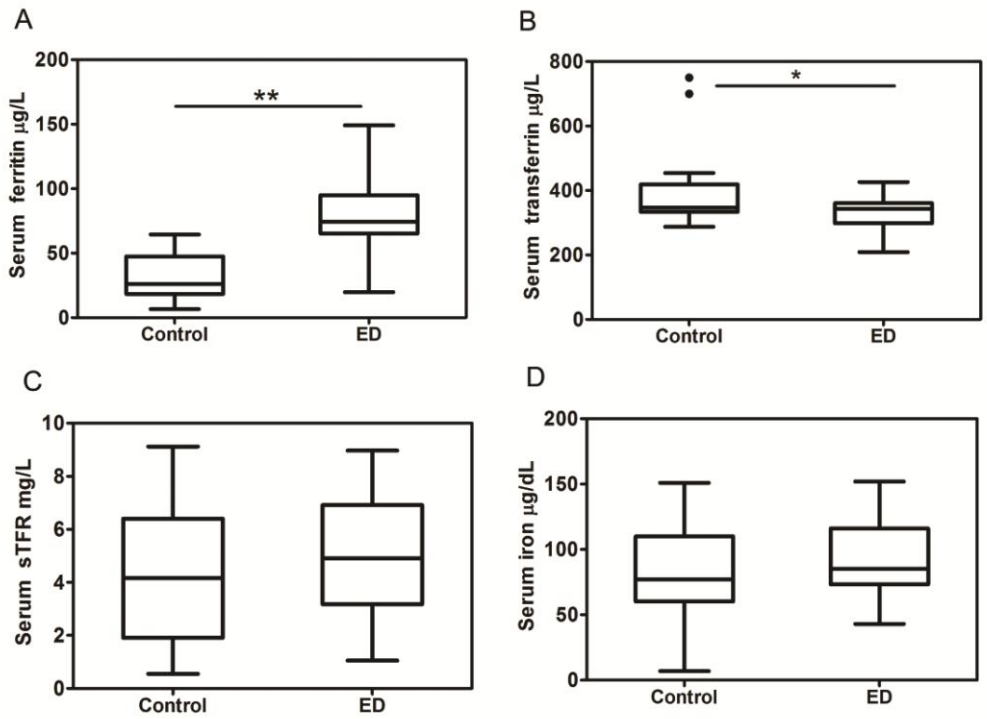

Figure 24: Comparison of serum ferritin, serotransferrin and serum transferrin receptor among ED and healthy controls. Statistical significance between control (n = 20) and ED (n = 20), a) Serum ferritin p = 0.002; b) serum Transferrin significantly decreased in ED compare to control p = 0.02; c) serum Transferrin receptor p = 0.477, d) serum Iron p = 0.29

6.12 Role of Copper in Eales' disease

CTR1

Eales' disease is peripheral neovascular disease and increased copper levels are reported in vitreous of the patients (6, 23, 53). In addition major copper protein ceruloplasmin was also reported to be elevated in this disease (51). Eales' disease patients PBMC were used to study CTR1 expression. CTR1 mRNA expression was compared with PBMC of control subjects and Eales' disease patients. Increased mRNA expression in Eales disease patients by 2.4 fold when compared to control was

seen (Figure. 25A). CTR1 ELISA in PBMC showed significant increase in protein level in ED (92.56 pg/µg ± 15.35, *p*= 0.0001) when compared to control (27.77 pg/µg ± 11.3) (Figure 25 B). Representative western blot images of CTR1 (Figure 25 C).

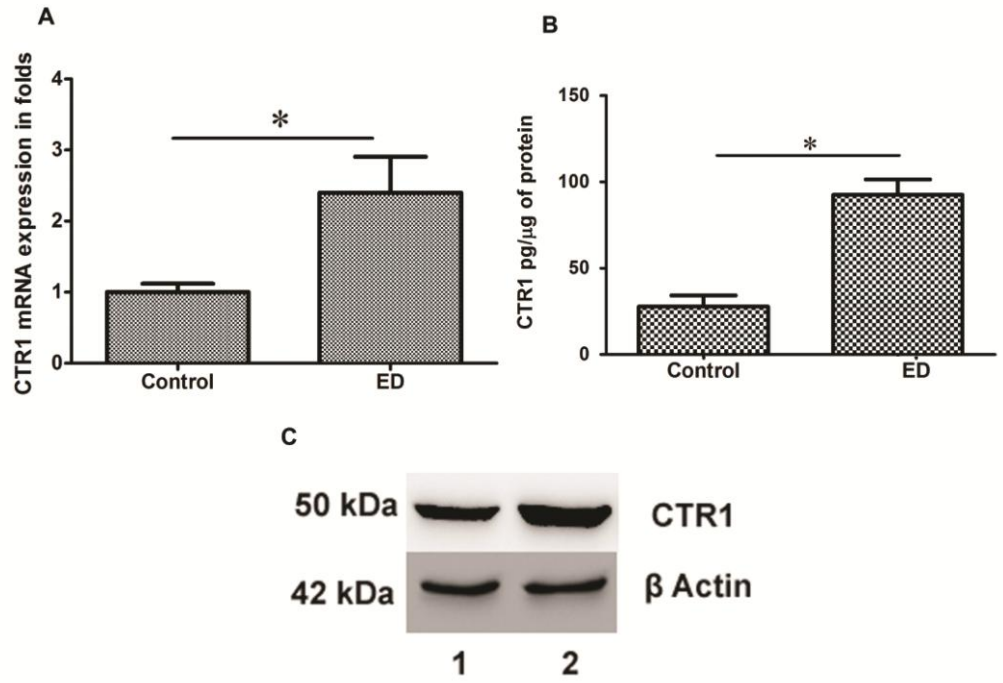

Figure 25: CTR1mRNA and protein expression in PBMC of control and Eales' disease A) Real time PCR CTR1 mRNA expression. B) CTR1 ELISA and C) Western blot in PBMC; lane 1 - control and lane 2 - Eales' disease.

Objective: 3. To clone the cDNA of identified protein in mammalian expression vector.

To transform in the cloned cDNA into cells and to overexpress and purify the protein.

The 88 kDa protein was identified as a complex of 3 proteins, in which haptoglobin was the top scoring protein. Since haptoglobin is a glycosylated and secreted protein, purified haptoglobin is preferred rather than the cloned protein. Although the findings on haptoglobin phenotype assessment had shown no statistical difference between the groups, in order to understand the role of Hp 2-2, a widely occurring phenotype of

haptoglobin (Control subjects and Eales' disease patients), was purchased from Sigma and its angiogenic effects were seen in Human Umbilical Vein Endothelial Cells (HUVEC) and effects in inflammatory condition, were seen in bacterial lipopolysaccharide (LPS) stimulated ARPE-19 cells. We have cloned galectin – 1 and overexpressed in COS-7 cells, similarly we have cloned and purified PE35 which are discussed in the sections 6.26 and 6.30 respectively.

Objective: 4 Functional implications of 88 kDa protein in the etiology of Eales' disease.

To study the effect of purified protein on angiogenesis and vitreal hemorrhage in cultured human retinal pigment cells and microvascular endothelial cells

6.13 Cytotoxicity of HUVEC and ARPE-19 cells by MTT assay

For carrying out functional characterization of haptoglobin in cell culture, purified protein was used. Various concentrations of haptoglobin (1, 2.5, 5, 10, 12.5, 15 μg/mL) was screened for cytotoxicity in ARPE-19 and HUVECs. Data is represented as mean percentages ± standard error of mean. Haptoglobin 2-2 is nontoxic and cell viability was more than 95 % in all tested concentrations (Figure 26).

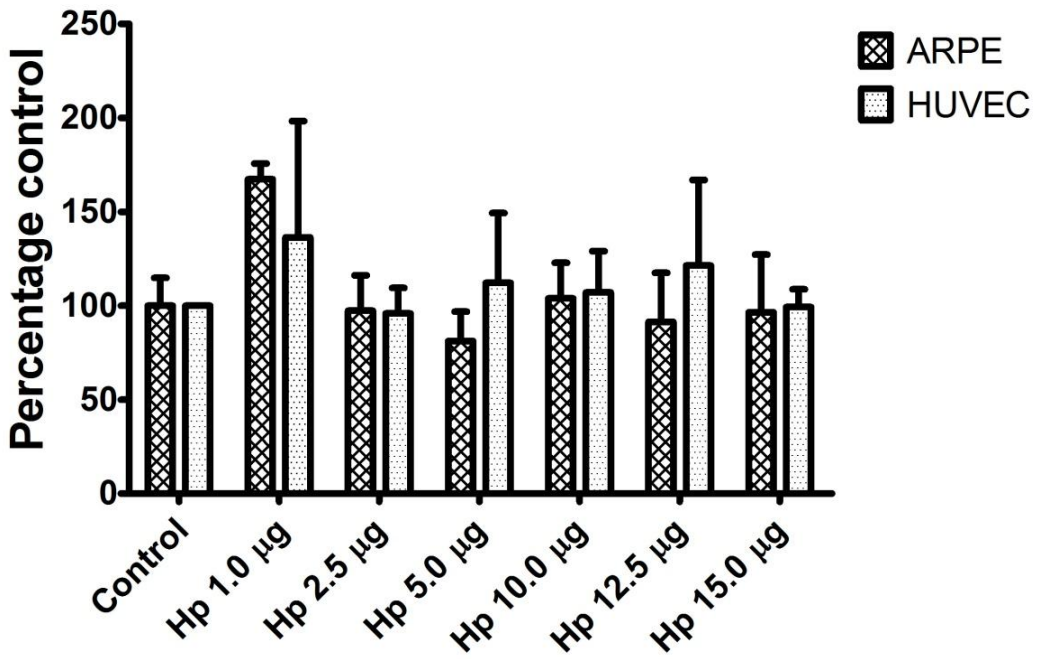

Figure 26: Cytotoxicity assay for haptoglobin treated cells.

HUVEC were treated with 1, 2.5, 5, 10, 12.5 and 15 µg/mL concentration of haptoglobin in EBM with 1 % FBS. Untreated HUVEC was used as a control for this assay. ARPE-19 cells were treated with 1, 2.5, 5, 10, 12.5 and 15 µg/mL concentration of haptoglobin in DMEM - F12 with 1 % FBS. Untreated ARPE-19 cells were used as a control for this assay. Cells were viable in all the tested concentrations.

6.14 Migration assay- wound healing assay

Various reports point out the involvement of haptoglobin in inducing migration of various cells. In mouse, LPS induced expression of haptoglobin, resulted in migration of fibroblasts. Similarly, arterial restructuring was delayed in haptoglobin knockout mice. Haptoglobin obtained from the sera of systemic vasculitis patients stimulated in vitro and in vivo matrigel angiogenesis assay. Effect of purified Hp 2-2 was tested by *in vitro* cell migration assay in HUVECs. Cells were treated with varying concentrations 2.5, 5, 10 µg/mL of haptoglobin for 24 h. VEGF at 10 ng/ mL was

used as positive control and untreated cells served as control. Weak migration was observed at all concentrations (Figure 27).

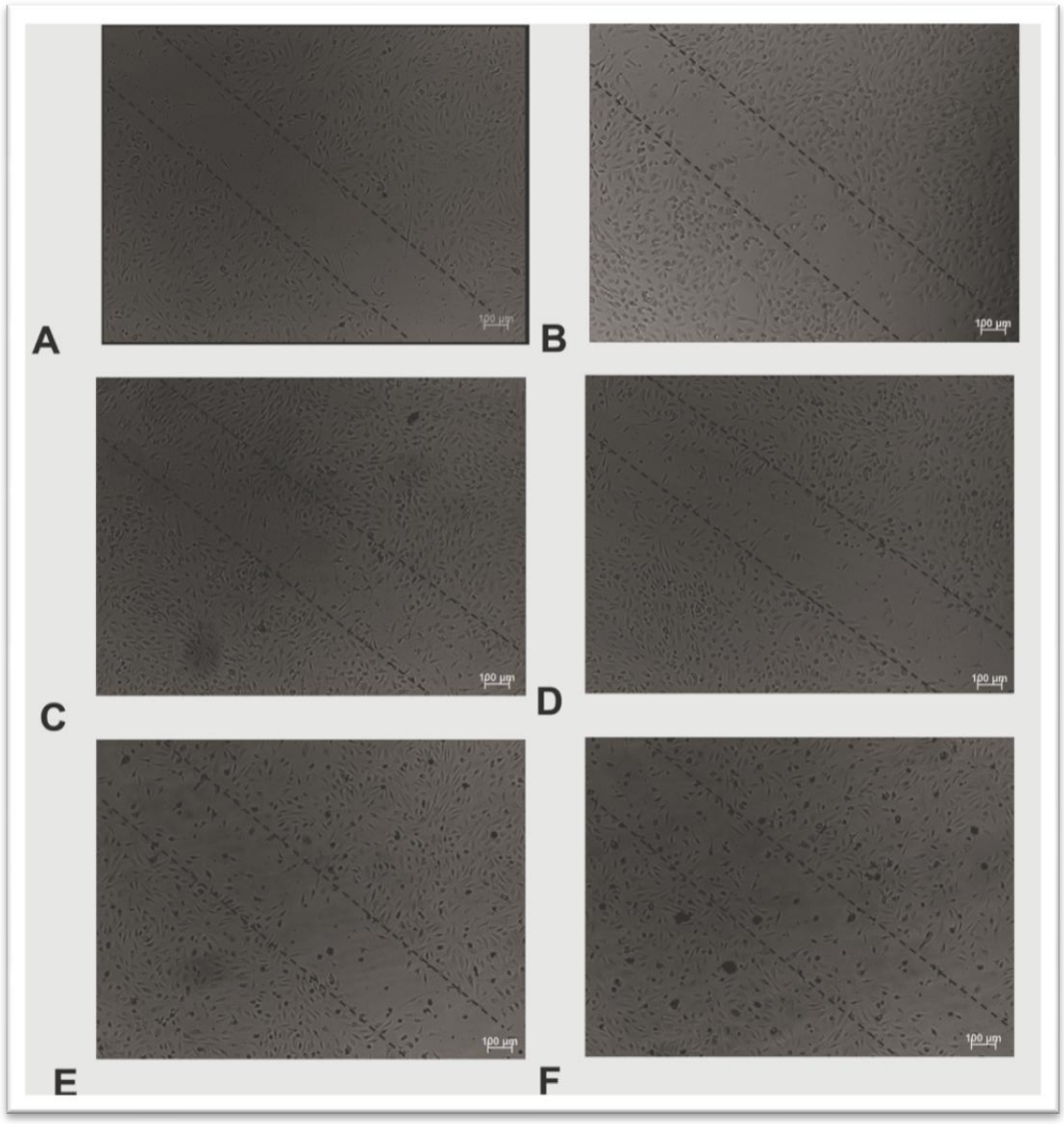

Figure.27 Migration assay for haptoglobin treated cells: Untreated HUVEC (A) served as control. HUVEC were (B) treated with 1 µg (C) 2.5 µg (D) 5.0 µg (E) 10 µg F) VEGF 10ng per mL concentrations of haptoglobin. HUVEC grown in growth factors rich medium (E) served as positive control. Haptoglobin weakly induced the migration of HUVEC at the concentration of 2.5 and 5.0 and 10.0 µg/mL.

6.15. *In vitro* Angiogenesis assay: Tube formation assay

HUVECs cells were used to evaluate the tube formation capacity of upon treatment with various concentrations 2.5, 5, 10 µg/mL of haptoglobin with proper controls. VEGF 10 ng/mL was used as positive control and untreated cells served as controls. Results show increased in Tube formation is increased by haptoglobin. Statistically significant increase was observed at 2.5 µg/mL and 5 µg /mL haptoglobin treated HUVECs (Figure 28).

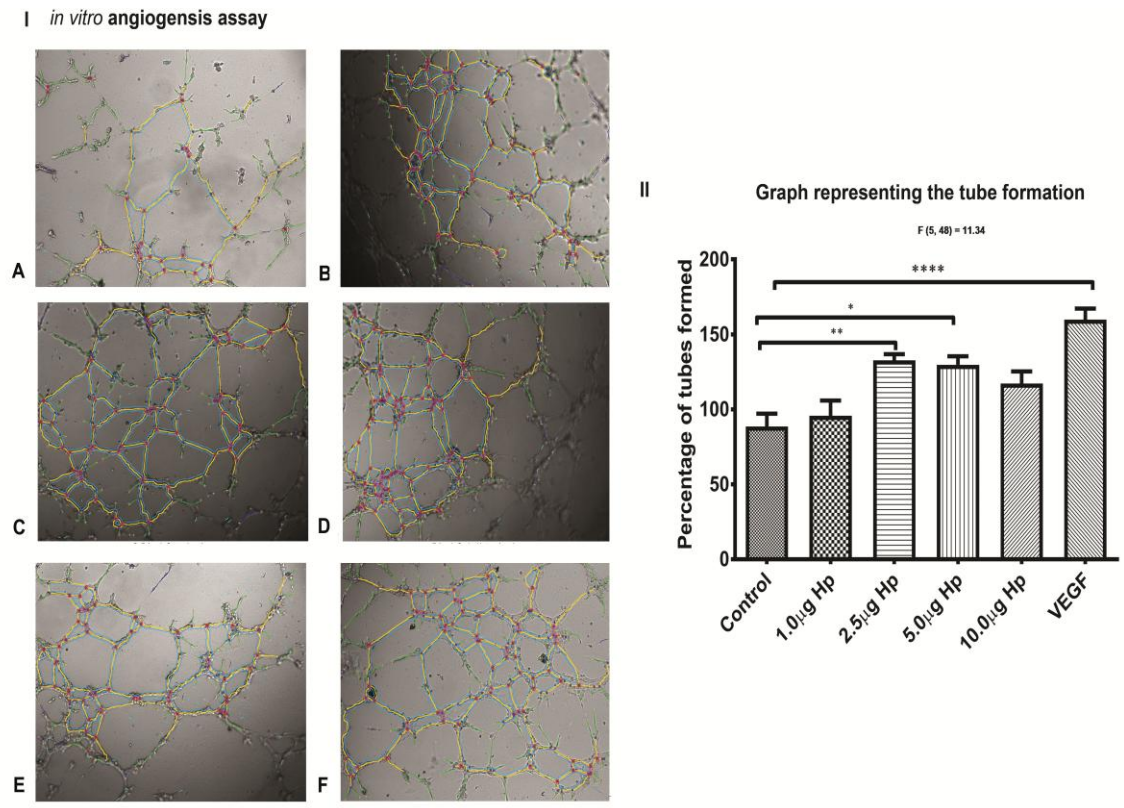

Figure 28: Matrigel assay *in-vitro* angiogenesis assay: A) HUVEC were treated with haptoglobin 2.5µg (B), 5.0µg (C) and 10 µg (D) per ml concentrations to score their pro/anti angiogenic ability. Untreated cells (A) served as control and VEGF (10 ng/ml) was used as positive control (E). The tube formation was significantly higher in the 2.5µg haptoglobin treated HUVEC B) **Quantification of matrigel *in-vitro* angiogenesis assay:** Image-J software was used to measure the tube length, which in turn represents angiogenic potential of the treated condition. Haptoglobin at 2.5µg concentration significantly induced tube formation in HUVEC compared to control. ($p<0.0096$).

6.16 Cell proliferation assay by crystal violet

HUVECs, were treated with varying concentrations of haptoglobin (1, 2.5, 5, 10, 12.5, 25, 50, 100 and 200μg/mL) for 24 h. Results showed that haptoglobin significantly increased proliferation at concentrations of 100 μg/mL (p = 0.0436) and 200 μg/mL (p = 0.0145) by 1.7 and 1.87 folds respectively. Lower concentrations did not show any significant change in proliferation (Figure 29).

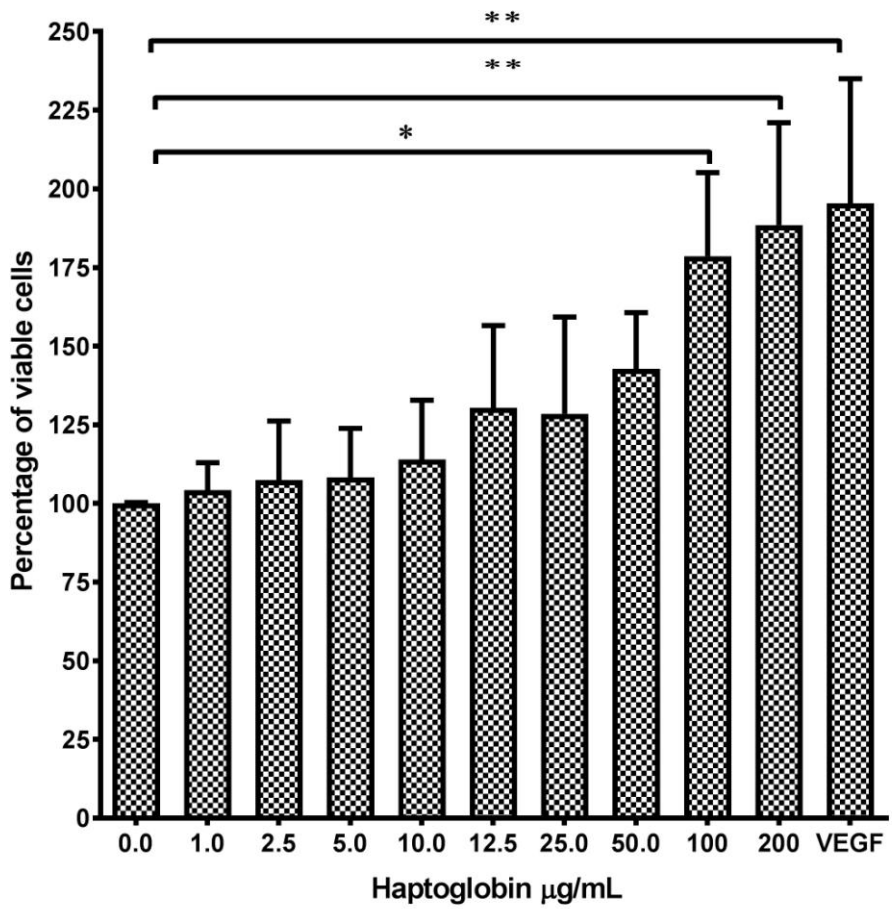

Figure 29: Proliferation assay using crystal violet for haptoglobin. Haptoglobin at concentrations of 100 and 200 μg/mL had significantly increased the proliferation in comparison to control (p = 0.0145). And haptoglobin treatment and VEGF at 10 ng/mL is used as positive control.

6.17 The role of haptoglobin in inflammation

ARPE-19 cells were treated with varying concentration of LPS (1 µg, 5.0 µg and 10.0 µg/mL) to induce inflammation. Expression of haptoglobin was found to be increased upon 5.0 µg and 10.0 µg/mL of LPS treatment (Figure 30).

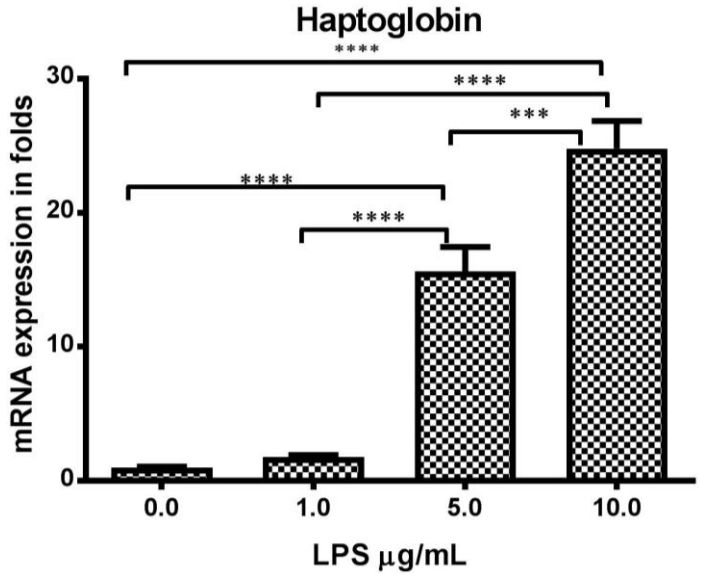

Figure 30: Expression levels of haptoglobin mRNA upon LPS treatment. One way ANOVAs with Tukey HSD post hoc test was used for comparison of means. 5.0 µg/mL of LPS concentration showed a significant increase in levels of haptoglobin mRNA ***p<0.001 compared to control and 1.0 µg/mL LPS. And 10 µg/mL of LPS showed a significant increase in levels of haptoglobin mRNA ***p<0.001 compared to control, 1.0 µg /mL and 5.0 µg /mL of LPS.

6.18 Haptoglobin down regulated LPS-induced expression of inflammatory genes

This study also probed the role of haptoglobin as an anti-inflammatory agent, using ARPE-19 stimulated with varying concentrations of LPS 1 µg/mL, 5 µg/mL and 10 µg /mL. ARPE-19 cells were stimulated with LPS and also co-treated with varying haptoglobin concentrations (2.5 µg/mL, 5.0 µg/mL and 10.0 µg/mL) for 24 h and the expression of pro inflammatory cytokines viz. IL-6, IL-8, TNF-α and MCP-1 were assessed at their transcript levels. The findings are presented as fold changes and the inhibitory effects of haptoglobin as measured by the expression of cytokines, were found to be statistically significant at all the tested concentrations. Fold changes of

cytokine mRNA in cells treated with LPS alone and LPS plus haptoglobin are represented as a bar chart.

6.19 ARPE-19 stimulated with 1µg LPS and anti-inflammatory effect of haptoglobin in a dose dependent manner

The effect of haptoglobin on 1 µg/mL of LPS treatment was compared by two way ANOVA and resulting statistical significance is also presented (Figure 31).

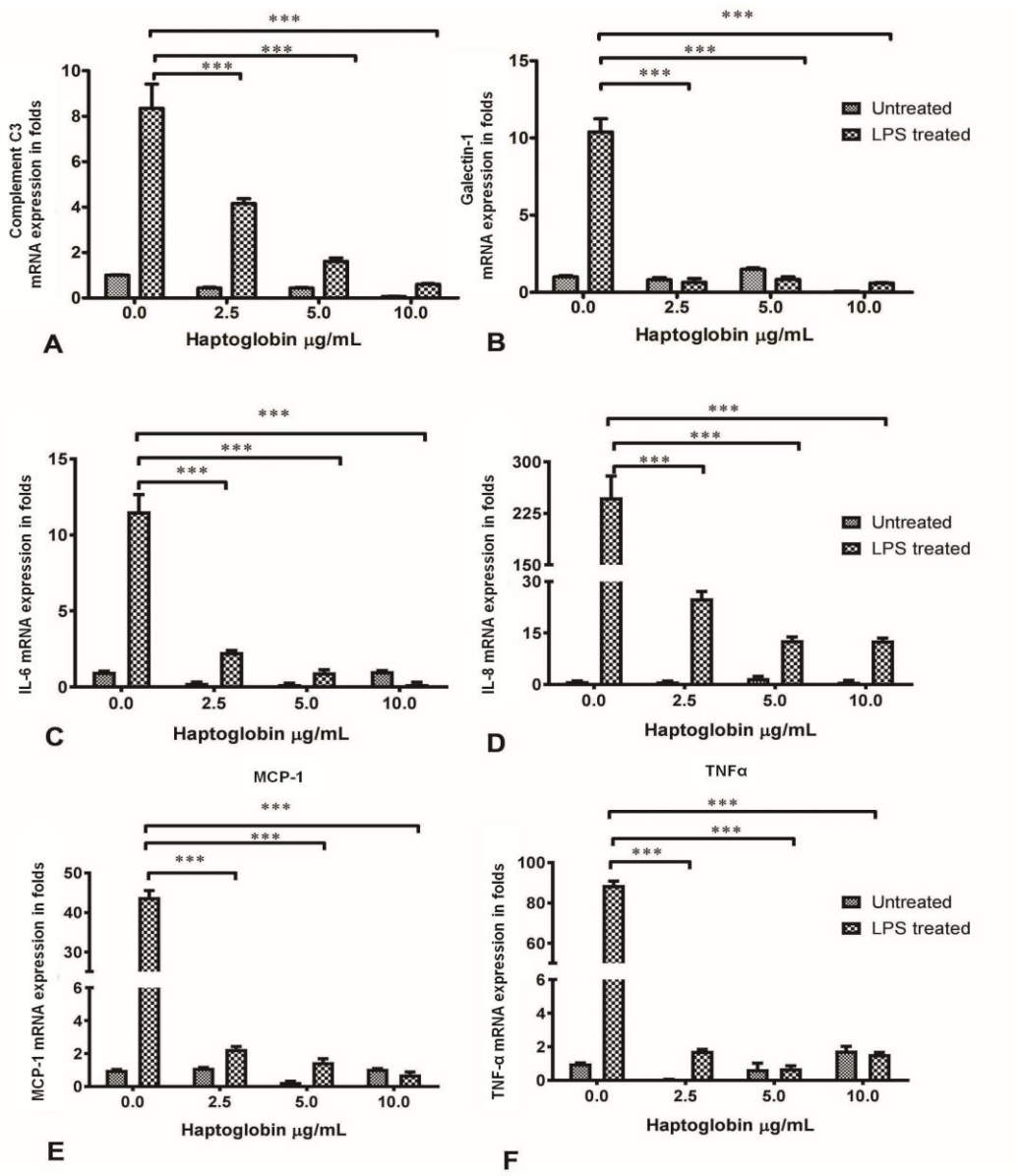

Figures 31: ARPE-19 stimulated with 1 µg/mL of LPS. Cells were co- treated with the 1µg/ml, 2.5 µg/ml, 5.0 µg/ml, 10 µg/ml of haptoglobin and mRNA expression was screened by qPCR.

Fold changes of complement C3 are as follows: A significant decrease in mean folds change was observed at all tested concentrations of haptoglobin when compared to cells with only LPS treatment ; Mean fold change values were presented as (mean ± SEM) $p<0.001$.

i) Control cells (untreated cells) - 1.00 ± 0.0161, **Cells treated with LPS alone** 8.346.55 ± 1.064 $p<0.001$; **ii) Treatment with haptoglobin 2.5 µg** 0.43 ± 0.037; **Co-treatment with LPS and haptoglobin 2.5 µg** - (4.15 ± 0.21 $p<0.001$); **iii) Treatment with haptoglobin 5.0 µg** 0.47 ± 0.026; **Co-treatment with LPS and haptoglobin 5.0 µg** (1.6 ± 0.15 $p<0.001$); **iv) Treatment with haptoglobin 10 µg**-0.066 ± 0.002857, **Co-treatment with LPS and haptoglobin 10 µg** (0.599 ± 0.037 $p<0.001$).

B) Fold changes of galectin-1 are as follows: A significant decrease in mean folds change was observed at all tested concentrations of haptoglobin when compared to cells with only LPS treatment ; Mean fold change values were presented as (mean ± SEM) $p<0.001$. **i) Control cells** (untreated cells) - 1.00 ± 0.084, **Cells treated with LPS alone** -10.38 ± 0.861 $p<0.001$; **ii) Treatment with haptoglobin 2.5 µg** -0.066 ± 0.0028; **Co-treatment with LPS and haptoglobin 2.5 µg** - (0.59 ± 0.037 $p<0.001$); **iii) Treatment with haptoglobin 5.0 µg** - 0.814 ± 0.137; **Co-treatment with LPS and haptoglobin 5.0 µg** (0.650 ± 0.25 $p<0.001$); **iv) Treatment with haptoglobin 10 µg**-1.487 ± 0.097, **Co-treatment with LPS and haptoglobin 10 µg** (0.829 ± 0.176 $p<0.001$).

C) Fold changes of IL-6 are as follows: A significant decrease in mean folds change was observed at all tested concentrations of haptoglobin when compared to cells with only LPS treatment ; Mean fold change values were presented as (mean ± SEM) $p<0.001$. **i) Control cells** (untreated cells) -1.00 ± 0.031, **Cells treated with LPS alone** -11.55 ± 0.778 $p<0.001$; **ii) Treatment with haptoglobin 2.5 µg** -0.28 ± 0.033; **Co-treatment with LPS and haptoglobin 2.5 µg** - (2.30 ± 0.068 $p<0.001$); **iii) Treatment with haptoglobin 5.0 µg** - 0.20 ± 0.037; **Co-treatment with LPS and haptoglobin 5.0 µg** (0.97 ± 0.113 $p<0.001$); **iv) Treatment with haptoglobin 10 µg-**

1.04 ± 0.0267, **Co-treatment with LPS and haptoglobin 10 µg** (0.199 ± 0.08 $p<0.001$).

D) Fold changes of IL-8 are as follows: A significant decrease in mean folds change was observed at all tested concentrations of haptoglobin when compared to cells with only LPS treatment - $p<0.001$.**i) Control cells (untreated cells) -**1.00 ± 0.031**, Treatment with LPS alone -** (248.5 ± 21.845, $p<0.0001$)**; ii) Treatment with the haptoglobin 2.5 µg -**0.89 ± 0.069, **Co-treatment with LPS and haptoglobin 2.5 µg -** (25.10 ± 1.412, $p<0.0001$); **iii) Treatment with the haptoglobin 5.0 µg -** 1.87 ± 0.448, **Co-treatment with haptoglobin 5.0 µg and LPS -** (12.89 ± 0.66, $p<0.0001$); **iv) Treatment with the haptoglobin 10 µg -** 0.84 ± 0.317, **Co-treatment with LPS and haptoglobin 10 µg -** (12.83 ± 0.46 $p<0.0001$).

E) Fold changes of MCP-1 are as follows: A significant decrease in mean folds change was observed at all tested concentrations of haptoglobin when compared to cells with only LPS treatment . $p<0.0001$.**i) Control cells (untreated cells) -** 1.00 ± 0.707**, Treatment with LPS alone-** (43.93 ± 1.149, $p<0.0001$)**; ii) Treatment with the haptoglobin 2.5 µg -**1.13 ± 0.804, **Co-treatment with LPS and haptoglobin 2.5 µg -** (2.28 ± 0.098, $p<0.0001$); **iii) Treatment with the haptoglobin 5.0 µg -** 0.27 ± 0.196, **Co-treatment with haptoglobin 5.0 µg and LPS -** (1.47 ± 0.153, $p<0.0001$); **iv) Treatment with the haptoglobin 10 µg -** 1.06 ± 0.753, **Co-treatment with LPS and haptoglobin 10 µg -** (0.72 ± 0.108 $p<0.0001$).

F) Fold changes of TNF-α are as follows: A significant decrease in the mean folds change was observed at all tested concentrations of haptoglobin when compared to cells with only LPS treatment $p<0.0001$.**i) Control cells (untreated cells) -** 1.00 ± 0.031**, Treatment with LPS alone -** (88.86 ± 1.392, $p<0.001$)**; ii) Treatment with the haptoglobin 2.5 µg -** 0.044 ± 0.014, **Co-treatment with LPS and haptoglobin 2.5 µg -** (1.76 ± 0.05, $p<0.0001$); **iii) Treatment with the haptoglobin 5.0 µg -** 0.651 ± 0.316, **Co-treatment with haptoglobin 5.0 µg and LPS -** (0.72 ± 0.099, $p<0.0001$); **iv) Treatment with the haptoglobin 10 µg -** 1.76 ± 0.223, **Co-treatment with LPS and haptoglobin 10 µg -** (1.55 ± 0.0703 $p<0.0001$).

6.20 ARPE-19 stimulated with 5µg of LPS and anti-inflammatory effect of haptoglobin in a dose-dependent manner

ARPE-19 cells were incubated in serum-free medium overnight and were stimulated with LPS of 5 µg/ mL concentration. Cells were simultaneously co-treated with final concentration of haptoglobin 2.5, 5.0, 10.0 µg/mL. At all treatment conditions mRNA expression of pro-inflammatory cytokines were measured after 24 h. The expression of mRNA was normalized to 18S rRNA. One way ANOVA with Tukey's Multiple Comparison Test was used for comparison of mean (fold change) untreated cells with the cells treated with LPS and haptoglobin co-treated (Figure 32).

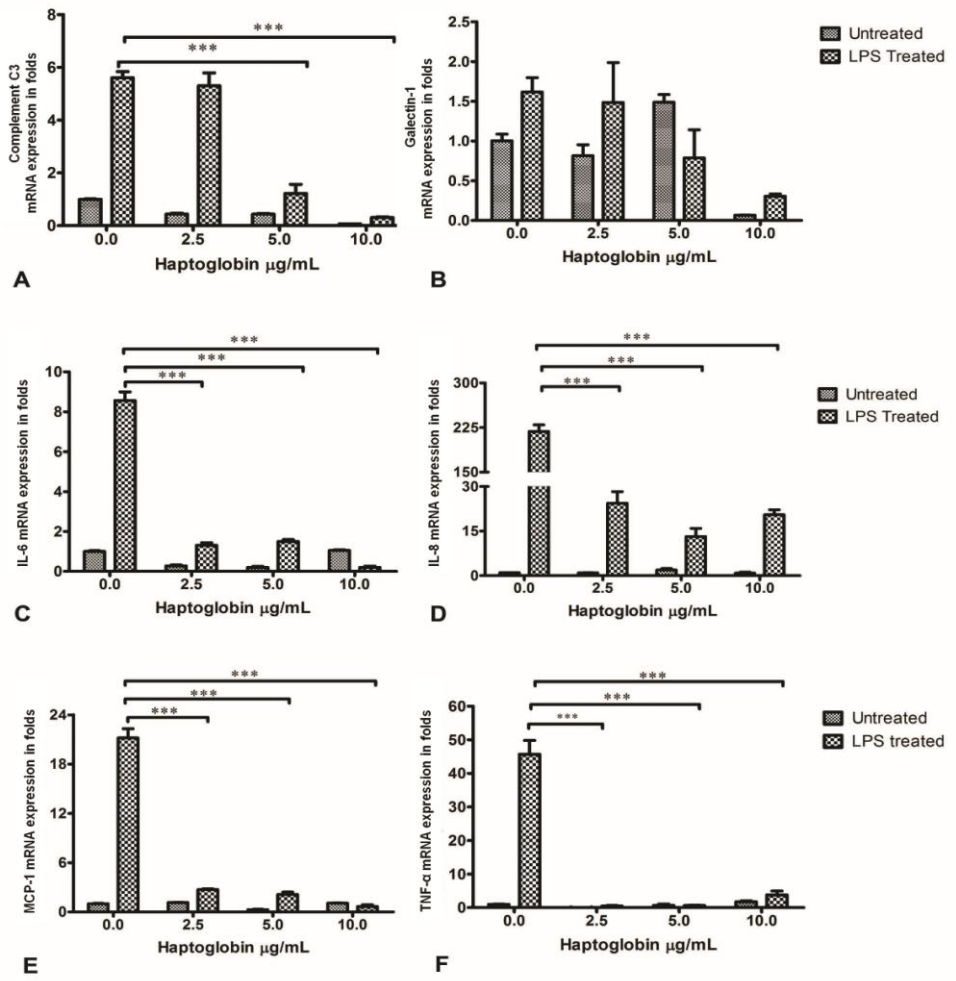

Figure 32: The ARPE-19 was treated with the 5.0 µg/ml of LPS. Cells were co-treated with 1 µg/ml, 2.5 µg/ml, 5.0 µg/ml, 10 µg/ml of haptoglobin and mRNA expression was screened by qPCR.

A) Fold changes of complement C3 are as follows: A significant decrease in mean folds change was observed at all tested concentrations of haptoglobin when compared to cells with only LPS treatment ; Mean fold change values were presented as (mean ± SEM) $p<0.001$. **Control cells** (untreated cells)-1.00 ± 0.0161, **Cells treated with LPS alone** 5.32 ± 0.56 $p<0.001$; **ii) Treatment with haptoglobin 2.5 µg** 0.43 ± 0.037; **Co-treatment with LPS and haptoglobin 2.5 µg -** (3.59 ± 0.92 $p<0.001$); **iii) Treatment with haptoglobin 5.0 µg** 0.47 ± 0.026; **Co-treatment with LPS and haptoglobin 5.0 µg** (2.32 ± 0.402 $p<0.001$); **iv)Treatment with haptoglobin 10µg-** 0.066 ± 0.02857, **Co-treatment with LPS and haptoglobin 10 µg** (0.47 ± 0.03 $p<0.001$)

B) Fold changes of galectin-1 are as follows: A significant decrease in mean folds change was observed at all tested concentrations of haptoglobin when compared to cells with only LPS treatment ; Mean fold change values were presented as (mean ± SEM) $p<0.001$. **Control cells** (untreated cells)-1.00 ± 0.084 , **Cells treated with LPS alone** 3.22 ± 0.25 $p<0.001$; **ii) Treatment with haptoglobin 2.5 µg** -1.436 ± 0.16 ; **Co-treatment with LPS and haptoglobin 2.5 µg** (1.48 ± 0.50 $p<0.001$); **iii) Treatment with haptoglobin 5.0 µg** - 0.814 ± 0.137; **Co-treatment with LPS and haptoglobin 5.0 µg** (1.435 ± 0.11 $p<0.001$); **iv)Treatment with haptoglobin 10µg-** 1.487 ± 0.097, **Co-treatment with LPS and haptoglobin 10 µg** (0.47 ± 0.0328 $p<0.001$)

C) Fold changes of IL-6 are as follows**.** A significant decrease in mean folds change was observed at all tested concentrations of haptoglobin when compared to cells with only LPS treatment ; Mean fold change values were presented as (mean ± SEM) $p<0.001$.**i) Control cells** (untreated cells)-1.00 ± 0.031, **Cells treated with LPS alone** 6.88 ± 1.80 $p<0.001$; **ii) Treatment with haptoglobin 2.5 µg** -0.28 ± 0.033; **Co-treatment with LPS and haptoglobin 2.5 µg -** (1.35 ± 0.231 $p<0.001$); **iii) Treatment with haptoglobin 5.0 µg** - 0.20 ± 0.037; **Co-treatment with LPS and haptoglobin 5.0 µg** (1.3803 ± 0.14 $p<0.001$); **iv)Treatment with haptoglobin 10µg-** 1.04 ± 0.0267, **Co-treatment with LPS and haptoglobin 10 µg** (0.37 ± 0.0102 $p<0.001$)

D) Fold changes of IL-8 are as follows**.** A significant decrease in mean folds change was observed at all tested concentrations of haptoglobin when compared to cells with only LPS treatment - $p<0.001$. **i) Control cells (untreated cells)**-1.00 ± 0.031**, Treatment with LPS alone**- (122.91 ± 12.5, $p<0.0001$)**; ii) Treatment with the haptoglobin 2.5 µg** -0.89 ± 0.069, **Co-treatment with LPS and haptoglobin 2.5 µg** - (34.43 ± 2.38 , $p<0.0001$); **iii) Treatment with the haptoglobin 5.0 µg** - 1.87 ± 0.448, **Co-treatment with haptoglobin 5.0 µg and LPS**- (25.227 ± 1.68, $p<0.0001$); **iv) Treatment with the haptoglobin 10µg**-0.84 ± 0.317, **Co-treatment with LPS and haptoglobin 10µg**- (29.28 ± 5.67 $p<0.0001$)

E) Fold changes of MCP-1are as follows**.** A significant decrease in mean folds change was observed at all tested concentrations of haptoglobin when compared to cells with only LPS treatment . $p<0.0001$. **i) Control cells (untreated cells)**-1.00 ± 0.707**, Treatment with LPS alone**- (13.70 ± 0.41, $p<0.0001$)**; ii) Treatment with the haptoglobin 2.5 µg** -1.13 ± 0.804, **Co-treatment with LPS and haptoglobin 2.5 µg** - (2.65 ± 0.38, $p<0.0001$); **iii) Treatment with the haptoglobin 5.0 µg** - 0.27 ± 0.196, **Co-treatment with haptoglobin 5.0 µg and LPS**- (2.88 ± 0.60, $p<0.0001$); **iv) Treatment with the haptoglobin 10µg**-1.06 ± 0.753, **Co-treatment with LPS and haptoglobin 10µg**- (1.04 ± 0.0420 $p<0.0001$)

F) Fold changes of TNF-α are as follows. A significant decrease in the mean folds change was observed at all tested concentrations of haptoglobin when compared to cells with only LPS treatment p<0.0001. **i) Control cells (untreated cells)**-1.00 ± 0.031**, Treatment with LPS alone**- (72.89 ± 13.7, $p<0.001$)**; ii) Treatment with the haptoglobin 2.5 µg** -0.044 ± 0.014, **Co-treatment with LPS and haptoglobin 2.5 µg** - (1.25 ± 0.19 , $p<0.0001$); **iii) Treatment with the haptoglobin 5.0 µg** - 0.651 ± 0.316, **Co-treatment with haptoglobin 5.0 µg and LPS**- (0.54 ± 0.13, $p<0.0001$); **iv) Treatment with the haptoglobin 10µg**-1.76 ± 0.223, **Co-treatment with LPS and haptoglobin 10µg**- (0.56 ± 0.14$p<0.0001$)

6.21 ARPE-19 stimulated with 10µg LPS and anti-inflammatory effect of haptoglobin in a dose-dependent manner

ARPE-19 cells were incubated in serum-free medium overnight and were stimulated with LPS at 10 µg /mL. Cells were simultaneously co-treated with final concentration

of haptoglobin 2.5, 5.0, 10.0 µg/mL. At all treatment conditions mRNA expression of pro-inflammatory cytokines were measured after 24 h. The expression of mRNA was normalized to 18S rRNA. One way ANOVA with Tukey's Multiple Comparison Test was used for comparison of mean (fold change) untreated cells with the cells treated with LPS and haptoglobin co-treated (Figure 33).

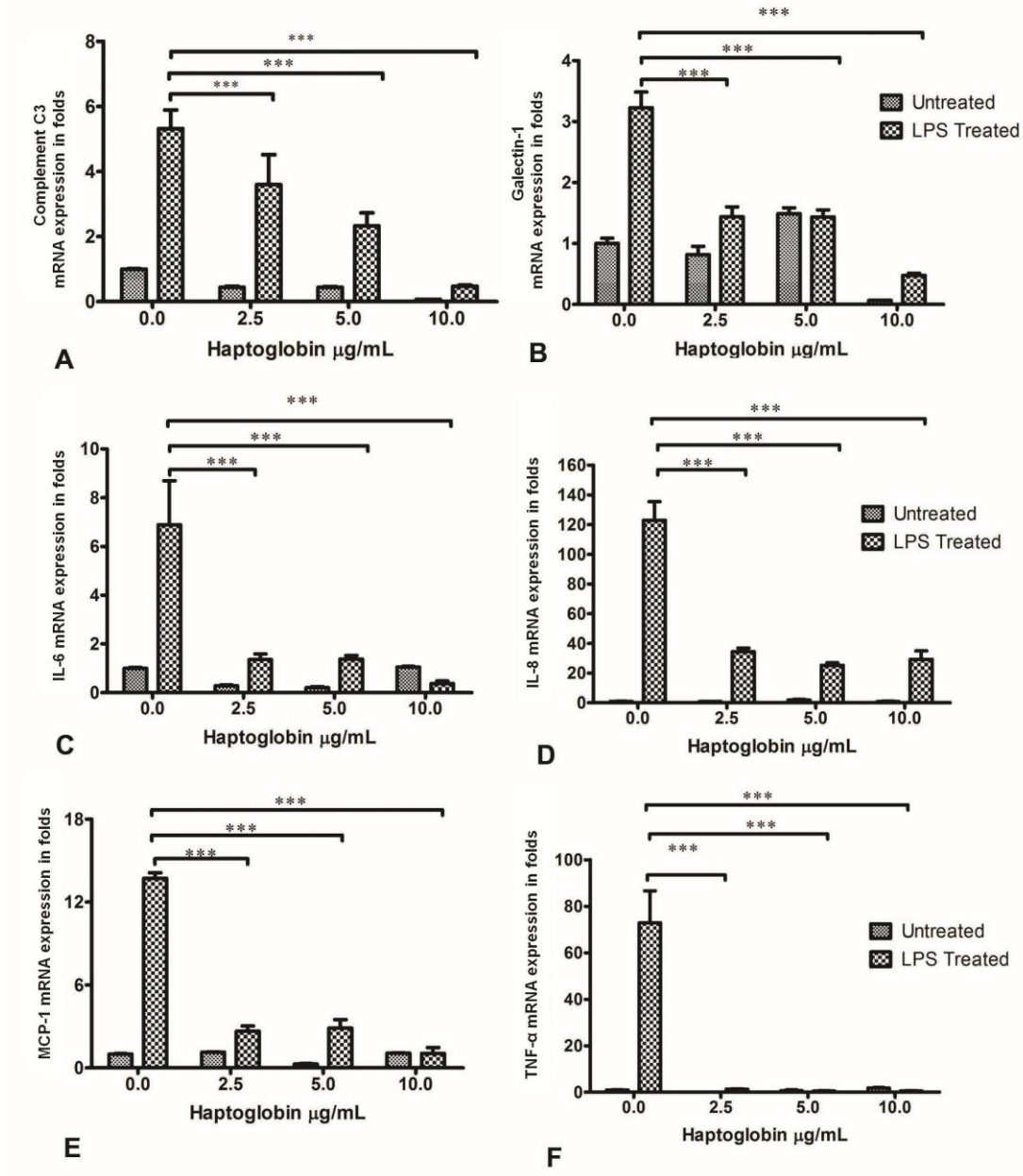

Figures 33: The ARPE-19 was treated with the 10 µg/ml of LPS. Cells were co-treated with 1 µg/ml, 2.5 µg/ml, 5.0 µg/ml, 10 µg/ml of haptoglobin and mRNA expression was screened by qPCR.

A) Fold changes of complement C3 are as follows**.** A significant decrease in mean folds change was observed at all tested concentrations of haptoglobin when compared to cells with only LPS treatment - $p<0.001$. **i) Control cells** (untreated cells)-1.00 ± 0.0161, **Cells treated with LPS alone** 5.32 ± 0.56 $p<0.001$; **ii) Treatment with haptoglobin 2.5 µg** 0.43 ± 0.037; **Co-treatment with LPS and haptoglobin 2.5 µg** - (3.59 ± 0.92 $p<0.001$); **iii) Treatment with haptoglobin 5.0 µg** 0.47 ± 0.026; **Co-treatment with LPS and haptoglobin 5.0 µg** (2.32 ± 0.402 $p<0.001$); **iv)Treatment with haptoglobin 10µg**- 0.066 ± 0.02857, **Co-treatment with LPS and haptoglobin 10 µg** (0.47 ± 0.03 $p<0.001$)

B) Fold changes of galectin-1 are as follows**.** A significant decrease in mean folds change was observed at all tested concentrations of haptoglobin when compared to cells with only LPS treatment - $p<0.001$. **i) Control cells** (untreated cells)-1.00 ± 0.084 , **Cells treated with LPS alone** 3.22 ± 0.25 $p<0.001$; **ii) Treatment with haptoglobin 2.5 µg** -1.436 ± 0.16 ; **Co-treatment with LPS and haptoglobin 2.5 µg** (1.48 ± 0.50 $p<0.001$); **iii) Treatment with haptoglobin 5.0 µg** - 0.814 ± 0.137; **Co-treatment with LPS and haptoglobin 5.0 µg** (1.435 ± 0.11 $p<0.001$); **iv)Treatment with haptoglobin 10µg**-1.487 ± 0.097, **Co-treatment with LPS and haptoglobin 10 µg** (0.47 ± 0.0328 $p<0.001$)

C) Fold changes of IL-6 are as follows**.** A significant decrease in mean folds change was observed at all tested concentrations of haptoglobin when compared to cells with only LPS treatment - $p<0.001$. **i) Control cells** (untreated cells)-1.00 ± 0.031, **Cells treated with LPS alone** 6.88 ± 1.80 $p<0.001$; **ii) Treatment with haptoglobin 2.5 µg** -0.28 ± 0.033; **Co-treatment with LPS and haptoglobin 2.5 µg** - (1.35 ± 0.231 $p<0.001$); **iii) Treatment with haptoglobin 5.0 µg** - 0.20 ± 0.037; **Co-treatment with LPS and haptoglobin 5.0 µg** (1.3803 ± 0.14 $p<0.001$); **iv)Treatment with haptoglobin 10µg**-1.04 ± 0.0267, **Co-treatment with LPS and haptoglobin 10 µg** (0.37 ± 0.0102 $p<0.001$)

D) Fold changes of IL-8 are as follows**.** A significant decrease in mean folds change was observed at all tested concentrations of haptoglobin when compared to cells with only LPS treatment - $p<0.001$.**i) Control cells (untreated cells)-**1.00 ± 0.031**, Treatment with LPS alone-** (122.91 ± 12.5, $p<0.0001$)**; ii) Treatment with the**

haptoglobin 2.5 µg -0.89 ± 0.069, **Co-treatment with LPS and haptoglobin 2.5 µg** - (34.43 ± 2.38 , p<0.0001); **iii) Treatment with the haptoglobin 5.0 µg** - 1.87 ± 0.448, **Co-treatment with haptoglobin 5.0 µg and LPS**- (25.227 ± 1.68, p<0.0001); **iv) Treatment with the haptoglobin 10µg**-0.84 ± 0.317, **Co-treatment with LPS and haptoglobin 10µg**- (29.28 ± 5.67 p<0.0001)

E) Fold changes of MCP-1 are as follows**.** A significant decrease in mean folds change was observed at all tested concentrations of haptoglobin when compared to cells with only LPS treatment - p<0.0001. **i) Control cells (untreated cells)**-1.00 ± 0.707**, Treatment with LPS alone**- (13.70 ± 0.41, p<0.0001)**; ii) Treatment with the haptoglobin 2.5 µg** -1.13 ± 0.804, **Co-treatment with LPS and haptoglobin 2.5 µg** - (2.65 ± 0.38, p<0.0001); **iii) Treatment with the haptoglobin 5.0 µg** - 0.27 ± 0.196, **Co-treatment with haptoglobin 5.0 µg and LPS**- (2.88 ± 0.60, p<0.0001); **iv) Treatment with the haptoglobin 10µg**-1.06 ± 0.753, **Co-treatment with LPS and haptoglobin 10µg**- (1.04 ± 0.0420 p<0.0001)

F) Fold changes of TNF-α are as follows**.** A significant decrease in mean folds change was observed at all tested concentrations of haptoglobin when compared to cells with only LPS treatment - p<0.0001. **i) Control cells (untreated cells)**-1.00 ± 0.031**, Treatment with LPS alone**- (72.89 ± 13.7, p<0.001)**; ii) Treatment with the haptoglobin 2.5 µg** -0.044 ± 0.014, **Co-treatment with LPS and haptoglobin 2.5 µg** - (1.25 ± 0.19 , p<0.0001); **iii) Treatment with the haptoglobin 5.0 µg** - 0.651 ± 0.316, **Co-treatment with haptoglobin 5.0 µg and LPS**- (0.54 ± 0.13, p<0.0001); **iv) Treatment with the haptoglobin 10µg**-1.76 ± 0.223, **Co-treatment with LPS and haptoglobin 10µg**- (0.56 ± 0.14p<0.0001)

6.22 ARPE-19 stimulated with TNF- α and anti-inflammatory effect of haptoglobin in a dose-dependent manner

ARPE-19 cells were incubated in serum-free medium overnight and were stimulated with TNF-α at 1 µg/mL. Cells were simultaneously co-treated with final concentration of haptoglobin 2.5, 5.0, 10.0 µg/mL. At all treatment conditions mRNA expression of pro-inflammatory cytokines were measured after 24 h. The expression of mRNA was normalized to 18S rRNA. One way ANOVA with Tukey's Multiple Comparison Test

was usedfor comparison of mean (fold change) untreated cells with the cells treated with TNF-α and haptoglobin co-treated (Figure 34).

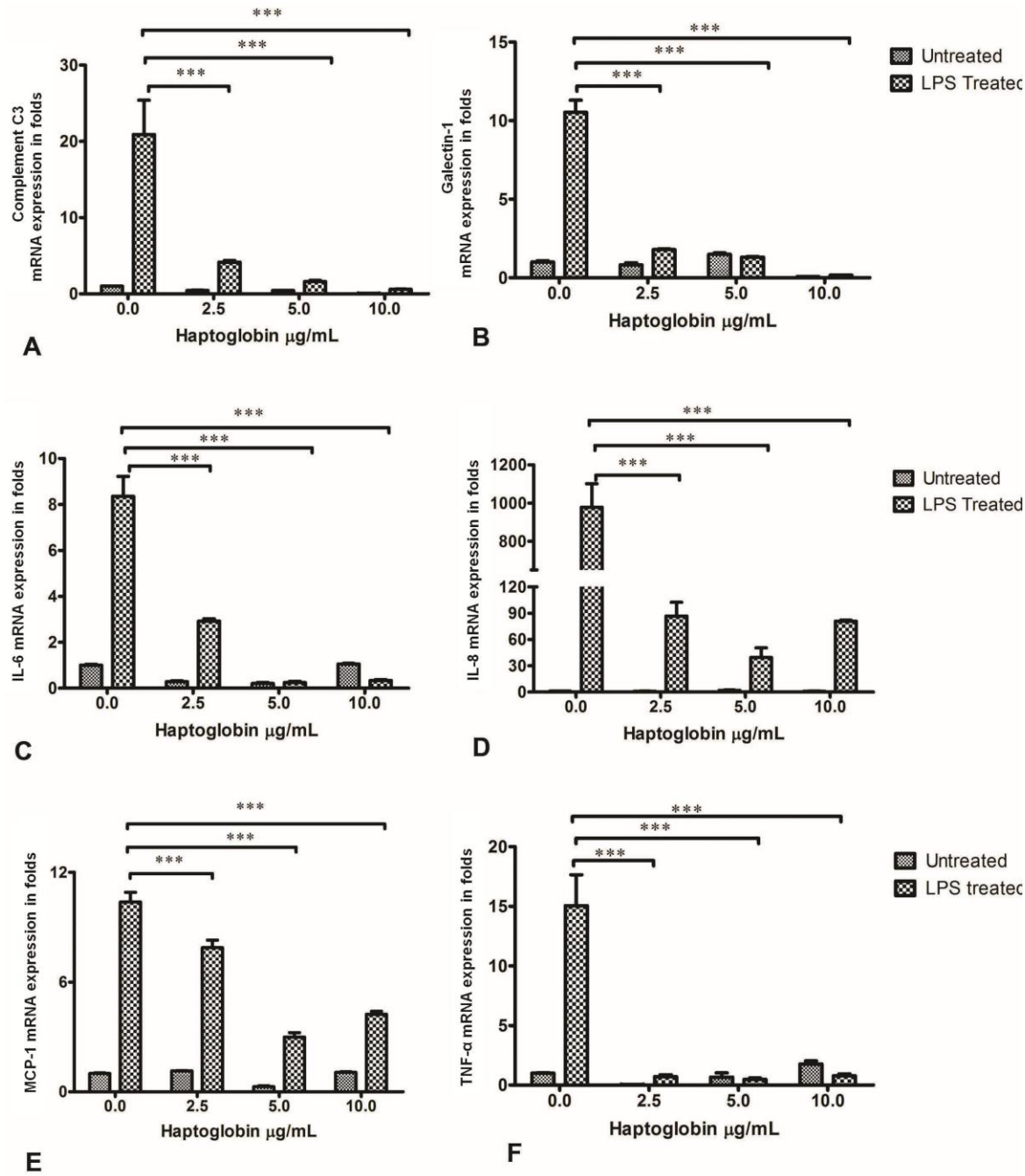

Figures 34: The ARPE-19 was treated with TNF-α of LPS. Cells were co-treated with 1 µg/ml, 2.5 µg/ml, 5.0 µg/ml, 10 µg/ml of haptoglobin and mRNA expression was screened by qPCR.

A) Fold changes of complement C3 are as follows**.** A significant decrease in mean folds change was observed at all tested concentrations of haptoglobin when compared to cells with only LPS treatment - $p<0.001$.**i) Control cells** (untreated cells)-1.00 ± 0.0161, **Cells treated with TNF-α alone** 5.60 ± 0.23 $p<0.001$; **ii) Treatment with haptoglobin 2.5 µg** 0.43 ± 0.037; **Co-treatment with TNF-α and haptoglobin 2.5 µg** - (5.30 ± 0.488 $p<0.001$); **iii) Treatment with haptoglobin 5.0 µg** 0.47 ± 0.026; **Co-treatment with TNF-αand haptoglobin 5.0 µg** (1.219 ± 0.34 $p<0.001$); **iv)Treatment with haptoglobin 10µg**- 0.066 ± 0.02857, **Co-treatment with TNF-α and haptoglobin 10 µg** (0.30 ± 0.02 $p<0.001$)

B) Fold changes of galectin-1 are as follows**.** A significant decrease in mean folds change was observed at all tested concentrations of haptoglobin when compared to cells with only LPS treatment - $p<0.001$.**Control cells** (untreated cells)-1.00 ± 0.084 , **Cells treated with TNF-α alone** 1.61 ± 0.18 $p<0.001$; **ii) Treatment with haptoglobin 2.5 µg** -1.436 ± 0.16 ; **Co-treatment with TNF-α and haptoglobin 2.5 µg** (1.48 ± 0.50 $p<0.001$); **iii) Treatment with haptoglobin 5.0 µg** - 0.814 ± 0.137; **Co-treatment with TNF-α and haptoglobin 5.0 µg** (0.78 ± 0.035 $p<0.001$); **iv)Treatment with haptoglobin 10µg**-1.487 ± 0.097, **Co-treatment with TNF-α and haptoglobin 10 µg** (0.30 ± 0.02 $p<0.001$)

C) Fold changes of IL-6 are as follows**.** A significant decrease in mean folds change was observed at all tested concentrations of haptoglobin when compared to **TNF-α** treated cells**. Control cells** (untreated cells)-1.00 ± 0.031, **Cells treated with TNF-A alone** 8.56 ± 0.435 $p<0.001$; **ii) Treatment with haptoglobin 2.5 µg** -0.28 ± 0.033; **Co-treatment with TNF-α and haptoglobin 2.5 µg** - (1.30 ± 0.13 $p<0.001$); **iii) Treatment with haptoglobin 5.0 µg** - 0.20 ± 0.037; **Co-treatment with TNF-α and haptoglobin 5.0 µg** (1.50 ± 0.08 $p<0.001$); **iv)Treatment with haptoglobin 10µg**-1.04 ± 0.0267, **Co-treatment with TNF-α and haptoglobin 10 µg** (0.206 ± 0.06 $p<0.001$)

D) Fold changes of IL-8 are as follows**:** A significant decrease in mean folds change was observed at all tested concentrations of haptoglobin when compared to TNF-A treated cells- $p<0.001$. **i) Control cells (untreated cells)**-1.00 ± 0.031**, Treatment with TNF-α alone-** (218.45 ± 11.02, $p<0.0001$)**; ii) Treatment with the haptoglobin**

2.5 µg -0.89 ± 0.069, **Co-treatment with TNF-α and haptoglobin 2.5 µg** - (24.26 ± 3.89 , p<0.0001); **iii) Treatment with the haptoglobin 5.0 µg** - 1.87 ± 0.448, **Co-treatment with haptoglobin 5.0 µg and TNF-A**- (13.15 ± 2.75 , p<0.0001); **iv) Treatment with the haptoglobin 10µg**-0.84 ± 0.317, **Co-treatment with TNF- α and haptoglobin 10µg**- (20.48 ± 4.7 p<0.0001).

E) Fold changes of MCP-1 are as follows: A significant decrease in mean folds change was observed at all tested concentrations of haptoglobin when compared to TNF- α treated cells. p<0.0001. **i) Control cells (untreated cells)**-1.00 ± 0.707**, Treatment with TNF- α alone**- (21.18 ± 1.11, p<0.0001)**; ii) Treatment with the haptoglobin 2.5 µg** -1.13 ± 0.804, **Co-treatment with TNF- α and haptoglobin 2.5 µg** - (2.72 ± 0.092, p<0.0001); **iii) Treatment with the haptoglobin 5.0 µg** - 0.27 ± 0.196, **Co-treatment with haptoglobin 5.0 µg and TNF-α** (2.12 ± 0.29, p<0.0001); **iv) Treatment with the haptoglobin 10µg**-1.06 ± 0.753, **Co-treatment with TNF- α and haptoglobin 10µg**- (0.67 ± 0.20 p<0.0001)

F) Fold changes of TNF-α are as follows: A significant decrease in the mean folds change was observed at all tested concentrations of haptoglobin when compared to TNF- α treated cells p<0.0001. **i) Control cells (untreated cells)**-1.00 ± 0.031**, Treatment with TNF- α alone**- (45.69 ± 4.12, p<0.001)**; ii) Treatment with the haptoglobin 2.5 µg** -0.044 ± 0.014, **Co-treatment with TNF- α and haptoglobin 2.5 µg** - (0.48 ± 0.13 , p<0.0001); **iii) Treatment with the haptoglobin 5.0 µg** - 0.651 ± 0.316, **Co-treatment with haptoglobin 5.0 µg and TNF- α** - (0.60 ± 0.092, p<0.0001); **iv) Treatment with the haptoglobin 10µg**-1.76 ± 0.223, **Co-treatment with TNF- α and haptoglobin 10µg**- (3.77 ± 1.176 p<0.0001).

6.23 Effect of haptoglobin on MAP kinase pathway and NFκB

LPS induces p38 mitogen activated protein kinase (MAPK) pathway which involved in pro-inflammatory cellular response and results in the expression of IL-1β, IL-6, IL-8 and TNFα (108). Since haptoglobin causes reduction of pro-inflammatory cytokine mRNA, effect of haptoglobin on p38 MAPK pathway was studied in LPS stimulated ARPE -19 cells. ARPE-19 cells were treated with LPS of 1 µg/mL and haptoglobin of 1 µg/mL for identifying their effect of p-38 activation. Cells were also co-treated with

of LPS and haptoglobin (1 μg/mL). One way ANOVA was used to compare mean of controls with the treatment conditions and results are given in mean percentages ± standard error of mean. The phosphorylation of p-38 MAPK is induced by haptoglobin (138.67 ± 13.12) and by co-treatment of haptoglobin and LPS (127.87 ± 8.13). However, there is no statistically significant difference is observed between the three conditions. The results of this experiment indicate that both haptoglobin and LPS induce phosphorylation of p-38 MAPK but did not show any additive effects (Figure 35).

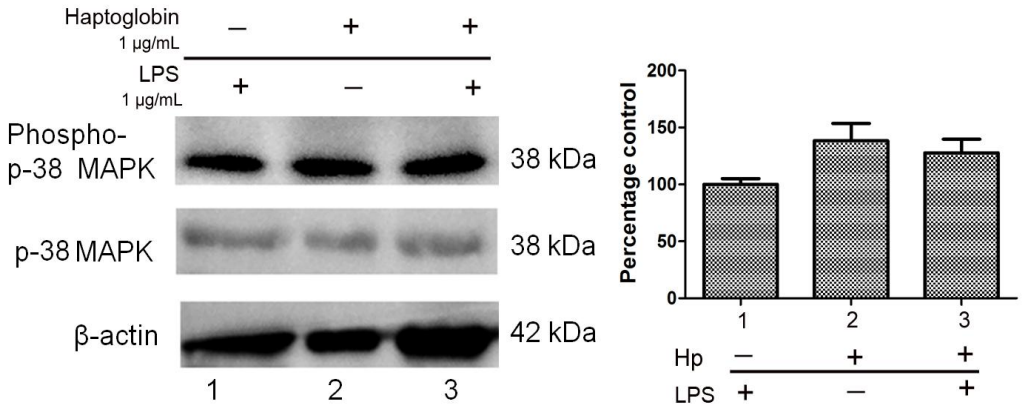

Figure 35: Effect of haptoglobin on MAP kinase activation . Lane 1: cells treated with 1 μg/mL of LPS, Lane 2: cells treated with 10 μg/mL of haptoglobin, Lane 3: cells treated with 1 μg/mL of LPS and co treated with 10 μg/mL of haptoglobin. The treatment of haptoglobin resulted in activation of p-38 MAPK.

6.24 Haptoglobin on NF-κB expression

Several investigators have reported increased NF-κB activity in human disease conditions. Targets for NF-κB include the genes corresponding to the pro inflammatory cytokines such as interleukins IL-1, IL-6, IL-8 and TNF. It also includes inducible nitric oxide synthase (iNOS), adhesion molecules, MMP, growth factors, major histocompatibility antigens (MHC class 1 and 2) and different acute

phase proteins (109). ARPE-19 cells were treated with LPS of 1 μg/mL served as control and compared with those cells co-treated with haptoglobin 1 μg/mL and 10 μg/mL. One way ANOVA was used to compare mean of controls with the treatment conditions and results are given in mean percentages ± standard error of mean. The results show the expression of NF-κB protein in ARPE-19 cells treated with LPS of 1 μg/mL. Expression of NF-κB was observed in cells treated with LPS alone served as control and cells co-treated with haptoglobin 1 μg/mL and 10 μg/mL. The results indicate treatment with haptoglobin 10 μg/mL concentration resulted in decreased expression of NFκB (5.13 ± 3.9, $p<0.0001$) and there is dosage dependent reduction of NFκB (Figure 36).

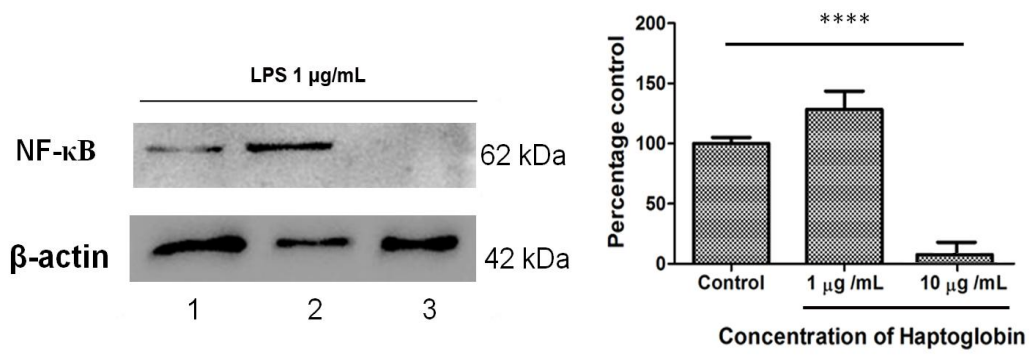

Figure 36: Suppression of NFκB by haptoglobin. Lane1: Control, Lane 2: 1 μg/mL of haptoglobin (122.245 ± 14.79) Lane 3: 10 μg /mL haptoglobin. The treatment of haptoglobin 10 μg/mL resulted in reduction NFκB with statistical significance (5.13 ± 3.9, $p<0.0001$).

6.25 Quantitative mRNA expression of galectin-1 in PBMC

Presence of galectin-1 was identified in the purified 88 kDa protein and its levels were found to be reduced in serum of Eales' disease patients. The levels of galectin-1 in Eales' disease were found to be decreased with statistical significance. In addition, mRNA expression was measured in the PBMC isolated from control and Eales disease patients and mRNA expression of galectin-1 was found to be reduced in Eales' disease patients (Figure 37). Galectin-1 is involved in a wide range of biological activity such as T-cell homeostasis, T-cell immune disorders, and inflammation and host– pathogen interactions. Galectin-1 silencing was carried out in ARPE-19 cells for understanding the effects of inflammation.

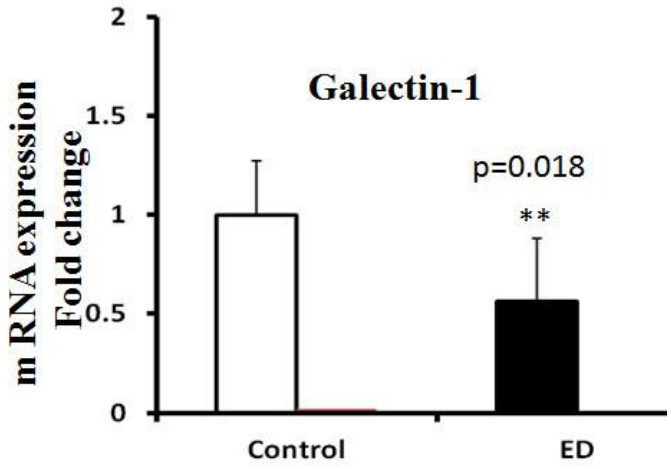

Figure 37: Reduced mRNA expression of galectin-1 in Eales' disease patients. The mRNA expression of galectin-1 in PBMC was compared between control and Eales' disease samples (n=20) and found to be reduced in Eales' disease compared to controls.

6.26 Cloning of galectin-1

Galectin-1, another protein of 88 kDa was found to be significantly down regulated in Eales' disease. Hence, the protein was cloned in pCMV 3x Flag vector.

6.26.1 Construction of p3X FLAG-MYC-CMV + Galectin-1

Infusion cloning method was implemented to get the, over expression of recombinant galectin-1. The galectin-1 insert was synthesized by PCR amplification with HUVEC mRNA as template. The galectin-1 cDNA was amplified by PCR and inserted into the mammalian expression vector, p3X FLAG-MYC-CMV using the restriction enzymes, HindIII and XbaI.

6.26.2 PCR amplification of galectin-1

From cDNA of HUVEC, galectin-1 gene was PCR amplified using infusion primers. Agarose gel electrophoresis of PCR product revealed a single band at 408 bp; this corresponds to the molecular size of galectin-1 gene. The band was eluted from the gel and was used for infusion reaction (Figure 38).

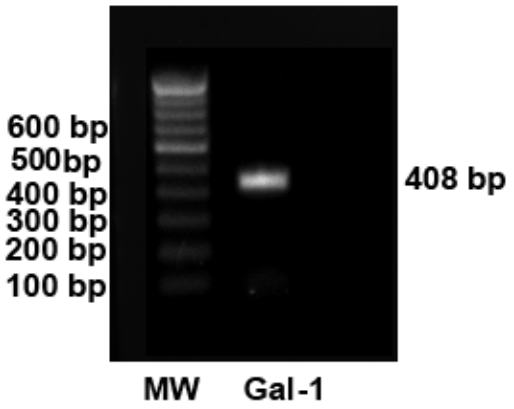

Figure 38: PCR amplification of galectin-1 insert. Amplified gal-1 insert is resolved by agarose gel electrophoresis.. Lane 1: MW Lane 2- PCR amplified galectin-1 insert (408 bp)

6.26.3 Linearization of p3X FLAG-MYC-CMV vector

Circular p3X FLAG-MYC-CMV vector was treated with HindIII and XbaI restriction enzymes overnight at 37^{o}C. The digested product was subjected to agarose electrophoresis and visualized. The specific band at 6.4 kbp was gel eluted and was used for infusion reaction (Figure 39).

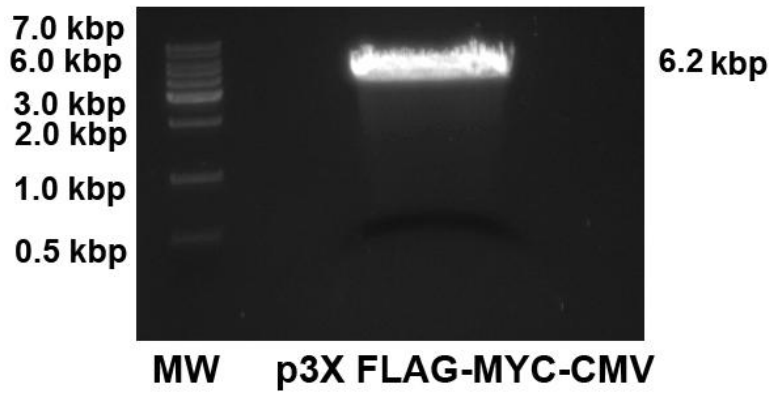

Figure 39: Linearization of p3X FLAG-MYC-CMV vector. Agarose gel electrophoresis of linearized p3X FLAG-MYC-CMV vector. Lane 1: MW Molecular size marker (0.5 – 10 kbp); Lane 2: Linearized p3X FLAG-MYC-CMV (6.2 kbp).

6.26.4 Infusion reaction

Infusion reaction was performed with eluted galectin-1 cDNA and linearized p3X FLAG-MYC-CMV vector. The resulted infusion product was transfected into competent M15 (pREP4) cells. The transfected cells were inoculated onto selective LB agar plate containing ampicillin (100 µg / mL) and incubated overnight at 37 ^{o}C. Colonies grown in the selective LB plate were further confirmed for complete vector construct.

6.26.5. Confirmation of p3X FLAG-MYC-CMV + galectin 1 vector construct

Colonies were randomly picked from the selective LB agar plate and were inoculated into LB media (containing ampicillin) and incubated overnight. Plasmid DNA from the overnight culture was isolated and restriction digestion was performed with HindIII and XbaI restriction enzymes. Restriction digestion product showed two bands at 6.4 kbp and 408 bp respective to the molecular size of linearized vector and galectin-1 cDNA insert (Figure 39). Thus the transformed M15 (pREP4) *E.coli* contains the complete p3X FLAG-MYC-CMV + galectin-1 construct. This was further confirmed by gene sequencing (Figure 40).

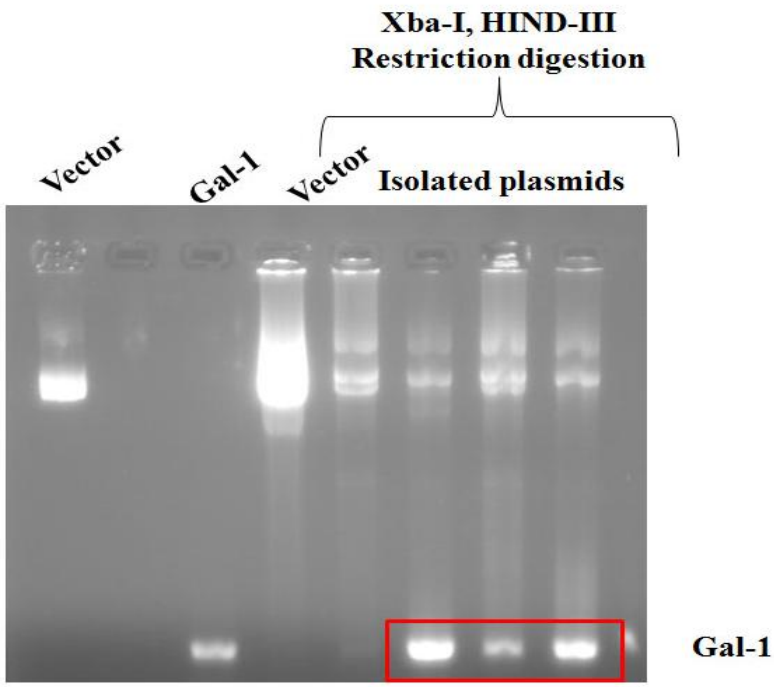

Figure 40: Confirmation of p3X FLAG-MYC-CMV + galectin 1 by restriction digestion. Agarose gel electrophoresis of p3X FLAG-MYC-CMV + galectin-1 vector digested using restriction enzymes HindIII and XbaI. Lane 1: Linearized p3X FLAG-MYC-CMV vector, Lane 3: galectin-1 insert, Lane 4: Undigested p3X FLAG-MYC-CMV vector; Lane 5: Digested p3X FLAG-MYC-CMV vector, Lane 6-8 Digested p3X FLAG-MYC-CMV + galectin-1 showing the galectn-1 insert at 408 bp.

6.26.6 Sequencing of galectin-1 gene in p3X FLAG-MYC-CMV vector constructs

The galectin-1 cDNA insert in the p3X FLAG-MYC-CMV + galectin-1 plasmid was sequenced with 3100-Avant Genetic analyzer. Output sequence was analyzed using the Bio Edit software tool. Resulted sequence had 100 % identity to the reference galectin-1 cDNA sequence from NCBI database with no mutation. Thus, transfected M15 (pREP4) E.coli (clone) strain harbors the complete p3X FLAG-MYC-CMV + galectin-1 plasmid constructs. Glycerol stocks of the transfected cells were prepared and stored at -80 ^{o}C for future usage (Figure 41).

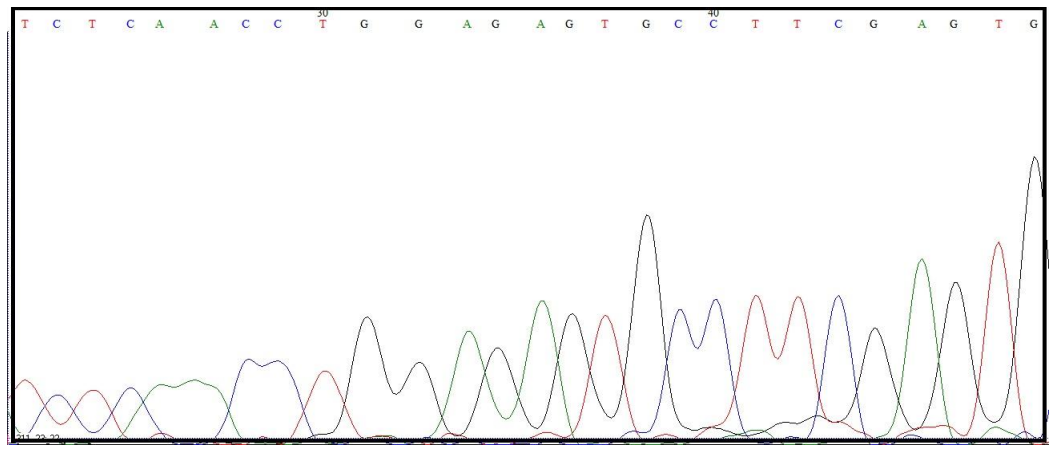

Figure 41: Sequencing of galectin-1: No mutation was observed in the sequence.

6.26.7 Overexpression of galectin-1 in COS-7 cells

The COS-7, an African green monkey kidney-derived cell line, was transfected with the p3X FLAG-MYC-CMV expression vector. The morphology and proliferation rate of COS-7-galectin-1 cells were similar to those of parental COS-7 cells. The expression level of galectin-1 in control vector COS-7 and COS-7-galectin-1 cells were examined at varying time points. Protein bands were detected in COS-7-galectin with the anti-galectin-1 antibody (Figure 42).

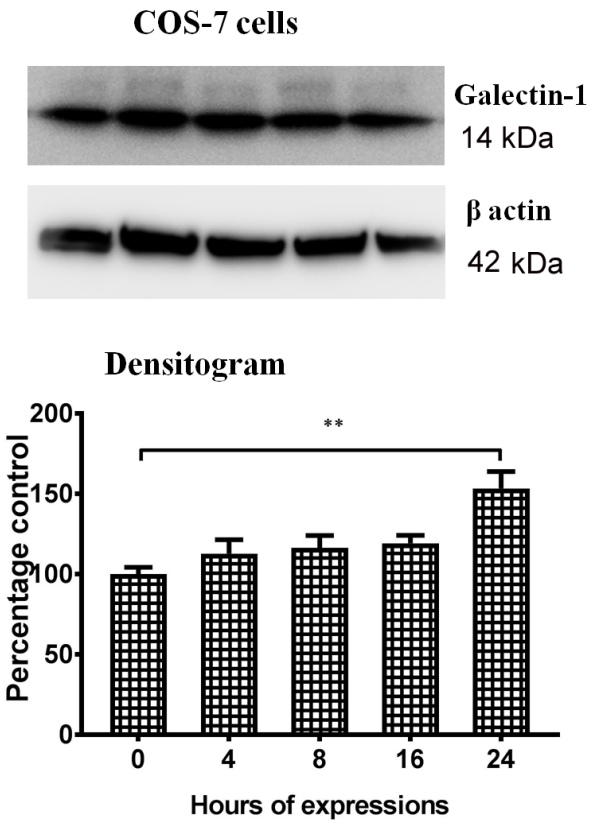

Figure 42: Optimization of time point for overexpression of galectin-1: Galectin expressions in COS-7-galectin-1 cells were examined at varying time points (0, 4, 8, 16, and 24 h). Protein bands with maximum intensity were detected at 24 h with statistical significance (**p<0.01).

6.26.8 Tandem affinity purification of overexpressed galectin-1 in COS-7 cells using FLAG tag

The expression levels of galectin-1 in COS-7 and COS-7-galectin-1 cells were examined. Using anti-FLAG -1 antibody immunoprecipitates, bands of COS-7 and COS-7-galectin-1 was compared. COS-7-galectin-1 cells showed significantly increased FLAG tag at 25 kDa compared to the control vector containing COS-7 cells (Figure 43).

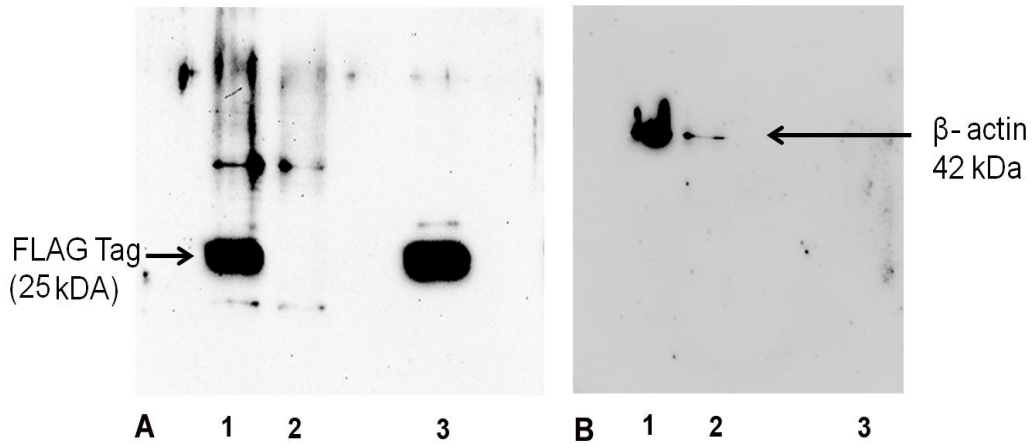

Figure 43: Tandem affinity purification of overexpressed galectin-1. A) Band at the region of 25 kDa was detected in the immunoprecipitate derived from COS-7- galectin-1 cells by anti-FLAG antibody. The 25-kDa band due to galectin-1 in the immunoprecipitates derived from COS-7 and COS-7-galectin-1 cells was also detected. B) Band of 42 kDa region was identified anti-β actin antibody, in COS-7-galectin-1 cells and parental COS-7 cells. Lane 1; overexpressed galectin-1, Lane 2: control vector, Lane 3: anti-FLAG -1 antibody immunoprecipitates COS-7-galectin-1 cells.

6.26.9 Identification of galectin-1 interacting proteins by mass spectrometry

In anti-FLAG -1 antibody immunoprecipitates, annexin, RNA binding motif protein, serine peptidase inhibitor and galectin 1 were identified. These proteins were found to be interacting and galectin-1 is a binding partner for the identified proteins (Table 29).

Protein Accession Protein Description	Protein score	Protein Avg Mass	Protein Seq Cover (%)	Protein. Matched Peptide Inten Sum
B4DNH8 Annexin	2956.218	21840.69	31.96	129434
A0A060D9J6 RNA binding motif protein 8A	945.6113	2352.452	100	4922
H7C1T1 Septin 2	708.9866	2985.425	79.31	13617
A0A024RD95 Serine peptidase inhibitor Kazal type 2	618.0439	9633.199	26.19	12995
P09382 Galectin 1	390.75	15057.89	25.93	79566

Table 29. The list of proteins identified in FLAG immunoprecipitated COS-7 cells lysates.

6.27 Silencing of galectin-1 in ARPE-19 and HUVEC using dicer substrate small interfering RNAs

Galectin-1 silencing was carried out with three concentrations, such as 10, 20 and 30 nM for the period of 24 h. Silencing of galectin-1 using 10 nM concentration of DsiRNA at 24 h time point has efficiently silenced the protein (Figure 44).

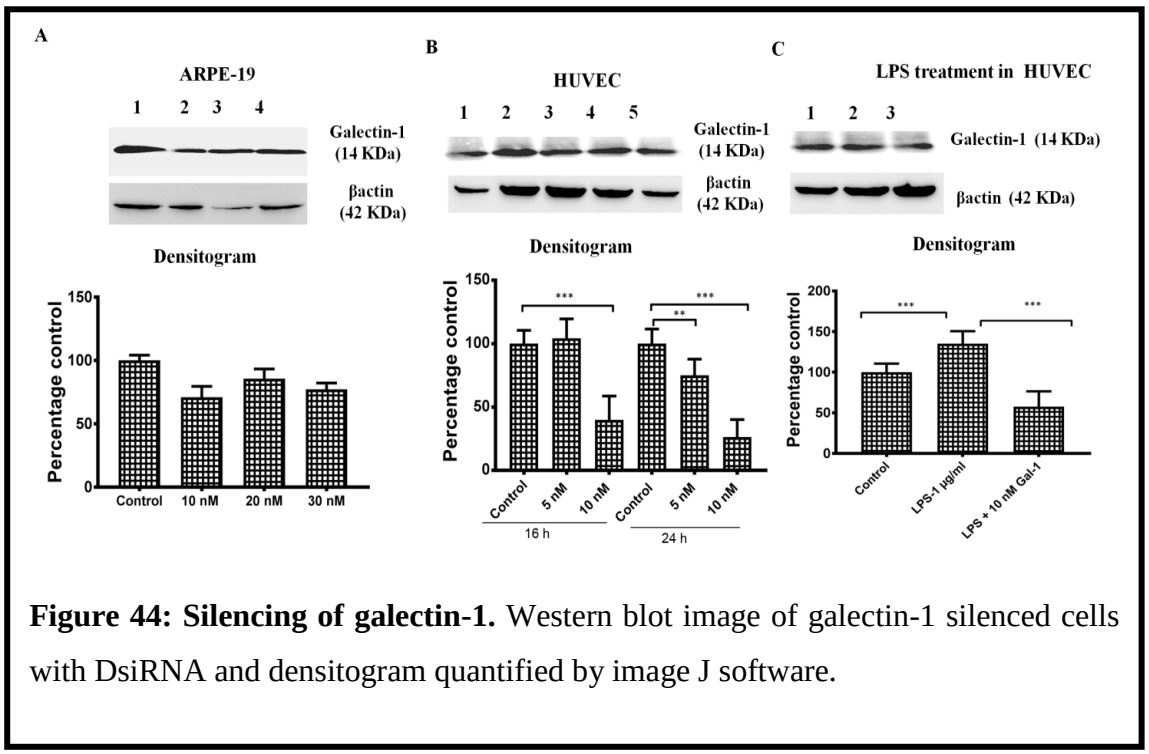

Figure 44: Silencing of galectin-1. Western blot image of galectin-1 silenced cells with DsiRNA and densitogram quantified by image J software.

6.28 Infectious Etiology

Proteomic analysis of serum and PBMC of Eales' disease patient samples using PLGS software showed the presence of *Mycobacterium tuberculosis* proteins. In addition to this MBP and IS 16110 also identified in PBMC of Eales' disease patients which confirms the presence of the organism in subjects (Table 30).

Protein Accession and Protein Description	Protein score	Protein Avg Mass	Protein seq Cover (%)	Protein Matched Peptide Inten Sum	Protein top3 Matched Peptide Inten Sum	Protein Matched Product Inten Sum
P9WIG7 **Uncharacterized PE family protein PE35 OS Mycobacterium tuberculosis strain ATCC 25618 H37Rv**	501.932	9927.8	10.1	27974	74247	14521
P95006 **Putative antitoxin VapB19 OS Mycobacterium tuberculosis strain ATCC 25618 H37Rv**	357.791	9453.6	23.53	113997	164053.5	38987
A0QVE0 **Ribosome recycling factor OS Mycobacterium smegmatis strain ATCC 700084 mc 2 155**	351.909	20824.55	8.11	51867	15830	30213

Table 30. The list of mycobacterial proteins identified in PBMC of ED patients.

6.29 PCR Screening for *Mycobacterium tuberculosis* PE35

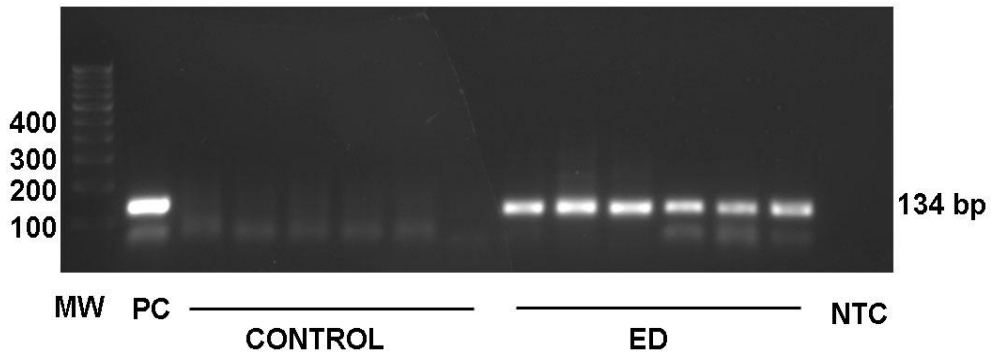

Figure 45: Detection of mycobacterial PE35 DNA in PBMC. Representative image of PE35 screening in PBMC of controls and ED patients. Representative image of PCR results obtained with DNAs extracted from the PBMC samples from patients with Eales' disease and control samples from healthy individuals and resolved in 2% ethidium bromide stained agarose gel. PE35 DNA was identified only in samples obtained from ED patients. The lanes are shown: MW- molecular weight markers, PC- positive control, control - samples from healthy volunteers, ED - Eales' disease patients sample and NTC - no template control.

The presence of PE35 gene expression was screened in PBMCs of 20 Eales' disease patients and control subjects. PE35 was identified in 17 out of 20 PBMC samples obtained from Eales' disease patients and none of the control subjects had shown the presence of the PE35 gene (Figure 45).

6.30 Cloning of PE35

6.30.1 PCR amplification of PE35

From the DNA of *Mycobacterium tuberculosis* (H37RV), PE35 gene was amplified using infusion primers. Agarose gel electrophoresis of PCR product revealed a single band at 300 base pairs; this corresponds to the molecular size of PE35 gene. The band was eluted from the gel and was used for infusion reaction (Figure 46).

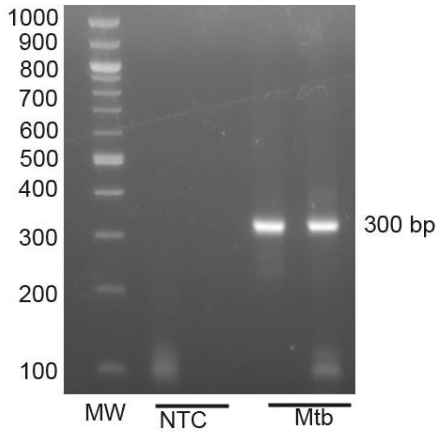

Figure 46: PCR amplification of PE35 insert. Agarose gel electrophoresis for PCR amplified PE35 DNA insert. Lane 1: MW Molecular size marker (100 – 1000 bp) Lane 2 & 3: NTC- no template control Lane 4 & 5: PCR amplified PE35 DNA insert (300 bp).

6.30.2 Linearization of pQE-30 Xa vector

Circular pQE-30 Xa vector was treated with StuI and HindIII restriction enzymes overnight at 37 ^{o}C. The digested product was subjected to agarose electrophoresis and visualized. The specific band at 3500 bp was gel eluted and was used for infusion reaction (Figure 47).

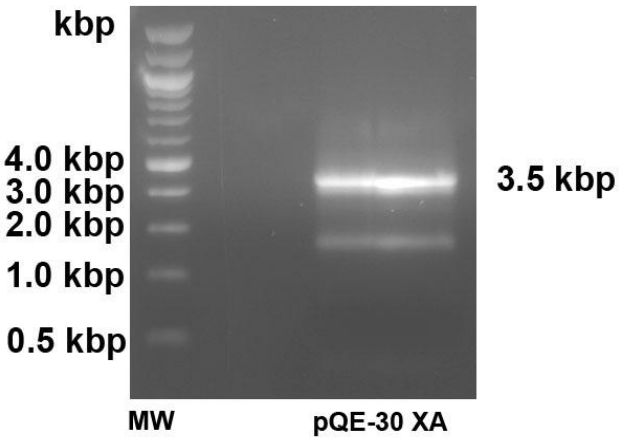

Figure 47: Linearization of pQE-30 Xa vector. Agarose gel electrophoresis of pQE-30 Xa vector which was treated with StuI and HindIII restriction enzymes. Lane 1: MW Molecular size marker (0.5 – 10 kbp), Lane 2 pQE-30 Xa linearized vector.

6.30.3 Infusion reaction

Infusion reaction was performed with eluted PE35 DNA and linearized pQE 30-Xa vector. The resulted infusion product was transfected into competent M15 (pREP4) cells. The transfected cells were inoculated onto selective LB agar plate containing kanamycin (30 μg / mL) and ampicillin (100 μg / mL) then incubated overnight at 37^{o}C. Colonies grown in the selective LB plate were further confirmed for the presence of the gene.

6.30.4 Construction of pQE-30 XA + PE35 vector

The infusion cloning method was implemented to get the purified recombinant PE35. The PE35 DNA insert was synthesized by PCR amplification from the template *Mycobacterium tuberculosis* (H37RV) DNA. The PE35 gene was amplified by PCR and inserted into the bacterial expression vector, pQE-30 Xa using the restriction enzymes, StuI and HindIII.

6.30.5 Confirmation of pQE-30 Xa + PE35 vector construct

Colonies were randomly picked from the selective plate and were inoculated into LB media (containing kanamycin and ampicillin) and incubated overnight. Plasmid DNA from the overnight culture was isolated and restriction digestion was performed with StuI and HindIII restriction enzymes. Restriction digestion product showed two bands at 3500 bp and 300 bp respective to the molecular size of linearized vector and PE35 DNA insert (Figure 48). Thus the transformed M15 (pREP4) *E.coli* contains the complete pQE – 30 Xa + PE35 construct. This was further confirmed by gene sequencing (Figure 49).

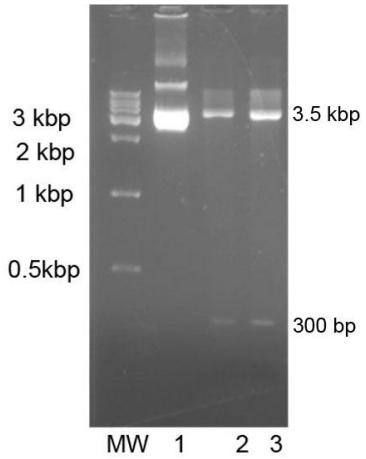

Figure 48: Confirmation of pQE-30Xa+PE35. Agarose gel electrophoresis of pQE-30Xa+PE35 vector digested using restriction enzymes StuI and HindIII. MW-Molecular size marker (0.5 bp – 10 Kbp); Lane 1: pQE-30Xa vector; Lane 2 & 3: pQE-30Xa + PE35 vector digested.

6.30.6 Sequencing of PE35 gene in pQE 30-Xa + PE35 vector constructs

The PE35 gene insert in the pQE-30Xa + PE35 plasmid was sequenced with 3100-Avant Genetic analyzer. Output sequence was analyzed using Bio Edit software tool. Resulted sequence had 100 % identity to the reference PE35 sequence from NCBI database with no mutation. Thus, transfected M15 (pREP4) E.coli (clone) strain harbors the complete pQE-30 Xa + PE35 plasmid construct. Glycerol stocks of the transfected cells were prepared and stored at -80^{o}C for future use).

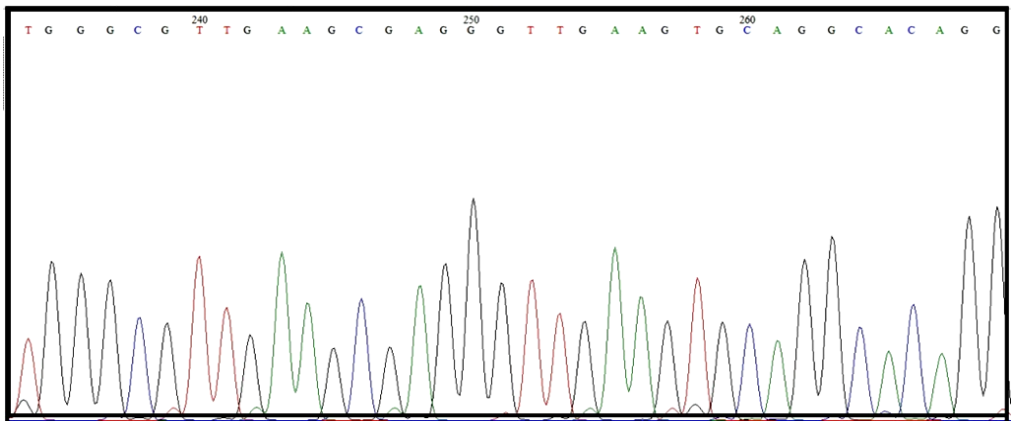

Figure 49: Sequenced image of PE35. No mutation was observed in the sequence of PE35.

6. 30.7 Expression of recombinant PE35

Optimization of IPTG induction

Cloned cells showed maximal expression of PE35 when induced with 1 mM IPTG for 4 h, as observed in figures 50 and 51. These optimized conditions were followed for protein overexpression and purification experiments.

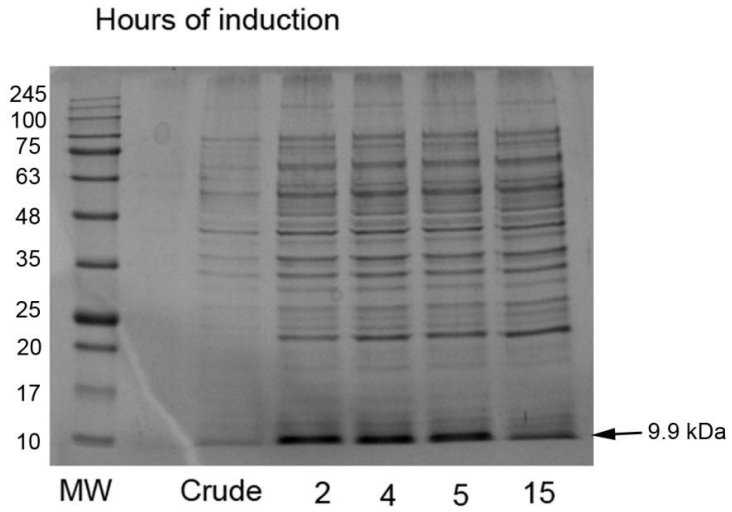

Figure 50: Optimization of IPTG induction time for expression of recombinant PE35. Cloned M15 cells were induced with 1 mM of IPTG for various time points. After induction, cells were lysed and resolved in 10 % SDS-PAGE. Lane 1: Molecular weight marker, Lane 2 & 3: Uninduced cells; Lane 4: IPTG induced for 2 h; Lane 5: IPTG induced for 4 h; Lane 6: IPTG induced for 5 h; Lane 7: IPTG induced for 15 h; Cloned cells induced with IPTG 0.2 mM for 5 h showed intense band at 9.9 kDa (respect to the size of PE35) and the overall protein profile was better when compared to the other time points.

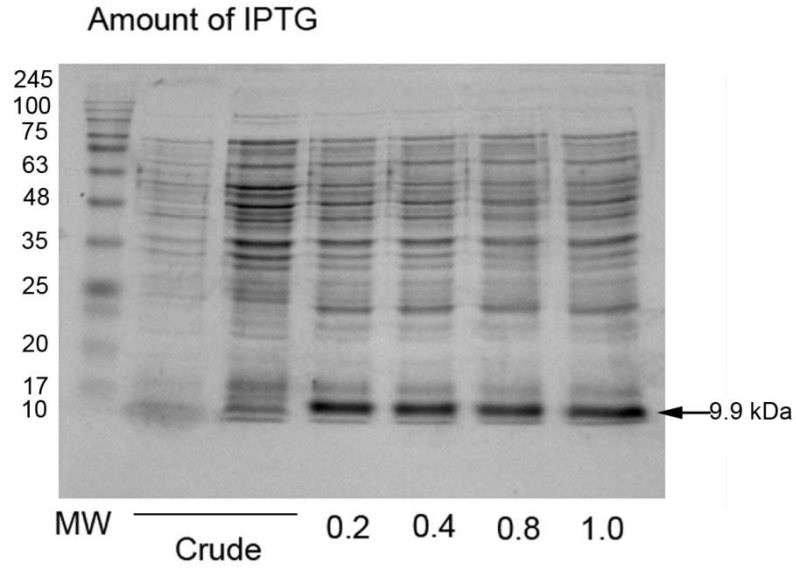

Figure 51: Optimization of IPTG concentration for expression of recombinant PE35. Cloned M15 cells were induced with various concentration of IPTG. After induction, cells were lysed and resolved in 10 % SDS-PAGE. Lane 1: Molecular weight marker (MW); Lane 2 and 3: Uninduced cells (Crude); Lane 4: Induced with 0.2 mM IPTG; Lane 5: Induced with 0.4 mM IPTG; Lane 6: Induced with 0.8 mM IPTG; Lane 7: Induced with 1 mM IPTG. Cloned cells induced with IPTG 0.2 mM showed intense band at 9.9 kDa (respective to the size of PE35) and overall protein profile was similar compared to the other concentrations and higher when compared to uninduced cells.

6.30.8 Purification of recombinant PE35 using Ni-NTA affinity chromatography

Cloned cells were induced with IPTG and PE35 protein was over expressed and purified using Ni-NTA agarose. By affinity displacement method, PE35 was eluted from Ni-NTA and purification was assessed by SDS-PAGE. The elution resulted in 9.9 kDa single band (Figure 52), corresponding to the molecular weight of PE35. Purification yield was about 1 mg per 100 mL of broth.

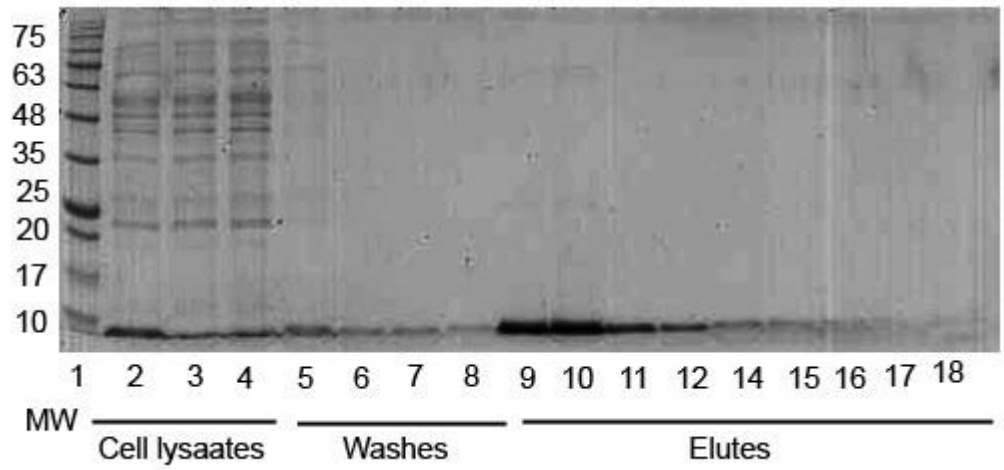

Figure 52: Silver stained 10 % SDS-PAGE gel showing the Ni-NTA affinity purification. Lane 1: Molecular size marker; Lane 2-4: Crude cell lysates; Lane 5-6: Ni-NTA unbound fraction; Lanes 7-8: fractions from 25 mM imidazole wash 1-2; Lanes 9-18: 250 mM imidazole eluted fraction (elutions 9 - 18).

6.30.9 Confirmation of purified PE35

Ni-NTA purified PE35 was further confirmed by western blotting and mass spectrometry. Purified protein was subjected to western blot and was probed with His tag and PE35 primary antibodies. A band of 10 kDa was observed in both, the PE35 and His tag western blots, which confirms the purity of Ni-NTA purified recombinant PE35 (Figure 53).

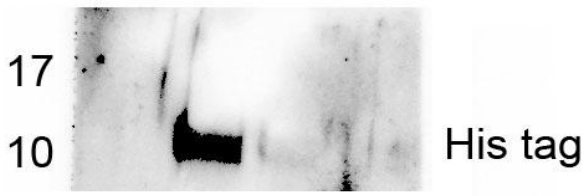

Figure 53: Confirmation of purified PE35 by western blot. Lane 1: Molecular weight marker, Lane 2: immunoreactivity in Ni-NTA purified PE35 sample probed with His tag antibodies.

6.31 PE35 is non-toxic to ARPE-19 cells

The cytotoxic effect of PE35 was studied in ARPE-19 cells by MTT assay. Cells were treated with PE35 (0.1–10000 ng/ mL) for the period of 24 h and percentage of cell viability was calculated. Treatment was not toxic to the cells at these concentrations (Figure. 54).

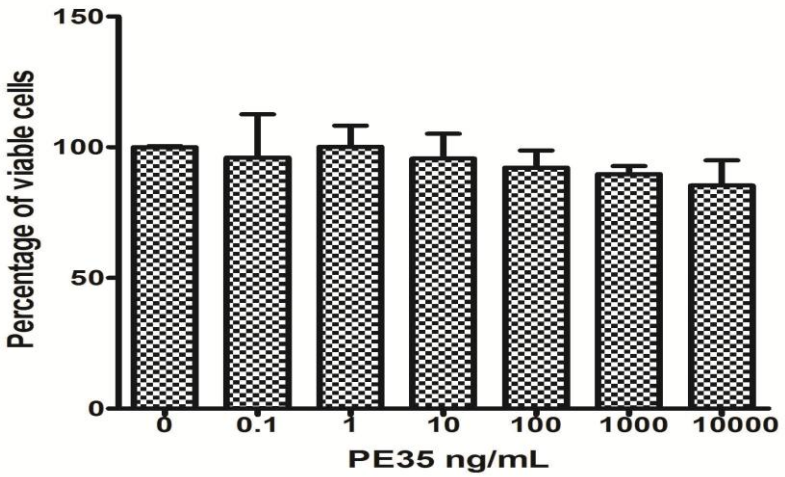

Figure 54: Cytotoxicity of PE35 in ARPE-19 cells by MTT assay. Cell viability after PE35 treatment was found to be more than 90 % at all tested concentrations.

6.32 PE35 induced expression of MCP-1, IL-8 and TNF-α genes

ARPE-19 cells were treated with varying concentrations of PE35 (1 ng, 10 ng, 100 ng, 1 µg and 10 µg /mL) for 24 h and the expression of pro-inflammatory cytokines viz. IL-6, IL-8, TNF-α and MCP-1 were assessed at their transcript levels. PE35 treatment at 10 µg/mL concentration increased the mRNA expression of IL-8, TNF-α and MCP-1 by 8 fold, 2.7 fold and 3 folds respectively. The findings are given as fold changes (Figure 55).

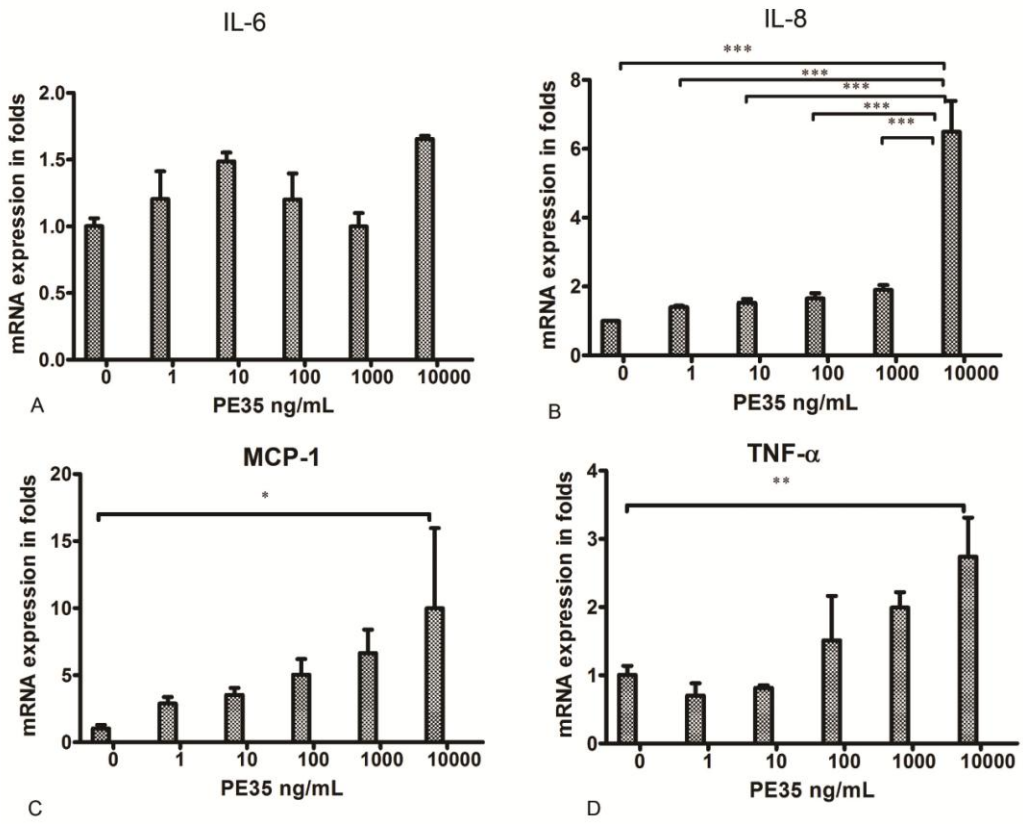

Figure 55: Inflammation is induced by PE35 in a dose-dependent manner.
ARPE-19 cells were incubated in serum-free medium overnight and were stimulated with purified recombinant PE35 protein in concentrations ranging from (0.1-10000 ng/mL. The mRNA expressions of pro-inflammatory cytokines were measured after 24 h. With 10 μg/mL of PE35 treatment, mRNA expression of all three cytokines except IL-6 were observed to raised. a) IL-6, b) 7 folds increase in IL-8 (p<0.001) c) 8 folds increase in MCP -1 (p<0.001) and d) 2.7 folds increase in TNF-α: (p<0.001), when compared to untreated cells. One way ANOVA was used for statistical analysis.

6.33 Effect of PE35 on mRNA expression of haptoglobin, complement C3, galectin-1 and VEGF

ARPE-19 cells were incubated in serum-free medium overnight and were stimulated with purified recombinant PE35 protein in concentrations ranging from (0.1-10000 ng/mL). The mRNA expressions of haptoglobin, complement C3, galectin-1 and

VEGF were measured after 24 h. Haptoglobin levels were not significantly raised. (*Ns)* b) Complement C3 levels were increased up to 10 folds with 10 µg PE35 (p<0.001), c) 2 folds of galectin-1 was raised with 1 and 10 µg (p<0.001) and d) 3 and 10 folds of VEGF (p<0.001), at concentration of 1 and 10 µg of PE35 when compared to untreated cells. One way ANOVA was used for statistical analysis (Figure 56).

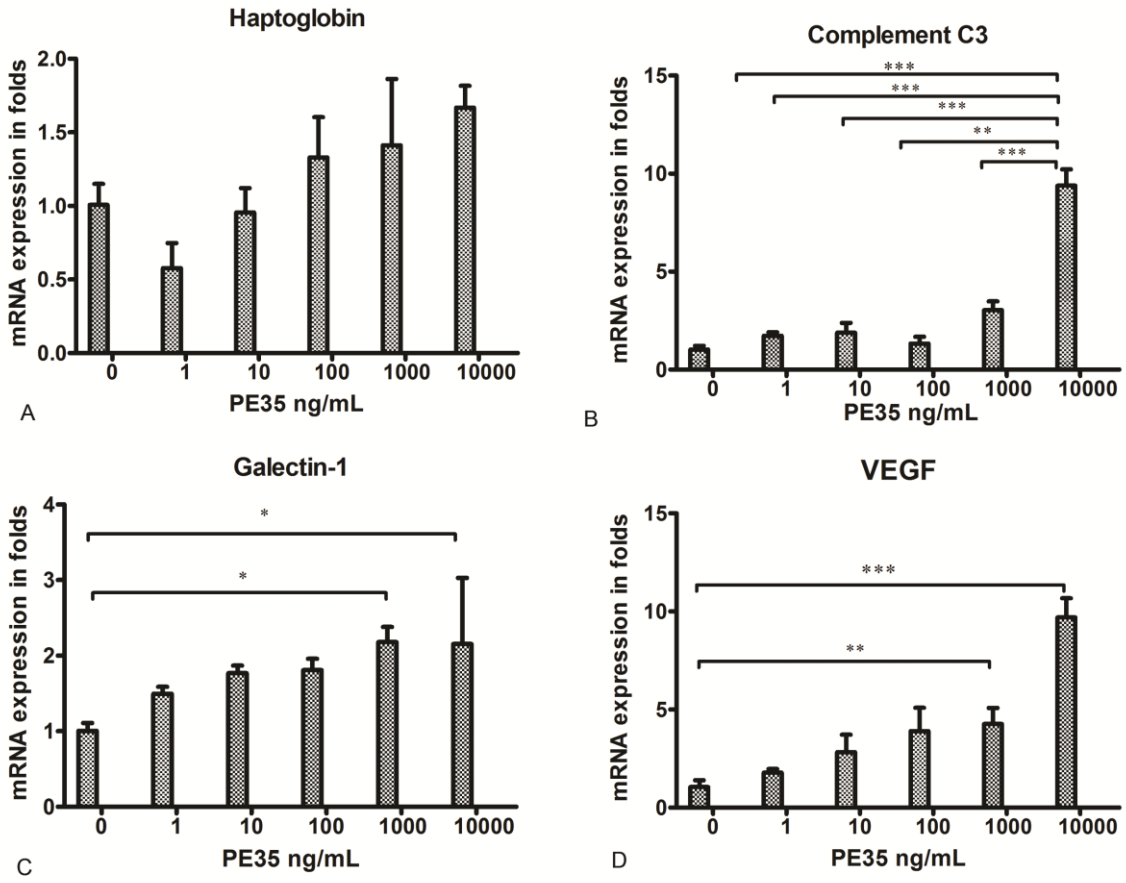

Figure 56: Expression levels of 88 kDa proteins (haptoglobin, complement C3 and galectin-1) and VEGF on PE35 treatment. mRNA expression levels of haptoglobin, complement C3, galectin-1 and VEGF upon PE35 treatment shown by real time PCR. Significant increase was observed in complement C3, galectin-1 and VEGF at 10 µg/mL of PE35 treatment (* indicates p<0.05; ** indicates p<0.01; *** indicates p<0.001).

6.34 Effect of PE35 on levels of 88 kDa proteins and VEGF in galectin-1 DsiRNA treated cells

Reduced galectin-1 levels and the presence of *Mycobacteria* PE35 was identified in Eales' disease. It was imperative to know the effect of silencing galectin-1 on PE35 treatment. Galectin-1 was silenced with 10 nM of DsiRNA in ARPE-19 and 10 nM scrambled DsiRNA treated cells were used as controls. Both control and galectin-1 DsiRNA treated Cells were co treated with 10 ng and 10 µg concentrations of PE35 for a period of 24 h. In addition mRNA levels of three proteins in 88 kDa complex, such as haptoglobin, complement C3 and galectin-1 were also measured. The mRNA expression of haptoglobin was 1.7 folds higher in 10 µg PE35 treated, galectin-1 silenced cells when compared with the scrambled DsiRNA treated cells. Similarly mRNA levels of complement C3 was 2.1 folds higher in 10 µg PE35 treated, galectin-1 silenced cells when compared with the scrambled DsiRNA treated cells, whereas galectin-1 levels remained unaltered (Figure 57).

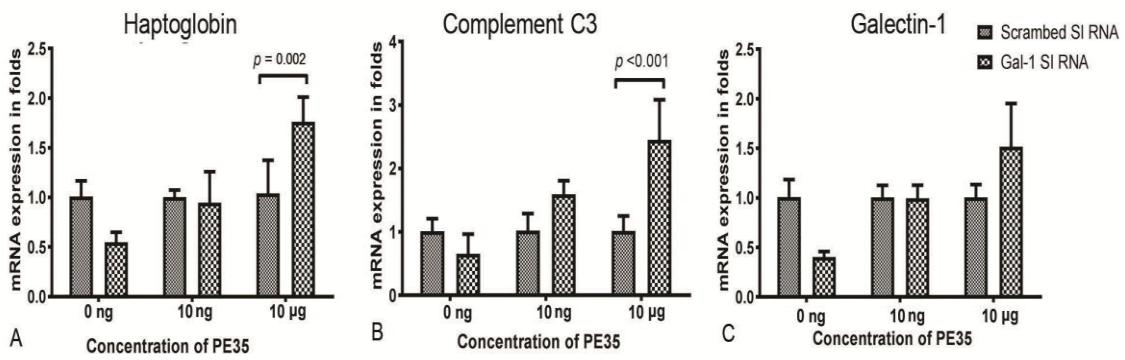

Figure 57: Levels of 88 kDa proteins (haptoglobin, complement C3 and galectin-1) on PE35 treatment in galectin-1 silenced ARPE-19 cells. mRNA expression levels of haptoglobin, complement C3 and galectin-1 upon PE35 treatment in galectin-1 silenced cells shown by real time PCR. Significant increase was observed in haptoglobin, complement C3 and galectin-1 at 10 µg/mL of PE35 treatment (* indicates $p<0.05$; ** indicates $p<0.01$; *** indicates $p<0.001$).

6.35 Effect of PE35 on levels of pro-inflammatory cytokines in the galectin-1 DsiRNA treated cells.

The mRNA expression levels of inflammatory cytokines IL-6, IL-8, MCP-1 and TNF-α were measured. The mRNA expression of IL-6 was 3.5 folds higher in 10 µg PE35 treated, galectin-1 silenced cells when compared with the scrambled siRNA treated cells. Similarly mRNA levels of complement IL-8, MCP-1 and TNF-α were 5.8, 4.9 and 5.2 folds higher in 10 µM PE35 treated, galectin-1 silenced cells respectively when compared with the scrambled siRNA treated cells (Figure 58).

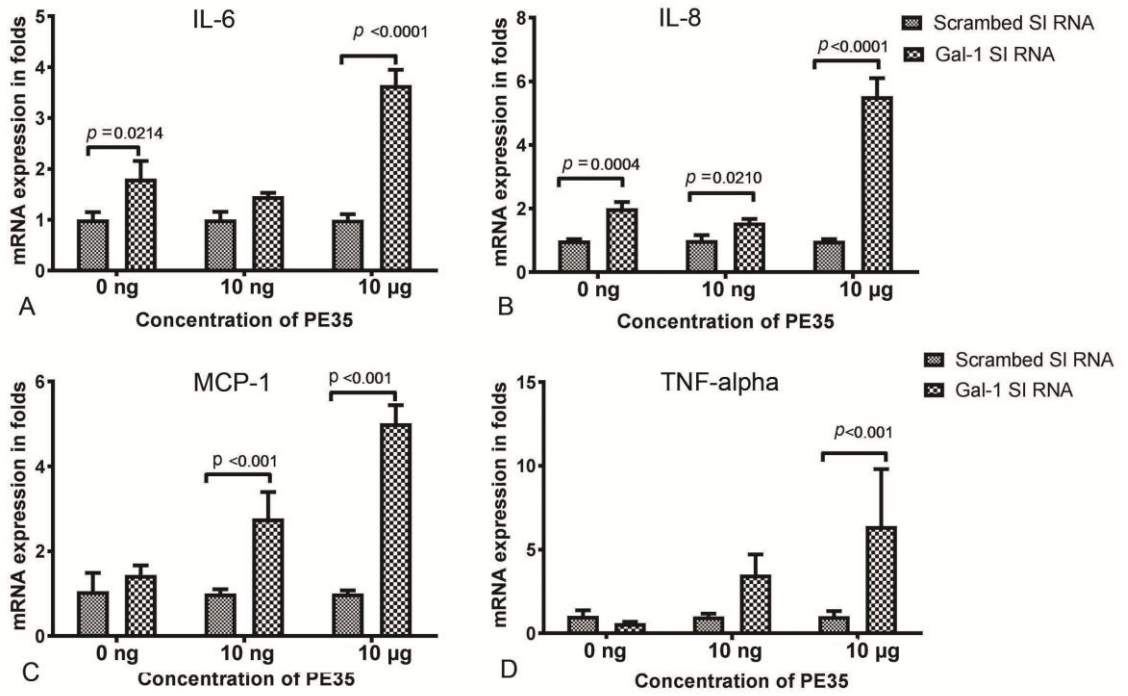

Figure 58: Effect of PE35 on pro-inflammatory cytokines in gal-1 silenced cells. mRNA expression levels of IL-6, IL-8, MCP-1 and TNF-α upon PE35 treatment in galectin-1 silenced cells shown by real time PCR. Significant increase was observed in all the pro-inflammatory cytokines at 10 µg/mL of PE35 treatment (* indicates $p<0.05$; ** indicates $p<0.01$; *** indicates $p<0.001$).

7. DISCUSSION

Eales' disease being an ocular inflammatory disease, affecting the peripheral retinal veins is generally diagnosed by exclusion of other similar disorders (6,23,110). An 88 kDa protein identified in Eales' disease patients was considered as a potential biomarker. The N- terminal end and some of the internal regions of novel 88 kDa protein was sequenced by automated Edman's degradation chemistry. Sequences thus obtained did not match with any known protein sequences in the human database. On further characterization, it was identified to be similar with haptoglobin in its electrophoretic mobility at the α2 globulin region; in its capacity to bind with hemoglobin and agglutinate RBC. Further analysis has also revealed its anti-TBARS activity (81).

In current study, purified 88 kDa protein was identified to be a complex of haptoglobin, complement C3 and galectin-1 by sophisticated Nano LC ESI MS MS.

MALDI-MS analysis revealed 88 kDa band in raw serum of Eales' disease patients as complement C3. However, nano LC coupled ESI- MS analysis for the identification of 88 kDa band from the serum of Eales' disease identified it to be a complex of 42 proteins. Haptoglobin, complement C3, and galectin-1 were top scoring hits along with many other systemic positive acute phase proteins, proteins of coagulation cascade (111), complement pathway (C5, C4A, C4B) and regulation complements (vitronectin, clusterin and vitronectin) (112) were identified. Enrichment analysis, of these 42 identified proteins with DAVID and PANTHER tools has shown the complement activation pathway along with coagulation cascade to be the major pathways. The crosstalks between these cascades were demonstrated by the ability of coagulation enzymes such as plasmin, kallikrein and thrombin to activate complement components (113-116). This process generates C5a and C3a which are involved in the inflammatory response (117, 118).

When the identified proteins were estimated in the serum of Eales' disease patients, the levels of haptoglobin were found to be elevated while those of galectin-1 were found to be decreased; complement C3 levels were found to be unaltered.

Inflammatory stages of Eales' disease was found to be correlated with elevated levels of the markers of inflammation like C-reactive protein and circulating interleukin IL-6 (14-16, 48, 119). Two such systemic positive acute phase proteins (APPs), Haptoglobin and complement C3 (120, 121) were identified in 88 kDa band. On estimation haptoglobin levels were found to be raised, in contrary the levels of complement C3 remained unaltered, and possibly due to its slower rate of synthesis than other acute phase proteins (122).

Co-immunoprecipitation of serum samples followed by mass spectrometric analysis was carried out, to find the interaction among the identified proteins. In serum samples, co-immunoprecipitation was carried out with the complement C3 antibody and identified haptoglobin and complement C3 as interacting partners. The presence of complement C3 in haptoglobin co-immunoprecipitated samples also strongly suggests their interaction. Further, these results were confirmed with the western blots and identified haptoglobin and complement C3 as interacting partners by these experiments for the first time.

Serum glycoprotein such as haptoglobin and immunoglobin M binds to an anti-inflammatory protein galectin-1 through set of specific glycan regions (123). The galectin-1 binding requires N glycans β (1-6) GlcNAc branching residues of a protein (124). Increased bi glycans (β-1,6 GlcNAc) and decreased α-2,6 sialic acid residues in haptoglobin of Eales' disease patients by MS and by lectin blot favors galectin-1 binding. Carlson *et al* have reported galectin-1 bound haptoglobin in sera of cancer patients that despite their normal haptoglobin levels in serum, had two folds higher galectin-1 binding (123). This binding was due to the presence of glycosylation change (123-126) MS analysis of N-glycosylation profiling in haptoglobin from Eales' disease patients samples was identified to be nonsialylated, biantennary glycan. Lectin blot analysis was performed in order to validate glycosylation changes (127, 128). Lectin blot with L-PHA showed increased tri-antennary and tetra-antennary glycopeptides with β-1,6-Nacetylglucosamine branches. These are residues for galectin-1 binding in the absence of capping with α-2,6-sialic acid residues. In addition, SNA lectin blot showed decreased levels of α-2,6-sialic acid capping in

haptoglobin of Eales' disease patients. This further justifies haptoglobin binding to galectin-1.

Haptoglobin is a positive acute phase protein. Its main physiological function is to bind free haemoglobin (Hb) in circulation and make iron available for recycling. Thus, haptoglobin prevents the loss of Hb through glomeruli and protects the kidneys from peroxidative damage. Haptoglobin 1-1, haptoglobin 2-1, and haptoglobin 2-2 are the three phenotypes expressed because of genetic polymorphism in humans (130-132). The anti-inflammatory nature of haptoglobin has been observed in the cell culture experiments of human PBMCs (133). Each phenotype differs in its anti-inflammatory nature (134) and in its anti-oxidative capacity (135). Of these phenotypes, haptoglobin 2-2 is associated with an increased risk of vascular complications (136-139) and further, the complex of haptoglobin 2-2 and hemoglobin is removed from circulation with less efficiency, thus contributing to an oxidative scenario (106). In order to associate phenotype of Haptoglobin with Eales' disease, phenotyping was performed in serum of patients and control subjects. As earlier reports (140), haptoglobin 2-2 phenotype is found to be widely occurring and there was no statistical difference observed among the groups.

Angiogenic functions of purified of haptoglobin were studied by *in vitro* angiogenesis assay. It showed that haptoglobin stimulated tube formation at the concentration of 2.5 μg/mL. This indicates the angiogenic activity of haptoglobin even in lower concentrations, which may be important in inflammatory diseases and may play a role in tissue repair. Proliferation assay in HUVECs showed that haptoglobin significantly increased proliferation. These results were obtained in accordance with the earlier reports (141, 142).

Retinal pigment epithelium (RPE) is involved in the formation of the outer blood-retinal barrier (BRB) through the development of tight junctions and contributes to the immune privilege of the retina by regulating the movement of fluids, solutes and toxic molecules across the BRB (143-146). RPE phagocytizes worn out photoreceptor membranes (147) and is involved in the immune responses of the eye, through the expression of Fas ligands, adhesion molecules (such as intercellular adhesion molecule-1, endothelial leukocyte adhesion molecule-1, platelet

endothelial cell adhesion molecule-1, and vascular adhesion molecule-1), major histocompatibility complex molecules and cytokines (148). In response to pro-inflammatory stimuli, RPE secrete IL-6, IL-8, MCP-1 and TNF-α (147, 148) and the levels of these cytokines were found to be elevated in the vitreous and serum samples of patients with Eales' disease (44). This inflammatory response of RPE cells eventually leads to the occlusion of the vascular lumen, resulting in retinal ischemia. Ischemic retinal vasculitis triggers a neo angiogenesis response, and is commonly seen in patients with Eales' disease (23). In order to mimic this condition, the association between inflammation and haptoglobin was studied by performing *ex vivo* experiments using ARPE-19 cells (which were treated with bacterial endotoxin, TNF-α and co-treated with haptoglobin). Pro-inflammatory cytokines, which have already been reported to be elevated in Eales' disease was measured. Our results revealed that treatment with haptoglobin resulted in the reduction of LPS-induced synthesis of IL-6, IL-8, and TNF-α, and MCP-1 by ARPE-19 in a dose dependent manner. Three concentrations of LPS (1, 5 and 10 μg/mL) were used to induce inflammation and there is a dose dependent increase in haptoglobin levels. Surprisingly, with increasing concentration of LPS, anti-inflammatory cytokines were reduced. This can be attributed to the anti-inflammatory effects of LPS induced haptoglobin. It was reported that IL-6 stimulates haptoglobin production by inducing STAT3 mediated transcription in rat and human hepatoma cells (149); a similar explanation could be responsible for our observation of a 1.5 fold rise in serum haptoglobin levels in Eales' disease patients as a response to raised IL-6.

LPS induces p38 mitogen activated protein kinase (MAPK) pathway which is involved in pro-inflammatory cellular response and results in the expression of IL-1β, IL-6, IL-8 and TNFα (108, 150). Since haptoglobin causes reduction of pro-inflammatory cytokine, effect of haptoglobin on p38 MAPK pathway was studied in LPS stimulated ARPE -19 cells. ARPE-19 cells were treated with LPS to induce p38 pathway. Subsequently cells were treated with haptoglobin and also in combination with LPS for identifying their effect on p-38 pathway. It was found that both haptoglobin and co-treatment of haptoglobin with LPS induced phosphorylation of p-38 MAPK. This shows anti-inflammatory property of haptoglobin is independent of p38 MAPK pathway.

The pro inflammatory cytokines such as interleukins IL-1, IL-6, IL-8, TNF-α., inducible nitric oxide synthase (iNOS), adhesion molecules, MMP, growth factors, major histocompatibility antigens (MHC- class 1 and 2) and different acute phase proteins are induced by NF-κB (109, 151). In order to understand whether the anti-inflammatory effect of haptoglobin is mediated through NFκB, inflammation was induced in ARPE-19 cells with LPS and compared with those cells co-treated with haptoglobin. LPS induced expression of NFκB is significantly reduced by the haptoglobin. Hence the anti-inflammatory effects of haptoglobin might be through the suppression of NFκB.

Galectin-1 and its ligands are involved in regulation of immune responses like T-cell pathogen interactions (152-156). Anti-retinal galectin-1 antibodies were present in uveitis patients' sera (157). Treatment with recombinant galectin-1 in an animal model of experimental autoimmune uveitis and arthritis, inhibited leukocyte infiltration and caused T cell apoptosis, thus alleviating the disease pathogenesis (158, 159). In the current study, galectin-1 was decreased at both the protein and transcript levels in Eales' disease patients. It was reported that the decreased galectin-1 levels could increase the Th1 population (160). This could partially explain the infiltration of T-lymphocytes in epiretinal and subretinal membranes and increased levels of Th1cell secreted proinflammatory cytokines (such as IL-10, and TNF-α), which is observed in Eales' disease patients (17, 119).

In order to find the interacting partners of galectin-1, the protein was cloned in a FLAG-tag vector and overexpressed in COS-7 cells. From the MS analysis of anti-FLAG-1 antibody immunoprecipitates (161), annexin, RNA binding motif protein, serine peptidase inhibitor and galectin 1 were identified as interacting partners. These proteins were found to be interacting with galectin-1. It is noteworthy that most of the proteins identified in 88 kDa band from raw serum were of serine protease inhibitor family (162, 163) and identification of serine peptidase inhibitor in this result further accentuates the interaction of galectin-1 with them (Table 13).

Inflammatory cytokines promote macrophage activation, nitric oxide production, and cytotoxic T lymphocyte proliferation, leading to phagocytosis and the destruction of microbial pathogens (164-166). Various researchers demonstrated the presence of *Mycobacterial* genome in surgically excised epiretinal membrane, and in the vitreous of Eales' disease patients but no cultivable organisms could be established (8, 9, 35, 36). In addition, Ashton hypothesized Eales' disease as a tuberculoprotein hypersensitivity reaction due to the presence of sequestered *Mycobacterium* in RPE (39). The presence of systemic inflammation in Eales' disease serum along with the reported presence of *M.tb* (8, 9, 35, 36, 167, 168) suggests, inflammation in Eales' disease might be due to this pathogen. Moreover, reduced galectin-1 also increases susceptibility of individuals to inflammation and it might have a role in retinal pathology. The coagulation and cascade complement pathway proteins in 88 kDa band is probably due to the presence of *Mycobacterium* genome in ERM and vitreous fluid of Eales' disease patients (8, 9, 35, 36, 167, 168). During ocular tuberculosis infection RPE sequesters *Mycobacterium* and it was observed in tubercular uveitis (169). RPE secretes pro-inflammatory cytokines in response to inflammatory stimuli.

This is the first report showing the presence of both the protein and genome of *Mycobacterium tuberculosis* PE35 (Rv3872) was identified in the PBMC of Eales' disease patients. PE35 gene is a member of PE_PPE family of proteins with conserved proline-glutamate residues (170-173) and present within RD1 (region of difference) locus, which is removed in all the vaccine strains of M. bovis BCG. RD1 locus is essential for the functioning of the ESAT-6 secretion system (ESX-1) and secretes CFP-10 and ESAT-6 which are associated with virulence and pathogenesis (174, 175). Apart from these, PE35 is necessary to induce anti-inflammatory response of IL-10 along with pro-inflammatory, chemotactic cytokine MCP-1 in THP-1 macrophages (176, 177). However, no studies were made on the effect of PE35 in production of pro-inflammatory cytokines which are mainly involved in pathogenesis of Eales' disease. Results revealed that, treatment of PE35 in ARPE-19 cells induced IL-8, TNF-α, and MCP-1 at transcript levels in a dose dependent manner. It was reported that chemoattractant cytokines IL-8 and MCP-1 were elevated in vitreous of

Eales' disease patients (178). MCP-1 is also mainly upregulated in *M. tuberculosis* infection (179) that recruits monocytes and T cells and promotes migration across an endothelium and involved in the initial response to *M. tuberculosis* infection (180). MCP-1 was reported to be angiogenic (181) and *in vitro* and *in vivo* experiments, since it increased migration and sprouting from aortal rings in endothelial cells and also caused angiogenesis in the matrigel plug assay (182). IL-8 recruits mainly neutrophils, to the inflammation and also have effects on endothelial cells in proliferation, increasing survival, and regulated angiogenesis (183, 184). TNF-α was found to be significantly raised in patients with Eales' disease and its levels were associated with severity of retinal periphlebitis (15, 16, 119). TNF-α is an acute phase protein which causes pro-inflammatory changes in vascular endothelial cells and thereby increasing leukocyte adhesion, transendothelial migration and increased vascular permeability and promote thrombosis (185-187). Effect of PE35 on the synthesis of proinflammatory cytokines in ARPE-19 cells were revealed in this study.

Reduced galectin-1 levels and the presence of *Mycobacteria* PE35 were observed in Eales' disease. It was imperative to know the effect of silencing galectin-1 on PE35 treatment. Galectin-1 was silenced in ARPE-19 cells followed by treatment with PE35. Among the three proteins of 88 kDa, the expression of haptoglobin was 1.7 folds and complement C3 was 2.1 folds increased whereas galectin-1 levels remained unaltered. Treatment with PE35 in galectin-1 silenced ARPE-19 cells resulted in increase of pro-inflammatory cytokines such as IL-6 by 3.5 folds, IL-8 by 5.8 folds, and MCP-1 by 4.9 folds and TNF-α by 5.2 folds. Reduction of galectin-1 results in further amplified synthesis of pro-inflammatory cytokines, haptoglobin and complement C3, which signifies the role of PE35 in induction of inflammation and production of 88 kDa proteins in Eales' disease.

Our previous studies, have shown, aberrations in iron and copper metabolisms (53, 60) the present work aims to comprehend the iron and copper metabolism. Silencing of CTR1 gene significantly reduced copper mediated ocular angiogenesis response in animal model (69) and to decipher involvement of copper homeostasis in Eales'

disease, CTR1 levels were estimated in PBMCs and found to be significantly elevated.These findings, implies strong role for copper mediated angiogenesis in Eales' disease.

Regulation of systemic iron level is a strict balance between iron storage and absorption. Intestinal iron absorption and macrophage iron recycling is highly synchronized and disturbances like infection and inflammation may lead to an imbalance in iron homeostasis (188-190). Various inflammatory markers IL-6, CD16+ monocytes with TLR2 expression were reported to be elevated in patients with Eales' disease (15, 19, 185). Reports, have shown iron accumulation in macrophages and vitreous (52,53) of Eales' disease patients. To observe, the systemic changes in iron metabolism, serum iron concentration was measured and no change was observed between control and Eales' disease subjects. This observation can be attributed, to the absence of hematological abnormality in these patients. Based on previous studies on alteration in intracellular iron, the molecules involved in iron storage were analyzed. The serum and ferritin levels were significantly increased in patients compared to controls. Furthermore, the increase of ferritin confers evidence towards intracellular iron accumulation. ROS generation, is induced when oxygen comes in contact with iron and copper, the metals which are accumulated within the cell which colud be possible explanation for oxidative stress in Eales' disease (191). Ferritin is a positive acute phase proteins that are increased during infection and inflammation (192, 193) which could be possible reason for increase in ferritin values.

This study had found, levels of circulating iron, soluble transferrin receptor were within normal range and comparable with those of control subjects; whereas, ferritin was increased, which occurs, this is possibly due to iron retention as a result of curbing infection, by limiting access to iron. In this study, may be due to iron retention by macrophages may be due to involvement of infection (192, 193). The limiting factor in our study group is the small sample size due to the lesser availability of fresh cases.

In conclusion, increase intracellular iron despite of normal serum iron levels, indicating the alterations in iron homeostasis. Increased intracellular iron, is the reason for oxidative stress, and could be the result of latent *Mycobacterium* infection and inflammation. Further investigation, is needed on the individually finding role of all 42 proteins in of 88 kDa protein band from serum. This might shed insight towards understanding molecular mechanism of the disease. From clinical perspective, we need better understanding, on the effect of latent TB infections and to design newer therapeutic options that are safer for example, considering use of iron / copper chelators along with an anti-inflammatory drug in Eales' disease.

In future, investigating the role of PE35 in animal models of ocular inflammation is essential to develop new therapeutic anti-inflammatory agents for the treatment of Eales' disease.

8. SUMMARY

Differentially expressed proteins were screened in serum of Eales' disease patients by 2DGE and native electrophoresis. The 88 kDa protein in serum, that is differentially expressed in Eales' disease, is composed of haptoglobin, complement C3 and galectin-1. It also contains complement regulators and proteins involved in blood coagulation. Nano LC coupled ESI MS analysis of purified 88 kDa protein confirms it to be a complex of haptoglobin, complement C3 and galectin-1. These proteins were validated by ELISA. Haptoglobin levels were increased; galectin-1 levels were decreased whereas levels of complement C3 were unaltered in Eales' disease. The complement C3 and haptoglobin present in 88 kDa protein complex were identified as interacting partners by MS analysis and western blot. In addition, haptoglobin of Eales' disease patients had shown increased amount of β-(1-6) GlcNAc branching and reduced sialic acid content which were identified by lectin blot and mass spectrometry. The β-(1-6) GlcNAc branching with reduced sialic acid capping indicates the favourable sites of galectin-1 binding. The disease conditions were mimicked in ARPE-19 and HUVEC cells by treating them with haptoglobin and silencing galectin-1. Although complement pathway proteins were observed in serum of Eales' disease patients, due to their unaltered levels, no further investigations were carried out.

In serum of Eales' disease patients, haptoglobin phenotype was screened and Hp 2-2 phenotype were widely seen among the groups. The presence of Hp 2-2 phenotype is reported to cause iron mediated oxidative stress. To understand alterations in iron and copper metabolism, levels of iron, ferritin, transferrin and soluble transferrin receptor were estimated in serum of Eales' disease patients. Ferritin levels were found to be elevated and transferrin levels were reduced in Eales' disease patients while levels of iron and soluble transferrin receptors were unaffected. Since copper is also associated to Eales' disease and angiogenesis, levels of CTR1 were estimated and found to be elevated. The Hp 2-2 phenotype of haptoglobin was tested for its anti inflammatory effect on LPS induced ARPE-19 cells. Since RPE forms blood retinal barrier and carries out macrophage like action in the ocular environment, human RPE derived cell line ARPE-

19 was used for studying inflammation. Angiogenic potential of haptoglobin, is evaluvated in human endothelial cells. Angiogenic and antiinflammatory effects of haptoglobin are identified in tested concentrations. Haptoglobin activates p38 MAPK and suppresses NFκB. Haptoglobin might act through NFκB to carry out its anti inflammatory function.

Galectin-1 was cloned to overexpress and to identify its interacting partners. Annexin, serum peptidase inhibitor, RNA binding protein were found to be interacting with galectin-1. In addition to the above findings, presence of PE35 protein of *Mycobacterium tuberculosis* were identified in PBMCs' Eales' Disease patients by mass spectrometry. The presence of PE35 gene of *Mycobacterium tuberculosis* is confirmed by the PCR. Inflammatory roles of PE35 were seen in ARPE -19 cells. It increased the levels of IL-8, MCP-1, TNF-α and also the 88 kDa proteins - complement C3 and galectin-1. To mimic Eales' disease, galectin-1 was silenced and PE35 was treated. In these cells, levels of proinflammatory cytokines, complement C3 and haptoglobin were increased. The levels of these cytokines were found to be elevated in vitreous and in serum of patients with Eales' disease (14, 15, 44, 185). Hence, the inflammation of RPE cells in Eales' disease may be due to the presence of *Mycobacterium tuberculosis*. This, inflammatory response of RPE cells may eventually leas to the occlusion of the vascular lumen resulting in retinal ischemia. Ischemic retinal vasculitis is commonly seen, in patients with Eales disease and triggers the neo angiogenesis response (23). This is the first work which connects, tubercular proteins, roles of haptoglobin, galectin-1, iron and copper in association with the Eales' disease pathogenesis.

Conclusion

The 88 kDa protein, a potential biomarker of Eales' disease, is identified as complex of haptoglobin, complement C3 and galectin-1. The complement C3 and haptoglobin are interacting partners and galectin-1 binds to haptoglobin due to decreased sialic acid residues. The levels of haptoglobin were elevated whereas the galectin-1 levels were reduced in serum of Eales' disease patients which might be due to the binding of galectin-1 with haptoglobin. Haptoglobin 2-2 phenotype is widely seen in the population which

was found to be anti inflammatory and angiogenic in tested concentrations. It reduces inflammation by suppressing NFκB pathway. In PBMCs of Eales' disease patients, bacterial PE35 protein was identified and its treatment in APRE-19, increases pro inflammatory cytokines. Galectin-1 silencing further amplifies the production of proinflammatory cytokine induced by PE35.

Increased ferritin, CTR1, and decreased transferrin were identified in Eales' disease patients. Inflammation caused by PE35 may be the reason for the elevated levels of these proteins. Haptoglobin can be developed as a therapeutic molecule to target inflammation in Eales' disease.

9. RECOMMENDATIONS

The current study revealed anti inflammatory potential of haptoglobin and PE35 in PBMCs of Eales' disease patients. Further investigation on anti inflammatory nature of haptoglobin would be warranted to develop it into a potential drug, and detailed studies on PE35 are also highly recommended.

10. IMPACT OF THE STUDY

Eales' disease results in irreversible loss of vision which can be prevented by early diagnosis and treatment. This disease is majorly reported from India. To develop diagnostic markers and to develop therapies for Eales' disease, studies are required on the etiopathogenesis of the disease. Since present study identified the presence of PE35 in Eales' disease, it may have important role in etiopathogenesis. Further studies on developing haptoglobin as anti inflammatory therapeutics can greatly help in clinical interventions of the Eales disease.

11. APPENDIX

11.1 Demographic data of Eales' disease patients

S. NO	Age in years	Sex	Clinical Diagnosis	Medications at time of collection
1.	25	Male	active vasculitis, cotton wool spot (OD,OS)	Nil
2.	20	Male	active vasculitis, vitreous hemorrhage	Nil
3.	21	Male	active vasculitis, vitreous hemorrhage	Nil
4.	26	Male	OD-perivasculitis,choroiditis	Nil
5.	20	Male	active vasculitis, vitreous hemorrhage, ED	Nil
6.	43	Male	Vasculitis	Nil
7.	18	Male	Active vasculitis, dispersed vitreous hemorrhage	Nil
8.	17	Male	Active vasculitis	Nil
9.	32	Male	Vitreous hemorrhage, healed vasculitis	
10.	42	Male	Vasculitis, mild vitreous hemorrhage	Nil
11.	33	Male	active vasculitis, neovascularization	Nil
12.	23	Male	active vasculitis, vitreous hemorrhage, Bronchial tuberculosis	Nil
13.	30	Male	active vasculitis, vitreous hemorrhage	Nil
14.	42	Male	peripheralvasculitis, vitreous hemorrhage, phlebitis, healed vasculitis	
15.	28	Male	active vasculitis, subhyaloid hemorrhage	Nil
16.	15	Male	active vasculitis, vitreous exudates, ED	Nil
17.	23	Male	active vasculitis, vitreous hemorrhage,	
18.	43	Male	active vasculitis, hemorrhage	Nil
19.	17	Male	active vasculitis, vitreous hemorrhage	Nil
20.	30	Male	Active vasculitis, vitreous hemorrhage,	Nil
21.	17	Male	periphlebitis	Nil,
22.	20	Male	active vasculitis, vitreous hemorrhage, tuberculosis	Nil

Mean age: 26.5 ± 9.2

11. 2 Demographic details of control subjects

S. NO	Mean age in years	Sex	Clinical Diagnosis	Medications at time of collection
1.	28 ± 4	Male	Nil	Nil

Characterization of a novel 88-kDa protein found in patients with Eales' disease.

CONSENT LETTER

The Research worker has explained the purpose of this study to me. I understand that Blood sample shall be taken for the research purpose that may help in understanding the disease mechanism of Eales' Disease.

I consent to participate in the study, having understood its objectives and outcome. I was informed about the strict maintenance and confidentiality of the results obtained. I voluntarily give my consent to participate and fully cooperate in this study.

Signature: _____

Date: _____

Name : _____

Parent/Guardian: _____

INSTITUTIONAL APPROVAL LETTER

SANKARA NETHRALAYA

e Molecular cloning, sequencing, overexpression and characterization of a novel 88KDA protein found in patients with Eales' disease

Dr. KNS presented the project. Members felt that this as a very useful project and possibly will help the institute to hold newer techniques. The project has been approved by the Research Sub-Committee.

VISION RESEARCH FOUNDATION

[Regd. Under Act XXI of 1860]

New No.41, Old No.18, College Road, Chennai - 600 006

ETHICAL COMMITTEE CLEARANCE CERTIFICATE

I, the ~~Undersigned Chairman~~/Member of the Ethical Committee, functioning in Vision Research foundation, Sankara Nethralaya, Chennai, have studied the proposed research ~~Subject~~/Project *"Identification, characterization, molecular cloning of differentially expressed proteins found in serum of patients with Eales' disease"* of **Mr. SARAVANAN.R,** a candidate applying for provisional registration and hereby give the certificate of clearance of approval by this Ethical Committee.

Station: Chennai,

Signature of the ~~Chairman~~/ Members of the Ethical Committee

VISION RESEARCH FOUNDATION
ETHICS SUB-COMMITTEE
No. 18, COLLEGE ROAD,
CHENNAI-600 006

Date : 13.12.2011

Name of the Institution:

DR. H.N. MADHAVAN. MD., Ph.D., FAMS, FIC PATH
President
Vision Research Foundation
Sankara Nethralaya,
New No: 41 (Old No: 18), College Road,
Chennai - 600 006, India.

Seal

Phone : 2827 1616, 2823 3556, 2831 1913 • Fax : 91-44-2825 4180
INTERNET e-mail : drhnm@snmail.org, nanu@snmail.org
WEB : http://www.sankaranethralaya.org

CLINICAL PROFORMA

Eales' disease

1. **S. No.** ☐☐☐☐

2. **Name** ☐ 3. **Age** ☐

4. **MRD NO.** ☐ ***Sex*** ☐ ***1. M*** **2. F**

5. **Onset of symptoms (days)** ☐

6. **Diagnosis of disease (anywhere)** ***1. Y*** **2. N** ☐

7. **Symptoms** ☐

1. Floaters 2. Black spots 3. Dimness of vision

4. Pain and redness 5. Others

8. **Systemic history** ☐

1. Tuberculosis
2. Diabetes mellitus
3. Hypertension
4. Collagen vascular disorder
5. Sarcoidosis
6. Hemoglobinopathies
7. Sickle cell disease
8. Any others (specify)
9. Nil

9. Prior treatment taken ☐

1. Topical steroid 6. Vitamin supplements/Antioxidants
2. Systemic steroid 7. Aspirin or dipyridazole with antiplatelet
3. Laser 8. Others (specify)
4. Vitrectomy.
5. Anti TB medication

10. Best corrected visual acuity OD ☐ OS ☐

1. 6/5, **2**. 6/6, **3**. 6/9, **4**. 6/12, **5**. 6/18, **6**. 6/24, **7**. 6/36, **8**. 6/60, **9**. 3/36, **10**. 3/60, **11**. 2/60, **12**. 1/60, **13**. CF, **14**. HM, **15**. PL, **16**. NPL.

11. Near Vision OD ☐ OS ☐

1. N6, **2**. N8, **3**. N10, **4**. N12, **5**. N18, **6**. N36 **7.** < N36

12. Anterior segment OD ☐ OS ☐

1. Lids **2**. Conjunctiva **3**. Cornea **4.** Sclera **5**. Iris **6**. Anterior chamber **7**. Pupil **8**. lens **9**. WNL, **10**. Others (specify)

13. Intra ocular pressure OD ☐ OS ☐

14. Fundus: OD ☐ OS ☐

1. Active **2**. Inactive **3**. Normal **4.** others

a. Periphlebitis

Extent of involvement OD ☐ OS ☐

0. No QD, **1**. 1QD **2**. 2QD **3**. 3QD, **4**. 4QD

b. Neovascularization OD ☐ OS ☐

NVD ☐ NVE ☐ Extent ☐ **0.** No QD, **1**. 1QD **2.** 2QD **3.** 3QD, **4.** 4QD

c. Retinitis proliferans

1. Vitreal ☐ ***1. Y*** **OD** **OS**
   ☐ ***2. N***
   ☐
2. ERM

3. Subretinal membrane **OD** **OS**

d.**Vitreous hemorrhage** ☐ ☐ ***1. Y***

e. Tractional RD ☐ ☐ ***2. N***

f. Combined RD ☐ ☐

15. Diagnosis ☐

16. Treatment ☐

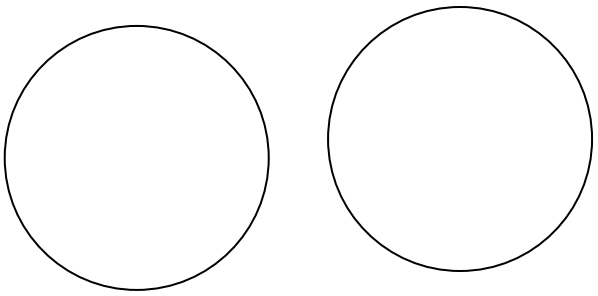

1. Central
2. Peripheral 3.Others (specify)

1. Laser 2. Systemic steroids 3. RD surgery 4. Vitamin supplementation 5. Others

12. References

1. Eales H. Primary retinal haemorrhage in young men. Ophthalmic Rev. 1882;1:41.

2. Eales H. Retinal haemorrhages associated with epistaxis and constipation. Brim Med Rev. 1980;9:262.

3. Puttamma ST. Varied fundus picture of central retinal vasculitis. Trans Asia Pacific Acad Ophthalmol. 1970;(3):520.

4. Das T, Biswas J, Kumar A, Nagpal PN, Namperumalsamy P, Patnaik B, et al. Eales' disease. Indian J Ophthalmol . 1994;42(1):3–18.

5. Das T. Collaborative Eales' Disease Study. Indian J Ophthalmol . 1994;42(1):1.

6. Biswas J, Sharma T, Gopal L, Madhavan HN, Sulochana KN, Ramakrishnan S. Eales disease--an update. Surv Ophthalmol . 2002;47(3):197–214.

7. Saxena S, Kumar D. New classification system-based visual outcome in Eales' disease. Indian J Ophthalmol . 2007;55(4):267–9.

8. Therese KL, Deepa P, Therese J, Bagyalakshmi R, Biswas J, Madhavan HN. Association of mycobacteria with Eales' disease. Indian J Med Res . 2007;126(1):56–62.

9. Singh R, Toor P, Parchand S, Sharma K, Gupta V, Gupta A. Quantitative polymerase chain reaction for Mycobacterium tuberculosis in so-called Eales' disease. Ocul Immunol Inflamm . 20(3):153–7.

10. Rishi P, Rishi E, Gupta A, Swaminathan M, Chhablani J. Vitreous hemorrhage in children and adolescents in India. J Aapos . 17(1):64–9.

11. Majji AB, Vemuganti GK, Shah VA, Singh S, Das T, Jalali S. A comparative study of epiretinal membranes associated with Eales' disease: a clinicopathologic evaluation. Eye . 2006;20(1):46–54.

12. Biswas J, Narain S, Roy S, Madhavan HN. Evaluation of lymphocyte proliferation assay to purified protein derivative, enzyme linked immunosorbant assay, and tuberculin hypersensitivity in Eales' disease. Indian J Ophthalmol . 1997;45(2):93–7.

13. Ishaq M, Karamat S, Niazi MK. HLA typing in patients of Eales disease. J Coll Physicians Surg Pak. 2005;15(5):288-90.

14. Sen A, Paine SK, Chowdhury IH, Mukherjee A, Choudhuri S, Saha A, et al. Impact of interleukin-6 promoter polymorphism and serum interleukin-6 level on the acute inflammation and neovascularization stages of patients with Eales' disease. Mol Vis . 17:2552–63.

15. Saxena S, Pant AB, Khanna VK, Agarwal AK, Singh K, Kumar D, et al. Interleukin-1 and tumor necrosis factor-alpha: novel targets for immunotherapy in Eales disease. Ocul Immunol Inflamm. 2009;17(3):201-06.

16. Sen A, Paine SK, Chowdhury IH, Mondal LK, Mukherjee A, Biswas A, et al. Association of interferon-gamma, interleukin-10, and tumor necrosis factor-alpha gene polymorphisms with occurrence and severity of Eales' disease. Invest Ophthalmol Vis Sci. 52(1):171-8.

17. Gong Y, Wei SH, Zhang MN, Jin X, Hou BK, Wang D. Serum interferon-gamma/interleukin-4 imbalance in patients with Eales' disease. Clin Exp Optom . 93(4):228–32.

18. Belge K-U, Dayyani F, Horelt A, Siedlar M, Frankenberger M, Frankenberger B, et al. The proinflammatory CD14+CD16+DR++ monocytes are a major source of TNF. J Immunol. 2002;168(7):3536–42.

19. Sen A, Chowdhury IH, Mukhopadhyay D, Paine SK, Mukherjee A, Mondal LK, et al. Increased Toll-like receptor-2 expression on nonclassic CD16+ monocytes from patients with inflammatory stage of Eales' disease. Invest Ophthalmol Vis Sci. 52(9):6940-8.

20. Sen DK, Sarin GS, Ghosh B, Acharya NR, Gurha N. Serum alpha-1 acid glycoprotein levels in patients with idiopathic peripheral retinal vasculitis (Eales' disease). Acta Ophthalmol . 1992;70(4):515–7.

21. Rajesh M, Sulochana KN, Sundaram AL, Krishnakumar S, Biswas J, Ramakrishnan S. Presence of a 88 kDa Eales protein in uveitis, tuberculosis, leprosy and rheumatoid arthritis. Med Sci Monit. 2003;9(2):CR95-9.

22. Sulochana KN, Rajesh M, Ramakrishnan S. Purification and characterization of a novel 88 kDa protein from serum and vitreous of patients with Eales' disease. Exp Eye Res . 2001;73(4):547–55.

23. Das T, Pathengay A, Hussain N, Biswas J. Eales' disease: diagnosis and management. Eye. 2010;24(3):472–82.

24. Hirsch J, Hansen KC, Burlingame AL, Matthay M a. Proteomics: current techniques and potential applications to lung disease. Am J Physiol Lung Cell Mol Physiol. 2004;287(1):L1–23.

25. Steely HT, Clark a F. The use of proteomics in ophthalmic research. Pharmacogenomics.2000;1(3):267–80.

26. Wardsworth. Recurrent retinal haemorrhage followed by the development of blood vessels in the vitreous. Ophthalmic Rev. 1887;6:289.

27. Elliot AJ. Recurrent intra-ocular hemorrhage in young adults (Eales' disease) with continuous subconjunctival therapy with hydrocortisone. Trans Am Ophthalmol Soc . 1958;56:383–8.

28. Charmis J. On the classification and management of the evolutionary course of Eales' disease. Trans Ophthalmol Soc UK. 1965;85:157–63.

29. Das T, Namperumalsamy P. Combined photocoagulation and cryotherapy in treatment of Eales' retinopathy. Preliminary report. Indian J Ophthalmol. 1986;35(5-6):108-18.

30. Saxena S, Kumar D. A new staging system for idiopathic retinal periphlebitis. Eur J Ophthalmol . 2004;14(3):236–9.

31. Gilbert TW. Periphlebitis and endovasculitis of retinal vessels. Klin M Monalsol Augeuh. 1935;94:335.

32. WC F. Some impressions derived from the study of recurrent hemorrhages in to the retina and vitreous of young persons. Trans Am Ophthalmol Soc. 1921;19:238–42.

33. Awasthi P, Mehrotra ML SS. Ocular conditions in pulmonary tuberculosis patients in India. Acta XX Concil Ophthalmol. 1966;1025.

34. Biswas J, Badrinath SS. Ocular morbidity in patients with active systemic tuberculosis. Int Ophthalmol . 1995;19(5):293–8.

35. Madhavan HN, Therese KL, Doraiswamy K. Further investigations on the association of Mycobacterium tuberculosis with Eales' disease. Indian J Ophthalmol . 2002;50(1):35–9.

36. Madhavan HN, Therese KL, Gunisha P, Jayanthi U, Biswas J. Polymerase chain reaction for detection of Mycobacterium tuberculosis in epiretinal membrane in Eales' disease. Invest Ophthalmol Vis Sci . 2000;41(3):822–5.

37. Dunlap NE, Bass J, Fujiwara P, Hopewell P, Horsburgh CR, Salfinger M, et al. Diagnostic standards and classification of tuberculosis in adults and children. Vol. 161, American Journal of Respiratory and Critical Care Medicine. 2000;1376–95.

38. Alsedà M, Godoy P. Tuberculin Reaction Size in Tuberculosis Patient Contact. Arch Bronconeumol. 2007;43(3):161–4.

39. Ashton N. Pathogenesis and aetiology of Eales' disease. Acta XIX Concil Ophtlmlmologicum. 1962;2-28.

40. Patricio MS, Portelinha J, Passarinho MP, Guedes ME. Tubercular retinal vasculitis. BMJ Case Rep. 2013.

41. Kono T, Yamana Y, Kurimoto S, Inomata H. [Histopathology of Eales' disease--retinal vascular changes and proliferations of preretinal membranes]. Nihon Ganka Gakkai Zasshi . 1985;89(9):1001–10.

42. Badrinath SS, Gopal L, Sharma T, Parikh S, Shanmugam MP, Bhende P, et al. Vitreoschisis in Eales' disease: pathogenic role and significance in surgery. Retina . 1999;19(1):51–4.

43. Rengarajan K, Muthukkaruppan VR, Namperumalsamy P. Biochemical analysis of serum proteins from Eales' patients. Curr Eye Res . 1989;8(12):1259–69.

44. Murugeswari P, Shukla D, Rajendran A, Kim R, Namperumalsamy P, Muthukkaruppan V. Proinflammatory cytokines and angiogenic and anti-angiogenic factors in vitreous of patients with proliferative diabetic retinopathy and eales' disease. Retina . 2008;28(6):817–24.

45. Koliopoulos J, Theodossiadis G, Palimeris G. The third component of complement (C'3) level in patients with uveitis. Mod Probl Ophthalmol . 1976;16:239–43.

46. Muthukkaruppan V, Rengarajan K, Chakkalath HR, Namperumalsamy P. Immunological status of patients of Eales' disease. Indian J Med Res . 1989;90:351–9.

47. Biswas J, Mukesh BN, Narain S, Roy S, Madhavan HN. Profiling of human leukocyte antigens in Eales' disease. Int Ophthalmol . 1997;21(5):277–81.

48. Saxena S, Kumar D, Kapoor S, Jain A. C-reactive protein in eales disease. Ann Ophthalmol 2002; 34(4):179–80.

49. Koch S, Kucharzik T, Heidemann J, Nusrat A, Luegering A. Investigating the role of proinflammatory CD16+ monocytes in the pathogenesis of inflammatory bowel disease. Clin Exp Immunol. 2010 Aug 1;161(2):332-41.

50. Jomova K, Valko M. Advances in metal-induced oxidative stress and human disease. Toxicology. 2011 May 10;283(2):65-87.

51. Selvi R, Angayarkanni N, Biswas J, Ramakrishnan S. Total antioxidant capacity in Eales' disease, uveitis & cataract. Indian J Med Res . 134:83–90.

52. Rajesh M, Sulochana KN, Ramakrishnan S, Biswas J, Manoharan PT. Iron chelation abrogates excessive formation of hydroxyl radicals and lipid peroxidation products in monocytes of patients with Eales' disease: direct evidence using electron spin resonance spectroscopy. Curr Eye Res. 2004;28(6):399-07.

53. Konerirajapuram NS, Coral K, Punitham R, Sharma T, Kasinathan N, Sivaramakrishnan R. Trace elements iron, copper and zinc in vitreous of patients with various vitreoretinal diseases. Indian J Ophthalmol. 2004;52(2):145-48.

54. Bhooma V, Sulochana KN, Biswas J, Ramakrishnan S. Eales' disease: accumulation of reactive oxygen intermediates and lipid peroxides and decrease of antioxidants causing inflammation, neovascularization and retinal damage. Curr Eye Res . 1997;16(2):91–5.

55. Sulochana KN, Biswas J, Ramakrishnan S. Eales' disease: increased oxidation and peroxidation products of membrane constituents chiefly lipids and decreased antioxidant enzymes and reduced glutathione in vitreous. Curr Eye Res 1999;18: 254-59

56. Stamler JS. Redox signaling: Nitrosylation and related target interactions of nitric oxide . Vol. 78, Cell. 1994. p. 931–6.

57. Rajesh M, Sulochana KN, Punitham R, Biswas J, Lakshmi S, Ramakrishnan S. Involvement of oxidative and nitrosative stress in promoting retinal vasculitis in patients with Eales' disease. Clin Biochem . 2003;36(5):377–85.

58. Yamakura F, Taka H, Fujimura T, Murayama K. Inactivation of human manganese-superoxide dismutase by peroxynitrite is caused by exclusive nitration of tyrosine 34 to 3-nitrotyrosine. J Biol Chem . 1998;273(23):14085–9.

59. Loh A, Hadziahmetovic M, Dunaief JL. Iron homeostasis and eye disease. Biochim Biophys Acta. 2009;1790(7):637–49.

60. Selvi R, Angayarkanni N, Bharathselvi M, Sivaramakrishna R, Anisha T, Jyotirmoy B, et al. Increase in Fe3+/Fe2+ ratio and iron-induced oxidative stress in Eales disease and presence of ferrous iron in circulating transferrin. Curr Eye Res. 2007;32(7–8):677-83.

61. Rouault TA. Post-transcriptional regulation of human iron metabolism by iron regulatory proteins. Blood cells, Mol {&} Dis. 2002;29(3):309–14.

62. Halliwell B. Antioxidant defence mechanisms: from the beginning to the end (of the beginning). Free Radic Res . 1999 Oct;31(4):261–72.

63. Prohaska JR, Gybina AA. Intracellular copper transport in mammals. J Nutr . 2004 May [cited 2016 Oct 19];134(5):1003–6.

64. Ashino T, Sudhahar V, Urao N, Oshikawa J, Chen G-F, Wang H, et al. Unexpected role of the copper transporter ATP7A in PDGF-induced vascular smooth muscle cell migration. Circ Res . 2010;107(6):787–99.

65. Tümer Z, Møller LB. Menkes disease. Eur J Hum Genet . 2010;18(5):511–8.

66. Petris MJ, Smith K, Lee J, Thiele DJ. Copper-stimulated endocytosis and degradation of the human copper transporter, hCtr1. J Biol Chem. 2003 14;278(11):9639–46.

67. Liang ZD, Stockton D, Savaraj N, Tien Kuo M. Mechanistic comparison of human high-affinity copper transporter 1-mediated transport between copper ion and cisplatin. Mol Pharmacol . 2009;76(4):843–53.

68. Blair BG, Larson CA, Safaei R, Howell SB. Copper transporter 2 regulates the cellular accumulation and cytotoxicity of Cisplatin and Carboplatin. Clin Cancer Res . 2009;15(13):4312–21.

69. Narayanan G, R. BS, Vuyyuru H, Muthuvel B, Konerirajapuram Natrajan S, Folkman J, et al. CTR1 Silencing Inhibits Angiogenesis by Limiting Copper Entry into Endothelial Cells. PLoS One . 2013;8(9):71982.

70. Resing KA, Ahn NG. Proteomics strategies for protein identification. FEBS Lett. 2005;579(4):885–9.

71. Yates JR, Ruse CI, Nakorchevsky A. Proteomics by Mass Spectrometry: Approaches, Advances, and Applications. Annu Rev Biomed Eng . 2009;11(1):49–79.

72. El-Aneed A, Cohen A, Banoub J. Mass Spectrometry, Review of the Basics: Electrospray, MALDI, and Commonly Used Mass Analyzers. Appl Spectrosc Rev . 2009;44(3):210–30.

73. Aebersold R, Mann M. Mass spectrometry-based proteomics. Nature. 2003 ;422(6928):198–207.

74. Staton CA, Reed MWR, Brown NJ. A critical analysis of current in vitro and in vivo angiogenesis assays. Vol. 90, International Journal of Experimental Pathology. 2009. 195–221.

75. Simpson RJ. Quantifying protein by bicinchoninic acid. Cold Spring Harb Protoc. 2008;3(8).

76. Waterborg JH, Matthews HR. The lowry method for protein quantitation. Methods Mol Biol. 1984;1:1–3.

77. Arndt C, Koristka S, Bartsch H, Bachmann M. Native polyacrylamide gels. Methods Mol Biol. 2012;869:49–53.

78. Simpson RJ. Rapid Coomassie blue staining of protein gels. Cold Spring Harb Protoc. 2010;5(4).

79. Dyballa N, Metzger S. Fast and sensitive colloidal coomassie G-250 staining for proteins in polyacrylamide gels. J Vis Exp. 2009;(30):2–5.

80. Morrissey JH. Silver stain for proteins in polyacrylamide gels: A modified procedure with enhanced uniform sensitivity. Anal Biochem. 1981;117(2):307–10.

81. Sulochana KN, Rajesh M, Ramakrishnan S. Purification and characterization of a novel 88 kDa protein from serum and vitreous of patients with Eales' disease. Exp Eye Res. 2001;73(4):547-55.

82. Jain A, Liu R, Xiang YK, Ha T. Single-molecule pull-down for studying protein interactions. Nat Protoc. 7(3):445-52.

83. Shevchenko A, Tomas H, Havlis J, Olsen J V, Mann M. In-gel digestion for mass spectrometric characterization of proteins and proteomes. Nat Protoc. 2006;1(6):2856-60.

84. Kinter M, Sherman NE. Protein sequencing and identification using tandem mass spectrometry . WileyInterscience series on mass spectrometry. 2000. 320.

85. Helsens K, Martens L, Vandekerckhove J, Gevaert K. MascotDatfile: An open-source library to fully parse and analyse MASCOT MS/MS search results. Proteomics. 2007;7(3):364–6.

86. Huang DW, Sherman BT, Lempicki RA. Systematic and integrative analysis of large gene lists using DAVID bioinformatics resources. Nat Protoc. 2009;4(1):44-57.

87. Mi H, Muruganujan A, Casagrande JT, Thomas PD. Large-scale gene function analysis with the PANTHER classification system. Nat Protoc. 8(8):1551-66.

88. Carrette O, Burkhard PR, Sanchez J-C, Hochstrasser DF. State-of-the-art two-dimensional gel electrophoresis: a key tool of proteomics research. Nat Protoc. 2006;1(2):812–23.

89. Rabilloud T, Lelong C. Two-dimensional gel electrophoresis in proteomics: A tutorial. Vol. 74, Journal of Proteomics. 2011. p. 1829–41.

90. Steel LF, Trotter MG, Nakajima PB, Mattu TS, Gonye G, Block T. Efficient and specific removal of albumin from human serum samples. Mol Cell Proteomics. 2003;2(4):262–70.

91. Smith FE, Herbert J, Gaudin J, Hennessy DJ, Reid GR. Serum iron determination using ferene triazine. Clin Biochem. 1984;17(5):306–10.

92. Bernard A, Lauwerys R. Turbidimetric latex immunoassay for serum ferritin. J Immunol Methods. 1984;71(2):141–7.

93. Kreutzer HGH. An Immunological Turbidimetric Method for Serum Transferrin Determination. Clin Chem Lab Med. 1976;14(1–12):401–6.

94. Samuelson G, Lönnerdal B, Kempe B, Elverby JE, Bratteby LE. Serum ferritin and transferrin receptor concentrations during the transition from adolescence to adulthood in a healthy Swedish population. Acta Paediatr. 2003;92:5–11.

95. Linke RP. Typing and subtyping of haptoglobin from native serum using disc gel electrophoresis in alkaline buffer: application to routine screening. Anal Biochem. 1984;141(1):55-61.

96. ATCC. ATCC ® ANIMAL CELL CULTURE GUIDE tips and techniques for continuous cell lines. Order A J Theory Ordered Sets Its Appl . 2011;1–40.

97. Liang C-C, Park AY, Guan J-L. In vitro scratch assay: a convenient and inexpensive method for analysis of cell migration in vitro. Nat Protoc . 2007;2(2):329–33.

98. Skovseth DK, Küchler AM, Haraldsen G. The HUVEC/Matrigel assay. Biol Methods Mol. 2007;360:253–68.

99. Baudin B, Bruneel A, Bosselut N, Vaubourdolle M. A protocol for isolation and culture of human umbilical vein endothelial cells. Nat Protoc . 2007;2(3):481–5.

100. Feoktistova M, Geserick P, Leverkus M. Crystal violet assay for determining viability of cultured cells. Cold Spring Harb Protoc. 2016(4):343–6.

101. Clontech. In-Fusion® HD Cloning Kit User Manual. In-Fusion Cloning . 2012;1(11614):1–15.

102. Zhu B, Cai G, Hall EO, Freeman GJ. In-Fusion assembly: seamless engineering of multidomain fusion proteins, modular vectors, and mutations. Biotechniques. 2007;43(3):354–9.

103. Untergasser A, Cutcutache I, Koressaar T, Ye J, Faircloth BC, Remm M, et al. Primer3--new capabilities and interfaces. Nucleic Acids Res . 2012 Aug;40(15):e115.

104. Thornton B, Basu C. Real-time PCR (qPCR) primer design using free online software. Biochem Mol Biol Educ. 2011;39(2):145–54.

105. Schmittgen TD, Livak KJ. Analyzing real-time PCR data by the comparative CT method. Nat Protoc. 2008;3(6):1101-08.

106. Delanghe JR, Langlois MR, Boelaert JR, van Acker J, van Wanzeele F, van der Groen G, et al. Haptoglobin polymorphism, iron metabolism and mortality in HIV infection. AIDS. 1998;12(9):1027-32.

107. Langlois, Martin ME, Boelaert, JR, et al. The haptoglobin 2-2 phenotype affects serum markers of iron status in healthy males. Clin Chem. 2000;46(10):1619-1625.

108. Neuder LE, Keener JM, Eckert RE, Trujillo JC, Jones SL. Role of p38 MAPK in LPS induced pro-inflammatory cytokine and chemokine gene expression in equine leukocytes. Vet Immunol Immunopathol. 2009;129(3–4):192–9.

109. Ghosh S, Hayden MS. New regulators of NF-kappaB in inflammation. Nat Rev Immunol . 2008;8(11):837–48.

110. Biswas J, Ravi RK, Naryanasamy A, Kulandai LT, Madhavan HN. Eales' disease-current concepts in diagnosis and management. J Ophthalmic Inflamm Infect. 2013;3(1):11.

111. Dunkelberger JR, Song WC. Complement and its role in innate and adaptive immune responses. Cell Res. 2010 Jan 1;20(1):34-50.

112. Palta S, Saroa R, Palta A. Overview of the coagulation system. Indian J Anaesth.2014 Sep 1;58(5):515.

113. Bennett WR, Yawn DH, Migliore PJ, Young JB, Pratt CM, Raizner AE, Roberts R, Bolli R. Activation of the complement system by recombinant tissue plasminogen activator. Journal of the American College of Cardiology. 1987 ;10(3):627-32.

114. Ghebrehiwet BE, Silverberg MI, Kaplan AP. Activation of the classical pathway of complement by Hageman factor fragment. J Exp Med. 1981;153(3):665-76.

115. Dobó J, Major B, Kékesi KA, Szabó I, Megyeri M, Hajela K, Juhász G, Závodszky P, Gál P. Cleavage of kininogen and subsequent bradykinin release by the complement component: mannose-binding lectin-associated serine protease (MASP)-1. PLoS One. 2011;6(5):e20036.

116. Schaiff WT, Eisenberg PR. Direct induction of complement activation by pharmacologic activation of plasminogen. Coronary artery disease. 1997;8(1):9-18.

117. Ricklin D, Hajishengallis G, Yang K, Lambris JD. Complement: a key system for immune surveillance and homeostasis. Nat Immunol. 2010;11(9):785–97.

118. Markiewski MM, Nilsson B, Nilsson Ekdahl K, Mollnes TE, Lambris JD. Complement and coagulation: strangers or partners in crime? Trends Immunol. 2007;28(4):184–92.

119. Sen A, Paine SK, Chowdhury IH, Mukherjee A, Choudhury S, Mandal LK, Bhattacharya B. Assessment of gelatinase and tumor necrosis factor-α level in the vitreous and serum of patients with Eales disease: role of inflammation-mediated angiogenesis in the pathogenesis of Eales disease. Retina. 2011 Jul 1;31(7):1412-20.

120. Gabay C, Kushner I. Acute-phase proteins and other systemic responses to inflammation. N Engl J Med. 1999;340(6):448–54.

121. Trey JE, Kushner I. The acute phase response and the hematopoietic system: the role of cytokines. Critical reviews in oncology/hematology. 1995;21(1-3):1-8.

122. Ritchie RF, Palomaki GE, Neveux LM, Navolotskaia O, Ledue TB, Craig WY. Reference distributions for complement proteins C3 and C4: a practical, simple and clinically relevant approach in a large cohort. J Clin Lab Anal. 2004;18(1):1-8.

123. Carlsson MC, Cederfur C, Schaar V, Balog CIA, Lepur A, Touret F, et al. Galectin-1-binding glycoforms of haptoglobin with altered intracellular trafficking, and increase in metastatic breast cancer patients. PLoS One. 6(10):6560.

124. Croci DO, Cerliani JP, Dalotto-Moreno T, Méndez-Huergo SP, Mascanfroni ID, Dergan-Dylon S, Toscano MA, Caramelo JJ, García-Vallejo JJ, Ouyang J, Mesri EA. Glycosylation-dependent lectin-receptor interactions preserve angiogenesis in anti-VEGF refractory tumors. Cell. 2014 Feb 13;156(4):744-58.

125. Leppänen A, Stowell S, Blixt O, Cummings RD. Dimeric galectin-1 binds with high affinity to α2, 3-sialylated and non-sialylated terminal N-acetyllactosamine units on surface-bound extended glycans. J Biol Chem. 2005 Feb 18;280(7):5549-62.

126. Patnaik SK, Potvin B, Carlsson S, Sturm D, Leffler H, Stanley P. Complex N-glycans are the major ligands for galectin-1,-3, and-8 on Chinese hamster ovary cells. Glycobiology. 2006 Apr 1;16(4):305-17.

127. Broekaert WF, Nsimba-Lubaki M, Peeters B, Peumans WJ. A lectin from elder (Sambucus nigra L.) bark. Biochem J. 1984;221(1):163-9.

128. Schwarz RE, Wojciechowicz DC, Park PY, Paty PB. Phytohemagglutinin-L (PHA-L) lectin surface binding of N-linked β1–6 carbohydrate and its relationship to activated mutant ras in human pancreatic cancer cell lines. Cancer lett. 1996;107(2):285-91.

129. Giblett ER. Haptoglobin: A review. Vox sanguinis. 1961;6(5):513-24.

130. Langlois MR, Delanghe JR. Biological and clinical significance of haptoglobin polymorphism in humans. Clinical chemistry. 1996;42(10):1589-600.

131. Sadrzadeh SM, Bozorgmehr J. Haptoglobin phenotypes in health and disorders. American journal of clinical pathology. 2004 Jun;121:S97-104.

132. Wassell J. Haptoglobin: function and polymorphism. Clin Lab. 2000;46(11–12):547-552.

133. Arredouani MS, Kasran A, Vanoirbeek JA, Berger FG, Baumann H, Ceuppens JL. Haptoglobin dampens endotoxin-induced inflammatory effects both in vitro and in vivo. Immunology. 2005;114(2):263-71.

134. Wang Y, Kinzie E, Berger FG, Lim SK, Baumann H. Haptoglobin, an inflammation-inducible plasma protein. Redox Rep. 2001;6(6):379-85.

135. Melamed-Frank M, Lache O, Enav BI, et al. Structure-function analysis of the antioxidant properties of haptoglobin. Blood. 2001;98(13):3693-3698.

136. Szafranek T, Marsh S, Levy AP. Haptoglobin: A major susceptibility gene for diabetic vascular complications. Exp Clin Cardiol. 2002;7(2–3):113-19.

137. Levy AP, Roguin A, Hochberg I, Herer P, Marsh S, Nakhoul FM, Skorecki K. Haptoglobin phenotype and vascular complications in patients with diabetes. N Engl J Med. 2000;343(13):969-70.

138. Hochberg I, Roguin A, Nikolsky E, Chanderashekhar PV, Cohen S, Levy AP. Haptoglobin phenotype and coronary artery collaterals in diabetic patients. Atherosclerosis. 2002;161(2):441-6.

139. Asleh R, Levy AP. In vivo and in vitro studies establishing haptoglobin as a major susceptibility gene for diabetic vascular disease. Vasc Health Risk Manag. 2005 Mar 1;1(1):19-28.

140. Padma T, Valli V V. ABO Blood Groups, Intestinal Alkaline Phosphatase and Haptoglobin Types in Patients with Serum Hepatitis. Hum Hered. 1988;38(367-371).

141. Cid MC, Grant DS, Hoffman GS, Auerbach R, Fauci a S, Kleinman HK. Identification of haptoglobin as an angiogenic factor in sera from patients with systemic vasculitis. J Clin Invest. 1993;91(3):977–85.

142. Park SJ, Baek SH, Oh MK, Choi SH, Park EH, Kim NH, Shin JC, Kim IS. Enhancement of angiogenic and vasculogenic potential of endothelial progenitor cells by haptoglobin. FEBS lett. 2009 Oct 6;583(19):3235-40.

143. Wenkel H, Streilein JW. Evidence that retinal pigment epithelium functions as an immune-privileged tissue. Invest Ophthalmol Vis Sci. 2000;41(11):3467-73.

144. Rizzolo LJ, Peng S, Luo Y, Xiao W. Integration of tight junctions and claudins with the barrier functions of the retinal pigment epithelium. Prog Retin Eye Res. 2011;30(5):296-323.

145. Cunha-Vaz J, Bernardes R, Lobo C. Blood-retinal barrier. Eur J Ophthalmol. 2010;21:S3-9.

146. Mazzoni F, Safa H, Finnemann SC. Understanding photoreceptor outer segment phagocytosis: use and utility of RPE cells in culture. Exp Eye Res. 2014;126:51-60.

147. McLaren MJ. Kinetics of rod outer segment phagocytosis by cultured retinal pigment epithelial cells. Relationship to cell morphology. Invest Ophthalmol Vis Sci. 1996;37(7):1213-24.

148. Holtkamp GM, Kijlstra A, Peek R, de Vos AF. Retinal pigment epithelium-immune system interactions: cytokine production and cytokine-induced changes. Prog Retin Eye Res. 2001;20(1):29-48.

149. Baumann H, Morella KK, Jahreis GP, MarinkoviÄ‡ S. Distinct regulation of the interleukin-1 and interleukin-6 response elements of the rat haptoglobin gene in rat and human hepatoma cells. Mol Cell Biol. 1990;10(11):5967-76.

150. Zhao Q, Wang X, Nelin LD, Yao Y, Matta R, et al. (2006) MAP kinase phosphatase 1 controls innate immune responses and suppresses endotoxic shock. J Exp Med 203: 131–140

151. Andreakos E, Sacre SM, Smith C, Lundberg A, Kiriakidis S, Stonehouse T, Monaco C, Feldmann M, Foxwell BM. Distinct pathways of LPS-induced NF-κB activation and cytokine production in human myeloid and nonmyeloid cells defined by selective utilization of MyD88 and Mal/TIRAP. Blood. 2004; 103(6):2229-37.

152. Motran CC, Molinder KM, Liu SD, Poirier F, Miceli MC. Galectin-1 functions as a Th2 cytokine that selectively induces Th1 apoptosis and promotes Th2 function. Eur J Immunol. 2008;38(11):3015-27.

153. Okumura CY, Baum LG, Johnson PJ. Galectin-1 on cervical epithelial cells is a receptor for the sexually transmitted human parasite Trichomonas vaginalis. Cellular Microbiol. 2008 Oct 1;10(10):2078-90.

154. Ouellet M, Mercier S, Pelletier I, Bounou S, Roy J, Hirabayashi J, Sato S, Tremblay MJ. Galectin-1 acts as a soluble host factor that promotes HIV-1 infectivity through stabilization of virus attachment to host cells. J Immunol. 2005 Apr 1;174(7):4120-6.

155. Garín MI, Chu CC, Golshayan D, Cernuda-Morollón E, Wait R, Lechler RI. Galectin-1: a key effector of regulation mediated by CD4+ CD25+ T cells. Blood. 2007 Mar 1;109(5):2058-65.

156. Camby I, Le Mercier M, Lefranc F, Kiss R. Galectin-1: a small protein with major functions. Glycobiology. 2006;16(11):137R-57R.

157. Romero MD, Muino JC, Bianco GA, Ferrero M, Juarez CP, Luna JD, Rabinovich GA. Circulating anti-galectin-1 antibodies are associated with the severity of ocular disease in autoimmune and infectious uveitis. Invest Ophthal Vis Scie. 2006 Apr 1;47(4):1550-6.

158. De Freitas Zanon C, Sonehara NM, Girol AP, Gil CD, Oliani SM. Protective effects of the galectin-1 protein on in vivo and in vitro models of ocular inflammation. Mol Vis. 2015;21:1036.

159. Rabinovich GA, Daly G, Dreja H, Tailor H, Riera CM, Hirabayashi J, Chernajovsky Y. Recombinant galectin-1 and its genetic delivery suppress collagen-induced arthritis via T cell apoptosis. J Exp Med. 1999;190(3):385-98.

160. Toscano MA, Commodaro AG, Ilarregui JM, Bianco GA, Liberman A, Serra HM, et al. Galectin-1 suppresses autoimmune retinal disease by promoting concomitant Th2- and T regulatory-mediated anti-inflammatory responses. J Immunol. 2006;176(10):6323-32.

161. Shevchenko A, Schaft D, Roguev A, Pijnappel WP, Stewart AF, Shevchenko A. Deciphering protein complexes and protein interaction networks by tandem affinity purification and mass spectrometry analytical perspective. Mol Cell Proteomics. 2002;1(3):204-12.

162. Kraut J. Serine proteases: structure and mechanism of catalysis. Annu Rev Biochem. 1977;46(1):331-58.

163. Hedstrom L. Serine protease mechanism and specificity. Chem Rev. 2002 ;102(12):4501-24.

164. Cavaillon JM. Cytokines and macrophages. Biomed Pharmacother. 1994 Jan 1;48(10):445-53.

165. Duque GA, Descoteaux A. Macrophage cytokines: involvement in immunity and infectious diseases. Secretion of Cytokines and Chemokines by Innate Immune Cells. 2015;19:6.

166. Kitasato A, Tajima Y, Kuroki T, Tsutsumi R, Adachi T, Mishima T, Kanematsu T. Inflammatory cytokines promote inducible nitric oxide synthase-mediated DNA damage in hamster gallbladder epithelial cells. World J gastroenterol. 2007; (47):6379-84.

167. McCaughan F, Holmes A, Lynn WA, Friedland JS. Mycobacterium tuberculosis infection complicated by Eales disease with peripheral neuropathy. Clin Infect Dis 2002;35(8):e89-91.

168. Singh UB, Mohapatra S, Wagh VK, Porwal C, Kaushik A. Association of Mycobacterium tuberculosis in the causation of Eales' disease: an institutional experience. Indian J Med Microbiol . 33 Suppl:43–5.

169. Rao NA, Saraswathy S, Smith RE. Tuberculous uveitis: distribution of Mycobacterium tuberculosis in the retinal pigment epithelium. Arch Ophthalmol. 2006;124(12):1777-79.

170. Brodin P, Majlessi L, Marsollier L, de Jonge MI, Bottai D, Demangel C, Hinds J, Neyrolles O, Butcher PD, Leclerc C, Cole ST. Dissection of ESAT-6 system 1 of Mycobacterium tuberculosis and impact on immunogenicity and virulence. Infect Immun. 2006;74(1):88-98.

171. Fortune SM, Jaeger A, Sarracino DA, Chase MR, Sassetti CM, Sherman DR, Bloom BR, Rubin EJ. Mutually dependent secretion of proteins required for mycobacterial virulence. Proc Natl Acad Sci U S A. 2005;102(30):10676-81.

172. Mukherjee P, Dutta M, Datta P, Dasgupta A, Pradhan R, Pradhan M, Kundu M, Basu J, Chakrabarti P. The RD1-encoded antigen Rv3872 of Mycobacterium tuberculosis as a potential candidate for serodiagnosis of tuberculosis. Clin Microbiol Infect. 2007;13(2):146-52

173. Ganguly N, Siddiqui I, Sharma P. Role of M. tuberculosis RD-1 region encoded secretory proteins in protective response and virulence. Tuberculosis. 2008 Nov 30;88(6):510-7.

174. Shaban K, Amoudy HA, Mustafa AS. Cellular immune responses to recombinant Mycobacterium bovis BCG constructs expressing major antigens of region of difference 1 of Mycobacterium tuberculosis. Clin Vaccine Immunol . 2013;20(8):1230–7.

175. Samten B, Wang X, Barnes PF. Mycobacterium tuberculosis ESX-1 system-secreted protein ESAT-6 but not CFP10 inhibits human T-cell immune responses. Tuberculosis. 2009;89 Suppl 1:S74-6.

176. Tiwari B, Soory A, Raghunand TR. An immunomodulatory role for the Mycobacterium tuberculosis region of difference 1 locus proteins PE35 (Rv3872) and PPE68 (Rv3873). FEBS J . 2014;281(6):1556–70.

177. Hanif SN, Al-Attiyah R, Mustafa AS. Cellular Immune Responses in Mice Induced by M. tuberculosis PE35-DNA Vaccine Construct. Scand J Immunol. 2011 Dec 1;74(6):554-60.

178. Murugeswari P, Shukla D, Kim R, Namperumalsamy P, Stitt AW, Muthukkaruppan V. Angiogenic potential of vitreous from Proliferative Diabetic Retinopathy and Eales' Disease patients. PLoS One . 9(10):e107551.

179. Orme IM, Cooper AM. Cytokine/chemokine cascades in immunity to tuberculosis. Immunology today. 1999 Jul 1;20(7):307-12.

180. Lin Y, Gong J, Zhang M, Xue W. Production of Monocyte Chemoattractant Protein 1 in Tuberculosis Patients. 1998;66(5):2319–22.

181. Goede V, Brogelli L, Ziche M, Augustin HG. Induction of inflammatory angiogenesis by monocyte chemoattractant protein-1. Int J Cancer. 1999 Aug 27;82(5):765-70.

182. Salcedo R, Ponce ML, Young HA, Wasserman K, Ward JM, Kleinman HK, Oppenheim JJ, Murphy WJ. Human endothelial cells express CCR2 and respond to MCP-1: direct role of MCP-1 in angiogenesis and tumor progression. Blood. 2000;96(1):34-40.

183. Hébert CA, Baker JB. Interleukin-8: a review. Cancer investigation. 1993 Jan 1;11(6):743-50.

184. Li A, Dubey S, Varney ML, Dave BJ, Singh RK. IL-8 Directly Enhanced Endothelial Cell Survival, Proliferation, and Matrix Metalloproteinases Production and Regulated Angiogenesis. J Immunol . 2003;170(6):3369-76.

185. Saxena S, Khanna VK, Pant AB, Meyer CH, Singh VK. Elevated tumor necrosis factor in serum is associated with increased retinal ischemia in proliferative eales' disease. Pathobiology . 78(5):261–5.

186. Petzelbauer P, Pober JS, Keh A, Braverman IM. Inducibility and expression of microvascular endothelial adhesion molecules in lesional, perilesional, and uninvolved skin of psoriatic patients. J Invest Dermatol. 1994;103(3):300-5.

187. Bradley. TNF-mediated inflammatory disease. J Pathol. 2008;214(2):149-60.

188. Duck KA, Connor JR. Iron uptake and transport across physiological barriers. Biometals. 2016 Aug 1;29(4):573-91.

189. Wang J, Pantopoulos K. Regulation of cellular iron metabolism. Biochemical Journal. 2011 Mar 15;434(3):365-81.

190. Ganz T. Systemic iron homeostasis. Physiol Rev . 2013;93(4):1721–41.

191. Sutton HC, Winterbourn CC. On the participation of higher oxidation states of iron and copper in Fenton reactions. Free Radic Biol Med. 1989 Jan 1;6(1):53-60.

192. Schaible UE, Kaufmann SH. Iron and microbial infection. NatRevMicrobiol . 2004;2(1740–1526.

193. Cassat JE, Skaar EP. Iron in infection and immunity. Cell host & microbe. 2013 May 15;13(5):509-19.

Ocular Immunology and Inflammation

ISSN: 0927-3948 (Print) 1744-5078 (Online) Journal homepage: http://www.tandfonline.com/loi/ioii20

Localization of Human Copper Transporter 1 in the Eye and its Role in Eales Disease

Iyer Gomathy Narayanan PhD, R. Saravanan MSc, M. Bharathselvi MSMLT, Jyotirmay Biswas MD & K. N. Sulochana PhD

To cite this article: Iyer Gomathy Narayanan PhD, R. Saravanan MSc, M. Bharathselvi MSMLT, Jyotirmay Biswas MD & K. N. Sulochana PhD (2016): Localization of Human Copper Transporter 1 in the Eye and its Role in Eales Disease, Ocular Immunology and Inflammation, DOI: 10.3109/09273948.2015.1071404

To link to this article: http://dx.doi.org/10.3109/09273948.2015.1071404

Published online: 25 Jan 2016.

Ocular Immunology & Inflammation, 2016; 00(00): 1–6
© Vision Research Foundation
ISSN: 0927-3948 print / 1744-5078 online
DOI: 10.3109/09273948.2015.1071404

Taylor & Francis
Taylor & Francis Group

ORIGINAL ARTICLE

Localization of Human Copper Transporter 1 in the Eye and its Role in Eales Disease

Iyer Gomathy Narayanan, PhD[1,2], R. Saravanan, MSc[3], M. Bharathselvi, MSMLT[1,2], Jyotirmay Biswas, MD[1,4], and K. N. Sulochana, PhD[1]

[1]*RS Mehta Jain Department of Biochemistry and Cell Biology, Vision Research Foundation, Sankara Nethralaya, Chennai, India,* [2]*Birla Institute of Technology and Science, Pilani, India,* [3]*Tamil Nadu Dr. MGR Medical University, Chennai, India, and* [4]*Uveitis Clinic, Medical Research Foundation, Chennai, India*

ABSTRACT

Purpose: Copper (Cu) is an essential trace element; however excess is toxic due to the pro-oxidant activity. Increased intracellular Cu levels in vitreous and monocyte were reported in Eales disease (ED) previously. Copper transporter1 (CTR1) maintains copper homeostasis and hence, we studied the presence of CTR1 in ocular tissues and its role in ED.

Methods: Real-time PCR, ELISA and Western blot experiments were performed in donor eyeballs tissues and PBMCs isolated from controls and ED. Immunostaining were performed for CTR1 from donor eyeballs and one ED case.

Results: CTR1 protein was expressed in all ocular tissues. PBMCs showed a three-fold increase in CTR1 protein in ED when compared with controls. Retinal sections from ED patients also revealed increased CTR1 protein expression in retinal tissues, compared with control.

Conclusions: CTR1 was significantly increased in ED when compared with controls, indicating its considerable role in the ED pathology.

Keywords: CTR1, Cu, Eales disease, PBMCs and inflammation

INTRODUCTION

Copper (Cu) is an essential micronutrient and is the third most abundant trace element required for various biological activities, after iron and zinc.[1] Cu is a cofactor for enzymes involved in cellular respiration, biosynthesis of neurotransmitter and maturation of peptide hormones. Conforti et al. in the early 1980s, demonstrated the role of Cu in acute inflammation.[2] Cu induces IL1, IL-2, IL-6, and IL-8, which activate NFκB, thereby triggering the inflammatory response.[3,4] Cu also plays an important role in angiogenesis and increased Cu levels have been reported to occur in corneal neovascularization; due to the presence of proinflammatory molecules and its role in inducing fibronectin synthesis.[5–7] Cu stimulates various factors such as VEGF, FGF1, and angiogenin.[8] Cu in its free form is potentially harmful, thus Cu homeostasis plays an important role in cellular function. Cu is transported from the liver to the cells, by ceruloplasmin (CP), where copper transporter 1 (CTR1), a transmembrane protein, imports Cu into the cells. Cu chaperones such as ATOX, cytochrome-*c* oxidase (CCO), distribute Cu to other Cu dependent proteins for their normal function. ATP 7A and 7B exports Cu from the cells, thus maintaining copper homeostasis.[9] The authors of this paper had previously studied the role of CTR1; other authors have also indicated that targeting CTR1 could be a strategy for inhibiting angiogenesis. CTR1 silencing reduced intracellular Cu levels, and inhibited cell migration and proliferation in both *in vivo* and *in vitro* conditions.[10–14]

Eales disease (ED) was first described by Henry Eales in the year 1880. ED is an idiopathic inflammatory disease that primarily affects young adult males and is

Received 24 February 2015; revised 6 July 2015; accepted 7 July 2015; published online 25 January 2016

Correspondence: K. N. Sulochana, RS Mehta Jain Department of Biochemistry and Cell Biology, Vision Research Foundation, No. 18, College Road, Chennai 600006, India. E-mail: drkns@snmail.org

Color versions of one or more of the figures in the article can be found online at www.tandfonline.com/ioii.

especially prevalent in the Indian subcontinent.[15] Inflammation, non-perfusion in peripheral veins, and retinal neovascularization are the hallmarks of ED. Repeated vitreous hemorrhage leads to a loss of vision. Factors such as autoimmunity, oxidative stress, and the possible role of *Mycobacterium tuberculosis* are associated with the pathology of ED. Increased levels of nitrotyrosine, free radicals, superoxide dismutase, and TBARS have all indicated the adverse role of oxidative stress in ED.[16,17] No laboratory test is indicated to diagnose the disease based on specific lipids, proteins or DNA analyses, and hence differential diagnosis is employed to make a conclusive finding. Treatments prescribed depend on the severity of the disease, based on which either oral steroids or laser photocoagulations are employed. Levels of inflammatory molecules such as TNFα, IL-6, and C-reactive proteins (CRP), have been reported to be elevated in ED.[18,19] Various reports have shown that trace elements such as iron and Cu have roles in free radical biology as prooxidants.[20] Thus, the involvement of the metal transporter, CTR1, was chosen to be the subject of study, with its levels serving as indicative for the role of Cu in ED.

MATERIALS AND METHODS

Human Sample

Human ocular tissues were obtained from the CU Shah eye bank. All materials procured were employed only with strict adherence to the protocols approved by the Institutional Review Board (IRB) of Vision Research Foundation, and in accordance with the tenets of the Declaration of Helsinki. The donor eyeballs were collected within 3–6 h of demise of the donor, who did not have any ocular disease. These eyeballs were procured with the consent of the donors' relatives. Five donor eyeballs with a mean age of 70 ± 8 years were used for the study. PBMCs were isolated from heparinized blood, collected from ED patients and healthy male volunteers who served as controls; in both cases with informed consent. Samples from control numbered five and Eales patients numbered four. Paraffin sections were taken from a rare ED case which was enucleated. The details of controls and patients are given in Tables 1–3.

TABLE 1. Details of healthy volunteer sample used in the study.

Sample	Age/sex	CTR1 protein level (pg/μg)
Control 1	27/M	47.44
Control 2	26/M	22.80
Control 3	27/M	18.83
Control 4	29/M	23.32
Control 5	34/M	26.43
Average		27.77

TABLE 2. Details of patients sample used in the study.

Sample	Age/sex	Clinical diagnosis	CTR1 protein level (pg/μg)
ED 1	37/M	Vasculitis, TB	86.99
ED 2	17/M	Active vasculitis	80.85
ED 3	15/M	Active vasculitis	87.24
ED 4	32/M	Active vasculitis	115.15
Average			92.56

TABLE 3. Details of PDR patients sample used in the study.

Sample	Age/sex	Clinical diagnosis
PDR 1	55/M	Neovascularization seen
PDR 2	67/M	Neovascularization seen
PDR 3	71/F	Neovascularization seen
PDR 4	68/M	Neovascularization seen
PDR 5	75/M	Neovascularization seen
PDR 6	54/M	Neovascularization seen
PDR 7	62/M	Neovascularization seen
PDR 8	49/F	Neovascularization seen

PDR, proliferative diabetic retinopathy.

Real-time PCR

Quantitative real-time PCR was performed using Applied Biosystems 7300 with SYBR Green Chemistry (Eurogentech, Belgium). Real-time PCR cycles followed the following steps: denaturation at 95ºC for 2 min, followed by 40 cycles of denaturation at 95ºC for 10 s, annealing at 60ºC for 20 s, and extension at 72ºC for 25 s. Each sample was run in triplicate and C_t was determined for the target transcripts. CTR1 (NM_001859.3) level was normalized to GAPDH (NM_002046) and real-time calculations were done using the $2^{-\Delta\Delta C}{}_T$ method. The primers used for human genes CTR1 were: forward primer 5′-GCG TAA GTC ACA AGT CAG CAT TC-; 3′ reverse primer; 5′-GCG TAA GTC ACA AGT CAG CAT TC- 3′, and GAPDH forward primer 5′-GAA CAT CCC TGC CTC TAC TG- 3′; reverse primer 5′-CGC CTG CTT CAC CTT C-3′.

ELISA and Western Blotting

For CTR1 ELISA (USCN, USA), tissues were weighed and lysed in MPER (Pierce, USA), and centrifuged at 1500 rpm for 10 min. Supernatant (50 μL) was used for ELISA. Protein estimation was done by the Bradford method. Protein at 50 μg concentration was loaded onto 10% SDS-PAGE, transferred in PVDF membrane; 5% non-fat

dry milk powder was used for blocking; CTR1 antibody (1:1000, anti-rabbit, Pierce, USA), and loading control β-actin antibody (1:1000, anti-mouse, Pierce, USA) were diluted in PBST and incubated overnight. Furthermore, they were probed for their respective secondary HRP antibody (1:7500) for 2 h. Membranes were developed using ECL (GE Healthcare, UK) and documented by Fluorochem CS3 (Bioscreen, India).

Immunofluorescence and Immunohistochemistry

Confocal microscopy for CTR1 localization was examined in 5 µm sections generated from tissue samples. The slides were deparaffinized and hydrated through exposure to graded alcohols (100% followed by 95%) and subsequently, by water. Antigen retrieval was performed in citrate buffer pH 6.0 for 2 min thrice in a microwave oven. Sections were incubated with CTR1 antibody (1: 100) at 4ºC overnight and non-immune mouse IgG was used for negative control. The same procedure as mentioned above was followed and the samples were stained using Novolink polymers (Leica Biosystems, UK) according to the manufacture's protocol.

Statistics

All the experiments including qPCR and ELISA were done in triplicate for donor eyeball tissues. Data are expressed as mean ± SD. Differences between the means of unpaired samples was evaluated by Student's unpaired t-test and $p < 0.05$ was considered to be statistically significant for real-time PCR. SPSS software was used to analyze ELISA results from donor and ED patients using the non-parametric Mann–Whitney test in the study.

RESULTS

CTR1 Expression in the Human Eye

CTR1 mRNA expression by qPCR in donor eyeball tissues were found to be elevated in the optic nerve head (ONH), and choroid, whereas its expression was lower in the iris and ciliary body than the retina (Figure 1A). ELISA for CTR1 showed that the protein was expressed in all ocular tissues. The expression varied in different tissues; protein levels were: in retina (0.29 ng /µg ± 0.18); in iris (0.23 ng/µg ± 0.027); in ciliary (0.14 ng/µg ± 0.06); in ONH (0.13 ng/µg ± 0.038); and in choroid (0.08 ng/µg ± 0.013), respectively (Figure 1B). Western blot analysis also showed the presence of CTR1 in all ocular tissues and these levels were comparable with that as seen from ELISA, observed in the banding patterns. The retina showed two bands for CTR1 indicating a multimeric form of CTR1 protein in western blot at 50 and 75 kD regions, supporting previous reports (Figure 1C).[21,22] Immunohistochemistry revealed the

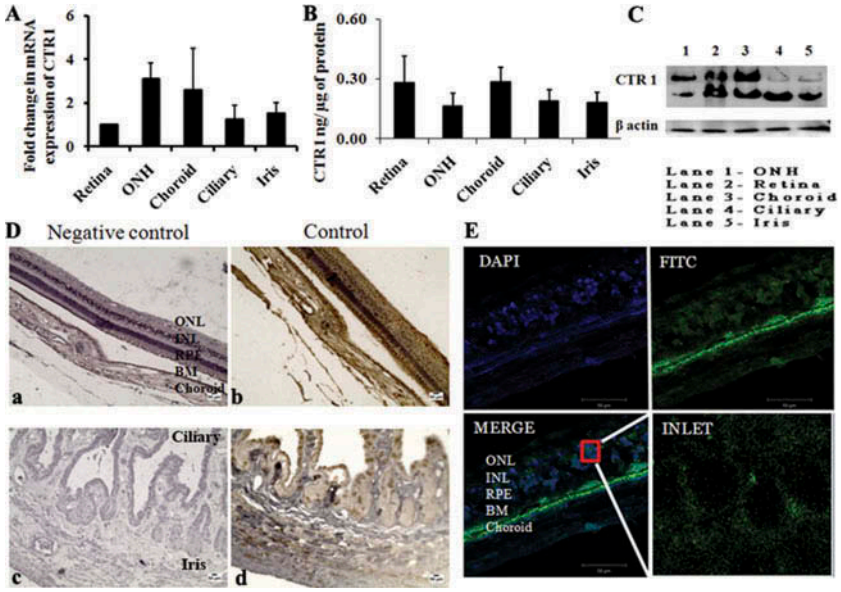

FIGURE 1. Localization of CTR1 in ocular tissue. (A) Real-time PCR for CTR1 showed increased mRNA expression in ONH and choroid; similar expression levels were seen in ciliary and iris in comparison to retina. (B) CTR1 ELISA showed retina, choroid levels to be when compared to iris, ciliary, and ONH, respectively. (C) Western blot analysis also showed the presence of CTR1 in tissues and β-actin was used as a loading control. (D) Microphotograph showing immunohistochemical staining of donor eyeball sections: retina and choroid are represented in (a) negative control and (b) control, respectively. While iris and ciliary are represented in (c) negative control and (d) control, respectively. (E) Confocal microscopy of the retinal sections showed presence of CTR1 in all the layers of retina.

presence of CTR1 in the retina, choroid, ciliary body, and the iris. ONH was not always present in the sections to confirm the presence of the protein (Figure 1D). Confocal microscopy image also confirmed the presence of CTR1 in all the layers of retina (Figure 1E).

CTR1 Level is Increased in Eales Disease

CTR1 was found to be present in all ocular tissues and thus, we looked for a disease model for Cu excess and angiogenesis. ED is one such disease where both excess Cu, and peripheral neovascularization in the eye have been reported. PBMCs were used from volunteers and ED patients to study CTR1 expression; their details have been listed in Tables 1 and 2. CTR1 mRNA expressions in PBMCs of healthy control and Eales disease subjects were compared. CTR1 mRNA expression was elevated by 2.4-fold in ED, when compared with controls (Figure 2A). CTR1 ELISA in PBMC showed significant increase in protein levels in ED (92.56 pg/μg ± 15.35) as compared with controls (27.77 pg/μg ± 11.3) (p = 0.0001) (Figure 2B). Western blot analysis also confirmed increased CTR1 levels in ED samples when compared with controls (Figure 2C). Immunohistochemical detection of CTR1 in the retinal region of the cross-section of the enucleated eye of ED case revealed extensive positive staining in the retina (Figure 2D) when compared with the donor eyeball (Figure 1D).

DISCUSSION

Copper plays important roles in both angiogenesis and inflammation, and hence the authors have taken Eales disease as a model to understand Cu's involvement in disease pathology. In our previous reports, we showed that there was a 0.6-fold increase in vitreous Cu of ED patients and a two-fold increase in circulating monocytes of ED pateints as compared with controls.[23,24] Reports have also shown the possible association of ED with mycobacterium infection. Ward et al. showed a bactericidal effect on tubercle bacilli at high physiologic levels of Cu.[25] Until now, no studies have been published on the presence of CTR1 in human ocular tissues; Holzer et al. had previously reported the absence of CTR1, based on one ocular sample.[26] Interestingly, in this report, ocular tissues demonstrated CTR1 at the level of mRNA and protein ranging from 0.29 to 0.08 ng/μg of tissue. Ugarte et al. showed higher Cu levels in RPE – choroid layer (9.0 ± 5.0 μg/g) as compared with neural retina (6.6 ± 1.4 μg/g of dry weight) by using ICP MS.[27] CTR1 mRNA and protein expression in ocular tissues varied among tissues possibly corresponding to varying Cu levels across these samples. ONH and choroid samples showed higher mRNA expressions but protein levels were found to be relatively lower than other tissues. Immunohistochemistry data showed the presence of CTR1 in the iris, cilary body, and choroid; the highest levels were recorded in the retina. Our previous work highlighted the role of CTR1 in angiogenesis; it also showed that excess levels of CTR1 in the retina could

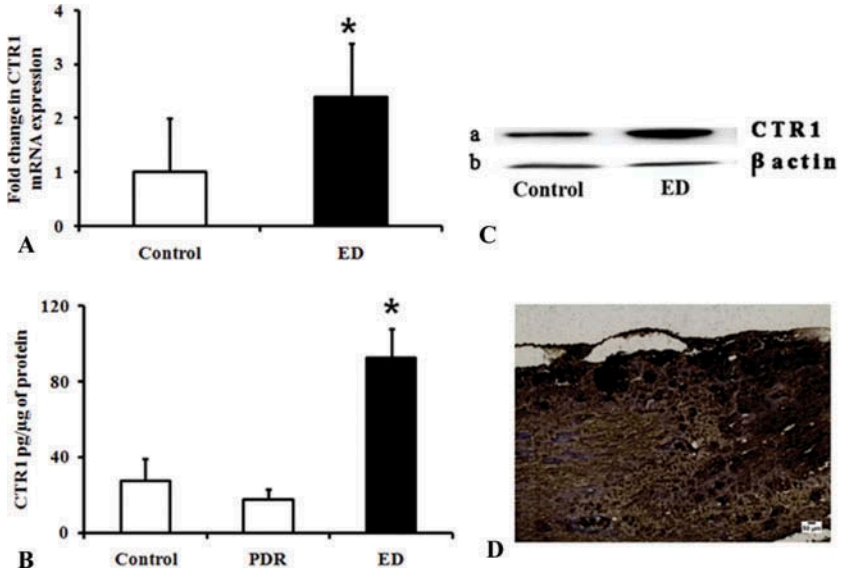

FIGURE 2. CTR1 levels in Eales disease. (A) Real-time PCR for CTR1 showed increased mRNA expression in Eales disease when compared with control. (B) CTR1 ELISA showed a three-fold increase protein in ED (p = 0.0001) when compared with control. Disease control PDR did not show any significant change when compared with control. (C) Western blot analysis also showed the presence of increased levels of CTR1 in ED when compared with control and β-actin was used as a loading control. (D) Microphotograph showing immunohistochemical staining for Eales disease, showing increased retinal positivity for CTR1 of the enucleated eyeball.

have been attributed to its increased vasculature. Further, localization of CTR1 by confocal microscopy revelaed the presence of CTR1 in both the membrane and the cytoplasmic region, which may be ascribed to the Cu transport mechanism of CTR1. CTR1 exists primarily as an internalized protein pool, rather than as an active membrane-bound transporter during active Cu transport. In addition to research on human tissues, Kuo et al. have also reported the presence of CTR1 in mouse RPE, outer limiting membranes and outer plexiform layers of the retina.[28] As increased Cu has been reported in ED, we undertook to study the level of CTR1. These results suggested an increased level of CTR1 mRNA and protein in the PBMCs of patients suffering from ED as compared with controls (Figure 2A–C). Previously, a case report published by Verma et al. showed increased VEGF and decreased PEDF in Eales patients having recurrent hemorrhage, and enucleation was performed due to a painful blind eye. Further, hematoxylin and eosin staining of the section showed retinal detachment, neovascularization in the retina with multiple vascular channels, and disorganized choroid with chronic inflammatory cell infiltration.[29] In this study, we followed up on the same patient to check the level of CTR1 in ED. Immunostaining of ED tissues showed increased positivity for CTR1 in retina when compared with donor tissues, indicating its role in ED (Figure 2D). The role of CTR1 in ocular angiogenesis and inflammation is unknown. Other than ocular tissues, CTR1 has been identified in brain tissues.[30] In Alzheimer disease, which is characterized by neurodegeneration due to aggregation and deposition of β-amyloid proteins, Cu is known to play a role in its pathology.[31] The role of CTR1 in Alzheimer's demonstrated that IFN-γ, a proinflammatory cytokine, regulates Cu homeostasis and induces CTR1 mRNA expression.[32] Wei et al. demonstrated that LPS induced inflammation was reduced by the Cu chelating agent tetrathiomolybdate (TTM). TTM decreased levels of NFκB, AP1, ICAM, MCP1, and TNF-α, thereby reducing inflammation in mice.[33,34] Iron chelators such as diethylenetriaminepentaacetic acid and desferrioxamine showed reduced TBARS levels in monocytes from ED.[35] Cui et al. demonstrated that another Cu chelating agent trientine hydrochloride decreased retinal inflammation induced by laser photocoagulation in rats.[36] Further research will help in explaining the role of CTR1 in ocular angiogenesis and inflammation. Collectively, our results indicate an important role for CTR1 in Eales disease.

CONCLUSION

In this study, we demonstrated the presence of CTR1 in all ocular tissues and the highest levels to be present in the retina. ED showed increased CTR1 expression in PBMC and retina, thus signifying the role of CTR1 in angiogenesis-related diseases.

ACKNOWLEDGMENTS

This work was funded by Department of Biotechnology, Ministry of Science and Technology (BT/PR12285/AGR/36/620/2009). We would like to thank IIT Madras for providing the confocal microscope facility.

DECLARATION OF INTEREST

The authors report no conflicts of interest. The authors alone are responsible for the content and writing of the paper.

REFERENCES

1. Goodman VL, Brewer GJ, Merajver SD. Copper deficiency as an anti-cancer strategy. *Endocr Relat Cancer*. 2004;11(2): 255–263.
2. Conforti A, Franco L, Milanino R, et al. Copper metabolism during acute inflammation: studies on liver and serum copper concentrations in normal and inflamed rats. *Br J Pharmacol*. 1983;79(1):45–52.
3. Hopkins RG, Failla ML, Copper Deficiency Reduces Interleukin-2(IL-2) Production and IL-2 mRNA in Human T-Lymphocytes. *J Nutr*. 1997;127(2):257–262.
4. Kennedy T, Ghio AJ, Reed W, et al. Copper-dependent inflammation and nuclear factor-kappaB activation by particulate air pollution. *Am J Respir Cell Mol Biol*. 1998;19(3): 366–378.
5. Gole GA, McAuslan BR, Ocular angiogenesis. Experimental models. *Trans Ophthalmol Soc N Z*. 1981;33:51–53.
6. Hannan GN, McAuslan BR, Modulation of synthesis of specific proteins in endothelial cells by copper, cadmium, and disulfiram: an early response to an angiogenic inducer of cell migration. *J Cell Physiol*. 1982;111(2):207–212.
7. Ziche M, Jones J, Gullino PM. Role of prostaglandin E1 and copper in angiogenesis. *J Natl Cancer Inst*. 1982;69(2):475–482.
8. Finney L, Vogt S, Fukai T, et al. Copper and angiogenesis: unravelling a relationship key to cancer progression. *Clin Exp Pharmacol Physiol*. 2009;36(1):88–94.
9. Banci L., Bertini I, Cantini F, et al. Cellular copper distribution: a mechanistic systems biology approach. *Cell Mol Life Sci*. 2010;67(15):2563–2589.
10. Ashino T, Sudhahar V, Urao N, et al. Unexpected role of the copper transporter ATP7A in PDGF-induced vascular smooth muscle cell migration. *Circ Res*. 2010;107(6):787–799.
11. Cai H. Wu JS, Muzik O, et al. Reduced 64Cu uptake and tumor growth inhibition by knockdown of human copper transporter 1 in xenograft mouse model of prostate cancer. *Journal of Nuclear Medicine*. 2014;55(4):622–628.
12. Brady DC, Crowe MS, Turski ML, et al. Copper is required for oncogenic BRAF signalling and tumorigenesis. *Nature*. 2014;509(7501):492–496.
13. Zimnicka AM, Tang H, Guo Q, et al. Upregulated copper transporters in hypoxia-induced pulmonary hypertension. *PLoS One*. 2014;9(3):e90544.
14. Narayanan G, Bharathidevi SR, Vuyyuru H, et al. CTR1 silencing inhibits angiogenesis by limiting copper entry into endothelial cells. *PLoS One*. 2013;8(9):e71982.
15. Biswas J, Sharma T, Gopal L, et al. Eales disease–an update. *Surv Ophthalmol*. 2002;47(3):197–214.

16. Saxena S, Khanna V, Kumar D, et al. Enhanced oxidative stress in Eales disease. *Ann Ophthalmol*. 2001;33(1):40–42.
17. Ramakrishnan S, Rajesh M, Sulochana KN. Eales' disease: oxidant stress and weak antioxidant defence. *Indian J Ophthalmol*. 2007;55(2):95–102.
18. Sen A, Paine SK, Chowdhury IH, et al. Impact of interleukin-6 promoter polymorphism and serum interleukin-6 level on the acute inflammation and neovascularization stages of patients with Eales' disease. *Mol Vis*. 2011;17:2552–2563.
19. Saxena S, Pant AB, Khanna VK, et al. Tumor necrosis factor-alpha-mediated severity of idiopathic retinal periphlebitis in young adults (Eales' disease): implication for anti-TNF-alpha therapy. *J Ocul Biol Dis Infor*. 2010;3(1):35–38.
20. Letelier ME, S. Sanchez-Jofre, L. Peredo-Silva, et al. Mechanisms underlying iron and copper ions toxicity in biological systems: Pro-oxidant activity and protein-binding effects. *Chem Biol Interact*. 2010;188(1):220–227.
21. Pabla N, Murphy RF, Liu K, et al. The copper transporter Ctr1 contributes to cisplatin uptake by renal tubular cells during cisplatin nephrotoxicity. *Am J Physiol Renal Physiol*. 2009;296(3):F505–F511.
22. Guo Y, Smith K, Petris MJ. Cisplatin stabilizes a multimeric complex of the human CTR1 copper transporter: requirement for the extracellular methionine-rich clusters. *J Biol Chem*. 2004;279(45):46393–46399.
23. Konerirajapuram NS, Coral K, Punitham R, et al. Trace elements iron, copper and zinc in vitreous of patients with various vitreoretinal diseases. *Indian J Ophthalmol*. 2004;52(2):145–148.
24. Rajesh M, Sulochana KN, Punitham R, et al. Involvement of oxidative and nitrosative stress in promoting retinal vasculitis in patients with Eales' disease. *Clin Biochem*. 2003;36(5):377–385.
25. Ward SK, Hoye EA, Talaat AM. The Global Responses of Mycobacterium tuberculosis to Physiological Levels of Copper. *J Bacteriol*. 2008;190(8):2939–2946.
26. Holzer AK, Varki NM, Le QT, et al. Expression of the human copper influx transporter 1 in normal and malignant human tissues. *J Histochem Cytochem*. 2006;54(9):1041–1049.
27. Ugarte M, Osborne NN, Brown LA, et al. Iron, zinc, and copper in retinal physiology and disease. *Surv Ophthalmol*. 2013;58(6):585–609.
28. Kuo Y-M, Gybina AA, Pyatskowit JW, et al. Copper transport protein (Ctr1) levels in mice are tissue specific and dependent on copper status. *J Nutr*. 2006;136(1): 21–26.
29. Verma A, Biswas J, Radhakrishnan S, et al. Intra-ocular expression of vascular endothelial growth factor (VEGF) and pigment epithelial-derived factor (PEDF) in a case of Eales' disease by immunohistochemical analysis: a case report. *Int Ophthalmol*. 2010;30(4):429–434.
30. Davies KM, Hare DJ, Cottam V, et al. Localization of copper and copper transporters in the human brain. *Metallomics*. 2013;5(1):43–51.
31. Squitti R, Hoogenraad T, Brewer G, et al. Copper status in Alzheimer's disease and other neurodegenerative disorders 2013. *Int J Alzheimers Dis*. 2013;2013:838274.
32. Zheng Z, White C, Lee J, et al. Altered microglial copper homeostasis in a mouse model of Alzheimer's disease. *J Neurochem*. 2010;114(6):1630–1638.
33. Wei H, Frei B, Beckman JS, et al. Copper chelation by tetrathiomolybdate inhibits lipopolysaccharide-induced inflammatory responses in vivo. *Am J Physiol Heart Circ Physiol*. 2011;301(3):H712–H720.
34. Wei H, Zhang WJ, McMillen TS, et al. Copper chelation by tetrathiomolybdate inhibits vascular inflammation and atherosclerotic lesion development in apolipoprotein E-deficient mice. *Atherosclerosis*. 2012;223(2):306–313.
35. Rajesh M, Sulochana KN, Ramakrishnan S, et al. Iron chelation abrogates excessive formation of hydroxyl radicals and lipid peroxidation products in monocytes of patients with Eales' disease: direct evidence using electron spin resonance spectroscopy. *Curr Eye Res*. 2004;28(6): 399–407.
36. Cui JZ, Wang XF, Hsu L, et al. Inflammation induced by photocoagulation laser is minimized by copper chelators. *Lasers Med Sci*. 2009;24(4):653–657.

Chapter

OXIDATIVE STRESS IN EALES' DISEASE: AN UPDATE

R. Saravanan and K. N. Sulochana
R.S. Mehta Jain Department of Biochemistry and Cell Biology,
Vision Research Foundation, Sankara Nethralaya, Chennai, India

ABSTRACT

Eales' Disease (ED) is an idiopathic, inflammatory, venous occlusive disease which primarily affects the peripheral retina of young adult males. The disease is more prevalent in the Indian subcontinent. ED was described by Henry Eales in 1880. Despite of the rigorous research effects, the etiopathogenesis of disease remains ambiguous. ED presents with inflammation, non-perfusion in peripheral veins, and retinal neovascularization. Loss of vision is due to repeated vitreous haemorrhage and its sequlae. Various research findings associate the disease with autoimmunity, oxidative stress and exposure to Mycobacterium *tuberculin* for the cause of the disease. There is no specific laboratory test available till date for its diagnosis. Therefore, the diagnosis of ED is arrived at by excluding other similar diseases. The scope of the present review is in highlighting the new findings on the strong association of oxidative stress with the disease.

There is strong evidence, for the involvement of oxidative stress and ED, both at the level of the local environment (i.e. vitreous humour and epiretinal membrane) and at systemic circulation. Elevated levels of thiobarbituric acid reactive substances (TBARS) were observed in serum,

vitreous and monocytes samples of ED, as compared to controls. We have reported damage to DNA and proteins, from the accumulated 8-hydroxy-2'deoxyguanosine and 3-Nitrotyrosine in leucocytes respectively. Elevated levels of homocysteine (Hcy), and its metabolite thiolactone (HcyTL), are observed in the disease and are associated with the functional impairment of proteins due to homocysteinylation. Plasma Hcy and HcyTL levels are positively correlated with TBARS, while plasma glutathione (GSH) is negatively correlated with Hcy and HcyTL levels. Increased oxidative stress is also evidenced from the accumulation of advanced glycation and lipid oxidation end products in epiretinal membranes, observed in patients with ED who underwent vitrectomy. The antioxidant enzymes superoxide dismutase (SOD) and glutathione peroxidase (GPX) and GSH levels were found to be reduced in the vitreous and the erythrocytes of patients with ED. Most interestingly, significant increase in the levels of intra-cellular iron and copper in circulating monocytes was observed in the vitreous of patients afflicted with ED. A novel iron binding protein, 88 kDa in molecular weight and with a presumable antioxidant function has been characterized for its possible role in ED as a biomarker, and its involvement in its etiopathogenesis. Several iron binding proteins in circulation have been analyzed systematically and have been found to vary in ED, indicating a strong role for iron in the disease. A complete study into the significance of iron binding proteins in the mechanism of the disease is needed to decode their relevance in etiopathogenesis, and for subsequent application of this knowledge in therapeutics.

Keywords: Eales' Disease, TBARS, oxidative stress, homocysteine, iron, copper and 88 kDa protein

INTRODUCTION

Eales' Disease (ED) was first described by Henry Eales in 1880 and 1882 [1]. In current scenario ED is described as an inflammatory disease which primarily affects peripheral retina of the males in between second and fourth decades of life [2]. The prevalence is remains relatively higher in the Indian subcontinent although this disease is very rarely reported in the western countries [2]. In 50-90% of cases it affects both the eyes [3]. ED is presented with three hall mark clinical signs such as the inflammation in the peripheral retinal veins followed sheeting and sclerosis of the veins, non-perfusion in peripheral veins and retinal neovascularization. Recurrent vitreous

haemorrhage from the neovascularized vessels is the major cause of tractional retinal detachment leading to loss of vision [4].

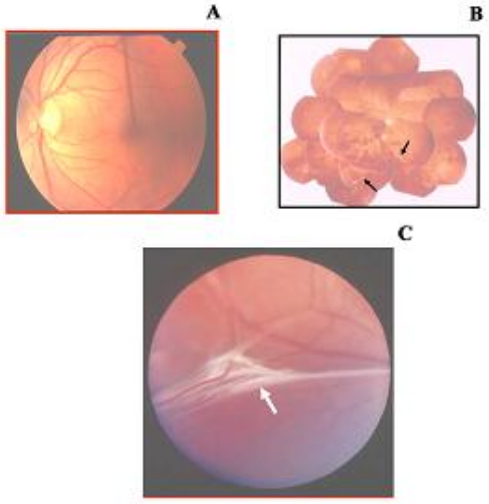

Figure 1. (A) Fundus picture of an healthy individual. (B) Montage fundus photograph of a patient with Eales' disease. Active inflammation of the retinal veins are denoted by arrow.(C) Fundus picture of a patients with ED in healed vasculitis stage, presenting with whitish fibrovascular sheahing.

Classification and assessment the severity of the disease is carried out as per new staging system described by Saxena *et al* [5].

Table1. New staging system for Eales's disease

Stage	Description
I	Periphlebitis of small (Ia) and large (Ib) caliber vessels with superficial retinal haemorrhages
IIa	Capillary nonperfusion
IIb	Revascularization elsewhere/of the disc
IIIa	Fibrovascular proliferation
IIIb	Vitreous haemorrhage
IVa	Traction/combined rhegmatogenous retinal detachment
IVb	Rubeosis iridis, neovascular glaucoma, complicated cataract, and optic atrophy

The natural course of the disease varies from remission to persistent progression to blindness [6].Various research findings associated autoimmunity, oxidative stress and exposure to *Mycobacterium tuberculin* as the cause of the disease. Many investigators favoured association of tuberculosis with ED, owing to the presence of *Mycobacterium tuberculosis* gene in the surgically excised epiretinal membrane and in the vitreous from the patients with ED. There is no growth in culture *M. tuberculosis* from vitreous aspirates and it was considered as the hypersensitivity to MTB [7,8]. The association is debatable since prevalence disease in particular gender, age and geographical locations remains unexplained. In addition tubercular retinal perivasculitis, characterized with the presence of vitreous snowball opacities [9] which is not seen in ED. There is speculation on involvement of the auto immunity in ED. Majji *et al* [10] reported presence of mast cells and eosinophils and Biswas *et al* [11, 12] demonstrated infiltration of T lymphocytes in the epiretinal membrane. Hence immunological mechanism of Eales' retinopathy is not precisely understood and needs further studies.

Despite of the meticulous research in ascertaining disease etiopathogenesis, it remains elusive till date. The diagnosis of ED is made clinically by omitting various systemic and ocular diseases mimicking in the inflammatory and proliferative phases of the diseases. There is no specific laboratory test available till date for its diagnosis [13]. However clinical diagnosis the following tests listed in the table were routinely carried out to exclude the other diseases mimicking ED.

The scope of the present review is in highlighting the findings on increased oxidative stress markers with decreased antioxidants levels and their strong association of with the disease.

OXIDATIVE STRESS

Cell efficiently and precisely maintains two major activities; first, energy level and second, redox status. Precise balance between the levels of free radicals and antioxidants are crucial, and any imbalance on either side is referred as oxidative or reductive stress.

Reactive oxygen intermediates (ROI) formed from consecutive one-electron reduction of oxygen (O_2). and they

Table 2. Investigations for Eales' Disease

To rule out the diseases mimic ED	Test
Leukemia and hematological diseases	Hemoglobin (Hb) Hemacrit(PCV) Total RBC count Total WBC count Differential WBC count
Sickle cell retinopathy	Sickle cell preparation Hemoglobin electrophoresis
Syphilis	Immunoglobin profile VDRL Treponema Pallidum Hemagglutination Test (TPHA)
Rheumatoid Arthritis	RA factor
SLE & other collagen diseases	Anti-nuclear antibody
Sarcoidosis	Serum angiotensin converting enzyme X-ray chest
Tuberculosis	Mantoux test Radiological tests X-ray chest PCR for *Mycobacterium tuberculosis* QuantiFERON - TB Gold IT test
Other tests:	Platelet count Erythrocyte sedimentation rate Reticulocyte count Plasma Glucose Fasting, Random and Postprandial Urea, creatinine Urine routine Basic coagulation test 1. Bleeding time 2. Clotting time 3. Clot retraction 4. Prothrombin time 5. Partial Thromboplastin Time (PTT)
Tests to assess the oxidative status	TBARS Vitamins A, E,C Superoxide Dismutase, Glutathione peroxidase, Glutathione

ROI comprises of superoxide anion radical ($O_2^{-}/O_2^{\bullet-}$), hydrogen peroxide (H_2O_2), and hydroxyl radical ($OH^{\bullet}$). Reactive oxygen species (ROS) includes ROI, ozone (O_3) and singlet oxygen (1_2O). The reactive nitrogen intermediates (RNI) directly influence ROI levels are nitric oxide radical (NO or $NO^{\bullet}$), nitrogen dioxide radical ($^{\bullet}NO_2$), nitrite (NO_2^{-}), and peroxynitrite ($ONOO^{-}$) [14].

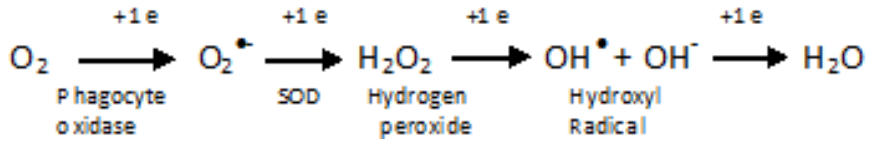

Figure 2. The step wise reduction of molecular oxygen via 1-electron transfers, producing ROS are shown in the above reaction.

NO and ROS acts as signalling molecules for various physiological functions. $O_2^{\bullet -}$ and $NO^{\bullet}$ at a lower concentrations play important roles in the cellular signalling and regulation [15].

$O_2^{\bullet -}$ and H_2O_2 produced within mitochondria reacts beneficially to the cellular stresses induced by aging, such as mitochondrial dysfunction and DNA damage [16]. They also induce autophagy, inflammation and involved in the host defence and DNA base excision repair systems [17]. In higher levels these reactive molecules can cause lipid per-oxidation, DNA oxidation and glycoxidation. ROS/RNS are short-lived and their half-life ranges from nanoseconds to minutes (minute for stable oxidants) [18]. The concentrations of free radicals are maintained in narrow limits by harmonizing their production and removal rates by enzymatic antioxidants, such as glutathione peroxidase (GPx), catalase and superoxide dismutase (SOD), or nonenzymatic antioxidants like glutathione (GSH), urate, carotenoids, cysteine, bilirubin, and flavonoids and dietary vitamin C (Ascorbic acid) and vitamin E (α-Tocopherol).

The status oxidative stress can be analyzed by the biomarkers of oxidative or nitrosative stress/ damage isolated from tissues and biological fluids. Markers of oxidative/nitrosative stress either directly detected (electron spin resonance) or by measuring stable metabolites formed [19]. The bio-markers of protein oxidation includes a) carbonyl groups formation b) total protein thiol content c) oxidized aliphatic amino acid residues d) oxidized tryptophan and tyrosine residues, nitrated tyrosine residues [20]. Bio-markers of lipid peroxidation includes a) malondialdehyde (MDA) b) conjugated dienes c) lipofuscin d) lipid peroxides and e) isoprostanes. TBARS determination was used as most common biomarker in samples obtained from patients with ED [21].

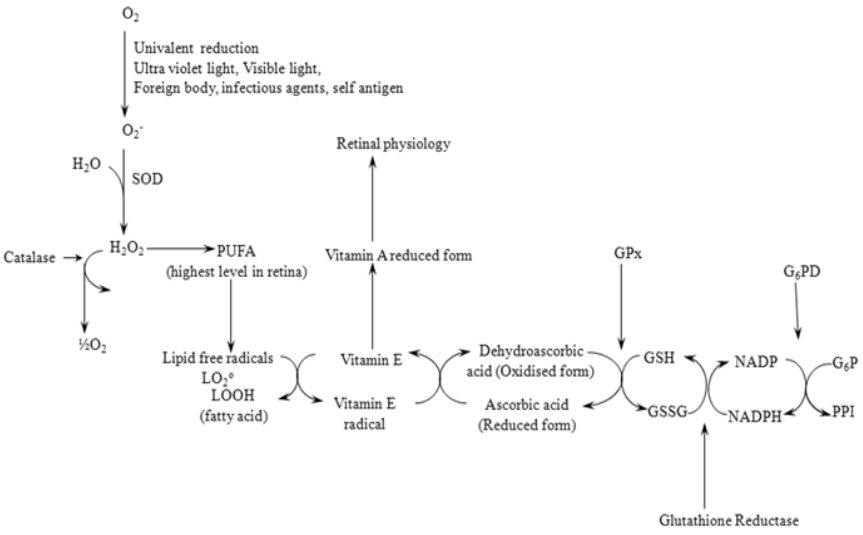

Figure 3. Schematic representation of antioxidant vitamins and GSH system in detoxification of ROS.

Free radical attack upon DNA generates a range of DNA lesions, including strand breaks and modified bases. $OH^\bullet$ attack on DNA leads to a large number of pyrimidine and purine derived base changes. 8-OHdG is considered to be the early biomarker to assess the intensity of free radical mediated DNA damage during inflammatory conditions [22].

Inflammation, angiogenesis and oxidative stress are shown to be interdependent in several human diseases [23]. ROS induced damage in ocular tissues reported in patients with uveitis [24].In experimental autoimmune uveitis higher concentration peroxynitrite was noted in photoreceptors. It also correlated with the pathologic oxidation in photoreceptors [25]. Armstrong et al. proposed a mechanism wherein elevated lipid, induces the synthesis of cytokines and growth factors during neovascularization (NV) in retina [26]. The free radicals, induced stress and damage along with antioxidant levels in the ED are discussed in following headings.

INFLAMMATION AND OXIDATIVE STRESS IN ED

During inflammation activated neutrophils and macrophages produces ROS and RNS [10,11]. The nitric oxide ($NO^\bullet$) and superoxide anion $O_2^{\bullet-}$ are

produced in reactions catalyzed by the enzymes nitric oxide synthase and the NADPH oxidase respectively [27].These $O_2^{\bullet-}$ and $NO\bullet$ radicals react to form peroxynitrite [28,29].

$$O_2^{\bullet-} + NO\bullet \rightarrow ONO_2^-$$

ED is associated with raised levels of inflammatory marker C-reactive protein [30] and circulating interleukin (IL-6) [31] in the inflammatory stage. Monocytes and non classical inflammatory $CD16^+$ monocytes subset were found raised in ED. $CD16^+$ monocytes numbers correlated with the levels of serum proinflammatory cytokines such as TNF-α, IL-6, IFN-γ, and IL-1β [32,33]. CD 16^+ monocytes reported to be major source of secreted TNF-α in blood [34]. The $CD16^+$ monocytes can be crucial regulators with the secretion of proinflammatory cytokines that bring about the inflammatory process in the retina [32].

It was observed that disruption of blood retinal barrier, results in the migration of circulating phagocytes in to the retina of the patients with ED [35]. The inflammation may have resulted in ROI generation and oxidative stress in the retina of the ED patients.

ROLE OF IRON IN OXIDATIVE AND NITROSATIVE STRESS IN ED

A variety of oxidative stress bio-markers were assayed in serum, plasma, monocytes, epiretinal membrane and vitreous of patients with ED. $O_2^{\bullet-}$ can be metabolized to a lesser reactive hydrogen peroxide by two isoenzymes of Superoxide dismutases (SOD) namely CuZn-SOD and Mn-SOD [36]. Decreased SOD activity and GSH levels with increased TBARS were reported in the monocytes of ED patients [37].

H_2O_2 and O_2 are formed from dismutation $O_2\bullet^-$, catalyzed the SOD [29].

$$\mathbf{2\ O_2^{\bullet-} + 2H^+ \xrightarrow{SOD} H_2O_2 + O_2}$$

H_2O_2 rapidly reacts with the other biomolecules is possible only when the reactions are catalyzed by metal-containing complexes or proteins [29]. Selvi *et al* demonstrated raised serum Fe^{3+}/Fe^{2+} ratio in ED and it was found to be

lowered after supplementation with antioxidant vitamins [38]. Fe^{3+} and $^{\bullet}$OH are formed when Fe^{2+} reacts with H_2O_2.

Fenton reaction

$$Fe^{2+} + H_2O_2 \longrightarrow Fe^{3+} + {}^{\bullet}OH + OH^-$$

The increased levels $^{\bullet}$OH free radicals were reported in the monocytes of patients with ED by using electron spin resonance spectrometry (ESR) [39].

$^{\bullet}$OH is a rapidly reacting molecule and a very strong oxidizing agent [40]. Its movement is diffusion limited [41] and it is able to react with all components of DNA bases as well as the deoxyribose backbone. DNA damage marker, 8-OHdG was found elevated by Gas chromatography-Mass spectrometry technique in the leucocytes patients with ED [37]. Treatment with iron chelator desferrioxamine, caused abrogation of $^{\bullet}$OH radical production, reduction in TBARS level, and increased SOD activity in monocytes from ED patients [39]. Desferrioxamine acts as powerful iron chelator, inhibits Fenton reaction and prevent the formation $^{\bullet}$OH. In oxidative stress or in induced inflammation, desferrioxamine treatment had ameliorated the complications of oxidative stress and mitigated the severity of inflammation [14]. From the above results we infer the $^{\bullet}$OH radical formed during an iron catalyzed reaction caused 8-OHdG and TBARS. Restoration of SOD activity after, vitamin supplement, desferrioxamine treatment suggests the exhaustion of antioxidants due to overproduction of free radicals.

In addition to the oxidative stress, nitrostative stress was also demonstrated in ED. In similar to ROS, RNS can also cause DNA damage, lipids and proteins. RNS can act as an oxidizing agent as well as nitrating agent [42]. Through the rapid reaction of $NO^{\bullet}$ and $O_2^{\bullet-}$, peroxynitrite ($ONOO^-$) is formed which can result in oxidation, nitrosation (addition of NO^+) or nitration (addition of NO_2). $NO^{\bullet}$ is generated by three nitric oxide synthase (NOS) isoforms present in tissues: neuronal NOS (nNOS), endothelial NOS (eNOS), and inducible NOS (iNOS). For production of $NO^{\bullet}$, iron, O_2, and reducing equivalents, are required [43,44]. NO has high-affinity binding to heme and non-heme iron [45,46]. We found increased levels iron and copper by using atomic absorption spectrometry in monocytes of patients with ED compared to controls. TBARS levels were also reported to be higher along with increased iNOs protein expression and the 3 nitrotyrosine (NTYR) in the ED monocytes. NTYR is a stable product of tyrosine nitration, biomarker of protein damage induced by peroxynitrite and other reactive nitrogen species [47]. $NO^{\bullet}$ is produced constitutively in nanomolar levels by eNOS and nNOS isoforms in the cells. iNOS expression in monocytes and macrophages is

stimulated by inflammation and produces NO$^{\bullet}$ in micromolar amounts [45]. After activation NO$^{\bullet}$ can overwhelm Cu, Zn-SOD reaction and produce ONOO [45,48]. Peroxynitrite inactivates MnSOD by nitration of the critical tyrosine-34residue [49]. The presence of excess iron and copper in monocytes along with OH$^{\bullet}$ radical, it is expected to damage biomolecules.

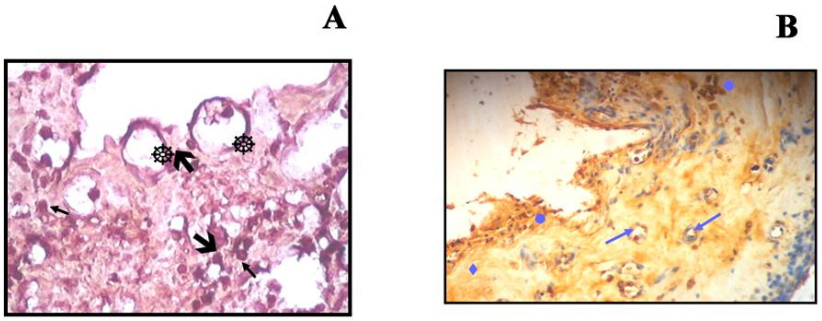

Figure 4. (A) iNOS immunolocalization in ERM. Strong expression could be noted in endothelium (arrow). (B) Immunolocalization of CML-AGE ERM-ED in the inflammatory cells is indicated by arrow (Mag. X 150).

PROTEIN DAMAGE IN ED

Free radicals produced during oxidative stress can damage the peptide backbone, resulting in the generation of protein carbonyls. Accumulation of carbonyl groups on protein results in series of chemical modifications, which ultimately leads to the formation of advanced protein oxidation products (APO) or advanced glycation end products (AGE) [50]. AGE on binding with its receptor on retinal microvascular cells (endothelial cells or pericytes) or retinal pigment epithelial cells, has been shown to induce the expression of cytokines, growth factors and proteases, leads to retinal neovascularization [51]. Carbonyls compounds are generated by the oxidation of several amino acid side chains by the formation of schiff's base adducts between lysine, histidine, and cysteine residues and α,β-unsaturated aldehydes, forming advanced lipoxidation end products (ALEs). And by glycation / glycoxidation of Lys amino groups, forming advanced glycation end product [52]. Protein carbonyl group content reduced antioxidants correlates severity of ED [53]. The AGE accumulation in ED patients mainly in the form of CML [54] occurred in spite of their normo glycemic status. Since CML and pentosidine formation are closely linked to oxidative processes. CML may be formed from

the lipid peroxidation (metal-catalyzed oxidation) as well as glycoxidation reactions [52].

HOMOCYSTEINE MEDIATED DAMAGE

Recently ED patients increased plasma homocysteine, homocysteine-thiolactone, TBARS, and decreased GSH levels [55]. Homocysteinemia may leads to production of reactive oxygen species such as H_2O_2, nitric oxide, the superoxide anion can form powerful oxidant peroxynitrite [56].These sequence of events impairs the antioxidant defenses [57]. Homocysteine-thiolactone with reacts with proteins results in homocysteinylation of protein lysine residues [55]. This leads to protein damage, and is associated with the functional impairment of in ED. It could be one of the etiological factors for ED [58].

SERUM PROTEIN MARKER 88 KDA IN ED

The 88 kDa, protein was purified using HPLC, was characterized to be a glycoprotein, present in the vitreous, ERM and serum of ED patients. The protein was sequenced by in the N- terminal end and some of internal regions by automated Edman's degradation chemistry. The sequences obtained revealed no match in the protein and DNA database search. It shared common properties with haptoglobin including the electrophoretic mobility at α2 globulin region, positive acute phase protein, hemoglobin binding, and agglutination of RBC. The molecular weight of haptoglobin is 44 kDa. It has anti TBARS activity and 8% thiols by mass and oxidized ferrous ion to ferric ion and is a ferro oxidase [59, 60]. Further investigations are required to understand the role of the protein in the etiopathogensis of ED. Its identity interactive partners and its role in inflammation and angiogenesis are ongoing.

INCREASED ROS AND WEAKENED ANTIOXIDANT SYSTEMS

Cytosol, the nuclear and mitochondrial matrices and extracellular fluids are protected by enzymatic and non-enzymatic antioxidant defence stratergies. Vitamin A, Tocopherols, carotenoids, and flavonoids in the lipid phase, While Ascorbate, glutathione, bilirubin, and thiols in the aqueous phase acts as

antioxidant molecules effectively reinforcing the defense provided by the enzymes superoxide dismutase, catalase and glutathione peroxidases. Researchers had reported the increased level of the TBARS with reduced levels of the antioxidants in ED [62-66]. Bhooma *et al.* had reported elevated TBARS level in erythrocytes as well as the decreased levels of vitamin E, vitamin C, vitamin A in serum of both the active and in the healed perivasculitis stages of ED [62]. Other studies had shown supplementation with vitamin E and C had lowered the TBARS levels and $Fe^{3+/}Fe^{2+}$ ratio; And also increased total antioxidant capacity (TAC) and vitamins levels in active vasculitis and healed vasculitis stages of ED [38]. Oral supplementation of vitamins E, C, and A, beta carotene; Cu; Zn; and Se for 3months, had significantly decreased the level of TBARS. It also increased the SOD activity, and GSH levels in the platelets from ED patients [63-65]. The clinical correlation or the benifical effects is not yet available.

FUTURE DIRECTIONS

Iron and copper are essential in the human body for the synthesis of variety of enzymes and other proteins that are involved in respiration, redox reactions and other metabolic pathways. Yet these two metals are potentially dangerous by their ability to participate in one-electron transfer reactions. This enables them to be powerful catalysts of autoxidation reactions. For instance, conversion of H_2O_2 to $OH^{\bullet}$ and decomposition of lipid peroxides to reactive peroxyl and alkoxyl radical. It is not only free metal ions that are catalytic. Haem and certain haem proteins can decompose lipid peroxides and interact with H_2O_2 to cause extensive structural and functional damage to the biomolecules. Therefore it is necessary to regulate the metabolism of these metal ions carefully, which are vital for physiological functions but are dangerous when their level exceeds the critical limit. The proteins which are involved directly or indirectly involved in regulation of iron metabolism are transferrin, haptoglobin (Hp) and Haemopexion (Hpx). The ferroprotein retains or exports ferric iron taken in dueodenum divalent metal transportor1 based on requirements. Ferric iron retained by the entrocytes in ferritin form. The exported iron is oxidized to the ferrous iron by hephastatin or ceruloplasmin and transported by transferrin. Ferroprotein is regulated by the hepicidin. Heme is transported by the heme-responsive gene 1 and oxidized by heme oxygenase 1 (HO-1) to produce ferrous iron.

ACKNOWLEDGEMENT

We thank M Bharathselvi, for her support and help in editing and proof reading the manuscript.

REFERENCES

[1] Eales H. Retinal hemorrhages associated with epistaxis and constipation. *Brim Med Rev* 1880;9:262-73.

[2] Das T, Biswas J, Kumar A, Nagpal PN, Namperumalsamy P, Patnaik B, et al. Eales' disease. *Indian J Ophthalmol* 1994;42(1):3-18.

[3] Biswas J, Ravi RK, Naryanasamy A, Kulandai LT, Madhavan HN. Eales' disease - current concepts in diagnosis and management. *J Ophthalmic Inflamm Infect*;3(1):11.

[4] Spitznas M, Meyer-Schwickerath G, Stephan B. The clinical picture of Eales' disease. *Albrecht Von Graefes Arch Klin Exp Ophthalmol* 1975;194(2):73-85.

[5] Saxena S, Kumar D. New classification system-based visual outcome in Eales' disease. *Indian J Ophthalmol* 2007;55(4):267-9.

[6] Kalsi R, Patnaik B. The developing features of phlebitis retinae (a vertical study). *Indian J Ophthalmol* 1979; 27: 87

[7] Therese KL, Deepa P, Therese J, Bagyalakshmi R, Biswas J, Madhavan HN. Association of mycobacteria with Eales' disease. *Indian J Med Res* 2007;126(1):56-62.

[8] Singh R, Toor P, Parchand S, Sharma K, Gupta V, Gupta A. Quantitative polymerase chain reaction for Mycobacterium tuberculosis in so-called Eales' disease. *Ocul Immunol Inflamm*;20(3):153-7.

[9] Gupta A, Gupta V, Arora S, Gupta A, Gupta V, Arora S, Dogra MR, Bambery P. PCR-positive tubercular retinal vasculitis Dogra MR, Bambery P. PCR-positive tubercular retinal vasculitis: clinical characteristics and management. *Retina* 2001;21(5):435-44.

[10] Forman HJ, Torres M. Redox signaling in macrophages. *Mol Aspects Med* 2001;22(4-5):189-216.

[11] Kobayashi SD, Voyich JM, Burlak C, DeLeo FR. Neutrophils in the innate immune response. *Arch Immunol Ther Exp (Warsz)* 2005;53(6):505-17.

[12] Majji AB, Vemuganti GK, Shah VA, Singh S, Das T, Jalali S. A comparative study of epiretinal membranes associated with Eales' disease: a clinicopathologic evaluation. *Eye (Lond)* 2006;20(1):46-54.

[13] Biswas J, Rao NA. Epiretinal membrane in Eales' disease and other vascular retinopathies. *Invest Ophllmlmol Vis Sci* 1990; **31**(Suppl): 369.

[14] Barry Halliwell JMCG, editor. *Free radicals in biology and medicine.* 4 ed. New York: Oxford University Press, 2007.

[15] Droge W. Free radicals in the physiological control of cell function. *Physiol Rev* 2002;82(1):47-95.

[16] Hekimi S, Lapointe J, Wen Y. Taking a "good" look at free radicals in the aging process. *Trends Cell Biol*;21(10):569-76.

[17] Scherz-Shouval R, Elazar Z. Regulation of autophagy by ROS: physiology and pathology. *Trends Biochem Sci*;36(1):30-8.

[18] Winkler BS, Boulton ME, Gottsch JD, Sternberg P. Oxidative damage and age-related macular degeneration. *Mol Vis* 1999;5:32.

[19] Valko M, Leibfritz D, Moncol J, Cronin MT, Mazur M, Telser J. Free radicals and antioxidants in normal physiological functions and human disease. *Int J Biochem Cell Biol* 2007;39(1):44-84.

[20] Dalle-Donne I, Rossi R, Colombo R, Giustarini D, Milzani A. Biomarkers of oxidative damage in human disease. *Clin Chem* 2006;52(4):601-23.

[21] Tsukahara H. Current status of redox markers in immunological and inflammatory diseases. *Rinsho Byori* 2005;53(8):759-67.

[22] Dizdaroglu M. Chemical determination of free radical-induced damage to DNA. *Free Radic Biol Med* 1991;10(3-4):225-42.

[23] Jackson JR, Seed MP, Kircher CH, Willoughby DA, Winkler JD. The codependence of angiogenesis and chronic inflammation. *Faseb J* 1997;11(6):457-65.

[24] Rao NA, Romero JL, Fernandez MA, Sevanian A, Marak GE, Jr. Role of free radicals in uveitis. *Surv Ophthalmol* 1987;32(3):209-13.

[25] Wu GS, Zhang J, Rao NA. Peroxynitrite and oxidative damage in experimental autoimmune uveitis. *Invest Ophthalmol Vis Sci* 1997;38(7):1333-9.

[26] Armstrong D, Ueda T, Ueda T, Aljada A, Browne R, Fukuda S, et al. Lipid hydroperoxide stimulates retinal neovascularization in rabbit retina through expression of tumor necrosis factor-alpha, vascular endothelial growth factor and platelet-derived growth factor. *Angiogenesis* 1998;2(1):93-104.

[27] Jarasch ED, Bruder G, Heid HW. Significance of xanthine oxidase in capillary endothelial cells. *Acta Physiol Scand Suppl* 1986;548:39-46.

[28] Kobayashi SD, Voyich JM, Burlak C, DeLeo FR. Neutrophils in the innate immune response. *Arch Immunol Ther Exp (Warsz)* 2005;53(6):505-17

[29] Bogdan C. Nitric oxide and the immune response. *Nat Immunol* 2001;2(10):907-16.

[30] Sandeep Saxena DK, Sangeeta Kapoor, Amita Jain. C-reactive protein in eales disease. *Annals of Ophthalmology* Winter 2002;34(4):179-180.

[31] Saxena S, Pant AB, Khanna VK, Agarwal AK, Singh K, Kumar D, et al. Interleukin-1 and tumor necrosis factor-alpha: novel targets for immunotherapy in Eales disease. *Ocul Immunol Inflamm* 2009;17(3):201-6.

[32] Sen A, Chowdhury IH, Mukhopadhyay D, Paine SK, Mukherjee A, Mondal LK, et al. Increased Toll-like receptor-2 expression on nonclassic CD16+ monocytes from patients with inflammatory stage of Eales' disease. *Invest Ophthalmol Vis Sci*; 2011; 52(9):6940-8.

[33] Gong Y, Wei SH, Zhang MN, Jin X, Hou BK, Wang D. Serum interferon-gamma/interleukin-4 imbalance in patients with Eales' disease. *Clin Exp Optom*; 2010;93(4):228-32.

[34] Belge KU, Dayyani F, Horelt A, Siedlar M, Frankenberger M, Frankenberger B, et al. The proinflammatory CD14+CD16+DR++ monocytes are a major source of TNF. *J Immunol* 2002;168(7):3536-42.

[35] Lightman S, Greenwood J. Effect of lymphocytic infiltration on the blood-retinal barrier in experimental autoimmune uveoretinitis. *Clin Exp Immunol* 1992;88(3):473-7.

[36] McCord JM, Fridovich I. Superoxide dismutase. An enzymic function for erythrocuprein (hemocuprein). *J Biol Chem* 1969;244(22):6049-55.

[37] Rajesh M, Ramesh A, Ravi PE, Balakrishnamurthy P, Coral K, Punitham R, et al. Accumulation of 8-hydroxydeoxyguanosine and its relationship with antioxidant parameters in patients with Eales' disease: implications for antioxidant therapy. *Curr Eye Res* 2003;27(2):103-10

[38] Selvi R, Angayarkanni N, Bharathselvi M, Sivaramakrishna R, Anisha T, Jyotirmoy B, et al. Increase in Fe^{3+}/Fe^{2+} ratio and iron-induced oxidative stress in Eales disease and presence of ferrous iron in circulating transferrin. *Curr Eye Res* 2007;32(7-8):677-83.

[39] Rajesh M, Sulochana KN, Ramakrishnan S, Biswas J, Manoharan PT. Iron chelation abrogates excessive formation of hydroxyl radicals and lipid peroxidation products in monocytes of patients with Eales' disease:

direct evidence using electron spin resonance spectroscopy. *Curr Eye Res* 2004;28(6):399-407.

[40] Koppenol WH, Stanbury DM, Bounds PL. Electrode potentials of partially reduced oxygen species, from dioxygen to water. *Free Radic Biol Med*;49(3):317-22.

[41] Buxton GV, Greenstock CL, Helman WP, Ross AB. Critical Review of Rate Constants for Reactions of Hydrated Electrons, Hydrogen Atoms and Hydroxyl Radicals (.OH/.O−) in Aqueous Solution. *Journal of Physical and Chemical Reference Data* 1988;17 513–886.

[42] Stamler JS. Redox signaling: nitrosylation and related target interactions of nitric oxide. *Cell* 1994;78(6):931-6.

[43] Werner ER, Gorren AC, Heller R, Werner-Felmayer G, Mayer B. Tetrahydrobiopterin and nitric oxide: mechanistic and pharmacological aspects. *Exp Biol Med (Maywood)* 2003;228(11):1291-302.

[44] Gorren AC, Mayer B. Nitric-oxide synthase: a cytochrome P450 family foster child. *Biochim Biophys Acta* 2007;1770(3):432-45.

[45] Toledo JC, Jr., Augusto O. Connecting the chemical and biological properties of nitric oxide. *Chem Res Toxicol*;25(5):975-89.

[46] Lancaster JR, Jr., Hibbs JB, Jr. EPR demonstration of iron-nitrosyl complex formation by cytotoxic activated macrophages. *Proc Natl Acad Sci U S A* 1990;87(3):1223-7.

[47] Rajesh M, Sulochana KN, Punitham R, Biswas J, Lakshmi S, Ramakrishnan S. Involvement of oxidative and nitrosative stress in promoting retinal vasculitis in patients with Eales' disease. *Clin Biochem* 2003;36(5):377-85.

[48] Beckman JS, Koppenol WH. Nitric oxide, superoxide, and peroxynitrite: the good, the bad, and ugly. *Am J Physiol* 1996;271(5 Pt 1):C1424-37

[49] Yamakura F, Taka H, Fujimura T, Murayama K. Inactivation of human manganese-superoxide dismutase by peroxynitrite is caused by exclusive nitration of tyrosine 34 to 3-nitrotyrosine. *J Biol Chem* 1998;273(23):14085-9

[50] Miyata T, Kurokawa K, Van Ypersele De Strihou C. Advanced glycation and lipoxidation end products: role of reactive carbonyl compounds generated during carbohydrate and lipid metabolism. *J Am Soc Nephrol* 2000;11(9):1744-52.

[51] Stitt AW. Advanced glycation: an important pathological event in diabetic and age related ocular disease. *Br J Ophthalmol* 2001;85(6):746-53.

[52] Fu S, Davies MJ, Stocker R, Dean RT. Evidence for roles of radicals in protein oxidation in advanced human atherosclerotic plaque. *Biochem J* 1998;333 (Pt 3):519-25.

[53] Rajesh M, Sulochana KN, Coral K, Punitham R, Biswas J, Babu K, et al. Determination of carbonyl group content in plasma proteins as a useful marker to assess impairment in antioxidant defense in patients with Eales' disease. *Indian J Ophthalmol* 2004;52(2):139-44.

[54] Swamy-Mruthinti S, Miriam KC, Kumar SK, Biswas J, Ramakrishnan S, Nagaraj RH, et al. Immunolocalization and quantification of advanced glycation end products in retinal neovascular membranes and serum: a possible role in ocular neovascularization. *Curr Eye Res* 2002;25(3):139-45.

[55] Bharathselvi M, Biswas J, Selvi R, Coral K, Narayanasamy A, Ramakrishnan S, et al. Increased homocysteine, homocysteine-thiolactone, protein homocysteinylation and oxidative stress in the circulation of patients with Eales' disease. *Ann Clin Biochem*;50(Pt 4):330-8.

[56] Loscalzo J. The oxidant stress of hyperhomocyst(e)inemia. *J Clin Invest* 1996;98(1):5-7.

[57] Nishio E, Watanabe Y. Homocysteine as a modulator of platelet-derived growth factor action in vascular smooth muscle cells: a possible role for hydrogen peroxide. *Br J Pharmacol* 1997;122(2):269-74

[58] Jakubowski H. Pathophysiological consequences of homocysteine excess. *J Nutr* 2006;136(6 Suppl):1741S-1749S.

[59] Sulochana KN, Rajesh M, Ramakrishnan S. Purification and characterization of a novel 88 kDa protein from serum and vitreous of patients with Eales' disease. *Exp Eye Res* 2001;73(4):547-55.

[60] Rajesh M, Sulochana KN, Sundaram AL, Krishnakumar S, Biswas J, Ramakrishnan S. Presence of a 88 kDa Eales protein in uveitis, tuberculosis, leprosy and rheumatoid arthritis. *Med Sci Monit* 2003;9(2):CR95-9

[61] Dalle-Donne I, Rossi R, Colombo R, Giustarini D, Milzani A. Biomarkers of oxidative damage in human disease. *Clin Chem* 2006;52(4):601-23.

[62] Bhooma V, Sulochana KN, Biswas J, Ramakrishnan S. Eales' disease: accumulation of reactive oxygen intermediates and lipid peroxides and decrease of antioxidants causing inflammation, neovascularization and retinal damage. *Curr Eye Res* 1997;16(2):91-5

[63] Srivastava P, Saxena S, Khanna VK, Kumar D, Nath R, Seth PK. Raised platelet thiobarbituric acid-reacting substances in proliferative Eales' disease. *Indian J Ophthalmol* 2000;48(4):307-9.

[64] Saxena S, Srivastava P, Khanna VK. Antioxidant supplementation improves platelet membrane fluidity in idiopathic retinal periphlebitis (Eales' disease). *J Ocul Pharmacol Ther*;26(6):623-6.

[65] Saxena S, Srivastava P, Kumar D, Khanna VK, Seth PK. Decreased platelet membrane fluidity in retinal periphlebitis in Eales' disease. *Ocul Immunol Inflamm* 2006;14(2):113-6.

DOI 10.1002/prca.201600068 *Proteomics Clin. Appl. 11, 1–2*, 2017, 1600068

RESEARCH ARTICLE

The 88-kDa Eales' protein in serum is a complex of haptoglobin, complement C3, and galectin-1 as identified by liquid chromatography coupled mass spectrometry

Saravanan Ramanujam[1,2], Bharathselvi Muthuvel[1,3], Babu Aravind C.[4], Jyothirmay Biswas[4] and N. Sulochana Konerirajapuram[1]

[1] R. S. Mehta Jain Department of Biochemistry and Cell Biology, Vision Research Foundation, Sankara Nethralaya, Chennai, India
[2] Department of Biochemistry, Tamil Nadu Dr MGR Medical University, Chennai, India
[3] Department of Biological Sciences, BITS, Pilani, Rajasthan, India
[4] Department of Uveitis, Medical Research Foundation, Sankara Nethralaya, Chennai, India

Received: April 21, 2016
Revised: August 25, 2016
Accepted: October 11, 2016

Purpose: Eales' disease (ED), an enigmatic inflammatory disease, affects peripheral retinal veins and thereby vision in males. This study was aimed at identifying and deciphering the role of a novel 88-kDa protein reported in the serum and vitreous of patients with ED.
Experimental design: The purified 88-kDa protein was identified by UPLC coupled ESI-QTOF-MS. The identified proteins were quantified in the serum from 20 ED patients and controls (age and sex matched), respectively by ELISA. The interaction of these proteins was studied using co-immunoprecipitation, western blot, and MS analyses. N-glycosylation of protein was observed by MS and lectin blot.
Results: The 88-kDa protein was identified to be a complex of haptoglobin, complement C3, and galectin-1. ELISA results showed a 1.5-fold increase in levels of haptoglobin ($p = 0.008$), with level of complement C3 unaltered and 1.2-fold decreased serum galectin-1 levels ($p = 0.003$) in ED patients compared to controls. Co-immunoprecipitation illustrated the interaction between haptoglobin and complement C3. Reduced sialylation and increased β-1, 6-*N*-acetyl-glucosamine branched N-glycans were observed in haptoglobin of ED patients.
Conclusion: The 88-kDa protein, a complex of haptoglobin, complement C3, and galectin-1, may play a potential role in ED pathogenesis while levels galectin-1 and haptoglobin may serve as potential biomarker of ED.

Keywords:
Complement C3 / Eales' disease / Galectin-1 / Haptoglobin / Mass spectrometry

Additional supporting information may be found in the online version of this article at the publisher's web-site

1 Introduction

Eales' disease (ED) is an idiopathic, inflammatory condition primarily affecting peripheral retinal veins and prevalent in the Indian subcontinent with a reported incidence of 1 in 200 to 250 ophthalmic patients [1]. Both eyes are affected in 90% of patients [2] and the disease predominantly affects young males between 15 to 45 years of age [3]. The disease progresses in a sequence of retinal periphlebitis, nonperfusion of retinal veins, and retinal neovascularization [4]. Neovascularization leads to recurrent vitreous hemorrhage, resulting in vision loss [5]. The etiology of ED remains unclear, although multiple factors such as tuberculin bacterial proteins, oxidative stress, and autoimmunity have been associated with it in prior reports [6–8]. Clinical diagnosis is made by excluding other mimicking diseases such as sickle cell retinopathy, syphilis, rheumatoid arthritis, diabetic retinopathy, and

Correspondence: Prof. Konerirajapuram N. Sulochana, R.S. Mehta Jain Department of Biochemistry and Cell Biology, Vision Research Foundation, Sankara Nethralaya, 41, College Road, Chennai 600006, India
E-mail: drkns@snmail.org

Abbreviations: **Co-IP**, co-immunoprecipitation; **ED**, Eales' disease; **PLGS**, ProteinLynx Global Server; **TBST**, TBS with Tween-20

Clinical Relevance

Eales' disease (ED) is an idiopathic retinal vasculitis, which impairs the vision in young adult males, predominately in Indian subcontinent. Despite rigorous research, the cause of the disease is unknown and presumed to have association with hypersentivity to a Mycobacterium tuberculin protein. A novel 88-kDa protein, with iron-binding and antioxidant properties, has been found in serum and vitreous of patients with ED. Insight into the identity of this protein is important to understand its role in the disease. This study was carried out to know the identity of this protein by using sophisticated LC-MS technique. The results revealed it to be a complex of haptoglobin, complement C3, and galectin-1. The findings presented in this article will have scope in the further understanding of the disease mechanism and development of newer targeted therapeutic strategies.

sarcoidosis. Due to the lack of specific diagnostic tests, various investigations are carried out to rule out these other plausible diseases [9]. Earlier a few studies have associated changes in circulating proteins such as increased levels of inflammatory cytokine IL-6, high-sensitivity C-reactive protein, elevated globulin, vascular endothelial growth factor, and the presence of a 23-kDa protein in the serum and vitreous samples obtained from patients with the disease [8–10].

In addition to these findings, a novel 88-kDa protein was identified, in the serum and vitreous and also immunolocalized in the epiretinal membranes of patients with ED. This protein has been characterized to have iron-binding capacity and antioxidant properties. Edman sequencing of this purified protein suggested that the sequence was unique [10]. Unraveling the identity of the 88-kDa protein is important for the diagnosis and understanding of the disease pathogenesis. MS-based proteomics is a powerful tool for discovery of proteins, which is increasingly being exploited for understanding the diseases of unknown etiology such as Behcet's disease, juvenile idiopathic arthritis, and type 1 diabetes [11–13]. We used proteomic approach for identifying 88-kDa protein by the LC-MS and evaluated the levels of identified proteins, which were significantly different compared to normal individuals, implying a role for these proteins in the disease mechanism.

2 Materials and methods

2.1 Patients and serum samples

This study was approved by the Institute's Research Board and Ethics Committee. Informed written consent for participating in the study was obtained from all the participants. The experiments pertaining to human subjects were performed in adherence to the tenets of the Declaration of Helsinki. This study included 20 ED patients, diagnosed by an ophthalmologist after detailed fundus examination, and 20 healthy adult volunteers as controls; between 15 and 45 years of age. The participants included were devoid of other systemic diseases, intake of vitamin supplements, and smoking or alcohol consumption. From each participant, 4 mL of venous blood was collected in plain tubes and was centrifuged at 3000 × *g*, 25°C for 10 min at room temperature, to separate serum from the blood. Serum samples were stored at −80°C until they were analyzed.

2.2 Sample preparation for mass spectrometry

2.2.1 In-gel tryptic digestion

Protein content of the serum samples were determined by the biuret method [14]. The serum of healthy controls subjects and ED patients was screened for the 88-kDa protein by loading 50 μg of serum protein and resolved on 7.5% native PAGE at 100 V by constant voltage mode, until the dye front reaches the bottom edge of the gel. The gel was stained for proteins with colloidal Coomassie stain.

The 88-kDa band was present only in samples of ED patients. The band was excised from the gel and transferred to 1.5 mL microcentrifuge tube. Gel pieces were alternately washed with 100% ACN and 100 mM NH_4CO_3 buffer in order to remove all free detergents by generating consecutive dehydration and hydration of the gels, respectively. Gel pieces were dried in a vacuum centrifuge (Speed Vac, Thermo Scientific Waltham, MA, USA) and incubated at 37°C for overnight with trypsin (13 ng/μL trypsin in 100 mM NH_4CO_3).

2.2.2 Purified 88-kDa protein preparation

Purification of the 88-kDa protein was carried out as per the method published by Sulochana et al. [10]. Briefly, serum samples from six ED patients were pooled (1 g protein) and precipitated with 70% ammonium sulfate. Precipitate was dialyzed with 10 mM phosphate buffer pH 7.4 for 48 h. After dialysis, the sample was centrifuged at 5000 × *g* for 30 min at 4°C; the supernatant was subjected to 5% PAGE preparative gel electrophoresis. The fractions, positive for 88-kDa protein, analyzed by gel electrophoresis and showing anti-TBARS activity were pooled and further subjected to HPLC purification

using octadecylsilane RP column. The protein was injected and eluted with isocratic buffer (10 mM phosphate buffer with 0.1 M sodium chloride and 50% methanol) at the flow rate of 0.2 mL/min. The elution was monitored and protein was resolved as a homogenous peak.

2.2.3 In-solution digestion

The fraction positive for 88-kDa protein (100 μg) and purified 88-kDa protein (100 μg) was subjected to in-solution tryptic digestion. Reduction was carried out using 100 mM dithiothreitol (56°C for 30 min) and alkylation was done using 200 mM iodoacetamide (room temperature for 30 min). Overnight digestion was carried out by adding 1 μg of trypsin in 1 μL of 100 mM NH_4CO_3 at 37°C [15].

2.2.4 Extraction of peptides

After overnight digestion of the in-gel digested sample, the supernatant was collected in fresh tube and the digested peptides were extracted with a buffer of 5% formic acid and 50% ACN and dried in a vacuum concentrator. Simultaneously, the in-solution tryptic digested sample was also subjected to vacuum drying.

The dried peptides from both in-gel and in-solution digested samples were reconstituted with 10 μL of buffer (2% ACN and 0.1% formic acid in Milli-Q water) and centrifuged at 18 000 × *g* for 10 min and filtered through 0.22 μm spin column filter. Both the supernatants were transferred to separate sample recovery vials (Waters Corporation, Milford, MA, USA) for further analysis [15].

2.2.5 Mass spectrometric analysis: UPLC-MS configurations for analysis

Nano ACQUITY UPLC system (Waters Corporation) uses two solvents, namely, solvent A (0.1% formic acid in water) and solvent B (0.1% formic acid in ACN). MPDS (Mass prep digestion standard, Waters Corporation) was used as a standard, analyzed prior to samples. More than 60% of the peptide sequence coverage for standard was considered as optimal for analysis of the test samples. MS/MS spectrum from GFP ([Glu1]-Fibrinopeptide B, Waters Corporation) m/z 785.8426 and LE (Leucine enkephalin, Waters Corporation) m/z 556.2741 were used to calibrate the TOF analyzer of mass spectrometer externally.

The GFP and LE were delivered at concentrations of 500 fmol and 1 ng/μL, respectively, to the mass spectrometer via a nano lock spray at a flow rate of 300 nL/min. For data correction after acquisition, the monoisotopic mass of the doubly charged ions in MS mode was used. Accurate mass data were collected in data-independent acquisition mode. The collision energy was ramped from 3.5 to 35 eV with the transfer collision energy at 10 eV in collision cells. The spectral acquisition scans rate was 0.6 s with a 0.1-s interscan delay. To each of the samples injected, tryptic digested protein from yeast enolase of 50 fmol concentration was spiked. The protein quantification of samples was calculated by ProteinLynx Global Server (PLGS) version 2.4.5 (label-free analytical methodology ("Hi3" method)) [16].

Tryptic digested peptides from the 88-kDa protein band were applied to the Symmetry C18 trapping column (180 μm × 20 mm, 5 μm) and flushed with 0.1% solvent B for 2 min at a flow rate of 15 μL/min. Sample elution from the analytical column (BEH 100 μm × 100 mm, 1.7 μm) was performed at a flow rate of 300 nL/min by increasing the organic solvent B concentration from 3 to 90% using step-up gradient over 120 min.

2.2.6 Data processing

Protein Lynx Global Server version 2.4.5 (Waters Corporation) was used to process LC-MS^E data. In brief, lockmass-corrected spectra were centroided, deisotoped, and charge-state-reduced to produce a single, accurate mass measured monoisotopic mass for each peptide and the associated fragment ion. The initial correlation of a precursor and a potential fragment ion was achieved by means of time alignment.

2.2.7 Database searches

All MS^E data obtained were processed in PLGS version 2.4.5 against *Homo sapiens* database (UniProtKB/Swiss-Prot), released in February 2016, to which sequences of proteins from MPDS (yeast enolase, rabbit Glycogen Phosphorylase b, yeast alcohol dehydrogenase, BSA) and porcine trypsin sequences had been added. A fixed modification of carbamidomethyl-C was specified, and variable modifications included were acetyl N-terminus, deamidation (N), deamidation (Q), oxidation (M), and N-glycosylation. One missed trypsin cleavage site was allowed. The precursor and fragment ion tolerances were determined automatically. The initial protein identification criteria used by the Identity E algorithm within PLGS required the detection of at least three fragment ions per peptide, seven fragment ions, and minimum one peptide per protein. For quantification of proteins by using Hi3 method, both the accession ID and amount of calibrating protein (Yeast alcohol dehydrogenase, 50 fmol) was entered in the workflow designer. The false discovery rate was set at 4%. All the experiments were done in accordance with minimum information about a proteomics experiment (MIAPE) guidelines.

2.2.8 ELISA for haptoglobin, complement C3, and galectin-1

Serum levels of haptoglobin (E-80HPT), complement C3 (ab108822), and galectin-1 (DGAL10) were determined with commercial ELISA kits, procured from Immunology

Consultants Laboratory (Portland, OR, USA), Abcam (Cambridge, UK), and R&D systems (Minneapolis, MN, USA), respectively. The linearity of the haptoglobin assay was within range 0.3125–200 ng/mL. Sensitivity of complement C3 ELISA is 0.6 ng/mL and dynamic range is 0.62–40 ng/mL. Minimum detectable doses of galectin-1 ranged 0.008–0.129 ng/mL and dynamic range of the assay is 0.313–20 ng/mL. All assays were performed in duplicates for 20 samples in each set, as per manufacturer's instructions. Appropriately, serum samples of 100 μL (diluted 1:50 000) for haptoglobin, 25 μL (dilution 1:100 000) for complement C3, and 10 μL (undiluted) for galectin-1 were used for quantification. In brief, standards/samples were incubated for 15 min in wells precoated with haptoglobin antibodies and for 2 h in precoated wells for both complement C3 and galectin-1 antibodies. Washing was carried out five times with wash buffer. To each well, 100 μL of HRP-conjugated respective primary antibodies were added and incubated for 15 min for haptoglobin and 60 min for complement C3 and galectin-1, followed by five times washing. Subsequently, wells were incubated with TMB substrate chromogen (100 μL) for 5 minfor haptoglobin and for 15 min for complement C3 and galectin-1. After the addition of 100 μL stop solution, plates were immediately read at 450 nm in spectramx M2^{e} (Molecular devices, Sunnyvale, CA, USA).

2.2.9 Co-immunoprecipitation

Serum samples (500 μg of protein) from three control and ED patients were used and analysis performed in triplicates. To remove nonspecific binding proteins, samples were precleared by incubating with A/G beads (Santa Cruz Biotechnology, Santa Cruz, CA, USA) for 3 h at 4°C. The contents were centrifuged at 2000 rpm for 2 min at 4 °C and supernatants were incubated with 1 μg of specific antibodies for 12 h at 4°C under rotary agitation to allow the formation of antibody–antigen complex.

For haptoglobin Ip, antihaptoglobin antibody (mouse, sc-69783) was used and anti-IgG antibody (mouse, sc-2025) was used as negative control. For complement C3 Ip, anti-complement C3 antibody (rabbit, ab181147) was used and IgG antibody (rabbit, sc-2027) was used as negative control.

To precipitate antigen–antibody complex, A/G beads were incubated at 4°C under rotary agitation for 2 h. After incubation, the tubes were centrifuged, and supernatant was decanted. Beads were boiled at 95°C for 2 min with 0.2% RapiGest (Waters Corporation) in Tris, pH 8.5, for 5 min, which permits separation of protein from protein-A/G beads. This solution was centrifuged and the supernatant was divided into two aliquots. One of them was subjected to in-solution tryptic digestion as described and with an additional step of adding 200 mM HCl prior to sample extraction and analyzed by MS. Simultaneously, the other aliquot of supernatant was boiled with 2× Lamelli buffer at 95°C and resolved in 10% SDS-PAGE [17] and subjected to western blot.

2.2.10 Western blot

The co-immunoprecipitation (Co-IP) samples were resolved in 10% SDS-PAGE, and electrotransfered to PVDF membrane (methanol prewetted). It was blocked with 5% BSA in PBST, pH 7.4, for 1 h at room temperature, then probed for the target protein with primary antibodies, viz., anti-complement C3 (rabbit, ab117244, 1:1000), anti-haptoglobin (goat, sc-68667, 1:1000), anti-IgG (mouse, sc-2025, 1:1000), and anti-IgG (rabbit, sc-2027, 1:1000) in 2.5% BSA as negative controls, for overnight at 4°C. After washing with PBST thrice, respective HRP-conjugated secondary antibodies (1:10 000 diluted in PBST) were added and the membranes were incubated at room temperature for 2 h. Membranes were washed in PBST thrice and developed using Clarity ECL Western Blotting Substrate (Bio-Rad), and imaged and documented using the FluorChem FC3 image analyzer (Protein Simple, San Jose, CA, USA).

2.2.11 Lectin blot

Serum protein of around 20 μg, from each of 20 controls and ED patients were separated by electrophoresis, and electrotransferred to the PVDF membrane. Subsequently membrane was incubated with 2 μg/mL biotinylated lectin for 30 min after blocking with 1% BSA in TBS with Tween-20 (TBST) for 1 h. L-phytohemagglutinin (L-PHA) was used for identification of β-1-6GlcNAc branching in tri- and tetra-antennary glycans and *Sambucus nigra* agglutinin (SNA) was used for identification of α-2-6-linked sialic acid. This is followed by washing with TBST and incubation for 2 h with streptavidin conjugated with HRP. Membranes were washed in TBST thrice and developed using the protocol as given in the section 2.2.9.

3 Results

3.1 The 88-kDa band consists of serum proteases and serum protease inhibitors family of proteins

The 88-kDa band (Fig. 1) in the alpha 2 globulin region of ED samples was excised, from three samples tryptic digested and analyzed by LC-ESI-MS/MS. The analysis revealed 40 proteins, including complement (C3, C5, C4A, C4B, vitronectin, clusterin, and plasma protease C1 inhibitor), coagulation components (plasmin, kallikrein, prothrombin) immunoglobins, and transport proteins. Most of these proteins belong to serine proteases of chymotrypsin family and serpins family. The hits were identical in all the three independent samples analyzed. The two top-scoring proteins are haptoglobin and complement C3 and the complete list of proteins identified in the 88-kDa band is given in Supporting Information Table 1.

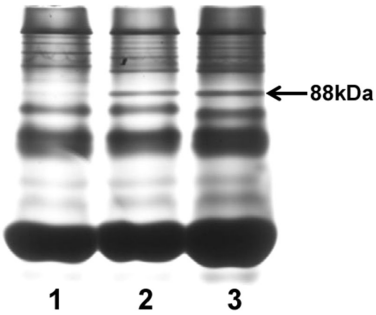

Figure 1. Representative native PAGE image of serum proteins obtained from control subjects and patients with ED. The image shown is of a 50 μg sample resolved on a 7.5% polyacrylamide gel under nondenaturing condition and stained with colloidal coomassie stain. Lane 1 depicts sample from healthy volunteers whereas the lanes 2 and 3 are samples from patient with ED. The presence of 88-kDa band is identified in the lanes 2 and 3, which is indicated by arrow in the image.

Serum samples from ED patients were fractionated with ammonium sulfate and resolved in preparative scale electrophoresis as described in Section 2.2.2.2, for the presence of 88-kDa protein. The LC-ESI-MS/MS analysis of fractions positive for 88-kDa protein revealed hits of haptoglobin, complement C3, and galectin-1 along with other proteins in all the three samples (Table 1).

3.2 Identification of purified 88-kDa protein as haptoglobin, complement C3, and galectin-1 by ESI-MS

The purified 88-kDa protein fraction was subject to in-solution tryptic digestion and subjected to LC-ESI-MS/MS. This analysis yielded only three hits, which were haptoglobin, complement C3, and galectin-1, shown in Table 2 and in Supporting Information Fig. 2a–c. The reproducibility was ascertained by analyzing in three sets. The presence of only three hits accentuates the purity of the sample. It is noteworthy that the analysis of in-gel tryptic digested 88-kDa band from ED patient serum and the in-solution tryptic digested purified fraction gave away the similar hits of haptoglobin and complement C3, along with galectin-1.

3.3 Estimation of haptoglobin, complement C3, and galectin-1 levels by ELISA

Serum levels of haptoglobin, complement C3, and galectin-1 from control and ED patients were estimated by ELISA. The levels of haptoglobin in serum were found to be significantly increased in ED patients compared to control subjects.

Table 1. The list of proteins identified with ESI MS in 88-kDa positive fractions obtained from the native preparative PAGE of the ED serum

Protein entry, protein description	Protein score	Protein average mass	Protein sequence cover (%)	Protein-matched peptide intensity sum
P00738, haptoglobin	2059.26	45 889.68	25.12	99 888
P01024, complement C3	2494.47	188 688.1	36.68	372 557
P09382, galectin 1	9137.65	15 057.89	45.19	203 300
P02768, serum albumin	4208.02	71 362.71	36.78	2 612 830
P02787, serotransferrin	3639.53	79 345.08	41.69	690 242
P02790, hemopexin	1126.67	52 417.79	27.06	142 448
P02763, alpha 1 acid glycoprotein 1	289.13	23 739.69	8.46	20 653
P16402, histone H1	141.61	22 349.92	9.5	36 682
Q9UKV3, apoptotic chromatin condensation inducer in the nucleus	76.67	152 260.85	7.38	28 780
Q5T200, zinc finger CCCH domain containing protein 13	11.85	197 319.92	0.48	988

UniProt accession numbers are listed along with PLGS scores, sequence coverage, and intensity.

Table 2. The list of proteins identified with ESI MS in purified (HPLC) 88-kDa protein in the ED serum

Protein accession, protein description	Protein score	Protein average mass	Protein sequence cover (%)	Protein-matched peptide intensity sum
P00738, haptoglobin	1995.47	45 889.68	57.14	580 473
P01024, complement C3	783.77	188 688.1	28.26	650 537
P09382, galectin 1	9758.47	15 057.88	76.3	766 672

UniProt accession numbers are listed along with PLGS scores, sequence coverage, and intensity.

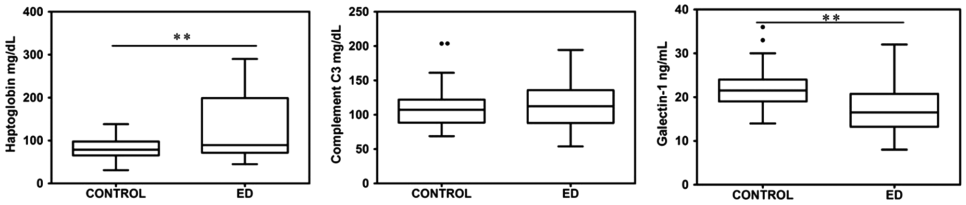

Figure 2. Serum levels of haptoglobin, complement C3, and galectin-1 proteins were estimated by ELISA. The levels of haptoglobin in serum were found to be significantly increased in comparison to control subjects. ($n = 20$, the levels of haptoglobin in control = 80.72 $\pm$ 25.33 mg/dL, ED = 131.12 $\pm$ 72.88 mg/dL, $p = 0.008$). Unaltered levels of complement C3 in control serum and ED serum were113.9 $\pm$ 37.49 and 115.4 $\pm$ 35.23 mg/dL, respectively, and difference among these groups was nonsignificant. Further, significantly lowered serum galectin-1 levels of ED patients in comparison to controls are shown ($n = 20$, Control = 22.50 $\pm$ 5.15 ng/mL, ED = 17.25 $\pm$ 5.46 ng/mL, $p =$ 0.003).

Complement C3 levels showed no significant change among control and ED groups. Levels of serum galectin-1 were significantly lower in ED samples in comparison to controls. Elevated levels of haptoglobin, decreased galectin-1 level, and unaltered C3 levels were found in serum of ED patients compared to control subjects (Fig. 2).

3.4 Comparative levels of estimated proteins among serum by ELISA, 88 kDa resolved by preparative electrophoresis, and purified 88-kDa protein by LC MS/MS

Serum haptoglobin complement C3 and galectin-1 levels quantified by ELISA were compared with levels measured by MS by Hi3 analysis of 88-kDa positive fractions and that of purified 88-kDa protein (Table 3). MS based protein estimation in whole serum (immuno depleted for albumin and immunoglobin) yielded 227 mg/dL of haptoglobin and 100 mg/dL of complement C3 meanwhile galectin-1 was undetected.

3.5 Identification of non-sialylated haptoglobin of ED patients

Haptoglobin identified in Co-IP of control subjects and ED patients were analyzed for glycosylation changes by MS. Haptoglobin has four known N-glycosylation sites (N184, N207, N211 and N241) and one of this glycosylated peptide 'MVSHH**N**^{184}LTTGATLINEQWLLTTAK' was found in our analysis. In the glycosylation profiling of control serum haptoglobin, N184 residue was identified to be mono sialylated biantennary species (Fig. 3A). Protein expression of haptoglobin was higher among of ED patients and in haptoglobin of ED patients 184residue was found to be nonsialylated biantennary N-glycan (Fig. 3B).

Increased, tri-antennary and tetra-antennary glycopeptides (containing α-linked mannose residues with β-1, 6-N-acetylglucosamine branches) and decreased α-2,6-sialic acid residues in haptoglobin of ED patients were observed by lectin blots when compared to control subjects (Fig. 3C).

3.6 Complement C3 interacts with haptoglobin

To address whether complement C3 associates with haptoglobin, we used ED patient serum for immunoprecipitation with anti-complement C3 antibody and anti-rabbit IgG. In complement C3 Co-IP, haptoglobin and other complement cascade proteins were obtained as hits (Table 4). MS analysis of negative control showed only nonspecific proteins (Supporting Information Table 2).

Similarly haptoglobin Co-IP with anti-haptoglobin antibody in ED serum revealed as lead hit Complement C3 suggesting its interaction with haptoglobin (Table 5). Only the nonspecific proteins were identified negative control Co-IP with anti-mouse IgG (Supporting Information Table 3).

Table 3. The three proteins identified in purified 88-kDa protein were measured in serum and in 88-kDa band

Protein accession, protein description	ELISA ($n = 20$)	88-kDa protein resolved by preparative electrophoresis ($n = 3$) in-gel digest analyzed LC-MS/MS	88-kDa purified protein ($n = 3$) in-solution digest LC-MS/MS
P00738, haptoglobin	131.12 $\pm$ 72.88 mg/dL	48.76 $\pm$ 11.25 ng/μL	6.6 $\pm$ 0.02 ng/μL
P01024, complement C3	113.9 $\pm$ 37.49 mg/dL	12.2 $\pm$ 2.415 ng/μL	2.95 $\pm$ 1.09 ng/μL
P09382, galectin 1	17.25 $\pm$ 5.46 ng/mL	0.27 $\pm$ 0.06 ng/μL	1.8 $\pm$ 0.8 ng/μL

Amount of haptoglobin was found to be increased in serum of ED patients and in 88-kDa protein.

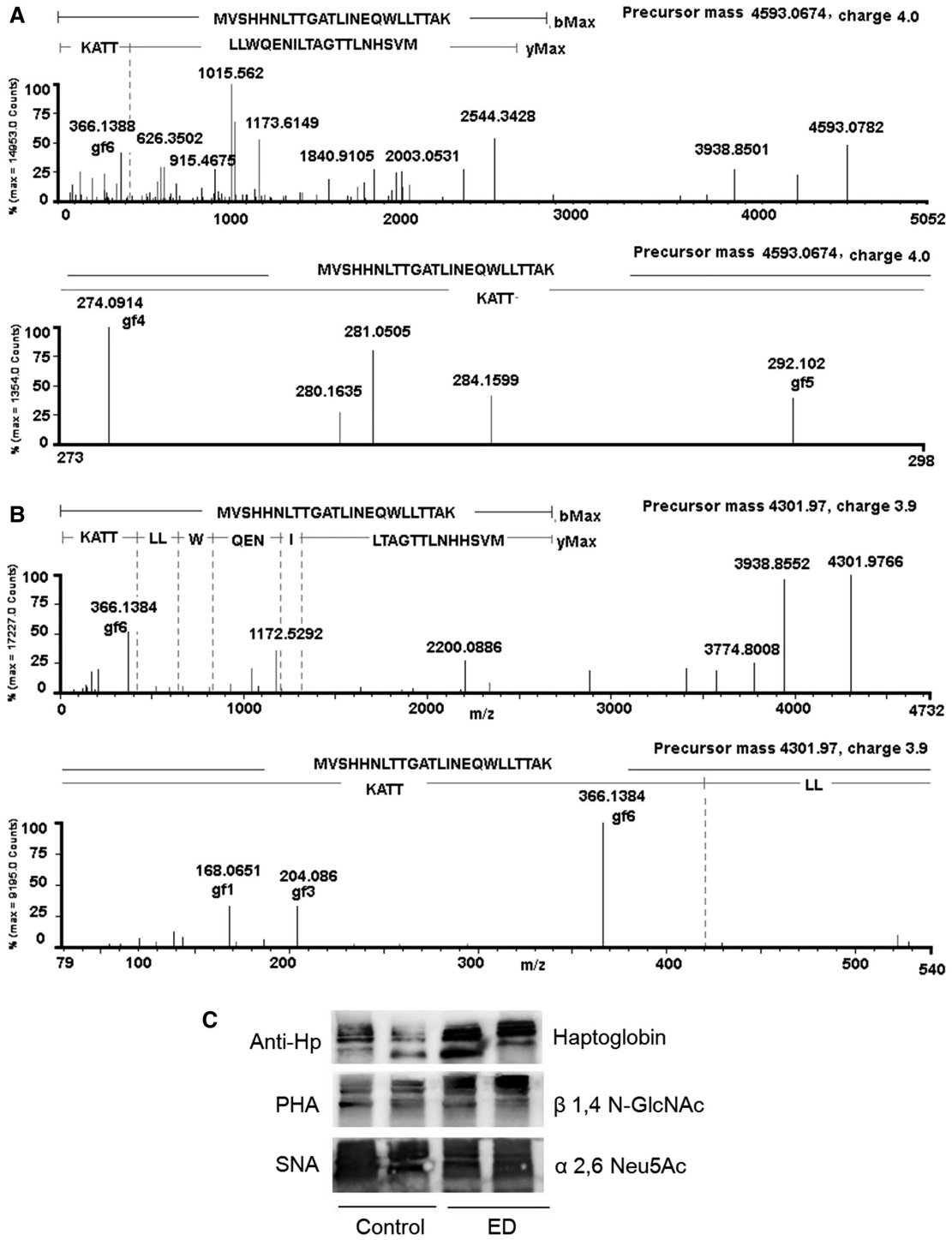

Figure 3. (A) N-glycosylation of haptoglobin peptide MVSHHNLTTGATLINEQWLLTTAK was from control samples. The mass of the peptide was 4593.0674 with identified glycan of Man2HexNAc2NeuAc1 + Man3HexNAc2. The observed fragment ions were 366.1395 (Man1HexNAc1), 292.1027 (NeuAc1), and 657.2354(Man1HexNAc1NeuAc1), which are indicative of sialylation. (B) N-glycosylation of haptoglobin peptide MVSHHNLTTGATLINEQWLLTTAK was from ED samples. The mass of the peptide was 4301.97 and identified to contain Man2HexNAc2 + Man3HexNAc2 glycosylation. In ED samples, mhp values are 292 Da lesser than controls, which accounts to loss of one sialic acid residue. The observed fragment ions were 204.0867 (HexNAc1) and (Man1HexNAc1) 366.1395 which corresponds to glycan residues. (C) Increased haptoglobin in ED patients was confirmed by western blot. Lectin blots showing increased tri- and tetra-antennary glycans, which were identified by PHA and SNA probing, showed a decrease in α-2, 6 sialic acid in ED patients compared to control. HexNAc, N-acetyl hexosamine; Man, mannose; NeuAc, N-acetylneuraminic acid.

Table 4. The list of protein sequences identified by ESI/LC/MS in complement C3 co-immunoprecipitated ED serum

Protein accession, protein description	Protein score	Protein average mass	Protein sequence cover (%)	Protein-matched peptide intensity sum
P00738, haptoglobin	70 515.26	45 889.68	59.11	8 435 820
P01024, complement C3 precursor	15 001.28	188 704.13	54.12	4 759 200
P01028, complement C4 precursor	2067.68	194 368.48	37.67	733 193
P01031, complement C5 precursor	400.387	190 042.42	17.6	167 061
P02679, fibrinogen gamma chain precursor	59 371.25	52 124.01	62.25	7 053 887
P02743, serum amyloid P component	474.60	25 501.20	13.45	58 262
P04004, vitronectin precursor	2894.29	55 104.03	20.92	182 319
P08603, complement factor H precursor H factor 1	3948.68	143 801.79	47.52	876 580

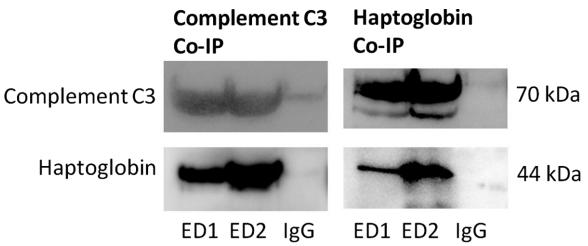

Figure 4. Western blot images of complement C3 and haptoglobin Co-IP. In Co-IP samples using complement C3, and haptoglobin antibodies, the presence of haptoglobin and complement C3 was identified respectively. These proteins were not detected in samples co-immunoprecipitated with respective control IgGs.

Interaction between complement C3 and haptoglobin Co-IP samples were confirmed by Western blot. Presence of haptoglobin and complement C3 bands in immunoprecipitated serum of ED patients was identified. Similarly, haptoglobin and complement C3 were identified in serum samples were immunoprecipitated with anti-haptoglobin antibody (goat, sc-68667) and probed with anti-complement C3 (rabbit, ab181147) and anti-haptoglobin (mouse, sc-69783) antibodies, as seen in case of complement C3 Co-IP (Fig. 4).

4 Discussion

ED, being an ocular inflammatory disease, affects the peripheral retinal veins, which is diagnosed by exclusion of other similar disorders. An 88-kDa protein identified in ED patients was considered as a potential biomarker. The 88-kDa protein resembles haptoglobin in its electrophoretic mobility at $\alpha 2$ globulin region and displayed some properties of haptoglobin such as hemoglobin binding, agglutinating RBC, and anti-TBARS activity. This was sequenced by automated Edman's degradation chemistry at the N-terminal and some of the internal regions. The sequence did not match with any known protein sequences available in the human database

Table 5. List of proteins identified in immunoprecipitates of haptoglobin by ESI/LC/MS

Protein accession, protein description	Protein score	Protein average mass	Protein sequence cover (%)	Protein-matched peptide intensity sum
P00738, haptoglobin	57 333.56	45 889.68	65.52	5 083 795
P00739, haptoglobin related protein	20 653.39	39 542.86	43.97	1 918 384
P0C0L5, complement C4 B	8783.28	194 291.5	34.12	1 058 353
P0C0L4, complement C4 A	8783.28	194 382.5	34.17	1 087 454
P69905, hemoglobin subunit alpha	8046.84	15 314.6	54.93	156 624
P02647, apolipoprotein A I	7559.90	30 777.87	41.57	165 152
P08603, complement factor H	3664.80	143 772.7	36.64	313 973
P00747, plasminogen	1391.02	93 306.41	23.58	143 102
P04004, vitronectin	1296.97	55 104.04	14.44	29 388
P01024, complement C3	880.95	188 688.1	19.96	142 136
P01019, angiotensinogen	149.69	53 439.43	5.15	11 260
P00751, complement factor B	137.86	86 901.64	7.46	14 933

and was considered as a unique protein [10]. This study reveals the 88-kDa protein as a complex of three proteins that was identified using MS analysis and their interaction was proven using immunoprecipitation.

Initially, to identify the protein we subjected the 88-kDa band, from ED serum for MS analysis. Positive acute phase proteins, haptoglobin and complement C3, were identified as top hits along with other 40 proteins. Number of proteins belongs to complement and coagulation pathway complement system were observed in this band and it was confirmed by both DAVID (Functional Annotation Chart) and PANTHER (statistical over-representation test) software analysis (Supporting Information Fig. 1 and Table 4) [18,19]. Both of these cascade components share conserved catalytic site system. The coagulation enzymes (plasmin, kallikrein, and thrombin) and pathogens are reported to activate complement components and thereby inducing series of inflammatory responses [20, 21]. The presence these proteins in 88-kDa band may have potential role in the ocular pathogenesis of ED which includes, inflammation, capillary occlusion, and peripheral nonperfusion. Since ED is believed to be tubercular vasculitis [3,6] and no study till date has substantiated, further research on the 88-kDa band for the presence of protein/proteins of infectious pathogen might be important to understand the nature of host-pathogen interaction.

To ascertain our findings, we subjected purified 88-kDa protein to MS analysis, which identified three proteins haptoglobin, complement C3, and galectin-1. Complement C3 is the most abundant component of complement cascade and is crucial in classical, lectin, and alternative pathways [22]. Interestingly, haptoglobin-2 precursor (Zonulin) is involved in complement activation of animals with acute lung injury, supporting their interaction [23]. We speculated if an interaction could take place between these acute phase proteins, which was confirmed by Co-IP and analysis with MS and western blot. For the first time we have demonstrated haptoglobin–complement interaction, along with altered levels of haptoglobin and galectin-1 in ED patients. However, unaltered levels of complement C3 may be due to its slower rate of synthesis than other acute phase proteins [24] or due its participation in the complement pathway as a result of persistent inflammation in ED.

The purified 88-kDa protein comprises galectin-1. It was reported that despite normal haptoglobin levels in sera of breast cancer, galectin-1 binding was twofold higher and this was attributed to the presence of glycosylation changes [25]. Our MS analysis of glycosylation changes in haptoglobin from ED samples was identified to be nonsialylated, biantennary glycan [26]. Lectin blot analysis was carried out to validate glycosylation changes and we found increased levels of tri- and tetra-antennary glycopeptides with β-1, 6-N-acetylglucosamine branches (L-PHA lectin). These residues are recognized as galectin-1 binding region in absence of α-2, 6-sialic acid capping residues [25, 27]. We also observed decreased α-2, 6-sialic acid capping in haptoglobin of ED patients (SNA lectin), thus enabling its binding to galectin-1. This explains the decrease in serum-free galectin-1 levels as a result of its binding with haptoglobin.

Galectin-1 is expressed in immune privilege sites. It is reported to suppress T-lymphocyte activation in uveitis, an acute inflammatory eye disease [28,29]. Additionally, in experimental autoimmune uveitis, complement plays a role in the induction of antigen specific T-cell responses [30]. Elevated pro-inflammatory cytokines in vitreous [31] as well as infiltration of T-lymphocytes in epiretinal and subretinal membranes were reported in ED patients [32]. We speculate the involvement of complement-mediated ocular inflammation, owing to presence of complement pathway components and association of mycobacterium genome in ED patients [6]. The ocular inflammatory reaction, in the disease, could be further aggravated by lower levels of galectin-1. However, specific complement activation studies are needed for complete understanding.

To our knowledge, this is the first report on proteome changes in ED and this study investigated the identity of 88-kDa protein as a complex of haptoglobin, complement C3, and galectin-1 that may play a role in the retinal inflammatory pathology of disease. Due to limited availability of vitreous samples from ED patients and nonavailability of animal model for the disease makes this study important as it facilitates the noninvasive identification of proteins associated with pathogenesis. This study is an example that demonstrates the power of proteomics in clinical intervention, by identifying the unknown proteins, elucidation of their interactive partners, and the involvement of the critical pathways in the disease pathogenesis. Detailed study of the individual proteins is needed for understanding the disease pathogenesis; its diagnosis and intervention warrant further research.

We thank ICMR for providing financial support (ICMR 53/18/2009-BMS), ICMR-JRF fellowship (3/1/3/JRF-2010/HRD-127(21362)) for the study, and R.S. Mehta Jain family who funded for the establishment of MS facility. Our sincere thanks to K. Gayathree and R. Swaminathan for their extensive help in proofreading the manuscript.

The authors have declared no conflict of interest.

5 References

[1] Puttamma, S. T., Varied fundus picture of central retinal vasculitis. *Trans. Asia Pacific Acad. Ophthalmol.* 1970, *520*.

[2] Duke-Elder, S., *System of Ophthalmology*, Henry Kimpton, London 1970.

[3] Biswas, J., Sharma, T., Gopal, L., Madhavan, H. N. et al., Eales disease—an update. *Surv. Ophthalmol.* 2002, *47*, 197–214.

[4] Spitznas, M., Meyer-Schwicherath, G., Stephan, B., Treatment of Eales' disease with photocoagulation. *Albrecht Von Graefes Arch. Klin. Exp. Ophthalmol.* 1975, *194*, 193–198.

[5] Saxena, S., Kumar, D., A new staging system for idiopathic retinal periphlebitis. *Eur. J. Ophthalmol.* 2004, *14*, 236–239.

[6] Therese, K. L., Deepa, P., Therese, J., Bagyalakshmi, R. et al., Association of mycobacteria with Eales' disease. *Indian J. Med. Res.* 2007, *126*, 56–62.

[7] Konerirajapuram, N. S., Coral, K., Punitham, R., Sharma, T. et al., Trace elements iron, copper and zinc in vitreous of patients with various vitreoretinal diseases. *Indian J. Ophthalmol.* 2004, *52*, 145–148.

[8] Rajesh, M., Sulochana, K. N., Ramakrishnan, S., Biswas, J. et al., Iron chelation abrogates excessive formation of hydroxyl radicals and lipid peroxidation products in monocytes of patients with Eales' disease: direct evidence using electron spin resonance spectroscopy. *Curr. Eye Res.* 2004, *28*, 399–407.

[9] Das, T., Pathengay, A., Hussain, N., Biswas, J., Eales' disease: diagnosis and management. *Eye (Lond.)* 2010, *24*, 472–482.

[10] Sulochana, K. N., Rajesh, M., Ramakrishnan, S., Purification and characterization of a novel 88 kDa protein from serum and vitreous of patients with Eales' disease. *Exp. Eye Res.* 2001, *73*, 547–555.

[11] Kalinina Ayuso, V., de Boer, J. H., Byers, H. L., Coulton, G. R. et al., Intraocular biomarker identification in uveitis associated with juvenile idiopathic arthritis. *Invest. Ophthalmol. Vis. Sci.* 2013, *54*, 3709–3720.

[12] Rifai, N., Gillette, M. A., Carr, S. A., Protein biomarker discovery and validation: the long and uncertain path to clinical utility. *Nat. Biotechnol.* 2006, *24*, 971–983.

[13] Zhang, Q., Fillmore, T. L., Schepmoes, A. A., Clauss, T. R. et al., Serum proteomics reveals systemic dysregulation of innate immunity in type 1 diabetes. *J. Exp. Med.* 2013, *210*, 191–203.

[14] Gornall, A. G., Bardawill, C. J., David, M. M., Determination of serum proteins by means of the biuret reaction. *J. Biol. Chem.* 1949, *177*, 751–766.

[15] Gundry, R. L., White, M. Y., Murray, C. I., Kane, L. A. et al., Preparation of proteins and peptides for mass spectrometry analysis in a bottom-up proteomics workflow. *Curr. Protoc. Mol. Biol.* 2009, Chapter 10, Unit10.25.

[16] Silva, J. C., Gorenstein, M. V., Li, G. Z., Vissers, J. P. et al., Absolute quantification of proteins by LCMSE: a virtue of parallel MS acquisition. *Mol. Cell. Proteomics* 2006, *5*, 144–156.

[17] Jain, A., Liu, R., Xiang, Y. K., Ha, T., Single-molecule pull-down for studying protein interactions. *Nat. Protoc.* 2012, *7*, 445–452.

[18] Huang da, W., Sherman, B. T., Lempicki, R. A., Systematic and integrative analysis of large gene lists using DAVID bioinformatics resources. *Nat. Protoc.* 2009, *4*, 44–57.

[19] Mi, H., Muruganujan, A., Casagrande, J. T., Thomas, P. D., Large-scale gene function analysis with the PANTHER classification system. *Nat. Protoc.* 2013, *8*, 1551–1566.

[20] Amara, U., Rittirsch, D., Flierl, M., Bruckner, U. et al., Interaction between the coagulation and complement system. *Adv. Exp. Med. Biol.* 2008, *632*, 71–79.

[21] Zipfel, P. F., Skerka, C., Complement regulators and inhibitory proteins. *Nat. Rev. Immunol.* 2009, *9*, 729–740.

[22] Ritchie, R. F., Palomaki, G. E., Neveux, L. M., Navolotskaia, O. et al., Reference distributions for complement proteins C3 and C4: a practical, simple and clinically relevant approach in a large cohort. *J. Clin. Lab. Anal.* 2004, *18*, 1–8.

[23] Moshage, H., Cytokines and the hepatic acute phase response. *J. Pathol.* 1997, *181*, 257–266.

[24] Rittirsch, D., Flierl, M. A., Nadeau, B. A., Day, D. E. et al., Zonulin as prehaptoglobin2 regulates lung permeability and activates the complement system. *Am. J. Physiol. Lung Cell Mol. Physiol.* 2013, *304*, L863–L872.

[25] Carlsson, M. C., Cederfur, C., Schaar, V., Balog, C. I. et al., Galectin-1-binding glycoforms of haptoglobin with altered intracellular trafficking, and increase in metastatic breast cancer patients. *PLoS One* 2011, *6*, e26560.

[26] Morelle, W., Michalski, J. C., Analysis of protein glycosylation by mass spectrometry. *Nat. Protoc.* 2007, *2*, 1585–1602.

[27] Croci, D. O., Cerliani, J. P., Dalotto-Moreno, T., Mendez-Huergo, S. P. et al., Glycosylation-dependent lectin-receptor interactions preserve angiogenesis in anti-VEGF refractory tumors. *Cell* 2014, *156*, 744–758.

[28] Romero, M. D., Muino, J. C., Bianco, G. A., Ferrero, M. et al., Circulating anti-galectin-1 antibodies are associated with the severity of ocular disease in autoimmune and infectious uveitis. *Invest. Ophthalmol. Vis. Sci.* 2006, *47*, 1550–1556.

[29] Toscano, M. A., Commodaro, A. G., Ilarregui, J. M., Bianco, G. A. et al., Galectin-1 suppresses autoimmune retinal disease by promoting concomitant Th2- and T regulatory-mediated anti-inflammatory responses. *J. Immunol.* 2006, *176*, 6323–6332.

[30] Jha, P., Sohn, J. H., Xu, Q., Nishihori, H. et al., The complement system plays a critical role in the development of experimental autoimmune anterior uveitis. *Invest. Ophthalmol. Vis. Sci.* 2006, *47*, 1030–1038

[31] Murugeswari, P., Shukla, D., Rajendran, A., Kim, R. et al., Proinflammatory cytokines and angiogenic and anti-angiogenic factors in vitreous of patients with proliferative diabetic retinopathy and Eales' disease. *Retina* 2008, *28*, 817–824.

[32] Badrinath, S. S., Gopal, L., Sharma, T., Parikh, S. et al., Vitreoschisis in Eales' disease: pathogenic role and significance in surgery. *Retina* 1999, *19*, 51–54.

